AGARD-R-692

AGARD

ADVISORY GROUP FOR AEROSPACE RESEARCH & DEVELOPMENT

7 RUE ANCELLE 92200 NEUILLY SUR SEINE FRANCE

AGARD REPORT No. 692

Wind Tunnel Corrections for High Angle of Attack Models

NORTH ATLANTIC TREATY ORGANIZATION

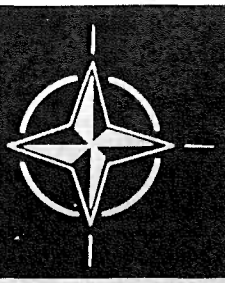

NORTH ATLANTIC TREATY ORGANIZATION

ADVISORY GROUP FOR AEROSPACE RESEARCH AND DEVELOPMENT

(ORGANISATION DU TRAITE DE L'ATLANTIQUE NORD)

AGARD Report No.692

WIND TUNNEL CORRECTIONS FOR HIGH ANGLE OF ATTACK MODELS

The material in this report was presented at an AGARD Fluid Dynamics Panel Round Table Discussion held in Munich, Germany on 8 May 1980.

THE MISSION OF AGARD

The mission of AGARD is to bring together the leading personalities of the NATO nations in the fields of science and technology relating to aerospace for the following purposes:

- Exchanging of scientific and technical information;
- Continuously stimulating advances in the aerospace sciences relevant to strengthening the common defence posture;
- Improving the co-operation among member nations in aerospace research and development;
- Providing scientific and technical advice and assistance to the North Atlantic Military Committee in the field of aerospace research and development;
- Rendering scientific and technical assistance, as requested, to other NATO bodies and to member nations in connection with research and development problems in the aerospace field;
- Providing assistance to member nations for the purpose of increasing their scientific and technical potential;
- Recommending effective ways for the member nations to use their research and development capabilities for the common benefit of the NATO community.

The highest authority within AGARD is the National Delegates Board consisting of officially appointed senior representatives from each member nation. The mission of AGARD is carried out through the Panels which are composed of experts appointed by the National Delegates, the Consultant and Exchange Programme and the Aerospace Applications Studies Programme. The results of AGARD work are reported to the member nations and the NATO Authorities through the AGARD series of publications of which this is one.

Participation in AGARD activities is by invitation only and is normally limited to citizens of the NATO nations.

Published February 1981

ISBN 92-835-0283-3

Printed by Technical Editing and Reproduction Ltd
Harford House, 7–9 Charlotte St, London, W1P 1HD

PREFACE

This report contains papers on various wind tunnel correction methods used in high angles of attack tests. The papers were solicited from the various NATO countries and presented in a round table discussion following the AGARD Fluid Dynamics Panel Symposium in Neubiberg, Germany in May 1980. Papers given and published here are from Canada, France, Germany, Netherlands, Sweden, United Kingdom and the United States.

Several wind tunnel wall correction methods in use or under study are presented here for closed, open and ventilated wall wind tunnels. The Mach number range is generally limited up to high subsonic speeds with some techniques only useful for incompressible flow. Wall correction techniques discussed along with their attributes and disadvantages include vortex lattice, panel, system of images, wall pressure and adaptive walls. The adaptive wall technique is a method to actively reduce or eliminate the need for wall correction and is becoming more favorable as development problems are solved.

Current testing in wind tunnels over this speed range should include documentation of pressures and/or flow angles in the inviscid flow near the tunnel walls. Such measurements facilitate (1) determination of magnitude of wall interference, (2) determination of equivalent free-flight test conditions, (3) correction for wall interference and (4) calculations for adaptive wall adjustments in tunnels which have variable geometry.

R.O.DIETZ
M.L.LASTER
Editors

PROGRAMME AND MEETING OFFICIALS

Chairman: Mr R.O.Dietz
Sverdrup-ARO Inc.
101 W Lincoln St
Tullahoma
Tennessee 37388, USA

MEMBERS

Prof. J.J.Ginoux
Director
Von Kármán Institute for Fluid Dynamics
Chaussée de Waterloo 72
B-1640 Rhode-Saint-Génèse
Belgium

Dr J.E.Green
Head of Aerodynamics Department
Royal Aircraft Establishment
Farnborough
Hants, GU14 6TD, UK

Mr L.H.Ohman
Head, High Speed Aerodynamics Lab.
National Aeronautical Establishment
National Research Council, Montreal Rd
Ottawa, Ontario K1A OR6, Canada

M.l'Ing. de l'Armement A.Coursimault
Section "Etudes Générales"
Service Technique de l'Aéronautique
4 Avenue de la Porte d'Issy
75996 Paris Armées, France

Ir. J.P.Hartzuiker
Chief, Compressible Aerodynamics Dept.
NLR, P.O. Box 90502
1006 BM Amsterdam
Netherlands

Prof. Dr Ing. B.Lashka
Institut für Stromungsmechanik der Tech.
Univers.
Bienroder Weg 3
D-3300 Braunschweig,
Germany

Prof. E.Mattioli
Director Istituto Meccanica Applicata
University di Ancona
Via della Montagnola 30
60100 Ançona, Italy

FLUID DYNAMICS PANEL

Chalrman: Dr K.J.Orlik-Rückemann
National Aeronautical Establishment
National Research Council
Montreal Road
Ottawa, Ontario K1A OR6, Canada

Deputy Chairman: M. l'Ing. en Chef B.Monnerie
Chef dc la Division d'Aérodynamique
Appliquée
ONERA
29 Avenue de la Division Leclerc
92320 Châtillon, France

PANEL EXECUTIVE

R.H.Rollins II

CONTENTS

CANADIAN STUDIES OF WIND TUNNEL CORRECTIONS FOR HIGH ANGLE OF ATTACK MODELS

M. Mokry
National Research Council Canada
National Aeronautical Establishment
Ottawa, Ontario

This paper is a brief account of wind tunnel interference studies relating to testing of high angle of attack models, carried out in Canada during the last decade. If any relevant Canadian work is omitted here, it is only because the author was unaware of its existence. The work of other AGARD countries is referenced here only when needed to indicate the origin of an idea or parallel development.

In the early seventies, the problem of wind tunnel interference on high angle of attack models was dealt with at Canadair, in connection with the research program aimed at the development of high lift technology for advanced aircraft. A vorticity distribution method[1] for the calculation of potential flow past multi-component airfoils in free air was extended[2] to flow past a multi-component airfoil in an infinite cascade and used to evaluate wall interference effects due to solid wind tunnel walls. Figure 1, taken from Ref. 2, shows schematically the generation of an infinite cascade used to model the flow past a four-component airfoil between two wind tunnel walls. The computation, utilizing vorticity panels in the infinite cascade mode, is performed on an eight-component configuration, consisting of the original airfoil and its mirror image. Unlike the usual approximations of wall effects by a few neighbouring images, this solution is exact (in the limit of decreasing panel lengths).

The computed pressure distributions for a 40 deg flap deflection are shown in Fig. 2; the solid line is the wind tunnel computation and the dashed line is the free air computation. Also shown for comparison is the experimental pressure distribution on a 2 ft chord model in the NAE 6 ft x 9 ft low speed wind tunnel. The theoretical curves indicate that there should be a negligible wall effect on lift at this flap deflection. The discrepancy between experiment and theory is apparently caused by viscous and three-dimensional effects which had not been accounted for in the method.

Figure 3 shows the result for the same airfoil with a 70 deg flap deflection. The potential flow theory shows a 4% loss in lift due to wind tunnel interference. The difference between experimental and calculated pressures is more pronounced than in the previous case, since the configuration is already in stall (beyond CL_{max}).

Using the methods based on viscous - inviscid interactions, e.g. Ref. 3, it should be possible to evaluate the effects of airfoil boundary layers on the pressure distributions and establish a better agreement between theory and experiment. However, the presence of boundary layers on the test section walls is an obstacle, since then the walls do not behave like perfect reflection planes and the concept of images would have to be modified, if not abandoned altogether.

At the National Aeronautical Establishment (NAE), the method of singularity distributions was later extended to compute wall interference effects in perforated wall test sections, assuming a linear relationship between the pressure coefficient and the normal component of velocity at the wall. The solution of the problem was separated into two parts: first, the construction of modified singularities (influence or Green's functions) satisfying the wall boundary conditions and, second, the solution for contour distributions of these singularities to satisfy the airfoil boundary conditions, in a procedure equivalent to that used in free air. The computation by a panel method is thus performed only on the original airfoil; no panels are placed on the walls. As the previously discussed cascade approach, this method is again exact. The case of solid walls is obtained as a special case of zero porosity. The source distribution version of the method is described in Refs. 4 and 5; the vortex distribution version in Ref. 6.

Unfortunately, experience with perforated walls indicates that the normal (cross-flow) component of velocity is a nonlinear function of the local pressure coefficient and, therefore, the applicability of wall interference corrections evaluated from linear porous wall theory is only limited. Particularly on the wall facing the suction side of the airfoil the normal velocity is strongly modulated by the rate of growth of the boundary layer, as discovered in Ref. 7. Figure 4 gives an example for a 20% perforated wall of the 15 in x 60 in test section of the NAE high speed wind tunnel. The flow disturbances at the walls were generated by a 10 in chord BGK 1 airfoil, located midway between the walls. Investigated is the boundary layer on the wall facing the suction side of the airfoil; on the other wall (pressure side) the boundary layer was almost completely bled into the plenum. The wall pressure coefficient C_p, measured by a static pressure pipe, is plotted against the ratio v_e/u_e of the normal and tangent velocities on the outer edge of the boundary layer. The normal velocity is deduced from the boundary layer development, computed according to the method of Ref. 8 which can handle suction and injection, matching the velocity profiles measured by boundary rakes at several stations along the wall. From Fig. 4 it is sufficiently clear that a linear relation, used in porous wall theory, does not adequately represent the basic nonlinear characteristics of the cross-flow. The curve shapes and the dependence on Mach number M and geometry of the tested airfoil (here represented by the angle of attack α) are in general agreement with observations in Ref. 9 (U.S.A.), based on direct measurements by a laser velocimeter.

Besides including the computation of wall boundary layers as an integral part of wall correction procedure, there are several ways of avoiding the difficulties with complicated boundary conditions of ventilated wind tunnel walls. Two of them have been extensively studied in Canada and are discussed here:

(1) development of wall correction procedure which uses boundary measurements, but does not require the knowledge of cross-flow properties, and

(2) development of ventilated walls which behave in a well predictable manner.

The first approach, based on the measurement of static pressures on the test section boundary was first successfully demonstrated[10] at ONERA, France. Assuming that the flow near test section walls is subsonic linearized, it is possible to estimate the far field of the model and separate from the wall pressure disturbance the part which is due to wall interference. Since the linearized pressure coefficient is proportional to the axial (streamwise) component of disturbance velocity, the velocity correction at the model position can be obtained as a solution of the Dirichlet problem in the test section interior. The cross-flow properties of the walls thus do not enter the problem.

The component of wall interference velocity normal to the tunnel axis is obtained as the harmonic conjugate of the axial component. Since the integration of Cauchy-Riemann equations involves an arbitrary constant, the determination of the angle of attack correction requires specification of the flow angle at an arbitrary distant point within the test section. A simple approach is to assume that the flow enters the test section in the direction parallel to the wind tunnel axis, but for a more reliable evaluation of the angle of attack correction an actual flow angle measurement should be carried out.

The difference between the ONERA method and the method developed at NAE, Ref. 11, is in the selection of test section boundaries and the construction of the solution. The ONERA method utilizes the concept of an infinitely long test section, Fig. 5a. However, since the pressures can be measured only over a finite length of the test section, the boundary values have to be extrapolated to infinitely distant upstream and downstream points. In Ref. 10, both components of wall interference velocity are obtained in one step, using the conformal mapping of the infinite strip onto the upper half-plane, where the solution is given by Cauchy's integral. The angle of attack correction at the position of the model is obtained assuming the flow parallel to the wind tunnel axis at the infinitely distant upstream point.

The NAE method[11] is based on the finite test section concept and utilizes the Fourier solution of the Dirichlet problem in a rectangle, Fig. 5b. This, in principle, requires that the static pressure be measured along the upstream and downstream sides of the rectangle in addition to the floor and ceiling pressures. However, if the latter are measured sufficiently far upstream and downstream of the model location, a simple interpolation between the floor and ceiling pressures will suffice. The evaluation of the coefficients of the infinite series solution by the fast Fourier transform makes the method very efficient and suitable for routine correcting of wind tunnel test data.

Examples of the evaluated wall interference corrections from measured wall pressures and forces on a high angle of attack model are given in Figs. 6-8, using unpublished test data by F.C. Tang of NAE. The static pressures along the 20% perforated walls of the 15 in x 60 in test section of the NAE high speed wind tunnel were measured by 1 in diameter static pressure pipes, attached to the centerlines of the walls. The force and pitching moment coefficients were measured by a three-component balance and compared with the values obtained by surface pressure integration. In addition, the wake drag was measured by the pitot-traverse method. The tested 12 in chord airfoil was equipped with a 4.5 in flap at the deflection angle of 35 deg, zero overlap and gap of 3% of the chord length.

In the coordinate system of Figs. 6-8, the quarter-chord of the airfoil is at $x/c = 0$ and CP is the wall pressure coefficient. The column of measured quantities contains: Rc the Reynolds number based on chord length, M the tunnel Mach number, α the geometrical angle of attack, CN, CX, and CM the normal force, axial force, and pitching moment coefficients obtained by balance measurements, A the cross-sectional area of the airfoil normalized by c^2, and c/h the chord to test section height ratio. In the column of computed quantities are: ΔM the Mach number correction, $\Delta\alpha$ the angle of attack correction, $c^*\partial\Delta M/\partial x$ and $c^*\partial\Delta\alpha/\partial x$ the variations of ΔM and $\Delta\alpha$ over the chord length, and M_{cor} and α_{cor} are the corrected values of M and α. The values CL_{cor}, CD_{cor}, and CM_{cor} are the corrected lift, drag, and pitching moment coefficients, obtained from the above corrections to stream quantities by standard techniques. The chordwise variations of ΔM and $\Delta\alpha$ are small in all three cases, indicating that the airfoil was tested in a reasonably uniform flow environment, corresponding to free air conditions at M_{cor} and α_{cor}.

The wall pressures in Fig. 6 were obtained with the airfoil at low incidence, in Fig. 7 at high incidence near CL_{max}, and in Fig. 8 in deep stall. The lift coefficients in Figs. 6 and 8 are nearly the same and so is the magnitude of wall pressure coefficients. However, contrary to the expectations from classical wall interference theory, the values of $\Delta\alpha$ differ markedly.

Figs. 9, 10, and 11 show the corrected and uncorrected CL vs. α curves, the drag polars, and the pitching moment polars respectively. The agreement between the lift coefficients obtained by the balance measurement and pressure integration in Fig. 9 is excellent. However, the correlation of drag polars in Fig. 10 is poor. It has been suggested in Ref. 12, that, unlike the wake drag which reflects only the viscous effects, the balance and pressure drags are subjects to inviscid forces which are due to the momentum transfer

through the test section boundaries.

Besides the analysis of drag forces on high angle of attack airfoils, the work at NAE is also continuing on extensions of the method of Ref. 11 to three-dimensional flows. Considered is the evaluation of wall interference corrections using the static pressure pipes attached to the test section floor and ceiling (two-rail arrangement) and also the additional pipes attached to the sidewalls (four-rail arrangement).

The task of developing a new type of a ventilated test section was undertaken in the Aerodynamics Laboratory of the Department of Mechanical Engineering at the University of British Columbia (UBC). A paper[13] at the seventh ICAS Congress described the unsatisfactory performance of the longitudinally slotted walls for high lift airfoil testing. Similarly to the case of perforated walls, one of the most disturbing features of slotted walls is the dependence of the theory on empirical factor which varies not only with the wall configuration, but also with the test model. Recently, more detailed studies of flow through slotted walls were published in Ref. 14 (Sweden) and Ref. 15 (U.S.A.).

The unsatisfactory empiricism of the longitudinally slotted and porous walls is a result of the partly separated flow through the walls. Therefore, it was proposed[16,17] to design a ventilated wall consisting of transverse slats, shaped as symmetrical airfoil sections, Fig. 12, which would operate within their unstalled incidence range. A singularity distribution method, such as the one described in Ref. 18, is a natural tool for studying the effects of different wall configurations. The boundary conditions to be satisfied are tangent flow on the solid wind tunnel wall, the airfoil wall slats, and the test airfoil, Kutta conditions at the trailing edges of all airfoil elements, and a free streamline pressure condition on the shear layer generated in the plenum. However, the potential flow calculations serve merely as a guide to a suitable wall configuration, which then has to be verified experimentally.

The reasons for using the transverse slotted wall on the suction side of the airfoil only are following:

(a) The pressure distribution on the pressure side of a high lift airfoil is dominated by stagnation pressure, see Figs. 2 and 3, and should undergo negligible change from free-air to tunnel conditions when the opposing wall is solid.

(b) On the suction side, the shear layer produced at the interface between the tunnel airflow and the stagnant plenum air enter the test section downstream of the model, see Fig. 13. If the other wall were slotted as well, the stagnant plenum air would be brought into the test section upstream of the model, and this air plus its bounding shear layer would degrade the test section flow near the airfoil.

(c) By analogy to the theoretical test section having one wall solid and the other formed by an open jet boundary, the angle of attack correction is expected to be minimized.

The last point brings us to the most important objective of this work, namely the development of a test section producing adequately low corrections to test data for a wide range of sizes, shapes and angles of attack of test airfoil. For many purposes "adequately low" would mean corrections of the order of 1% to pressure, force and moment coefficients, and it should be possible to maintain such low corrections for relatively large models at high angles of attack.

An experimental verification of the above test section concept was demonstrated in the 388 mm x 915 mm insert of the UBC low-speed closed-circuit wind tunnel. One wall was surrounded by plenum and could be fitted with airfoil shaped slats of NACA 0015 section and chords of 46 mm (small slats) or 92 mm (large slats), at zero incidence. A full range of wall open area ratios (OAR) could be tested. The test airfoils were mounted on the turntable of a six-component balance. Figure 14, adapted from Ref. 16, shows experimental values of the lift curve slope, m, (per degree) of NACA 0015 in the presence of walls having OAR = 0, 60, 70, and 80%. The results show a convergence toward a free air (c/h=0) lift curve slope value of 0.093/deg and indicate small corrections for all airfoil sizes in the range of OAR between 60% and 70%, in accordance with potential flow predictions.

This encouraging finding together with other experimental verifications in Refs. 16 and 17 is an indication that the described concept of the low-correction or "tolerant" test section could be a viable alternative to the far more complex concept of a "self-correcting" wind tunnel.

REFERENCES

1. Mavriplis, F., "Aerodynamic Research on High Lift Systems," Canadian Aeronautics and Space Journal, Vol. 17, 1971, pp. 175-183.

2. Mavriplis, F., "Aerodynamic Prediction and Design Methods of Aircraft High Lift Systems," Proceedings of the Aerodynamics Seminar of May 15, 1974, National Research Council of Canada, March 1975.

3. Choo, D.O., "Predicting Multi-Element Airfoil Flows," Contract #1SX78-00083, HITECH Canada Ltd./National Research Council Canada, Feb. 1980.

4. Mokry, M., "Calculation of Flow Past Multi-Component Airfoils in a Perforated Wind Tunnel,"C.A.S.I. Trans., Vol. 7, March 1974, pp. 19-24.

5. Mokry, M., "Influence Function Method in Wind Tunnel Wall Interference Problems," AGARD-CP-174, Proceedings of the AGARD Conference on Wind Tunnel Design and Testing Techniques, London, Oct. 1975, pp. 15.01-15.10.

6. Mokry, M., "Calculation of the Potential Flow Past Multi-Component Airfoils Using a Vortex Panel Method in the Complex Plane," Aero. Rept. LR-596, National Research Council Canada, Nov. 1978.

7. Chan, Y.Y., "Boundary Layer Development on Perforated Walls in Transonic Wind Tunnels," LTR-HA-47, National Aeronautical Establishment, National Research Council Canada, Feb. 1980.

8. Chan, Y.Y., "Compressible Turbulent Boundary Layer Computations Based on Extended Mixing Length Approach", C.A.S.I. Transactions, Vol. 5, March 1972, pp. 21-27.

9. Jacocks, J.L., "An Investigation of the Aerodynamic Characteristics of Ventilated Test Section Walls for Transonic Wind Tunnels," Dissertation, The University of Tennessee, Dec. 1976.

10. Capelier, C., Chevallier, J.-P., and Bouniol, F., "Nouvelle méthode de correction des effets de parois en courant plan," La Recherche Aérospatiale, Jan.-Feb. 1978, pp. 1-11.

11. Mokry, M. and Ohman, L.H., "Application of the Fast Fourier Transform to Two-Dimensional Wind Tunnel Wall Interference," Journal of Aircraft, Vol. 17, 1980, pp. 402-408.

12. Peake, D.J. and Bowker, A.J., "A Simple Streamwise Momentum Analysis to Indicate an Empirical Correction to Angle of Incidence in Two-Dimensional Transonic Flow, Due to a Perforated Floor and Ceiling of the Wind Tunnel," LTR-HA-11, National Aeronautical Establishment, National Research Council Canada, Jan. 1973.

13. Parkinson, G.V. and Lim, A.K., "On the Use of Slotted Walls in Two-Dimensional Testing of Low Speed Airfoils," Seventh ICAS Congress, Rome, 1970; C.A.S.I. Transactions, Vol. 4, Sept. 1971, pp. 81-87.

14. Berndt, S.B., "Inviscid Theory of Wall Interference in Slotted Test Sections," AIAA Journal, Vol. 15, Sept. 1977, pp. 1278-1287.

15. Everhart, J.L. and Barnwell, R.W., "A Parametric Experimental Study of the Slotted-Wall Boundary Condition," NASA Conference Publication 2045, Advanced Technology Airfoil Research, Hampton, March 1978, Vol. 1, pp. 459-471.

16. Williams, C.D. and Parkinson, G.V., "A Low-Correction Wall Configuration for Airfoil Testing," AGARD-CP-174, Proceedings of the AGARD Conference on Wind Tunnel Design and Testing Techniques, London, Oct. 1975, pp. 21.1-21.7.

17. Parkinson, G.V., Williams, C.D., and Malek, A., "Development of a Low-Correction Wind Tunnel Wall Configuration for Testing High Lift Airfoils," ICAS Proceedings 1978, Vol. 1, Lisbon 1978, pp. 355-360.

18. Kennedy, J.L. and Marsden, D.J., "Potential Flow Velocity Distribution on Multi-Component Airfoil Sections," Canadian Aeronautics and Space Journal, Vol. 22, 1976, pp. 243-256.

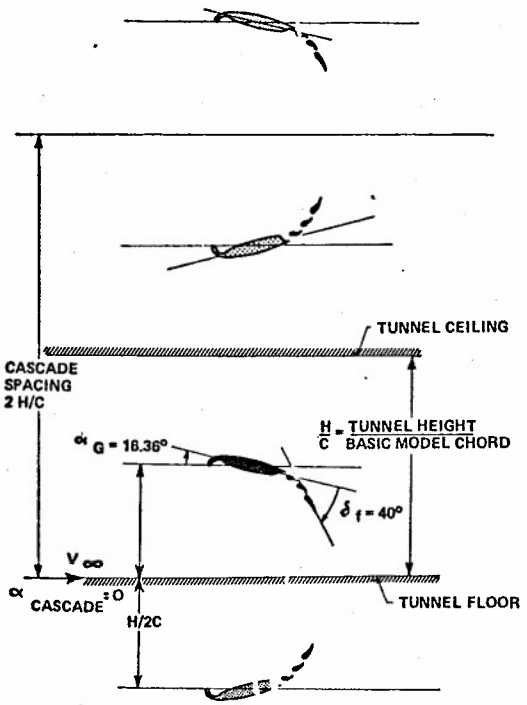

(Courtesy of F.Mavriplis,Ref.2)

Fig.1 Eight-element cascade system simulating a high lift airfoil between wind tunnel walls

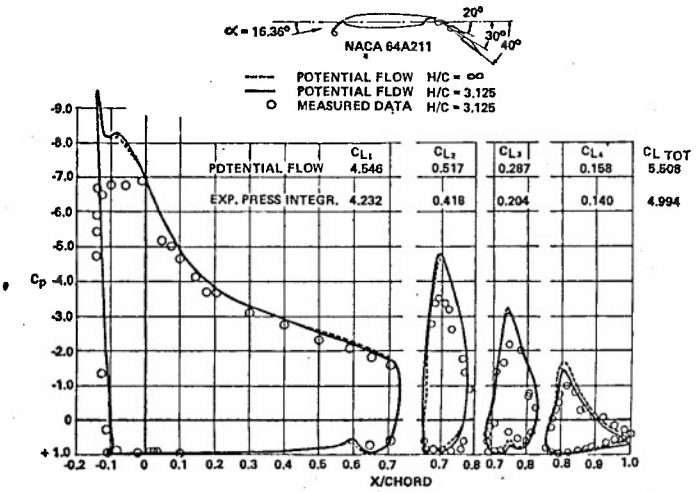

(Courtesy of F.Mavriplis,Ref.2)

Fig.2 Computed W.T. wall effect on pressure distribution and comparison with experimental data at $\delta_f = 40°$

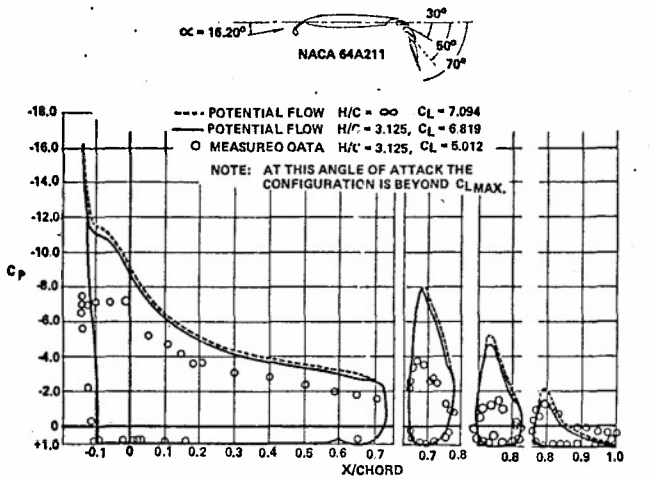

(Courtesy of F.Mavriplis,Ref.2)

Fig.3 Computed W.T. wall effect on pressure distribution and comparison with experimental data at $\delta_f = 70°$

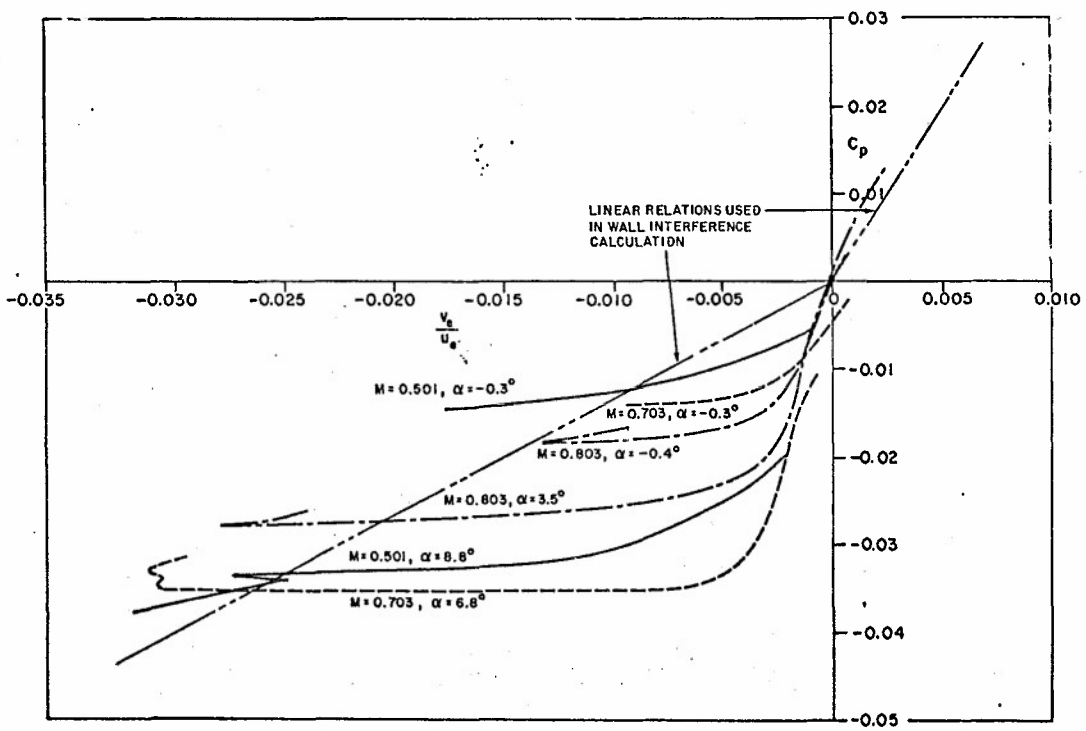

(Courtesy of Y.Y.Chan,Ref.7)

Fig.4 Normal velocities at the edge of the boundary layer as a function of pressure coefficient

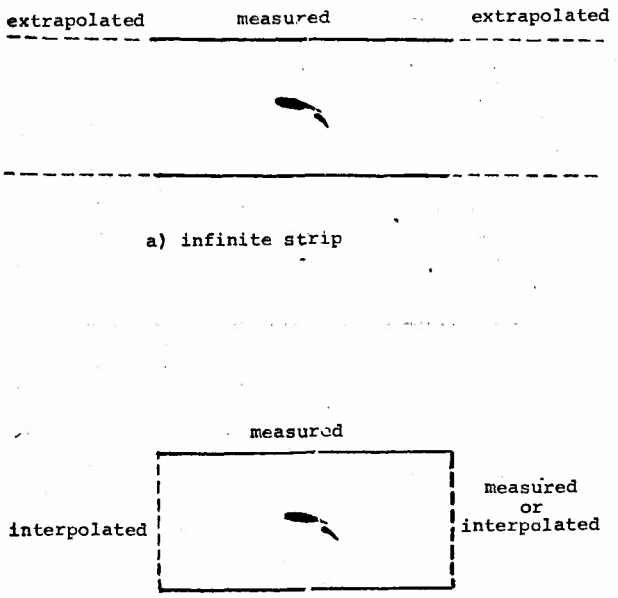

Fig.5 Determination of boundary pressures

	$\Delta M = -0.0047$
$Re = 2.13 \times 10^8$	$\Delta\alpha = -2.050^\circ$
$M = 0.2313$	$c \times \delta\Delta M/\delta x = 0.0004$
$\alpha = 0.130^\circ$	$c \times \delta\Delta\alpha/\delta x = -0.090^\circ$
$CN = 1.9924$	
$CX = 0.1532$	$M_{cor} = 0.2266$
$CM = -0.6354$	$\alpha_{cor} = -1.920^\circ$
$A = 0.1390$	$CL_{cor} = 2.0834$
$c/h = 0.2000$	$CD_{cor} = 0.0895$
	$CM_{cor} = -0.6621$

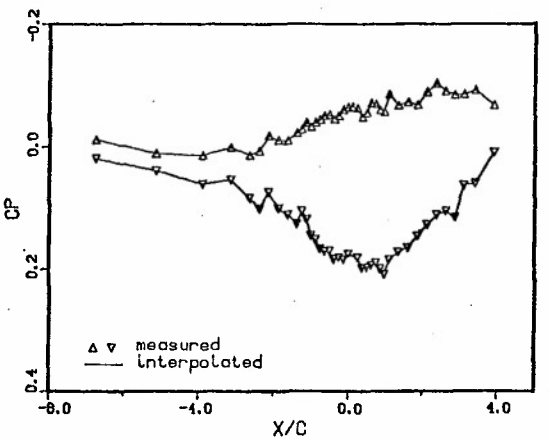

Fig.6 Measured wall pressures for a two-component airfoil at low lift. Wall corrections evaluated according to Ref.11

Rc = 2.13×10^6	ΔM = -0.0060
M = 0.2309	Δα = -3.314°
α = 16.948°	c×δΔM/δx = 0.0009
CN = 3.4136	c×δΔα/δx = -0.021°
CX = -0.6527	
CM = -0.5857	M_{cor} = 0.2249
R = 0.1390	α_{cor} = 13.634°
c/h = 0.2000	CL_{cor} = 3.6526
	CD_{cor} = 0.1781
	CM_{cor} = -0.6163

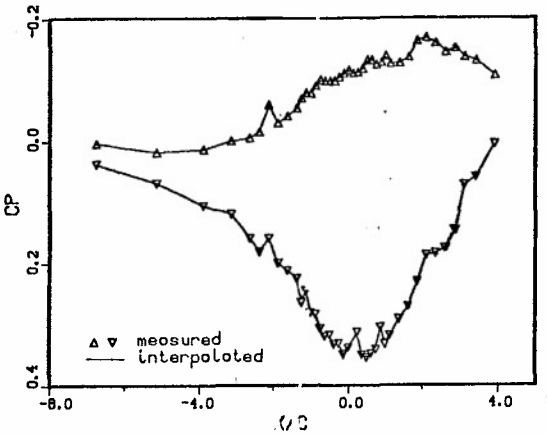

Fig.7 Measured wall pressures for a two-component airfoil near maximum lift. Wall corrections evaluated according to Ref.11

Rc = 2.13×10^6	ΔM = -0.0027
M = 0.2309	Δα = -1.280°
α = 18.902°	c×δΔM/δx = 0.0012
CN = 1.9855	c×δΔα/δx = 0.024°
CX = -0.1443	
CM = -0.4833	M_{cor} = 0.2283
R = 0.1390	α_{cor} = 17.622°
c/h = 0.2000	CL_{cor} = 1.9792
	CD_{cor} = 0.4728
	CM_{cor} = -0.4942

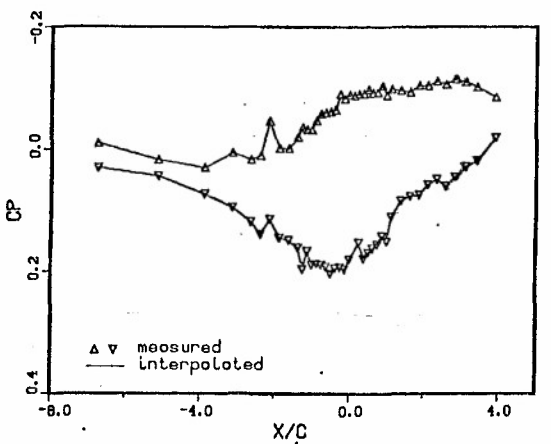

Fig.8 Measured wall pressures for a two-component airfoil in stall. Wall corrections evaluated according to Ref.11

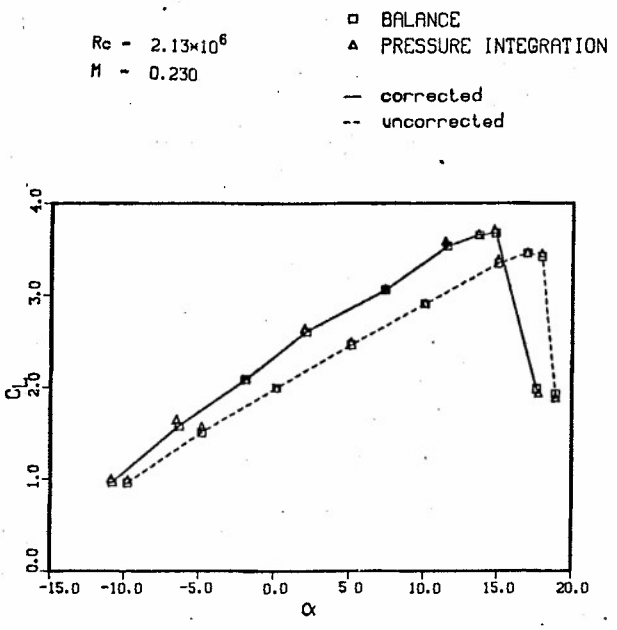

Fig.9 Corrected and uncorrected lift curves for a two-component airfoil

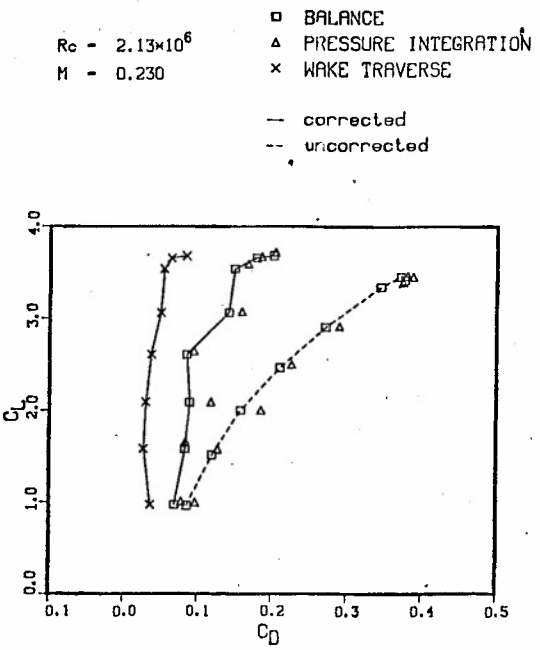

Fig.10 Corrected and uncorrected drag polars for a two-component airfoil

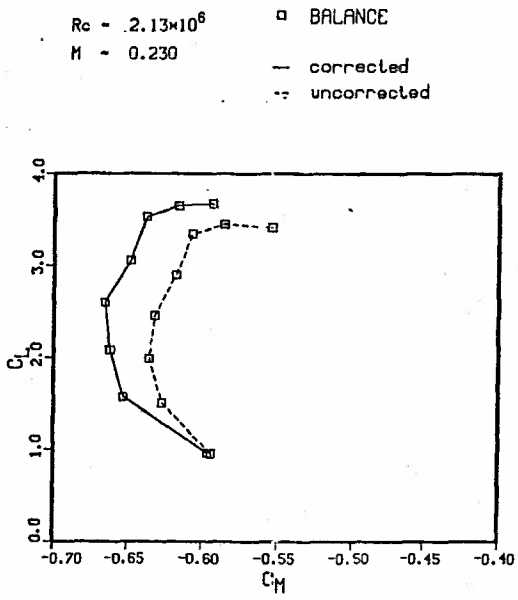

Fig.11 Corrected and uncorrected pitching moment polars for a two-component airfoil

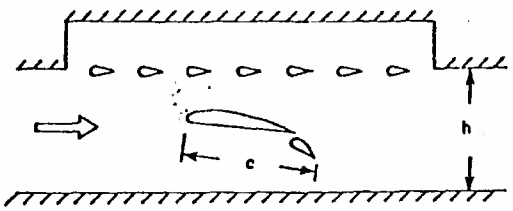

Fig.12 Schematic of the low correction test section (Adapted from Ref.17)

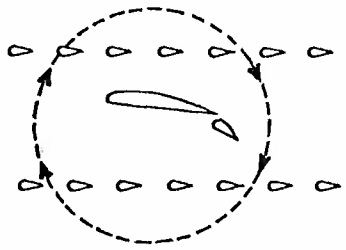

Fig.13 Illustrating the effect of airfoil circulation on flow through slotted walls

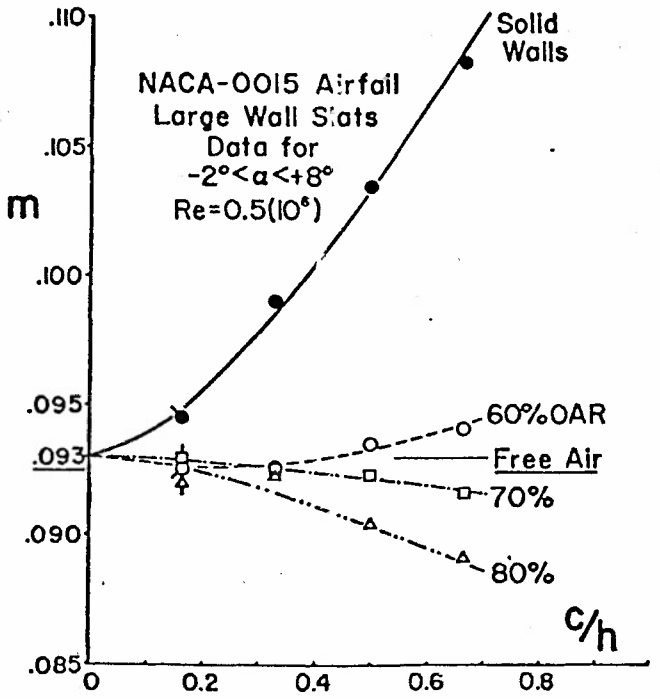

Fig.14 Effects of airfoil size and open area ratio of the slotted wall on the measured lift curve slope (Adapted from Ref.16)

A REVIEW OF THE "WALL PRESSURE SIGNATURE" AND OTHER TUNNEL CONSTRAINT CORRECTION METHODS FOR HIGH ANGLE-OF-ATTACK TESTS

by

J. E. Hackett
D. J. Wilsden
W. A. Stevens

Lockheed-Georgia Company, Marietta, Georgia, USA

Summary

Recent U. S. developments concerning correction techniques for high angle-of-attack testing are reviewed in general terms and the results are presented of a letter survey on the methods now in use. The majority of the paper concerns the determination of corrections from wall pressure measurements. The application of the "wall pressure signature" technique is demonstrated in experiments on several types of models. The method is shown to provide good estimates of tunnel blockage effects and extension to lift interference is discussed. It appears that correctability will be limited more by the problem of determining the effects of tunnel-induced velocity gradients than by our ability to determine the flow field. It is suggested that passive, boundary measurement technology will diffuse first into high angle-of-attack production testing, possibly followed by partially adaptive tunnel techniques.

1.0 Introduction

1.1 Overview

The present meeting concerns methods of correcting for wind tunnel constraint effects on models at high angle of-attack throughout the subsonic and transonic flight regime, including the effects of powered lift and directed thrust. These requirements are a substantial challenge to present-day and to evolving technologies so a review of all the relevant topics would be very comprehensive. An attempt will be made in this overview to at least mention most of the relevant topics, but the scope of the remainder of the paper will be more limited.

New approaches to correcting tunnel data for boundary interference have recently become practical as a result of continuing improvements in data acquisition and in both on- and off-line computing. Flow measurements at or near the tunnel boundaries can now be included as a starting point for tunnel correction procedures, rather than solely model-geometry as in the past. This avoids two problems: the need to estimate explicitly the effective aerodynamic shapes of models with separated flows and, in high speed tunnels, the theoretical difficulties which arise for ventilated test section walls which have differing inflow and outflow characteristics.

Correction for tunnel effects involves two stages which are not always distinguishable in traditional approaches. These are determination of tunnel-induced changes in flow field velocities and determination of consequent changes in surface pressure or force. Neither problem is easy but the first can at least be "self-contained" in the sense that interference velocities can be found independently of model measurements if conditions at the tunnel boundaries are determined.

Interference Flows

In solid-walled tunnels, pressure measurements at the tunnel surfaces may be used to determine singularity strengths which define the model envelope, including both regions of open or closed separation and the far-wake displacement surface. The degree of detail available in the model description is a function of the number and disposition of the tunnel surface measurements employed as boundary conditions to the problem. It will be seen in a later section of this paper that the number of measurements actually required is practical for modern data acquisition and reduction systems. Having determined the singularity strengths which represent the model envelope, image methods or their equivalent may be used to compute the interference flow field.

In porous or slotted-walled tunnels, the procedure is similar in principle but less straightforward in application. Normal velocities are now present at the tunnel boundaries and these must be measured. To avoid local effects near slots or holes in the tunnel surface, a control surface is usually defined a short distance inside the physical boundary. The experimental techniques are more difficult than before because the normal velocities are small. Pressure probes used to measure pitch angle are quite inconvenient and may lack the desired sensitivity. The use of the laser velocimeter has been suggested for flow measurements near the boundary.

The above methods are essentially extensions of traditional techniques. The important difference is that, rather than relying on known model geometry and "guesstimated" wake profiles, new more reliable information, i.e. measured boundary conditions, is employed to size and locate the singularities which describe the effective model/wake surface.

Effect at the Model

The fact that the interference flow field is calculable does not guarantee that its effects on the model will be. For simple attached flow cases surface pressure correction may be straightforward. Measured forces or moments may be also correctable, in moderate velocity gradients, though with somewhat less confidence. However, if tunnel-induced velocity gradients are large enough to modify the character of the model's viscous flows substantially, proper correction may be difficult or impossible. Little guidance can be derived from the literature concerning what constitutes an excessive interference gradient in this sense.

Even if the nature of the viscous effects is proper, moment correction (in particular) in high angle-of-attack tests may not be trivial. As pointed out by Heyson, each of the three moments involved in typical angle-of-attack plus yaw cases could be affected by one or more of the three spatial gradients of each velocity component. Though not all of the nine gradient terms may affect a particular moment, it is evident that careful thought and work is needed to produce an effective and reliable correction scheme.

The traditional solution to the above problem is to use models which are small in relation to tunnel cross section and accept the resulting small Reynolds number. This is the approach now being taken in testing models of fighters at high angles-of-attack. However, power simulation requirements frequently dictate the use of relatively large models, particularly in V/STOL tests. The continuing use of large, existing facilities for these tests indicates that there will be a continuing need for correction procedures for tests with high levels of interference.

Adaptive and Partially Adaptive Wind Tunnels

Adaptive wind tunnel technology has been developing steadily during the past decade. Here, the first, wall-sensing stage is the same as described above but the measured wall data are used to determine surface contour modifications or wall porosity changes which eliminate interference velocities within the test section. The technology is currently well advanced for two dimensional testing and the principles for extension to three dimensions are understood. However, the practical difficulties for three dimensional application are quite impressive. Even when these are overcome, there is a substantial body of opinion that no more than one or two such tunnels will be commissioned in the U. S. within the next decade. Nonetheless, such tunnels will be very valuable for providing "benchmark" test results for checking high angle-of-attack results from conventional tunnels.

A number of compromise solutions have been suggested which lie between the entirely passive and fully adaptive approaches. Some of these recognize that the principle problem concerns velocity gradients, since even gross tunnel-induced changes in mean angle-of-attack or speed cause little difficulty in applying corrections. Kemp has suggested the interesting concept of the "correctable" wind tunnel which is adaptive only to the degree that velocity gradients are removed. Once the mean interference velocities are determined in such a tunnel, completion of the correction process is likely to be trivial.

Another compromise solution, suggested by Joppa, is to employ a three-dimensional system which is adaptive only in the lifting direction. While this can remove longitudinal variations in angle-of-attack and blockage, the impact upon transverse gradients, which may also be significant, is unknown. One of the difficulties with such "mixed" systems is determining the residual corrections. The fact that the effective floor and roof contours are irregular in shape and change from data-point to data-point may limit the usefulness of this particular compromise.

Research along the traditional line of tailoring porous or slotted walls for minimum interference has also continued in recent years. Variation of porous wall open area and the use of "tailored" slots designed via recently developed methods are being pursued for tests on limited classes of models. This work, also, is relevant to high angle-of-attack testing, particularly if it can be combined with passive wall sensing schemes, since it is applicable to the present-day tunnels which will be the mainstay for production testing for a considerable time to come.

1.2 Literature and Letter Surveys

In preparation for the present paper literature and letter surveys were made on the subject of high angle-of-attack testing.

The literature survey involved both standard computer search techniques and personal follow-up. To keep the references within bounds the survey was restricted to U. S. work published after 1973: prior work may be found via AGARD CP 174 (1975) or AGARDograph 109 (1966). After eliminating papers not relevant to high angle-of-attack testing, about fifty remained which are categorized in the Reference section of this paper. Many of the References will not be cited directly; however, all were reviewed while preparing the present paper.

A survey letter was sent to appropriate personnel in nine aircraft companies, seven government agencies and four other organizations. Questions related to currently used test and correction methods and their shortcomings and to future plans. Opinions were solicited regarding computer applications and adaptive-wall tunnels. The replies showed an almost universal conversatism in the production testing community: models are made sufficiently small that corrections may be neglected or can be calculated conventionally. In most cases the techniques in use are backed by large- versus small-tunnel test comparisons. The exceptions to the "small model" philosophy concerned fighter testing (Reference 22) and automobile testing (Reference 8).

Peitzman, in Reference 22, describes an empirical approach which combines the standard "Pope"-type solid-plus-wake blockage correction method at low angles of attack with a "continuity" method at high angles. In the "continuity" method, a q-value is used which corresponds to uniform flow through a tunnel cross section reduced by the projected frontal area of the model. A linear combination of the two methods is used between 40- and 90-degrees. The method was applied to tests in a 7' x 10' tunnel involving two models of the YF17 having 1.05 ft. and 2.80 ft. span (.03- and .08-scale), wing planform areas of .45% and 3.2%, respectively of the tunnel cross sectional area and total planform areas of 0.9% and 6.4%. A blockage correction, to q, of approximately 14% was obtained at 90-degrees angle-of-attack for the larger model. Though the Reference 22 method worked well, it is empirical and the "continuity" method, in particular, is not well founded. Its use would be unwise without further correlation except for fighter configurations similar to the YF17 at small relative model size.

In Reference 8, Wilsden describes the application of the "wall pressure signature" method in automobile testing. This method is a developed version of that given in AGARD CP 174. The method is applied in tests upon production cars and vans in the Lockheed 16½ x 23½' wind tunnel in which model cross-sections of 5 to 10% of tunnel area are involved. Recent correlations and newer theoretical developments will be described in Section 2.

2.0 Recent Developments in the Lockheed "Wall Pressure Signature" Method

2.1 Introduction

Since its first appearance in Reference 24, the wall pressure signature method for blockage estimation has been refined in certain aspects, various new correlations have been performed and some progress has been made in the development of pressure and force correction procedures for nonuniform interference flows. These developments are described in detail in Reference 26 and will be reviewed in subsection 2.2. Recently, a new, non-iterative approach to wall signature analysis has been developed which is more rapid and more flexible than the original method. The same principles have been applied in pilot studies regarding the determination of tunnel-induced upwash for lifting models. These new developments will be described in subsection 2.3. As a point of departure, the remainder of this subsection will describe the general approach and its relationship to other methods.

Outline of Blockage Estimation Method

In a typical experiment (Figure 1) wall pressures are measured along the centerlines of the tunnel walls or roof. If lift is present, the mean of corresponding floor and roof pressures can be taken or sidewall pressures are used to determine souce and sink strengths, spans, and locations on the tunnel centerline (Figure 2) which define an effective body which corresponds to the displacement surface of the test model and its wake.

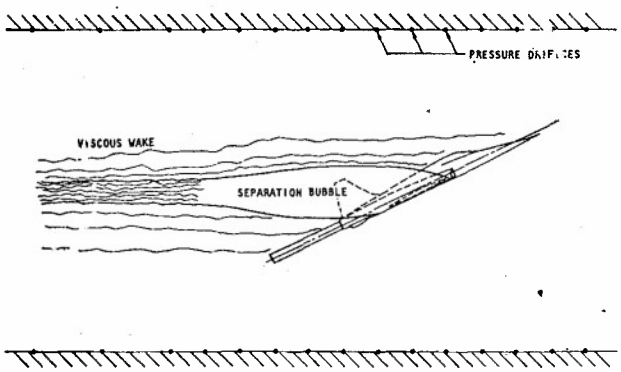

FIGURE 1 DETERMINATION OF WALL PRESSURE SIGNATURE IN A TYPICAL CASE.

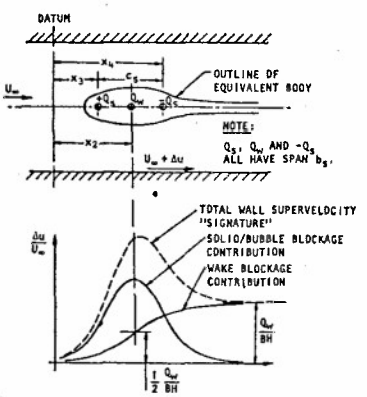

FIGURE 2 EFFECTS, AT A WIND TUNNEL WALL, OF SOLID/BUBBLE AND OF VISCOUS WAKE BLOCKAGE.

A typical wall supervelocity signature for a separated flow case (Figure 2, lower) includes a velocity peak, just aft of the model, which reflects the presence of the expanding separation bubble which closes further downstream leaving a viscous wake. The asymptote downstream is a result of the displacement thickness of this wake.

For analysis, the measured profile is resolved into symmetric and anti-symmetric parts, as shown in the lower part of Figure 2. This simplifies the subsequent steps since the symmetric part corresponds to solid/bubble blockage and the anti-symmetric part reflects wake blockage. Resolution of these components from the measured signature is achieved via an iterative procedure.

The wake blockage parameters, Q_w and x_2, emerge directly from the wake signature analysis. However, to obtain the solid blockage parameters Q_s and c_s, a chart look-up technique is employed as illustrated in Figure 3. Preparation of the working charts is discussed in References 24 and 25. Inputs to the charts are now the symmetric part peak height $(\Delta u/U)_{max}$ and half width at half peak height, $\Delta x/B$, from the resolved signature, together with the source and sink span (b_s/B) which is estimated from model geometry.

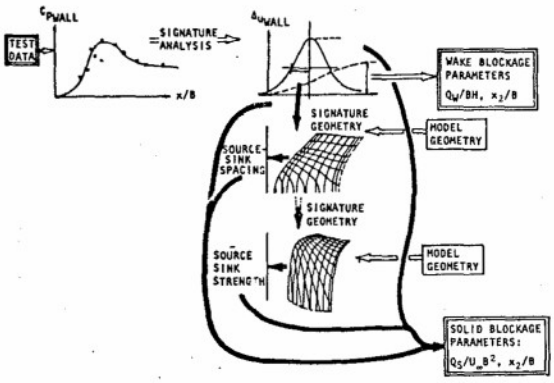

FIGURE 3 DETERMINATION OF SOLID/BUBBLE AND WAKE BLOCKAGE PARAMETERS FROM A WALL PRESSURE SIGNATURE

In essence, the above analysis is an engineering solution of a set of algebraic equations involving five nonlinear terms (source and sink spans and locations) and two linear terms (source and sink strengths). Multiple solutions are possible and it is necessary to demonstrate that appropriate roots are obtained by the above procedure. Reference 25 describes a Lockheed study using a nonlinear solver algorithm which accepts sets of seven wall pressures as inputs and returns as roots the seven aerodynamic variables. The program was provided with an initial guess of the roots and on varying the guess converged to differing roots. It was established that the source/sink strengths were "hard" variables (i.e., lead to closely spaced roots) and their streamwise locations were "soft". The table to the right of Figure 4 shows a number of sets of roots obtained for a normal-plate experiment. The left part of the figure shows that the corresponding distribution of interference velocity at the tunnel centerline was affected very little. The chart method produces solutions very close to those from the nonlinear analysis.

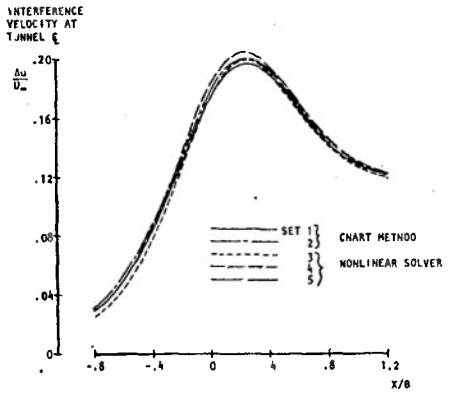

SET #	$\frac{Q_S}{U_\infty}$	$\frac{Q_W}{U_\infty}$	$\frac{x_2}{B}$	$\frac{x_3}{B}$	$\frac{x_4}{B}$	$\frac{b_2}{B}$	$\frac{b_{3,4}}{B}$	COMMENTS
1	96	42	.11	-.21	.44	.05	.05	b_S = .05B CHART METHOD
2	93	42	.11	-.25	.46	.30	.30	b_S = .30B
3	113	42	.03	-.12	.38	.30	.35	
4	121	42	.29	-.18	.43	.30	.45	NONLINEAR SOLVER.
5	121	44	.59	-.18	.51	.30	.45	

FIGURE 4 THE NATURE AND CONSEQUENCES OF MULTIPLE SOLUTIONS TO THE WALL PRESSURE INVERSE PROBLEM (NORMAL PLATE S/C = 9.5%).

Calculated Flows

Interference effects may be calculated anywhere in the test section by the wall pressure signature method. Figure 5 shows incremental pressure coefficients, at four tunnel cross sections, induced by the image system for a large sphere and its wake at a subcritical Reynolds number. The corresponding supervelocities on the tunnel centerline increase from 7.5% at the front of the sphere to 9.8% at its maximum diameter and rise to 11.3% and 11.2% at planes C and D due to the expanding separation bubble. Interference velocity decreases downstream of C as the separation bubble closes.

Though axial variation is very marked, the lower part of Figure 5 shows that the percentage variations at any one cross section are not large – particularly in the region occupied by the model. It may be inferred from continuity considerations that the blockage-induced lateral velocities are also small. This is confirmed by calculation.

It is sometimes instructive to calculate streamlines for the effective body corresponding to the source, source, sink solution. Figure 6 shows some body shapes for a 15-inch sphere and a 9-inch normal disc tested in a 30- by 43-inch wind tunnel. Considering that only three point singularities are used, the effective shapes blend with the model outlines very well. As is evident from Figures 5(a) and 5(b), the change in wake character through sphere transition Reynolds number is well depicted. It is interesting to note that the subcritical wake occupies 24.9% of the tunnel cross-section, at maximum diameter, compared with 13.7% for the model itself. Generally similar results are obtained for a circular disc mounted normally to the flow [Figure 5(c)]. The calculated body diameter at the model station approximates the disc diameter very closely.

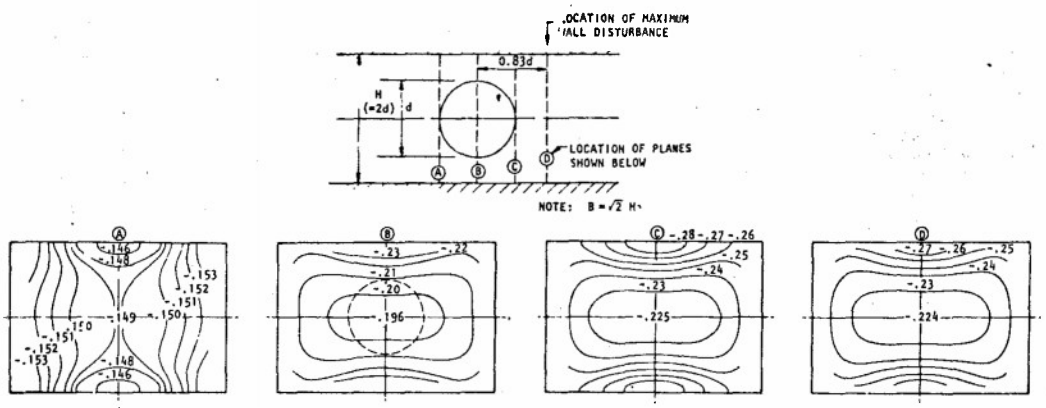

FIGURE 5 DISTRIBUTION OF BLOCKAGE-INOUCED PRESSURE COEFFICIENTS, ACROSS THE TUNNEL CROSS-SECTION, FOR A LARGE SUBCRITICAL SPHERE (S/C = 13.7%).

In the subcritical case (Figure 5), the calculated wake occupies a substantial proportion of the tunnel area and it appears likely that interference will distort it. To estimate the magnitude of the change, body shapes were calculated with and without interference velocity increments. It was found that the change in shape, due to the tunnel, was almost too small to draw separately (see Reference 26). As the model is very large compared with those used for routine tests, it appears that blockage-induced distortion of separation bubbles may not be a limiting factor.

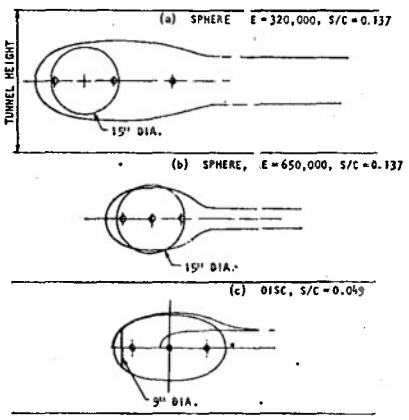

FIGURE 6 EFFECTIVE BODY SHAPES IN 30" x 42" TUNNEL.

Comparisons With Other Methods

Blockage correction methods fall broadly into two classes, requiring geometric or geometric plus measured tunnel data, respectively. In the absence of pressure data from the tunnel, aerodynamic estimates have to be made which are often conjectural. Figure 7 shows a comparison between results from five blockage estimation methods applied to bluff models, using data taken largely from Reference 8. The "free air" data, in the last column, is derived either from sub-scale models (for the idealized sedan) or correspond to accepted values for the idealized shapes (sphere and normal plate).

	AREA RATIO METHOD	THOM	MENSEL	MASKELL	WALL PRESSURE SIGNATURE	FREE AIR DATA
IDEALIZED SEDAN S/C = 5.65%	-2.8%	-7.4%	-7.2%	-9.6%	-8.9%	-9.0%
VAN S/C = 10.16%	-5.1%	-22.1%	-20.3%	--	-22.9%	--
SUBCRITICAL SPHERE S/C = 13.7%	-7.0%	-13.4%	-17.9%	-27+ -32%	-29.3%	-30.0%
NORMAL FLAT PLATE S/C = 16.7%	-9.0%	-19.0%	-27.0%	-52.0%	-47.0%	-45.5%

FIGURE 7 BLOCKAGE CORRECTIONS TO ORAG COEFFICIENT BY VARIOUS METHODS.

It is evident that the two geometric methods give lower blockage estimates than two of the three methods employing tunnel measurements. Hensel's method, published in 1951 (Reference 23) relies upon the wall pressure measurement as does the present wall-pressure signature method. However, it has been found that use of pressures "opposite to the model location" as recommended by Hensel leads to uncertainty, since strong pressure gradients are usually present at this location (see Figure 4). Hensel's method has been revised recently, in a pilot study at Lockheed, to use the entire pressure signature. Another feature of the Hensel method is that it uses doublets to model the flow. This renders the method less flexible than the wall pressure signature method, which permits variable source-sink spacing. This can be important for long models or models with thick wakes. Corrections via the Hensel method are generally lower than by wall pressure signature method – noticeably so in the case of the sphere in Figure 7.

Maskell's method determines dynamic pressure correction from an empirical relationship involving measured drag or, in a variant of the method, measured drag in combination with base pressure. Maskell shows that the drag coefficient is proportional to base pressure, for square plates, and notes that non-square plates exhibit varying base pressure across their span. In the equation* $\Delta q/q = \eta C_D\, S/C$, η is assigned tabulated values which vary from 2.77 to 2.13 for plate aspect ratios in the range 1 to 10. Maskell's method is fundamentally based and gives good results for normal flat plates. However, in other applications, determination of base pressure for direct use in the method may be questionable not only because of aspect ratio effects, but also if vortex separation exist in the vicinity of the separation bubble. If the tabulated values of η are used, there may be practical difficulties in distinguishing bubble drag from other drag components or in estimating the aspect ratio of the separation bubble. Though Maskell asserts that an η value of 2.5 ± 0.25 is reasonably accurate in situations where q-corrections are of order 10%, the spread in estimated corrections becomes unacceptable for large models (see Figure 7).

It has been noted already that the wall pressure signature method may be regarded as an extension or generalization of the Hensel method. It may also be shown that the present method, when implemented in its original form (Ref. 24) exactly parallels Maskell's approach while avoiding both base pressure measurements and estimation of η. The relationship between the two methods is examined further in Reference 26.

2.2 Correction of Pressures and Forces

Having determined the spatial distribution of the three components of interference velocity, as described above, the correction process is completed by determining their effects upon the test model. This presents as great a challenge as determining the interference velocities themselves, and our ability to obtain reliable, accurate corrections depends upon the amount of detailed aerodynamic data available from the model.

Surface Pressures

It is demonstrated in Reference 26 that surface pressure measurements may be corrected successfully for blockage by applying x-dependent interference velocity ratios to local surface velocities and then recalculating C_p. It is shown that it is unnecessary to consider transverse velocities, even for large models, but it is essential to ratio the surface velocities since simple superposition implies velocity vectors which violate local tangency conditions at the model surface. The corresponding surface pressure correction equation is

$$C_{p_c}(x) = \frac{C_{p_u}(x) - 1}{\left(1 + \frac{\Delta u(x)}{U_\infty}\right)^2} - 1.$$

Figure 8 shows pressures measured on the surface of the 15-inch sphere in a 30" x 43" wind tunnel, designated C_{p_U} and in a 16½' x 23½' wind tunnel, designated C_{p_∞}. Blockage increases both the peak and the wake suctions significantly in the small tunnel. Correction via the above equation leads to good correlations except that large tunnel peak suctions are slightly higher.

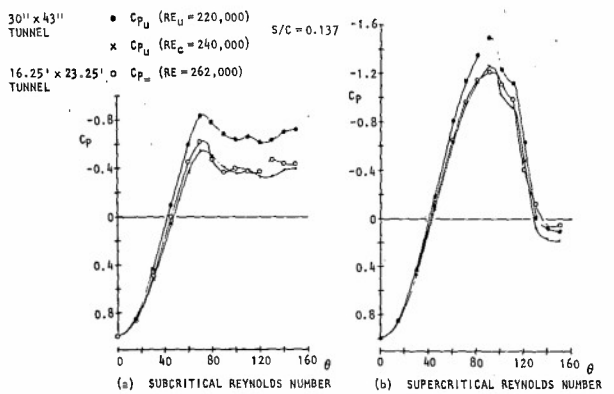

FIGURE 8 APPLICATION OF BLOCKAGE CORRECTIONS TO SPHERE SURFACE PRESSURE MEASUREMENTS.

To avoid confusion with blockage velocity ratio, Maskell's ϵ has been replaced by η.

Similar tests encompassing the transitional Reynolds number, reported in Reference 26, lead to the conclusion that use of the above correction equation gives corrected small tunnel data which are comparable with and no less credible than results from similar tests in the large tunnel. In correcting Reynolds number, the interference velocity ratio calculated at the peak suction location was employed. Model center values were a reasonable approximation to this.

Force Corrections

It is possible in principle to determine force corrections from the pressure corrections indicated above. However, this is frequently impractical and alternative means are needed which are less detailed but which reflect interference gradient effects properly. To correct spatially-distributed loads for spatially-distributed interference effects, two general approaches may be considered, based respectively upon test model properties or measurements and upon fundamental results for a theoretical flow model derived from wall pressures and other data.

If a good analytic counterpart to the test configuration exists, this may be used in dividing measured total loads between the model's components, prior to correcting them. Measured pressures may also be used in this procedure. In the absence of these options, it may be necessary to instrument a model to measure those component loads which cannot be estimated confidently. (In multi-tunnel tests on a NASA fan-in-wing model, for example, a metric tailplane was used and a particular division of loads between the wing surface and the embedded fans was assumed.) Next, the sensitivity of each component to changes in dynamic pressure or angle-of-attack must be estimated. This will generally be straightforward for dynamic pressure changes but will involve uncertainties with regard to angle of attack. Finally, the various effects are summed and used to correct the measured loads.

The source, source, sink blockage flow model, or its lifting counterpart, may be used in principle not only to estimate the interference flow field, but also for estimating the corresponding force and moment changes. So far, this general approach has been applied only to the evaluation of "horizontal buoyancy" drag. This analysis will be used to illustrate the principles involved.

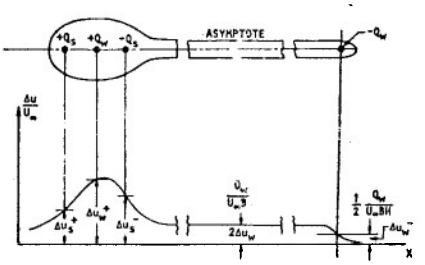

FIGURE 9 FLOW MODEL FOR BLOCKAGE ESTIMATION

As was seen previously, each source, source, sink combination determined from wall pressures may be used to generate an effective body with a defined area distribution and with defined pressures on its surface. In principle, the body shape, its free-air surface pressures and the tunnel-induced increments could be calculated, the pressure correction could be applied, and appropriate integrations could be performed to determine the corresponding drag increments. However, the same result is obtained much more easily by considering the drag of the sources and sinks themselves. Using the notation shown in Figure 9, this gives, for the forward body

$$\Delta D_{MODEL} = \rho(-\Delta u_s^+ Q_s - \Delta u_w^+ Q_w + \Delta u_s^- Q_s)$$

Recognizing that the whole-body, potential-flow drag on the body sketched in Figure 9 is zero, we may write alternatively

$$\Delta D_{MODEL} = -\rho\, u_w^- Q_w$$

Substituting $u_w^- = \frac{1}{2}(Q_w/BH)$ and nondimensionalizing yields

$$\Delta C_D = -\frac{BH}{S}\left[\frac{Q_w}{U_\infty BH}\right]^2$$

where BH represents tunnel area. The above horizontal buoyancy correction is combined with the dynamic pressure correction to give

$$C_{D_c} = \frac{C_{D_u} + \Delta C_D}{(1 + \epsilon_M)^2}$$

where ϵ_M is the value of $\Delta u/U_\infty$ at the model location.

Application of the above equation to the flat plate data analyzed in Reference 24 gave very similar but slightly smaller corrections compared with those calculated by the older method. The normal flat plate drag coefficient which resulted was 1.20, slightly greater than Hoerner's quoted value. Figure 10 shows new data, for a family of floor-mounted rectangular flat plates. For W4, the largest plate, the uncorrected drag coefficient is almost double the corrected value and the deviation of this point from the earlier trend is probably significant. However, it appears that the above method can be applied successfully to models having C_{D_o} S/C values of at least 0.12 and highly separated flows.

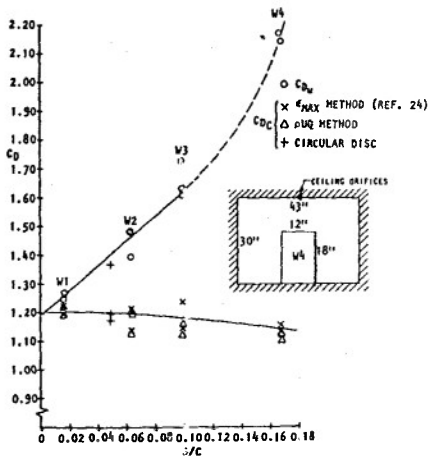

FIGURE 10 DRAG OF RECTANGULAR PLATES IN THE 30" x 43" TUNNEL.

The same rectangular models were tested as flat-plate wings which, being mounted from the floor as shown in Figure 10, had a whole wing aspect ratio of 3. Angle-of-attack corrections, determined via standard methods, were generally less than one degree. The results are shown in Figure 11.

Despite the very large size of wing W4 (circles) and despite the presence of an uncontrolled boundary layer on the tunnel floor, the lift correlation between the four models is excellent over the linear $C_L - \alpha$ range. There was a tendency for smaller models to stall earlier, which was probably due to the greater adverse influence of the floor boundary layer. The lift curve slope is about 10% greater than that given by simple wing theory; probably on account of lift from edge vortices at the wing tip. The largest wing gave the best overall result and was the least affected by the uncontrolled floor boundary layer which degraded the drag correlation somewhat in the linear-C_L range (see Reference 26).

Figure 12 extends the lift and drag data to 90-degrees angle of attack, i.e. the normal flat plate case. Uncorrected data are also shown for the largest plate. The correlation between models remains good except in the immediate post-stall region. Here, it appears that the floor boundary layer again had an adverse effect on the smaller models, this time in delaying the approach to the second lift peak.

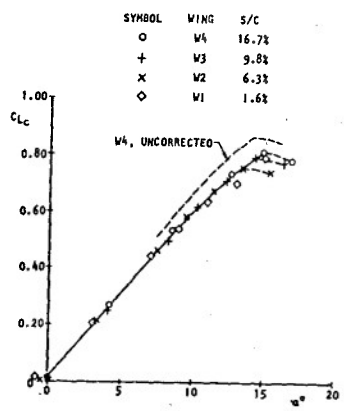

FIGURE 11 LIFT CORRELATION FOR FOUR AR-3 FLAT PLATE WINGS.

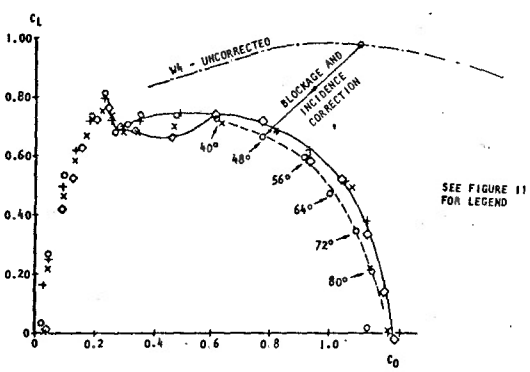

FIGURE 12 DRAG POLAR FOR AR-3 FLAT PLATE WINGS AT HIGH ANGLES OF ATTACK.

The above results show that the combined blockage and conventional angle-of-attack corrections produce good results for large wings, including one for which C_L S/C was 0.134. In the presence of a floor boundary layer, the largest semi-span model gave the best results. Similar force studies on spheres yielded less conclusive results due to hysteresis and other test difficulties described in Reference 26. However, it was concluded that the corrected small tunnel drag data were no less credible than those measured in the large tunnel.

2.3 Reformulation and Matrix Solution

The wall pressure signature method, described above, is now being used at the Lockheed-Georgia 16½ x 23½-foot wind tunnel, and is also being implemented at other tunnels in the U.S. In the period from 1975 to 1978 the method was refined as described above and the run time per data point was reduced from about 30 seconds to 3 seconds on a late '60's vintage computer (CDC 1700). Nonetheless the computation time was considered excessive for on-line applications in a 'production' wind tunnel.

In setting up the source, source, sink blockage model for the present wall pressure signature program, a decision was made to accept the difficulty of determining unknown source positions in exchange for better physical insight and the ability to implement the procedure in chart form. However the need for faster operation and for an additional, angle-of-attack correction capability has lead to a study of a different method which employs multiple singularities at fixed positions. This approach is inherently faster because wall influence matrices, their inverses and centerline interference matrices can be precalculated and used non-iteratively. In view of previous experience the revised techniques have been applied first to the blockage problem (see below). Significant improvements in run time have been achieved, but the new method is neither well enough understood, nor correlated sufficiently to be considered yet as a substitute for the present approach.

A welcome consequence of the matrix approach, when applied to angle-of-attack correction is that an estimate is obtained of the axial distribution of loads. This may provide at least a partial solution to the problem mentioned in Subsection 2.2, of loads assignment during blockage correction. It remains to be seen how this will work out in practice.

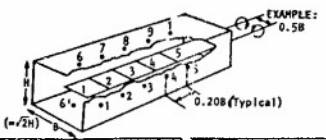

Location	Source Coefficients					Vortex Coefficients				
	1	2	3	4	5	1	2	3	4	5
SIDEWALL 1	0.5000	0.1440	0.0388	0.0115	0.0033	+.4033	+.2016	+.0895	+.0379	+.0154
SIDEWALL 2	0.8560	0.5000	0.1440	0.0388	0.0115	+.6052	+.4033	+.2016	+.0895	+.0379
SIDEWALL 3	0.9611	0.8560	0.5000	0.1440	0.0388	+.7160	+.6052	+.4033	+.2016	+.0895
SIDEWALL 4	0.9885	0.9611	0.8560	0.5000	0.1440	+.7691	+.7160	+.6052	+.4033	+.2016
SIDEWALL 5	0.9967	0.9885	0.9611	0.8560	0.5000	.7939	+.7691	+.7160	+.6052	+.4033
ROOF 6	0.5000	0.0832	-.0081	-.0082	-.0034	0.41.3	0.2755	0.1176	0.0458	0.0175
ROOF 7	0.9168	0.5000	0.0832	-.0081	-.0082	0.2755	0.4113	0.2755	0.1176	0.0458
ROOF 8	1.0081	0.9168	0.5000	0.0832	-.0081	0.1176	0.2755	0.4113	0.2755	0.1176
ROOF 9	1.0082	1.0081	0.9168	0.5000	0.0832	0.0458	0.1176	0.2755	0.4113	0.2755
ROOF 10	1.0034	1.0082	1.0081	0.9168	0.5000	0.0175	0.0458	0.1176	0.2755	0.4113
FLOOR 6'	0.5000	0.0832	-.0081	-.0082	-.0034	-.4113	-.2755	-.1176	-.0458	-.0175
FLOOR 7'	0.9168	0.5000	0.0832	-.0081	-.0082	-.2755	-.4113	-.2755	-.1176	-.0458
FLOOR 8'	1.0081	0.9168	0.5000	0.0832	-.0081	-.1176	-.2755	-.4113	-.2755	-.1176
FLOOR 9'	1.0082	1.0081	0.9168	0.5000	0.0832	-.0458	-.1176	-.2755	-.4113	-.2755
FLOOR 10'	1.0034	1.0082	1.0081	0.9168	0.5000	-.0175	-.0458	-.1176	-.2755	-.4113

FIGURE 13 INFLUENCE MATRICES FOR SOURCE AND VORTEX ARRAYS.

Influence Matrices for Source and Vortex Arrays

Figure 13 shows example influence coefficient matrices for line source and horseshoe vortex arrays for a rectangular tunnel having $\sqrt{2}$ width-to-height ratio. All of the coefficients correspond to axial velocity increments except the influence of the horseshoe vortex system at the sidewall surface, which is of course a vertical velocity, as indicated in the table. Source coefficients are normalized upon mainstream velocity and tunnel area; vortex coefficients are normalized upon mainstream velocity and the square root of tunnel area. At a given point, the roof and floor coefficients have like signs for sources but opposite signs for the vortex array: angle-of-attack and blockage effects can therefore be separated readily by considering the sum and difference velocities from corresponding locations on the tunnel roof and floor.

There is no theoretical need to use sidewall pressures, in fact, we shall see that there are reasons not to. In practice and particularly in large tunnels, the use of floor instrumentation is undesirable on account of susceptibility to damage and complications related to turntables and model supports. From this viewpoint the combined use of sidewall and roof static pressures is preferable. Measurement of sidewall vertical velocities is undesirable because of the potential for damage to pitch probes, and because of possible errors arising from trailing vortex drift.

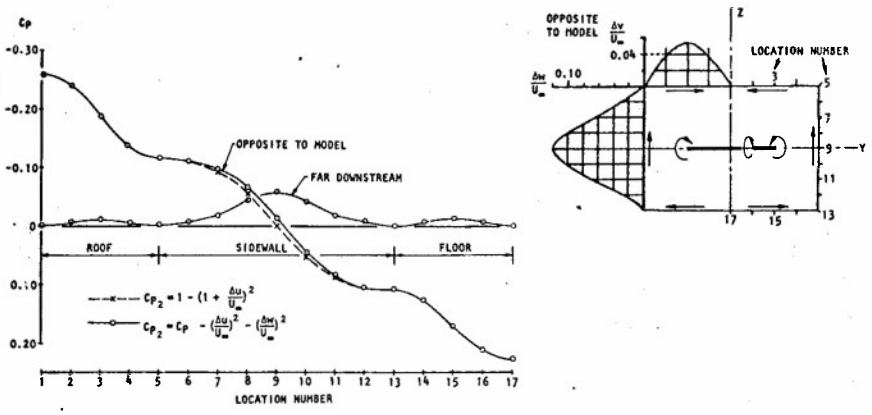

FIGURE 14 TUNNEL SURFACE PRESSURES FOR A HORSESHOE VORTEX, ($C_L/AR = 1.0$)

Figure 14 shows an example of the distribution of surface pressures induced by a horseshoe vortex. This vortex spans 50% of the tunnel width and has strength corresponding to unit (C_L/AR). The corresponding $C_{L_{hb}}$ value of $\sqrt{2}$ is well within the limit for tunnel flow breakdown. At mid-sidewall the vertical velocity opposite to the model is approximately 12% of mainstream (see inset). This causes a sidewall suction C_p of about 0.015. However, far downstream the suction is four times this. This would have the effect of reducing slightly the vortex strength returned by a Δu-dependent procedure and increasing the apparent wake source strength. Because of the nature of the C_p equation, correction for this effect must be retrospective and a second pass through the analysis may be needed when wall signatures are used in high lift tests.

Application of the Matrix Method

In essence, the source influence matrices (Figure 13) comprise a 0.5000 term at every location, associated with a downstream sink, superposed upon an antisymmetric array representing the effects of the local sources. Both constituent matrices are singular but their sum is not. The left side of Figure 15 shows a tunnel roof influence matrix (upper array), its inverse (middle) and the inverse times a center-tunnel influence matrix (lower array). The middle array is used to determine source strengths from an experimental, roof Δu, blockage signature. The combined array in the lower block is used to determine centerline interference directly from the roof signature.

It is evident from Figure 15 that the source inverse matrix has alternating signs, is poorly damped and has large elements below the leading diagonal. In application to a 'noisy' experimental signature, a strongly-varying, alternating-sign source array can be anticipated. The upper part of Figure 16 confirms this. For this example three wall signatures were computed for source, source, sink arrays at 0.18 spacing, using source and sink spans b/B of 0.30, 0.50 and 0.70. When these were input to an influence matrix corresponding to a 0.50-span case the source arrays depicted in the upper part of Figure 16 were obtained. Checks showed that, in every case, the input wall signature was properly matched by the solution. For the 0.5-span case the original source strengths were properly returned.

	SOURCE-SINK SYSTEM					HORSESHOE VORTEX SYSTEM				
$A_{R/F}$	0.5000	0.0832	-.0081	-.0082	-.0034	0.4113	0.2755	0.1176	0.0458	0.0175
	0.9168	0.5000	0.0832	-.0081	-.0082	0.2755	0.4113	0.2755	0.1176	0.0458
	1.0081	0.9168	0.5000	0.0832	-.0081	0.1176	0.2755	0.4113	0.2755	0.1176
	1.0082	1.0081	0.9168	0.5000	0.0832	0.0458	0.1176	0.2755	0.4113	0.2755
	1.0034	1.0082	1.0081	0.9168	0.5000	0.0175	0.0458	0.1176	0.2755	0.4113
$A^{-1}_{R/F}$	+3.295	-0.947	+0.231	-0.028	+0.015	+4.915	-4.470	+2.066	-0.818	+0.246
	-7.507	+5.422	-1.434	+0.254	-0.028	-4.470	+8.968	-6.308	+2.707	-0.818
	+8.630	-9.931	+5.956	-1.434	+0.231	+2.066	-6.308	+9.700	-6.308	+2.066
	-8.426	10.590	-9.931	+5.422	-0.947	-0.818	+2.707	-6.308	+8.968	-4.470
	+6.576	-8.426	+8.630	-7.507	+3.295	+0.246	-0.818	+2.066	-4.470	+4.915
$A^{-1}_{R/F} * A_C$	+0.398	+0.116	+0.228	-0.131	+0.181	+0.409	+0.173	-0.151	+0.079	-0.056
	-6.855	+3.254	-0.165	-0.128	+0.273	-1.391	+2.049	-0.750	+0.187	-0.072
	+4.725	-6.216	+3.466	-0.743	+0.493	-0.165	-0.145	+0.948	-0.206	-0.049
	-9.653	+8.663	-5.958	+2.201	+0.429	-1.011	+1.940	-1.596	+1.507	-0.354
	+3.997	-7.672	+8.045	-6.080	+2.819	-0.763	+1.079	+0.218	-0.523	+0.701

FIGURE 15 APPLICATION OF INFLUENCE MATRICES.

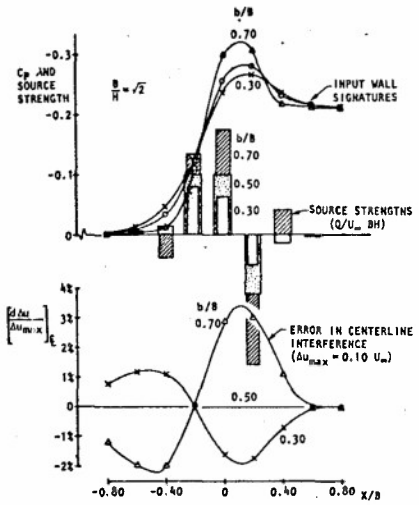

FIGURE 16 BLOCKAGE SOLUTION: SENSITIVITY TO SPAN EFFECTS (CONSTANT MATRIX, $C_{D_o}(S/C) = 0.20$).

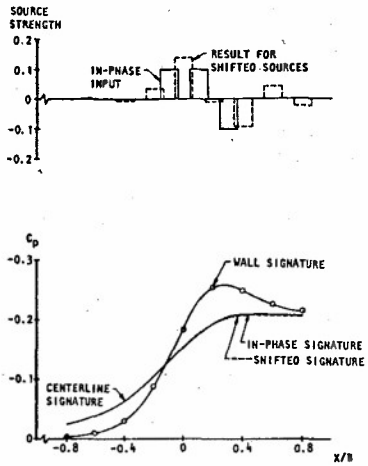

FIGURE 17 EFFECT OF SOURCE-SINK PHASE ON MATRIX METHOD RESULTS, B = 0.60 B

The lower part of Figure 16 shows that, despite the large errors in source and sink strengths, the distributions at the centerline deviated surprisingly little from the correct, 0.5-span, signature. This is encouraging and indicates that even quite major errors in source span estimation may not have serious repercussions. Figure 17 shows the results of a similar exercise, with the source array misphased relative to the source which generated the "experimental" signature. Misphasing had almost no effect on calculated interference.

To explore the ability of the new method to analyze complex signatures, an experimental example having a double-peaked wall pressure signature was selected (see Figure 18). This was generated experimentally by a highly lifting, jet flap model which caused tunnel flow breakdown in the case shown. The first peak in the wall signature corresponds to model blockage and the second is related to flow separation from the tunnel floor aft of the model. Though the second peak should be represented by sources or sinks located at floor level, these were placed at the tunnel centerline for the present illustration. The number of centerline singularities equalled the number of experimental points (circles, upper plot) and the matrix solution passed through every point. The corresponding centerline interference signature is illustrated in the lower plot (circles). To determine the impact at the model position of the second peak, a further case was run with it removed (triangles). The effect at the model location (x/B = 0) is surprisingly small.

As mentioned previously, the matrix method is sensitive to data scatter. Though the scatter in the Figure 18 case produced no problems it has become apparent that some smoothing is desirable and this has been achieved within the matrix solution itself. An influence matrix is set up with a row for each data point but with a reduced number of columns (i.e. singularities). The matrix is made square by using a least squares analysis in which all data is used. Figure 19 shows a least squares solution to the problem illustrated in Figure 18. Nine singularities, rather than the previous nineteen were used and the smoothed curve approximates the wall pressure signature quite well. There is some change to the centerline interference signature in Figure 19, as compared with Figure 18; however, we have no standard by which to judge which is "correct".

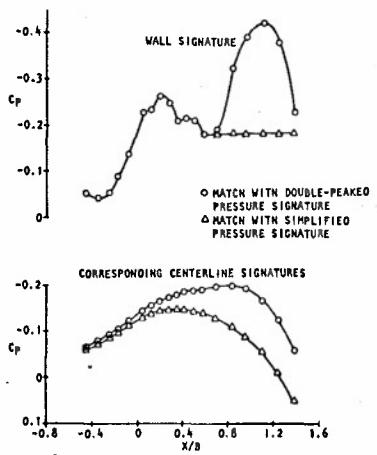

FIGURE 18 APPLICATION OF MATRIX METHOD TO A COMPLEX WALL PRESSURE SIGNATURE.

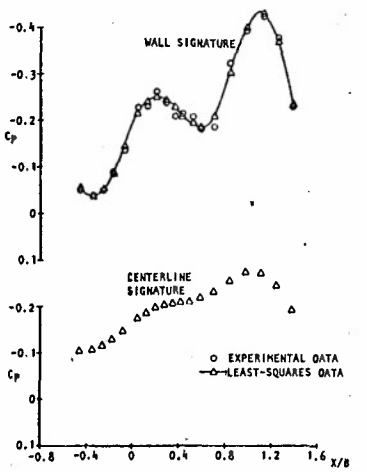

FIGURE 19 APPLICATION OF LEAST-SQUARES METHOD.

Application to Angle-of-Attack Correction

The tunnel roof influence matrix for the horseshoe vortex array (see Figure 13) is symmetric about the leading diagonal, rather than anti-symmetric as for sources. The inverse retains the alternating sign property, but the leading diagonal is now dominant. In view of this, the solution may be better behaved than for sources.

Pilot, angle-of-attack correction runs were made following the same general approach as for the source study of Figure 16. The overall results gave angle-of-attack corrections which agreed well with conventional estimates despite oscillating vortex strength solutions. However, the overall sensitivity to span effects was greater for the vortex model than for sources. Figure 20, upper, shows three tunnel roof pressure signatures for idealized models having the same lift (C_L (S/C) = 0.20), but differing spans. It was assumed that, in the hypothetical experimental case, the span was unknown and a 0.50B span was assumed throughout the analysis. The vortex strengths returned by applying the 0.5B matrix to each signature deviated from each other much less than for the corresponding source-source-sink study (Figure 16). Despite this, the percentage errors in centerline interference were somewhat greater.

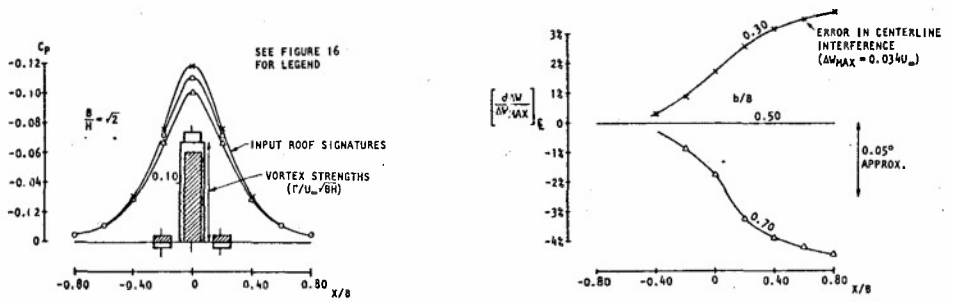

FIGURE 20 ANGLE-OF-ATTACK SOLUTION: SENSITIVITY TO SPAN EFFECTS
[CONSTANT MATRIX FOR b = 0.5B. C_L (S/C) = 0.20]

Bearing in mind that the angle-of-attack analysis of Figure 20 and the blockage analysis of Figure 16 were both made at the same force level, it may be shown that the correct selection of span is considerably more important for vortices than it is for sources at likely values of model L/D. However, the sensitivity is such that span selection within ±0.10% of the actual value will hold errors to an acceptable level. The possibility also exists of determining vortex span from tunnel surface measurements. Figure 21(a) shows that there is little prospect for discriminating between vortex strength and vortex span on the basis of the shapes of streamwise ceiling pressure signatures. However, it is evident from Figure 21(b) that there are good prospects for deriving vortex span from transverse pressure profiles at the model location.

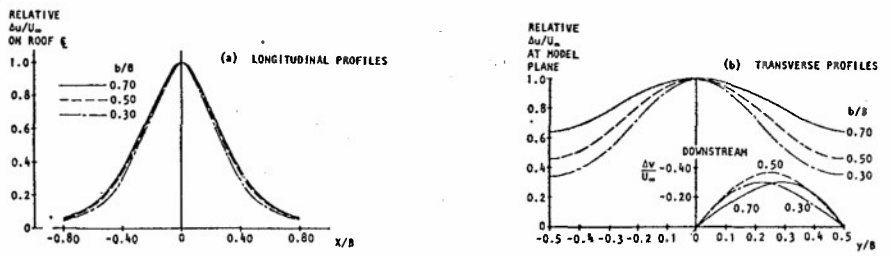

FIGURE 21 EFFECT OF BOUND VORTEX SPAN ON ROOF SUPERVELOCITIES NEAR MODEL LOCATION.

3.0 Discussion

The demands of high angle-of-attack testing tax existing wind tunnel corrections technology across a broad front. However, after many years of relatively slow progress, new advances are being made which promise to bring production testing out of the "horse-and-buggy" stage and change the present, small-model, small corrections philosophy. This has especial relevance today because of the need for energy conservation and because of the increasing cost of wind tunnel construction.

The new advances are made possible predominantly by recent increases in computer power and reductions in computation costs. The advances have also fostered the growing science of computer fluid dynamics and have raised the feasibility of flow recomputation as a "correction" method. Though this is becoming a reality for airfoil section design and testing it will be a considerable time before a similar attack will be practical for highly three-dimensional flows such as those over aircraft models at high angles-of-attack. Correction of test data, i.e. the semi-empirical removal of unwanted tunnel effects, will therefore continue to hold prime importance.

Increased model size brings with it the ability to improve internal instrumentation, to install power simulators more readily and to improve reading accuracy as well as to increase Reynolds number. Before any of these desirable features can be exploited, however, the test engineer must ask "Will the data be correctible?" At all levels of testing, the question resolves into two aspects, concerning the flow physics and the data needed to compute the correction.

It was shown in Section 2 that the prospects are good for defining the tunnel-induced flow field from a practical number of measurements at or near the test-section boundaries. However, an exception to this occurs when a sonic region occupies a substantial proportion of the tunnel cross section or approaches a tunnel surface. The prospects are also good for deriving corresponding corrections successfully in pre- and post-stall situations, provided the loads on major components can be measured or estimated. However, incipient stall and immediate post-stall flows are likely to be gradient-sensitive and this may limit model size in fixed-geometry tunnels. There is a clear need for sensitivity studies which determine the permissible imposed axial gradients for typical airfoil sections or wings.

Tunnel-related wake distortion may limit correctability in V/STOL tests, especially if powered flows impinge upon tunnel surfaces. This is a pressing problem in large tunnels where full-scale vehicles are tested. Despite a number of attempts to use adaptive techniques in this situation, no practical solution has emerged. It is not yet clear to what extent the difficulty can be relieved using the new correction techniques described in Section 2.3 (see Figure 18).

The second aspect of correctability – concerning data needed to compute corrections – divides naturally into tunnel surface- and model-related parts. Tunnel surface instrumentation for solid-walled tunnels represents a fairly modest, one-time cost involving probably two scanivalves. The requirement is somewhat greater for porous-walled tunnels and better methods are needed for measuring normal-to-wall velocities. Part of the data needed to calculate the correction to a particular model measurement is often the measurement itself. This is all that is required from the model in pressure distribution tests and in some force tests. However extra data are needed to correct six-component balance measurements and means must be available for distributing loads between components in order to compute gradient-dependent corrections, particularly to moments.

It is possible to eliminate one of the weaker links in the above procedure – that of assigning loads to individual model components – by using adaptive walls. It is of interest to consider a minimally adaptive tunnel in which changes are made only to "upper" and "lower" tunnel surfaces and only as needed to remove axial gradients. Such an approach would reduce the recurring cost of model instrumentation. However, the magnitude of the task of providing partially, as opposed to fully adaptive walls, has not been defined and cost effectiveness studies are needed which consider such trades. Possible difficulties in defining the mean flow and determining residual corrections for partially adaptive schemes should also be reviewed.

A significant factor in promulgating emerging technologies concerns acceptance by the test engineer. When the pressure-signature, blockage-correction method was first developed (see Section 2), this was a major reason for adopting the "chart" method (Section 2.2) rather than the more direct but less intelligible matrix approach (Section 2.3). Conversations with the testing community concerning fully adaptive tunnels have revealed deeply ingrained reservations concerning the "calibration" of these tunnels. A partially adaptive tunnel used with a baseline calibration would be more acceptable to the test engineer.

4.0 Conclusions

Recent U. S. developments wind tunnel test and corrections technology have been reviewed which are applicable to high angle-of-attack testing. The needs are such that the applicable techniques encompass a large proportion of current research on tunnel test technology.

An overview of the relevant factors is given in Section 1, together with the results of a limited literature review and of a letter survey involving members of the tunnel testing community in the United States. Developments in the use of measurements at tunnel surfaces for determining corrections are reviewed. These include both improvements to the iterative approach published by Hackett and Wilsden in 1975 (see Sections 2.1 and 2.2) and some early results from a new, non-iterative technique (Section 2.3).

The definition of the tunnel-induced flow field, using wall measurements, has been accomplished for low speed flows and extension to high subsonic speeds appears feasible provided that supercritical flow is not extensive. Experiments have shown that surface pressures may be corrected successfully even on quite a large model.

The most difficult aspect of the correction process is to determine the consequences of tunnel-induced velocity gradients. The effects on moments, in particular, may require either experimental or theoretical input in order to assign loads to particular model components. However new work is needed to determine the sensitivity of viscous effects – particularly the stall- to tunnel-induced gradients.

The above topics are reviewed in Section 3, which also includes a discussion of adaptive-wall techniques. A possible compromise is to adapt the walls only to a zero gradient condition, rather than to a configuration for zero interference. This might involve only upper and lower tunnel surfaces and might prove more acceptable to the practicing test engineer than a fully adaptive scheme.

It appears that passive, boundary measurement technology may diffuse first into high angle-of-attack production testing, possibly followed by some form of partially adaptive tunnel technology. However, much remains to be done concerning the application of adaptive techniques to configurations with highly three-dimensional flows.

Acknowledgements

The authors are indebted to Mr. R. A. Boles and to Mr. D. E. Lilley, both of Lockheed-Georgia, for their parts in performing the experiments which are described in this paper.

Much of the correlation work described was performed under NASA Contract NAS2-9883. Work on the matrix methods (Section 2.3) was accomplished under the Lockheed-Georgia Independent Research and Development program. The authors are responsible for the opinions expressed in this paper.

References

Reviews and Compendia

1. Garner, H. C.; Rogers, E. W. E.; Acum, W. E. A.; Maskell, E. C.: "Subsonic Wind Tunnel Wall Corrections." Agardograph 109 October 1966.

2. Meyson, H. H.: "General Theory of Wall Interference for Static Stability Tests in Closed Rectangular Test Sections and in Ground Effect." NASA TR R-364 September 1971.

3. Goethert, B. M.: "Technical Evaluation Report on the Fluid Dynamics Panel Symposium on Wind Tunnel Design and Testing Techniques." AGARD-AR-97 August 1976.

4. Pindzola, M.; Binion, T. W.; and Chevallier, J. P.: "Comments on Wall Interference Control and Corrections," AGARD CP-187 Paper 4A June 1975.

5. Polhamus, E. C.: "Technical Evaluation Report on the Fluid Dynamics Panel Symposium on High Angle-of-Attack Aerodynamics." AGARD-AR-145 August 1979.

6. Whitfield, J. D. (Ed.): "Aerodynamic Testing - A Look at Future Requirements." AIAA Paper No. 78-765 April 1978.

7. Collins, F. G.: "Summary of the 1977 USAF/DSR/ASEE Summer Design Study Program on the Integration of Wind Tunnels and Computers." AIAA Paper 78-783 April 1978.

8. Wilsden, D. J.: "A Review of Blockage Correction Methods for Automobile Testing in Wind Tunnels." Lockheed-Georgia Company Engineering Report No. LG79ER0050 March 1979.

Correction by Deterministic Methods

9. Binion, T. W.: "An Investigation of Three-Dimensional Wall Interference in a Variable Porosity Transonic Wind Tunnel." AEDC TR-74-76 October 1974.

10. Binion, T. W.: "An Experimental Study of Several Wind Tunnel Wall Configurations Using Two V/STOL Model Configurations." AEDC TR-75-36 July 1975

11. Lo, C. F.; Glassman, H. N.: "Calculation of Interference for a Porous Wall Wind Tunnel by the Method of Block Cyclic Reduction." AEDC TR-75-98 November 1975.

12. Kraft, E. M., and Lo, C. F.: "Analytical Determination of Blockage Effects on a Perforated-Wall, Transonic Wind Tunnel," *AIAA Journal* 1977 p 511.

13. Everhart, J. L.; Barnwell, R. W.: "A Parametric Experimental Study of the Interference Effects and the Boundary Condition Coefficient of Slotted Wind Tunnel Walls." AIAA Paper No. 78-8D5 April 1978.

Theoretically-Oriented Methods

14. Murman, E. M.: "Computation of Wall Effects in Ventilated Transonic Tunnels." AIAA Paper No. 72-1007 September 1972.

15. Murman, E. M.; Bailey, F. R.; and Johnson, M. H.: "TSFOIL - A Computer Code for 2-D Transonic Calculations, Including Wind-Tunnel Wall Effects and Wave Drag Evaluation." NASA SP347, Part II, 1975, pp 769-788.

16. Murman, E. M.: "A Correction Method for Transonic Wind Tunnel Wall Interference." AIAA Paper No. 79-1533, July 1979.

17. Bhately, I. C.; Mann, M.; Ballhaus, W. F.: "Evaluation of Three-Dimensional Transonic Methods for Analysis of Fighter Configurations." AIAA Paper No. 79-1528 July 1979.

18. Lachle, G. C.: "Horizontal Buoyancy Effects on the Pressure Distribution of a Body in a Duct." *Journal of Hydronautics*, pp 61-67, April 1979.

19. Joppa, R. G.: "A Method of Calculating Wind Tunnel Interference Factors for Tunnels of Arbitrary Cross Section " NASA CR-845 July 1967.

20. Heltsby, J. L.; Dietz, W.: "A Vortex Lattice Technique for Computing Ventilated Wind Tunnel Wall Interference." AEDC TR-79-21 June 1979.

21. Heard, C. A.: "Wind Tunnel Wall Corrections for Arbitrary Planforms and Wind Tunnel Cross Sections." Masters Thesis, Naval Postgraduate School, Monterey, June 1977.

22. Pletzman, F. W.: "Determination of High-Attitude Wall Corrections in a Low Speed Wind Tunnel." AIAA Paper No. 78-810 April 1978.

Correction Using Measurements at Tunnel Boundaries

23. Hensel, R. W.: "Rectangular Wind Tunnel Corrections Using the Velocity-Ratio Method." NACA TN2372 June 1951.

24. Hackett, J. E.; Wilsden, D. J.: "Determination of Low Speed Wake Blockage Corrections via Tunnel Wall Static Pressure Measurements." AGARD CP 174 Paper 23 October 1975.

25. Hackett, J. E.; Wilsden, D. J.: "Estimation of Tunnel Blockage from Wall Pressure Signatures: A Review of Recent Work at Lockheed-Georgia." AIAA Paper No. 78-828 April 1978 (Also submitted to the AIAA Journal).

26. Hackett, J. E.; Wilsden, D. J.; Lilley, D. E.: "Estimation of Tunnel Blockage from Wall Pressure Signatures: A Review and Data Correlation." NASA CR 152,241 March 1979.

27. Kemp, W. B.: "Toward the Correctable-Interference Transonic Wind Tunnel." AIAA 9th Aerodynamic Testing Conference Proceedings pp 31-38 1976.

28. Kemp, W. S.: "Transonic Assessment of Two-Dimensional Wind Tunnel Wall Interference Using Measured Wall Pressures." NASA CP 2045 pp 473-486 1978.

29. Lo, C. F.: "Tunnel Interference Assessment by Boundary Measurements." *AIAA Journal*, pp 411-413 April 1978.

30. Blackwell, J. A.: "Wind Tunnel Blockage Correction for Two-Dimensional Transonic Flow." *Journal of Aircraft*, April 1979, pp 256-263 (Also AIAA Paper 78-806).

31. Hinson, B. L.: "3-D Transonic Wing Data Acquisition and Evalaution." Proceedings, AFOSR/AFFDL Program Review of Research in External Aerodynamics, June 1979. See also AIAA Paper No. 80-0003.

"Self-Correcting" Wind Tunnels

32. Lo, C. F.: "Wind Tunnel Wall Interference Reduction by Streamwise Porosity Distribution. *Journal of Aircraft* April 1972 pp. 547-550.

33. Ferri, A.; Baronti, P.: "A Method for Transonic Wind Tunnel Corrections." *AIAA Journal*, January 1973.

34. Sears, W. R.: "Self-Correcting Wind Tunnels." *Aeronautical Journal*, February/March 1974, pp. 80-89.

35. Vidal, R. J.; Erickson, J. C.; Catlin, P. A.: "Experiments with a Self-Correcting Wind Tunnel." AGARD CP 174 Paper 11 October 1975.

36. Goodyer, M. J.: "The Self-Streamlining Wind Tunnel." Symposium on Wind Tunnel Design and Testing Techniques AGARD CP 174 Paper 13 October 1975.

37. Bernstein, S.; Joppa, R. G.: "Development of Minimum Correction Wind Tunnels." AIAA Paper No. 75-144. See also *Journal of Aircraft* April 1976.

38. Weeks, T. M.: "Reduction of Transonic, Slotted Wall Interference by Means of Slot Contouring." AFFDL TR-74-139, March 1975.

39. Sears, W. R.; Vidal, R. J.; Erickson, J. C.: "Interference-Free Wind Tunnel Flows by Adaptive-Wall Technology." ICAS Paper No. 76-D2 or *Journal of Aircraft* November 1977.

40. Lo, C. F.; Kraft, E. M.: "Convergence of the Adaptive-Wall Wind Tunnel." *AIAA Journal* January 1978 pp 67-72.

41. Vidal, R. J.; Erickson, J. C.: "Experiments on Supercritical Flows in a Self-Correcting Wind Tunnel." AIAA Paper No. 78-788 April 1978.

42. Sears, W. R.: "Adaptive Walls With Imperfect Control." *Journal of Aircraft*, May 1979 pp 344-348.

43. Dowell, E. H.: "A Compliant Wall Supersonic Wind Tunnel." AIAA Paper No. 79-0110, July 1979.

44. Bodapati, S.; Schairer, E.; Davis, S.: "Adaptive Wall Wind Tunnel Development for Transonic Testing." Paper submitted to the 11th AIAA Testing Conference.

Other Topics

45. Erickson, G. E.: "Water Tunnel Flow Visualization Insight into Complex Three-Dimensional Flow Fields." AIAA Paper No. 79-1530 July 1979.

46. Daughterty, N. S.; Steinle, F. W.: "Transition Reynolds Number Comparisons in Several Major Transonic Tunnels." AIAA Paper 74-627, July 1974.

47. Mouch, T. N.; Nelson, R. C.: "The Influence of Aerodynamic Interference on High Angle-of-Attack Wind Tunnel Testing." AIAA Paper 78-827 April 1978.

48. Olson, L. E.: The Effect of Viscosity on Wind-Tunnel Wall Interference for Airfoils at High Lift." AIAA Paper No. R-1534 July 1979.

49. Nark, T. C.: "Powered Lift Testing." AIAA Paper No. 79-0706.

AMELIORATIONS ENVISAGEES POUR RESOUDRE LES PROBLEMES RENCONTRES AU COURS D'ESSAIS A GRANDE INCIDENCE DE MAQUETTES EN SOUFFLERIE

par Xavier VAUCHERET

Office National d'Etudes et de Recherches Aérospatiales (ONERA)
92320 Châtillon (France)

RESUME

Parmi les problèmes rencontrés lors de l'exécution d'essais en soufflerie de maquettes à grande incidence, trois sont sélectionnés ici : effets de parois, interaction de dards supports et vibrations au-delà du décrochage.

L'état de l'art des corrections des effets de parois, systématiquement appliquées en soufflerie à caractère industriel, est exposé avec de nombreuses comparaisons entre souffleries ou entre vol et soufflerie. Les modélisations nécessaires des maquettes en atmosphère illimitée font apparaitre des lacunes dans le cas de tourbillons d'apex et de jets actifs des maquettes.

Simultanément, d'autres méthodes de corrections sont développées en FRANCE pour pallier aux hypothèses simplificatrices et aux limitations de la méthode classique. Ainsi AMD-BA a développé la méthode des petits pavés et ONERA, la méthode des signatures maquettes sur les parois des veines d'essais. Cette dernière méthode, déjà utilisée en essais bidimensionnels industriels pour des veines ventilées cylindriques, est étendu au tridimensionnel. Son extension au cas des veines déformées constituera une étape intermédiaire de l'étude des parois autoadaptables.

Il est insisté, en conclusion, sur les méthodes de contrôle de la validité des méthodes de correction des effets de parois.

EXPECTED IMPROVEMENTS ON HIGH ANGLE OF ATTACK MODEL TESTING

Office National d'Etudes et de Recherches Aérospatiales (ONERA)
92320 Châtillon (France)

SUMMARY

Several problems were encountered during tests at high angle of attack in wind tunnels. Three are selected here : wall interference, sting interference and vibrations beyond the stall.

The state of the art on wall interference, systematically applied to the development tests, is showed with several comparisons between wind tunnels or between flight and tunnels tests. The models used in unconfined flow point out some deficiencies as regards apex vortex and active jets.

Simultaneously, other correction methods are developed in FRANCE to palliate the assumptions and limits of the classical method. Thus AMD-BA works on the vortex lattice method and ONERA on the model signatures on the test section walls. This method, already used in 2D flow for development tests with ventilated cylindrical test sections, is extended at the 3D case, as a first stage for distorted but non streamlined walls.

As a conclusion, the control of the validity of the wall interference correction method is analysed.

INTRODUCTION

Les prévisions de perfórmances d'avion sont étsblies à partir de nombreuses données parmi lesquelles les essais en soufflerie tiennent un rôle majeur. En même temps que la fourniture des résultats de mesures, le spécialiste de soufflerie doit effectuer les corrections nécessaires pour que le constructeur puisse disposer des meilleurs éléments d'appréciation de la validité et de la précision des résultats. En dehors des comparaisons entre résultats d'essais en vol et en soufflerie qui nécessitent de recourir à des méthodes d'extrapolation, les essais de fidélité et les comparaisons de résultats obtenus dsns différentes soufflerles ou différentes configurations de veines d'esaais constituent des guides précieux pour juger les améliorations à apporter aux méthodes de corrections.

Des programmes de comparsison de résultats d'esssis ont ainsi été réalisés en supersoniqua sur maquettes étalons AGARD [1] puis plus récemment en transsonique sur maquettes étalons ONERA[2]. De telles confrontations sont bien entendu spécifiques des maquettes utilisées et en particulier devrsient être développées dans le domsine des grsndes incidences sur avion civil ou militaire.

Lors des comparaisons des résultats provenant de divers essais effectués dans diverses veines d'essais, il y a lieu de tenir compte des qualités de l'écoulement aussi bien stationnaire (ascendance, gradient longitudinal de pression) qu'instationnaire (turbulence, bruit), des effets de parois et des champs des dards supports et des conditions de traitement des mesures surtout lorsque des vibrations interviennent.

Si certaines corrections peuvent être effectuées ssns ambiguité telles que celles d'sscendance et de poussée d'Archimède, d'autres corrections telles que celles des effets de parois peuvent poser des problèmes si les effets des autres paramètres modifient les caractéristiques sérodynamiques des maquettes. Il y s donc lieu de s'sssurer de l'effet de ces paramètres tels que turbulence ou bruit, avant d'aborder les corrections des effets de parois, sous peine de mélanger différentes influences ce qui conduirait slors à douter des méthodes de corrections. Ceci risque d'être particulièrement délicat dans les domaines où ls susceptibilité des résultats aux paramètres indiqués devient élevée et lorsque l'influence des divers paramètres ne peut être étudiée isolément car il n'est pas encore possible de les fsire varier.

L'ONERA s déjà publié des travaux [3 , 4] sur des comparaisons de résultats dont certsins concernaient le domaine des incidences élevées Les sujets qui seront ici abordés concernent particulièrement le domaine des incidences élevées ou plus précisément le domaine d'incidence pour lequel des décollements importsnts existent. Le sujet principsl concernera les effets de parois en présence de décollements et les diverses méthodes de corrections en service pour essais industriels ou envisagées dans le futur [5] . L'influence des dards supports sera rapidement abordée ainsi qu'une tentative de modélisation du comportement vibrstoire des msquettes en de.d autour et au delà du décrochage.

I - CORRECTIONS DES EFFETS DE PAROIS

I.1 - Méthode analytique

I.1.1 - Corrections en l'absence de décollements

Il est seulement rappelé ici que ls méthode analytique de corrections nécessite la formulation d'hypothèses de conditions aux limites sur les psrois de la veine d'essais et la modélisation des potentiels maquettes en atmosphère illimitée. Ces modélisations peuvent être plus ou moins élaborées selon les tailles des maquettes vis à vis des dimensions des veines d'essais [4] . On reviendra sur ce point su parsgrsphe 1.1.5.

La méthode analytique est systématiquement sppliquée pour corriger les résultats d'essais dsns les soufflerles à carsctère industriel de l'ONERA.

I.1.2 - Corrections en présence de décollements

Pour tenir compte de ls présence de décollements, une correction supplémentaire est ajoutée aux corrections de blocage de volume et de sillsge. A l'inverse de ces dernières, établies à partir d'une modélisation de maquette, ls correction de décollement est dérivée de la théorie semi-empirique de MASKELL [6 , 7] fondée sur ls notion d'esu morte. Les deux hypothèses fondamentales de cette théorie sont rappelées seulement ici.

La première hypothèse consiste à sssimiler l'écoulement décollé dans le cas d'une aile à grande incidence au bulbe d'eau morte derrière une plsque perpendiculaire au vent. Si ce bulbe est bien décelable dans les visualisations au tunnel hydrodynamique derrière une aile en incidence ou avec des voleta braqués, VAYSSAIRE [9] note que dans le css de tourbillons d'apex bien organisés et portants, la notion d'eau morte n'est justifiée qu'en aval du point d'éclatement du tourbillon et ce d'autant plus que le tourbillon est diffus à grande incidence et avec un éclatement proche du bord d'attaque.

La deuxième hypothèse de MASKELL consiste en une addition pure et simple du coefficient ε_D aux deux autres coefficients de blocage de volume ε_S et de sillage ε_W (figure 1) dans la correction du nombre de Mach M ou de la pression cinétique q . Cette superposition linéaire correspondrait à une apparition de décollement au bord de fuite de voilure et à son extension progressive à toute l'envergure de l'aile.

Le coefficient de blocage de décollement ε_D (figure 1) est proportionnel à l'incrément de traînée C_{D_D} engendré par les décollements. Ce supplément de traînée est déduit de l'écart entre la polaire expérimentale et la mise en équation polynomiale de la polaire dans le domaine exempt de décollements. Le coefficient de proportionnalité θ intervenant dans ε_D est déduit de tarage des veines d'essais à l'aide de plaques perpendiculaires au vent de divers allongements [8] λ_a . La fonction $\theta(\lambda_a)$ indiquée figure 1 a été obtenue en veine guidée. D'après d'autres tarages effectués par VAYSSAIRE [9] en veine semi guidée de la soufflerie BREGUET, une valeur voisine de 2 serait à considérer pour θ . En outre, d'après des tarages en bidimensionnel, il n'est pas exclu que la valeur de θ dépende de l'incidence.

I.1.3 - Applications préliminaires

En vue de valider la théorie de MASKELL, des comparaisons de réaultats corrigés , dana diverses soufflerles ont été présentées en 1972 par VAYSSAIRE [9] . Un bon accord était obtenu entre les résultats corrigés d'une maquette d'avion de transport à flèche de voilure de 25 degrés dans deux configurations de la veine de la soufflerie $\Sigma 4$ de St Cyr : guidée et à parois horizontales perforées. Pour un rapport entre l'aire de la section veine C et la surface de voilure S de 24 les résultats corrigés étaient confondus jusqu'à Mach 0,85.

Dans le cas d'une maquette de Mirage F à flèche de voilure de 48 degrés, en configuration hypersustentée, l'accord des courbes de portance corrigées dana trois aoufflerles différentes S5 Toulouse, S2 Chalais et S1 St Cyr, pour des rapports C/S respectivement de 19.3, 9.6 et 5.1 (figure 2) était assez bon malgré l'importance des corrections pour le cas C/S = 5.1.

La confrontation de ces résultats corrigés avec lea résultats des essais en vol, en configuration trains rentrés ou sortis, (figure 3) était considérée comme largement satisfaaante par le constructeur même dans des cas où l'estimation du terme ε_D était grande par rapport aux autres termes ε_S et ε_W .

I.1.4 - Comparaisons de résultats dans les soufflerles S1MA et F1

Depuis l'entrée en service en 1977 de la nouvelle soufflerie basse vitesse pressurisée F1 de l'ONERA, de nombreuses comparaisons entre les résultats obtenus dans cette soufflerie et dans la soufflerie S1 de Modane ont été effectuées à même Reynolds sur mêmes maquettes. La soufflerie F1 possède une veine rectangulaire guidée de 15,75 m2 d'aire ; la nouvelle veine à fentes de la soufflerie S1MA à une aire de 40,44 m2 (figure 6). Les maquettes passées à F1 et S1 présenteront donc des corrections d'effets de parois notables à F1 et négligeables à S1, de telle sorte que les résultats obtenus à S1 peuvent servir de référence aux corrections appliquées à F1.

En outre, il a été vérifié sur une maquette de petites dimensions du Mirage G8, (rapports C/S de 28,4 et 73,0 à F1 et S1) que les qualités des écoulements des deux veines d'essais conduisaient à des résultats parfaitement identiques (figure 4). Un décalage constant de la stabilité résulte des différences de montage, en dard à S1 et sur mât à F1. Dès lors, il était possible de comparer des résultats sur maquettes de tailles plus grandes et d'étudier les effets de parois sans risque d'influence d'autres paramètres.

La comparaison des résultats corrigés d'une maquette au 1/10 du MERCURE 100 dans les deux soufflerles montre une bonne concordance (figure 5) en configuration croiaière bien que l'envergure relative de la maquette soit de 0,68 à F1. Les polaires équilibrées obtenues à F1 à 3,9 bars de pression génératrice sont comparées aux résultats donnés par la modélisation faite par les AMD.BA et correspondant aux essais en vol (figure 6). La concordance est très bonne en configuration croisière et décollage. Les résultats de vol à l'atterrissage correspondent à la position train sorti alors que les essais en soufflerie ont été effectués train rentré : on vérifie cependant la bonne cohérence vol-soufflerie grâce à l'existence de résultats de vol au décollage donnant l'influence de la sortie du train d'atterrissaga.

Dana tous les exemples qui viennent d'être donnés jusqu'ici, les flèches de bord d'attaque sont telles que les voilures sont exemptes d'écoulement tourbillonnaire d'apex. La figure 7 illustre les difficultés qui apparaissent dans le cas de fortes flèches avec des portances tourbillonnaires marquées. Les courbes correspondant aux valeurs non corrigées et corrigées à F1 permettent d'apprécier l'importance des corrections : la concordance entre les valeurs corrigées à F1 et S1MA n'est pas entièrement satisfaisante dans les zones à forts décollements au delà de l'inflèchissement de la courbe de portance. Dans le cas de la figure 7, la correction de blocage de décollement est appliquée à partir de l'incidence d'inflèchissement de la courbe $C_L(\alpha)$: S1 (figure 8) : les courbes corrigées sont intitulées"corrected 1" sur planches 7 et 8. Si la correction de blocage de décollement avait été appliquée à l'incidence d'apparition du tourbillon, S2 de figure 8, les courbes corrigées seraient cellea intituléea "corrected 2" sur les planches

8 et 9. La figure 9 montre l'importance relative des coefficients de traînée de décollement $C_{D_{S1}}$ et $C_{D_{S2}}$ tandis que la figure 8 donne les corrections de nombre de Mach ($M_c - M_u$) dans les 2 cas de bornes de décollement. La figure 8 montre bien qu'aux incidences élevées la correction la plus importante est celle de blocage sur la pression cinétique (trajets BC1 ou BC2) alors que la correction d'incidence (trajets AB) est modérée. On voit donc apparaître dans le cas de portances tourbillonnaires la difficulté de mise en oeuvre de la théorie de MASKELL.

D'une part,on a vu que le tourbillon non éclaté n'était pas assimilable à une zone d'eau morte donc que la borne inférieure d'incidence de décollement doit être plutôt à l'infléchissement de C_L (points S2) et pourrait être, en basse vitesse, bien définie par le minimum de la courbe $C_A(\alpha)$ (figure 9).

D'autre part, la mise en équation polynomiale de la polaire conduisant à la valeur de la traînée de décollement C_{D_S} devrait être $C_{D_{S2}}$ issue de la polaire induite en $C_L^2/\pi\lambda_a$ distincte de la polaire expérimentale dès l'apparition du tourbillon qui donne un supplément de C_D.

Il y a donc ambiguité dans l'application de la théorie semi-empirique de MASKELL par suite d'une absence de modélisation progressive de la traînée induite par le tourbillon lorsque l'incidence croît donc lorsqu'il se déplace vers le plan de symétrie avion et éclate en un point progressant vers le bord d'attaque.

Dans le cas d'une portance tourbillonnaire moins accusée du fait d'un braquage de becs par exemple, (figure 10) la confrontation est meilleure en $C_L(\alpha)$. Toutefois la comparaison entre résultats corrigés à F1 et SIMA est moins bonne en ce qui concerne la stabilité et la traînée.

I.2 - Schématisation des maquettes

La méthode analytique, comme la méthode des signatures qui sera évoquée au paragraphe 1.3, nécessite une schématisation de l'écoulement autour de la maquette en atmosphère illimitée. S'agissant de calculs correctifs, la modélisation, fondée sur un support théorique admissible, doit être raisonnable et rester assez simple pour ne pas entraîner de trop longues durées de calcul. Il serait en effet inutile d'apporter des raffinements supplémentaires si ceux-ci ne conduisaient qu'à de faibles variations des corrections. La difficulté principale réside dans la définition d'un niveau suffisant d'élaboration des modélisations ; la meilleure méthode de contrôle de ce niveau reste encore la vérification des effets secondaires entraînés par la prise en considération de descriptifs plus élaborés de la modélisation.

Il ne faut pas oublier que le support théorique de la schématisation de la maquette est complété de valeurs expérimentales, globales telles que C_L, C_D ou locales telles que des répartitions de pressions ou des mesures clinométriques. En outre, des coefficients correcteurs sont associés à certains termes de corrections pour tenir compte d'expérimentations de base.

I.2.1 - Termes de blocage

La plupart du temps, les modélisations sont très simples, doublet et source, pour les termes de blocage de volume et de sillage. Les intensités de doublets sont déduites du volume maquette et de coefficients correcteurs tenant compte de l'élancement du fuselage et de l'épaisseur relative de voilure. L'intensité des sources est directement liée à la mesure de la traînée C_D maquette ou de la traînée de sillage de profil C_{D_W}.

L'emploi de multisingularités, réparties sur la maquette, permet de respecter mieux la géométrie de celle-ci mais au prix d'un alourdissement des calculs.

Pour les termes de poussée d'Archimède, induits par les gradients longitudinaux de blocage, la loi des aires maquette est incluse pour améliorer la correction résultante de traînée.

Les décollements entraînent une correction supplémentaire calculée à partir de la théorie semi-empirique de MASKELL. Les difficultés d'emploi en présence de tourbillons d'apex, progressivement éclatés, ont été indiquées au paragraphe 1.1. Des améliorations devraient être apportées dans ce cas comme en présence de spoïlers pour s'affranchir des tarages préliminaires des veines d'essais à l'aide de plaques planes.

Dans le cas de maquettes actives, pour lesquelles les jets sont simulés, des études seraient nécessaires pour effectuer les corrections utiles tenant compte de la forme et de l'emplacement des jets et calculer les modifications des termes de volume et de sillage en blocage.

I.2.2 - Termes de portance

Les corrections d'incidence et de courbure de champ font intervenir les valeurs mesurées C_L, C_m, $\partial C_L/\partial\alpha$ et $x/\bar{c}$ et des coefficients de correction précalculés en fonction de divers paramètres. Actuellement ces paramètres peuvent être :

- forme de veine et porosité des parois
- envergure relative de maquette $\tau = 2s/B$
- flèche de voilure Λ
- type de répartition de circulation en envergure $\Gamma(y)$
- excentrement vertical de maquette $\mu = d/R$

En outre, la position de la nappe tourbillonnaire par rapport à la maquette peut être imposée, par exemple au point neutre obtenu en essais.

Les influences de ces divers paramètrea sont illustrées par quelques exemples donnés figures 11 et 12. En ce qui concerne la répartition de circulation en envergure $\Gamma(y)$, elle est suppcsée constante lorsque l'incidence varie dans les résultats corrigés donnés au paragraphe 1.1. Le calcul des coefficients de corrections d'incidence et de courbure de champ, locaux ou intégrés en envergure $\bar{\delta}$, $\bar{\delta}_1$, peut être effectué pour un cas quelconque de répartition . et il serait possible de tenir compte de l'évolution de celle-ci en incidence si l'équipement maquette permet d'accéder à $\Gamma(y)$.

Les exemples qui vont être donnés ci-après, issus d'essais sur une aile à flèche variable [10] montrent qu'il y aurait lieu de tenir compte de l'évolution avec α de la distributiun $\Gamma(y)$.

La figure 13 donne la courbe de portance globale de l'aile mise en flèche à 60 degrés en incompressible en fonction de α . Cette courbe, ainsi que la polaire, montre nettement le point A d'apparition du tourbillon d'apex. De A à B le tourbillon se développe et commence à éclater sur la voilure en B avec perte progressive de portance ; en C l'éclatement est intense et la traînée croît rapidement. La figure 14 donne le réseau des forces normales C_N , intégrées à partir des pressions relevées sur chaque corde, en fonction de la position y de la corde et de l'incidence α . La perte de portance locale apparaît à une incidence variant de 20 à 32 degrés pour une corde se déplaçant de l'extrémité à l'emplanture où la perte de portance est plus accusée. De ce fait, les répartitions $C_N(y)$ plates à faible incidence deviennent plutôt triangulaires dès 20 degrés d'incidence. Les figures 15 et 16 montrent le même phénomène à Mach 0,92 avec en outre des discontinuités nettes des courbes C_N, α en extrémité de voilure.

L'influence de la déflexion de la nappe tourbillonnaire en incidence n'a paa encore été étudiée car elle nécessite la miae en oeuvre de sondages clinométriques en aval de la voilure rarement exécutés.

Habituellement les corrections d'incidence et de courbure de champ sont calculées en valeur moyenne par intégration sur l'envergure de la maquette. En fait, il est possible d'accéder aux corrections sur chaque corde de voilure et de déterminer le vrillage de l'aile équivalente corrigée en atmosphère illimitée. La figure 17 montre que la correction locale d'incidence, proportionnelle à δ_0 , évoluera différemment en envergure selon le type de répartition de circulation utilisé pour une même envergure relative τ de maquette : les variations $\delta_0(y)$ sont dans le cas de la figure 17, de signes opposés sur la voilure, sauf en son extrémité. De même lors d'une comparaison de résultats sur même maquette dans des veines de dimensions différentes il y a lieu dc considérer que le vrillage dû aux corrections peut être différent. Ainsi pour une même répartition elliptique $\Gamma(y)$, la figure 17 montre que pour des envergures relatives τ de 0,4 et 0,8 le vrillage sera de signe opposé donc que les voilures équivalentes corrigées seront différentes.

Dans tout ce qui précède, la nappe tourbillonnaire est supposée horizontale. Il y aurait lieu, à grande incidence et dans les cas hypersustentés, de tenir compte de la déflexion de la nappe tourbillonnaire à l'aide de méthodes telles que celles décrites par HEYSON [11] . Ici encore un support expérimental à partir de visualisations serait nécessaire pour tenir compte d'une répartition en envergure de la déflexion et son influence sur les corrections devrait être examinée avant d'appliquer des raffinements de schématisation maquette.

I.3 - Autres méthodes de corrections des effets de parois

I.3.1 - Méthode des petits pavés

La méthode des petits pavés, initiée par JOPPA, a été développée par AMD.BA [12] . Cette méthode permet de tenir compte des dimensions de la veine et de la nature des parois découpées en élémenta rectangulaires d'intensité tourbillonnaire inconnue. Il est ainsi possible de l'appliquer à des géométries quelconques de veine, à des longueura quelconques de parois ventilées et à des emplacements quelconques de maquettes en veine. Bien entendu plus le descriptif de veine sera détaillé , plus les durées de calcul augmenteront. Cette méthode requiert, comme la méthode analytique, une modélisation des maquettes.

I.3.2 - Méthodc des signatures des maquettes

Devant les incertitudes existant sur les conditions aux limites imposées sur les parois ventilées (non linéarités, amplification par les couches limites), et les limites d'application des méthodes classiques dans les domaines de nombre de Mach élevé ou par suite de la présence de décollements plus ou moins organisés, ONERA a développé une autre méthode [5] en relation avec le concept dea parois auto-adaptable [13] . Cette méthode est basée aur la mesure des signatures de la maquette sur les parois de la veine d'essais.

Le cslcul des corrections a tout d'abord été basé sur ls mesure de la seule composante longitudinale de la vitesse de perturbation. La maquette est encore représentée par un nombre restreint de singularités proportionnées aux forces mesurées dans l'hypothèse d'un écoulement compressible linésrisé. De nombreuses applications en courant plan ont conduit à son utilisation en essais industriels. La figure 18 donne les résultats bruts et corrigés obtenus dans la soufflerie S3 de Modane sur un profil décroché. Le regroupement des résultats est correct bien que les corrections en parois perforées soient élevées. Les coefficients de traînée C_{D_P}, déduits des intégrations de pressions sur le profil s'accordent bien après correction alors qu'en parois perforées les C_{D_P} bruts dépassaient les traînées de sillage. La figure 19 donne les signatures nettement différentes selon la nature des parois ayant conduit aux mêmes valeurs de α, C_L et C_{D_P} au voisinage du décrochage.

Les signatures d'une maquette tridimensionnelle à aile delta ont été relevées sur les parois de la veine, rendue guidée, de la soufflerie S3 Chalais. A Mach 0,7 et pour deux incidences de 10 et 32 degrés, la dernière en présence d'un décollement prononcé, les courbes présentées sont issues des signatures : demi sommes (figure 20) et différences (figure 21) directement liées respectivement aux termes de blocage et de portance. Le caractère tridimensionnel de la signature en portance (différence) est nettement accusé à la plus forte incidence.

La méthode des signatures est en voie de généralisation en faisant appel à la connaissance supplémentaire de la direction de l'écoulement sur la surface de contrôle. Dans le domaine compressible linéaire, le champ de maquette, y compris les effets des supports et des décollements, en écoulement illimité, est déduit de l'ensemble des deux composantes de perturbation sur la surface de contrôle et substitué aux champs des singularités représentatives de la maquette lorsque celles-ci sont incertaines.

L'extension au transsonique, domaine supersonique léger inclus, en écoulement bidimensionnel, faisant appel aux mêmes principes et aux méthodes de petites perturbations transsoniques sera développée prochainement par ONERA. L'application locale, et non plus seulement globale, des corrections, qui apparaîtra nécessaire lors des domaines linéaires, a été traitée sur quelques cas subcritiques.

I.3.3 - Parois autoadaptables

L'extension de la méthode des signatures au contrôle de la composante transversale de la vitesse de perturbation sur une surface voisine des parois, en fonction de la composante longitudinale, permet d'assurer l'élimination des effets de parois. L'application de ce principe a été effectuée dans la soufflerie T2, au moyen de parois pleines déformables [13]. L'adaptation des parois en écoulement bidimensionnel et le calcul éventuel de corrections résiduelles par la méthode des signatures ont été réalisés sur le profil NACA 0012 à T2 et seront complétés par des essais sur des profils CAST 7.

En écoulement tridimensionnel, l'application des parois auto adaptables soulève des difficultés pratiques. Une adaptation partielle des parois horizontales, alliée à des corrections résiduelles basées sur les signatures, complèterait les essais effectués en tridimensionnel à S3Ch avec des parois non déformées, indiquées au paragraphe précédent.

II - INFLUENCE DES SUPPORTS DE MAQUETTES

Les supports de maquettes ne sont en principe pas considérés dans les corrections des effets de parois. Le principe de superposition des trois écoulements suivants est admis : écoulement autour de la maquette, isolée, en atmosphère illimitée, écoulement induit par les parois et écoulement perturbateur dû à la présence des supports de maquettes en présence des parois.

Des calculs théoriques du champ règnant autour des supports de maquettes sont souvent effectués à partir de multisingularités sur la périphérie des supports. La difficulté dans le cas des dards placés à grande incidence réside dans le calcul du champ perturbateur incluant les sillages en aval des dards. En l'absence de tels calculs, des sondages de l'écoulement autour des supports à l'emplacement maquette restent encore la meilleure méthode permettant d'accéder aux corrections induites par les supports. En général seules des mesures de répartitions longitudinales de pressions sont effectuées pour accéder aux corrections de poussée d'Archimède ΔC_{D_g} nécessaires pour établir le bilan de traînée d'un avion civil. Des sondages clinométriques complémentaires permettraient d'accéder à la perturbation déflexion sur empennage horizontal.

Un exemple des résultats de sondages en pressions à Mach 0,8 dans la soufflerie S2 de Modane est donné figure 22. Les répartitions longitudinales de pressions, le long de la droite qu'occuperait l'axe maquette aux différentes incidences, sont mesurées à l'aide d'une sonde multiprises en l'absence et en présence du dard support de maquette. Même à de faibles incidences, la variation du gradient de pression, entraîne des variations des corrections de poussée d'Archimède, sur la partie arrière du fuselage, non négligeables avec M et α.

Dans un tout autre domaine d'incidence, une étude de l'influence des dards supports de missiles a été effectuée en subsonique élevé dans la soufflerie S3 de Modane [14]. Les résultats, bien que non généralisables à d'autres configurations de maquette, donnent un ordre de grandeur des corrections à apporter aux résultats de mesure. Les réductions de force normale C_N provoquées par la présence du support de dard prolongeant la maquette sont inférieures à 2 % à Mach 0,7 et atteignent 7 % à Mach 0,9 (figure 23). Le dard de balance, prolongeant le missile, même avec un diamètre inférieur à celui du fuselage (ici 0,65 D), induit un léger supplément de portance par atténuation des effets d'extrémités sur le fuselage en incidence. Il y a lieu de noter [15] qu'un montage sur mât dorsal réduirait C_N, à l'inverse du dard droit, et d'une quantité importante par altéra-

tion de l'organisation tourbillonnaire du sillage du fuselage. La simulation du jet du propulseur (figure 23) provoque, à partir de 40 degrés d'incidence, un accroissement de C_N de l'ordre de 10 % à 60 degrés, donc un effet de signe opposé à celui du support d'incidence.

Le champ du support de dard a pour effet d'augmenter les incidences locales, davantage sur les gouvernes que sur les ailes, et de réduire les vitesses de l'écoulement. Ce ralentissement est confirmé d'une part par l'accroissement de la pression au culot de la maquette et par la signature de l'ensemble maquette-dard mesurée sur le plancher de la veine d'essais (figure 23) donné à titre d'exemple pour $\alpha = 60°$. Cependant, le champ des sous-vitesses locales induit par le support, qui a tendance à réduire les charges aérodynamiques sur la maquette est prépondérant vis à vis de l'effet d'augmentation de l'incidence moyenne, ces deux résultats ayant des effets contraires. L'influence du jet du propulseur sur la signature au plancher de la veine est négligeable ce qui semble indiquer que le jet ne crée qu'une modification des incidences locales sans altérer les vitesses de l'écoulement.

III - VIBRATIONS DES MAQUETTES AUTOUR DU DECROCHAGE

Les maquettes, montées en dard, sont parfois soumises à des vibrations de fortes amplitudes autour et au delà du décrochage. Outre que le problème de la sécurité des maquettes réquiert une réduction des amplitudes de vibrations, des filtrages appropriés des meaures s'avèrent nécessaires pour pouvoir réduire la dispersion des résultats et fournir au constructeur les meilleures caractéristiques aérodynamiques moyennes au delà du décrochage.

Au cours d'essais à basse vitesse, dans la soufflerie pressurisée F1, sur une maquette d'avion civil montée en dard, des vibrations importantes sur le mode de flexion fondamentale du dard ont été rencontrées pour certains cas de configuration d'atterrissage. L'évolution dans le temps des amplitudes conduisait alors l'expérimentateur à limiter le domaine des incidences explorées.

Une approche de calcul de prévision des amplitudes a été élaborée à l'ONERA : elle est basée sur la seule connaissance des coefficients aérodynamiques stationnaires. L'équation générale du mouvement est établie, sans approximation, pour des mouvements d'amplitude modérée autour d'une incidence moyenne élevée variant avec le temps selon un cycle défini. La résolution de cette équation, à l'aide des méthodes classiques de mécanique non linéaire conduit aux évolutions de la fréquence et de l'amortissement avec l'amplitude du mouvement. Lorsque des instabilités sont rencontrées, provenant des seuls termes de rigidité aérodynamiques négatifs au delà du décrochage, l'effet cumulatif des amortissements négatifs conduit à des cas d'amplification des amplitudes.

La figure 24 donne ainsi en incompressible pour trois évolutions types des forces aérodynamiques, autour du centre instantané de la ligne de dard, avec l'incidence, les variations de l'amortissement et de l'amplitude qui seraient obtenus au cours d'un cycle de montée et descente en incidence. Dans ce cas l'incidence maximale est de 24 degrés et la vitesse de balayage d'incidence de 0,5 degrés par seconde. Selon l'intensité de décrochage, l'amortissement devient plus négatif donc l'amplitude croît. Le phénomène se compliqua si des cycles limites peuvent être présenta et en particulier l'amortissement est modifié par l'amplitude. De ce fait les amplitudes en incidences croissantes et décroissantes sont différentes. En particulier l'effet cumulatif peut être tel qu'une divergence dynamique soit atteinte.

La figure 25 montre la susceptibilité des amplitudes de vibration à un paramètre essentiel, la vitesse de balayage en incidence, lorsque celle-ci augmente l'échelle des temps peut être telle que les instabilités n'ont pas le temps de s'établir et les amplitudes sont, dans le cas illustré, nettement réduites.

Selon les niveaux d'amplitudes, des filtrages plus ou moins drastiques peuvent être appropriés pour accroître la validité des polaires et courbes aérodynamiques en valeurs moyennes.

CONCLUSIONS : Contrôle de la validité des corrections des effets de parois

Les calculs de corrections des effets de parois appliqués à des maquettes de dimensions raisonnables conduisent,dans bien des cas,à des comparaisons de résultats, obtenus dans diverses souffleries, honorables. Des corrections classiques déduites de la méthode analytique, ne nécessitant que des durées réduites de calcul sont bien adaptées aux souffleries à caractère industriel et effectuées aystématiquement par ONERA. Cette méthode est perfectible par amélioration des modélisations des maquettes. Ainsi les évolutions en incidence des répartitions de portance en envergure et des déflexions des nappes tourbillonnaires de voilure pourraient être considérées dès lors qu'elles seraient connues. A forte incidence, dans le cas de voilure à forte flèche, des modèlea réalistes dea développements du tourbillon d'apex et de son éclatement restent à développer. Il en va de même pour la prise en considération des jets actifs des maquettes.

D'autres méthodes de corrections des effets de parois sont en cours de développement. La méthode des petita pavés, développée par AMD.BA peut s'avérer nécessaire pour des veines et des longueurs de parois ventilées courtes ainsi que dans le cas de formes compliquées de veines. La méthode des signatures en pressions des maquettes sur les parois des veines d'essais présente un progrès intéressant par l'affranchissement des conditions limites linéaires, criticables en parois perforées et des étalonnages de leur porosité. De telles méthodes, nettement plus lourdes en durées d'essais ou de calculs, seraient utilisées en essais industriels dans les cas où la méthode classique s'avèrerait insuffisante.

Le principal problème restant, est la validation des méthodes de corrections des effets de parois. En ce qui concerne les schématisations des maquettes, il est toujours loisible de vérifier que des modélisations plus élaborées n'entraînent que des modifications mineures des corrections donc qu'elles sont superflues. La comparaison entre des résultats provenant de diverses origines reste toujours un élément décisif mais nécessitant une critique approfondie et délicate pour s'assurer que les écarts observés résultent bien des corrections des effets de parois et non de l'influence d'autres paramètres parfois prépondérants. En outre, il y a lieu de discriminer la part due aux dispersions de mesures et à leurs traitements. (figure 26)

La comparaison vol - soufflerie, évidemment la plus intéressante en définitive, fait appel à des corrections multiples et souvent bien supérieures aux effets de parois telles que les influences des supports de maquette [16] , les transpositions en Reynolds et la prise en compte de l'aéroélasticité [17] .

A partir de nombreuses comparaisons vol-soufflerie effectuées sur le Concorde, AEROSPATIALE conclue que les variations et les grandeurs des caractéristiques aérodynamiques à haute incidence déterminées en soufflerie sont retrouvées sur l'avion en vol [18] .

La comparaison entre résultats sur même maquette dans diverses configurations de parois d'une même veine d'essais est intéressante par l'invariance de certains paramètres tels que turbulence, interaction de supports, mais insuffisante car elle peut cacher une erreur systématique si une correction dépend peu de l'état des parois.

La comparaison entre résultats sur maquettes homothétiques dans diverses souffleries est de loin la plus délicate car elle fait intervenir les qualités respectives des écoulements de diverses souffleries et la susceptibilité des maquettes à ces qualités. D'autre part, il y a lieu de s'assurer de l'homothétie non seulement au sens macroscopique mais encore au sens état de surface et aéroélasticité des maquettes. Enfin si les états de parois des veines d'essais comparées et si les tailles relatives de maquettes diffèrent, les états de maquettes corrigées équivalentes peuvent différer notablement en vrillage et cambrure.

La comparaison entre résultats sur même maquette et même support dans différentes souffleries permet d'éliminer des causes d'écarts mais non d'obvier aux difficultés résultant des qualités d'écoulement spécifiques à chaque soufflerie et des états de maquettes corrigées équivalentes.

Une perspective d'avenir, qui relève indirectement des méthodes de corrections des effets de parois, développée depuis quelques années, est le concept des parois autoadaptables. Actuellement des perspectives encourageantes s'ouvrent pour les applications en écoulement bidimensionnel.

REFERENCES

[1] A review of measurements on AGARD calibration models
AGARDOGRAPH 64 (1961)

[2] POISSON-QUINTON Ph - VAUCHERET X.
Prévision des caractéristiques aérodynamiques d'un avion à partir de la comparaison des résultats sur une maquette étalon dans diverses grandes souffleries transsoniques.
AGARD CP 242 (1977)

[3] VAUCHERET X - VAYSSAIRE J.C.
Corrections de parois en écoulement tridimensionnel transsonique dans des veines à parois ventilées
AGARD CP 174 (1975)

[4] VAUCHERET X.
Corrections de parois en soufflerie transsonique. Porosité équivalente
Publication ONERA 1977-3

[5] CAPELIER C - CHEVALLIER JP - BOUNIOL F.
Nouvelle méthode de correction des effets de parois en courant plan
La Recherches Aérospatiale n° 1978-1

[6] MASKELL E.C.
A theory of the blockage effect on bluff bodies and stalled wing in a closed wind-tunnel
A R C R et M 3400 (1963)

[7] MASKELL E.C.
Bluff bodies and high lift aystems
AGARDOGRAPH 109 (1966)

[8] FAIL R - LAWFORD J.A - EYRE R.C.W
Low speed experimenta on the wake charactariatics of flat platea normal to an air stream
A R C R et M 3120 (1957)

[9] VAYSSAIRE J.C.
Corrections de blocage dana les esaaia en soufflerie. Effeta des décollementa
AGARD F D P Liabonne (1972)

[10] MIRANDE J. - SCHMITT V. - WERLE H.
Système tourbillonnaire présent à l'extrados d'une aile en flèche à grande incidence
AGARD CP 247 (1978)

[11] HEYSON H.H
Wind tunnel wall effects at externe force coefficienta
Intern - Congress of Subsonic Aeronautica (1967)

[12] VAYSSAIRE JC - LANGOT M - MENARD M.
Adaptation de la méthode de JOPPA à une soufflerie à perméabilité variable
AGARD CP 210 (1976)

[13] CHEVALLIER JP
Soufflerie transsonique à parois auto-adaptables
AGARD CP 174 (1975)

[14] REGARD D
Essai en soufflerie de missile à grande incidence. Influence du dispositif d'essai en subsonique élevé
22 nd Israël Annual Conference on Aviation and Astronautica (1980)
ONERA TP 1980 - 16

[15] DIETZ W.E.- ALSTATT M.C.
Experimental investigation of support interference on an ogive cylinder at high incidence
AIAA 78 - 165 (1978)

[16] BERGER J -(AEROSPATIALE.)
Comparaison entre les prévisions déduites des essais en soufflerie et les résultats de vol en croisière.(Airbus et Concorde).
AGARD CP n° 242 (1977)

[17] PELAGATTI C - PILON J.C - BARDAUD J - AEROSPATIALE.
Analyse critique des comparaisons des résultats de vol aux prévisions de soufflerie pour des avions de transport subsonique et supersonique.
AGARD CP n° 187 (1975).

[18] COLLARD D. -(AEROSPATIALE.)
Comportement à haute incidence d'un avion de transport à aile à grand élancement.
AGARD CP n° 247 (1978).

BLOCKAGE CORRECTIONS

$$M_c = M_u \left[1 + \left(1 + 0.2 M_u^2 \right) \varepsilon \right]$$

$$q_c = q_u \left[1 + \left(2 - M_u^2 \right) \varepsilon \right]$$

$$\varepsilon = \varepsilon_S + \varepsilon_W + \varepsilon_D$$

SOLID $\quad \varepsilon_S = \dfrac{V_m}{C^{3/2}} \, \Omega_S \, \dfrac{i}{\beta_c^3}$

WAKE $\quad \varepsilon_W = \dfrac{S C_{D_u}}{4C} \, \Omega_W \, \dfrac{1 + 0.4 M_c^2}{\beta_c^2}$

STALL $\quad \varepsilon_D = \dfrac{S C_{D_D}}{C} \, \dfrac{\theta}{2} \, \dfrac{1}{\beta_c^3}$

$$\theta \sim 2.8 - 0.068 \, \beta \lambda_a \qquad (1 < \beta \lambda_a < 10)$$

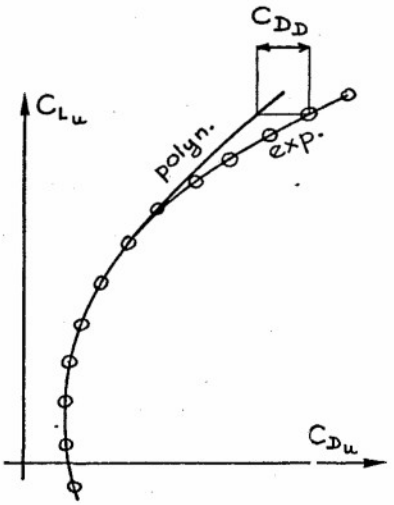

Fig. 1 : Coefficients de corrections de blocage

MIRAGE F FLAPS AND SLATS DOWN

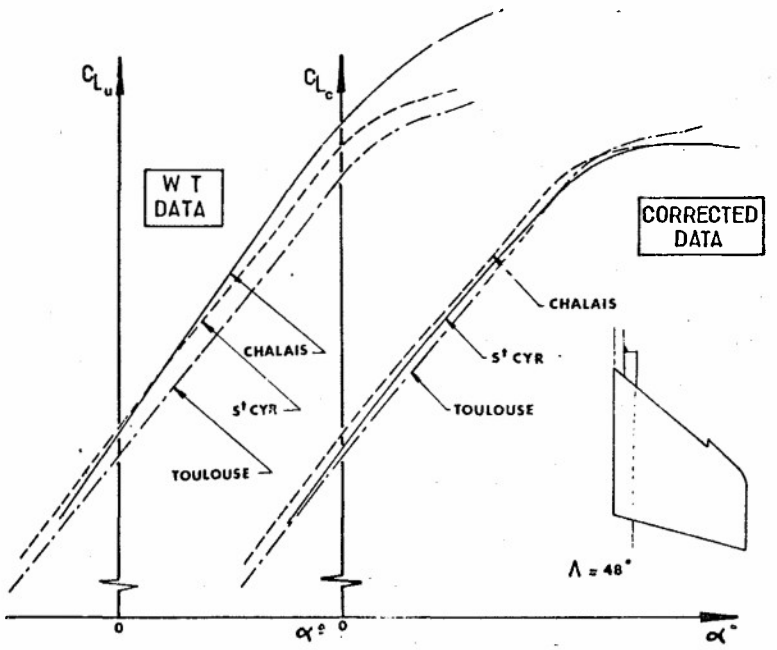

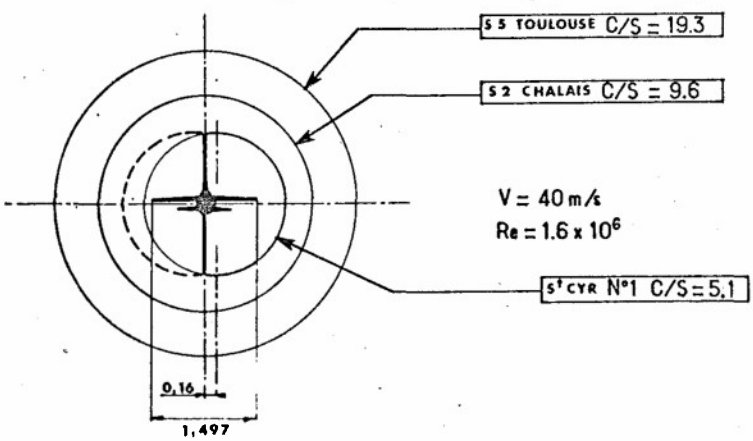

Fig. 2 : Comparaisons de résultats de soufflerie MIRAGE F hypersustenté

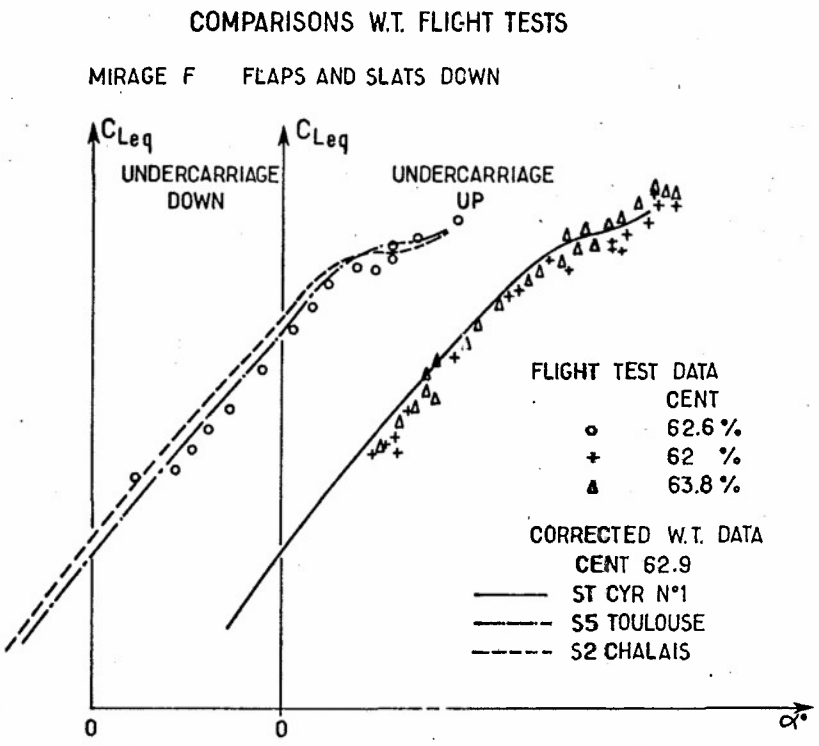

Fig. 3 : Comparaisons vol-soufflerie MIRAGE F hypersustenté

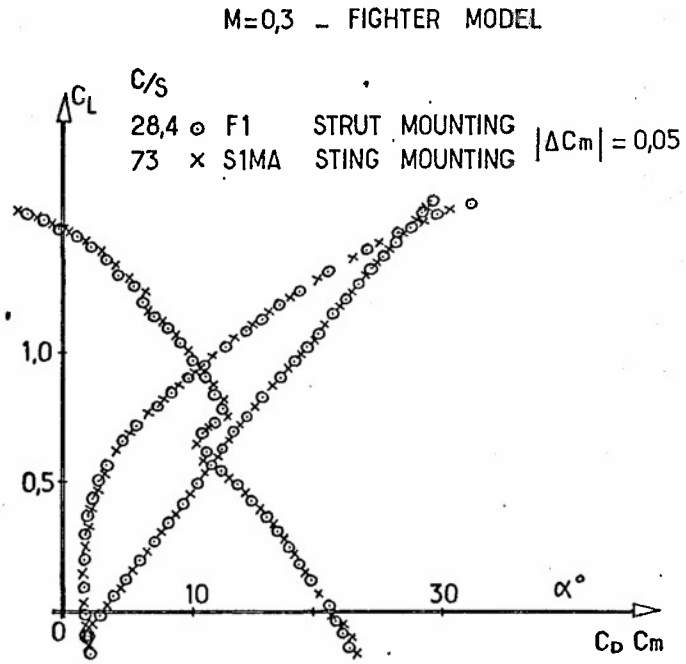

Fig. 4 : Comparaison des souffleries - F1 - S2MA Avion de combat - configuration lisse

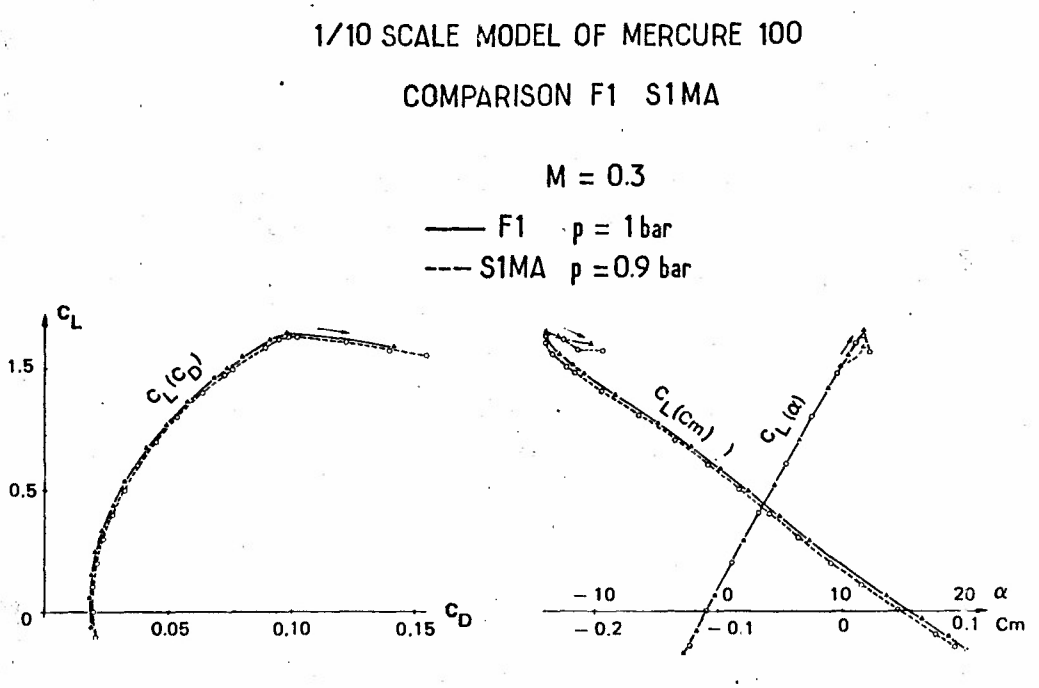

Fig. 5 : Comparaison des souffleries F1 - S1MA MERCURE 100 (éch. 1/10 - configuration croisière

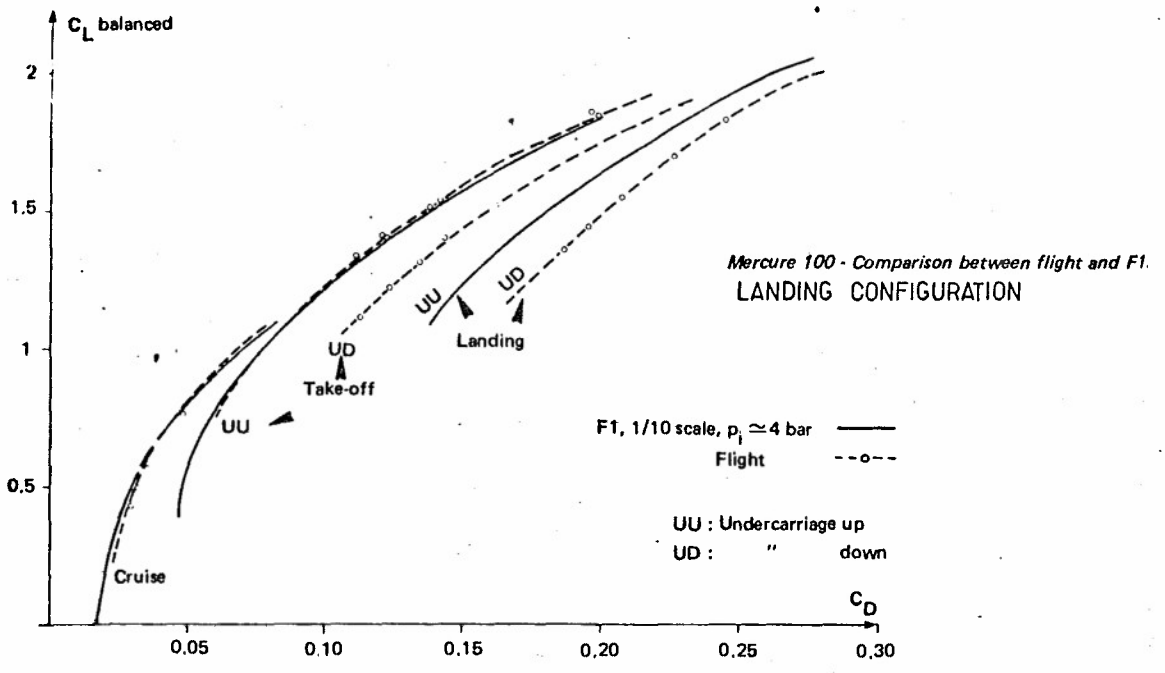

Fig. 6 : Comparaison vol - soufflerie MERCURE 100 - polaires équilibrées

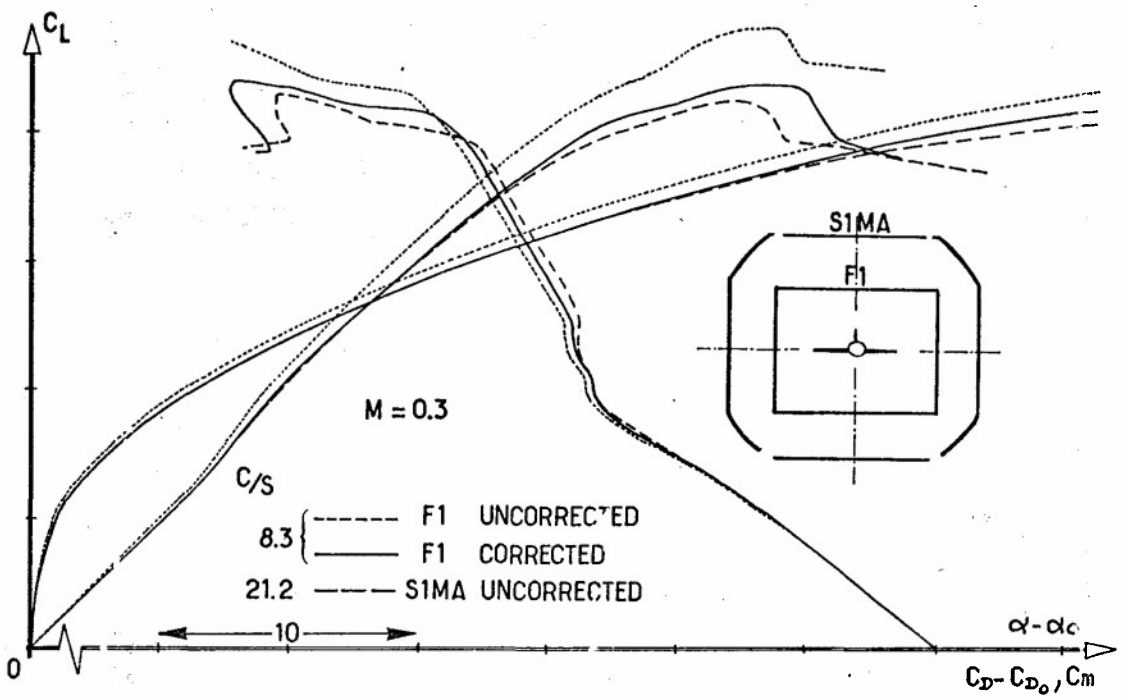

Fig. 7 : Comparaison des souffleries F1 - S1MA Maquette à forte flèche - Configuration lisse

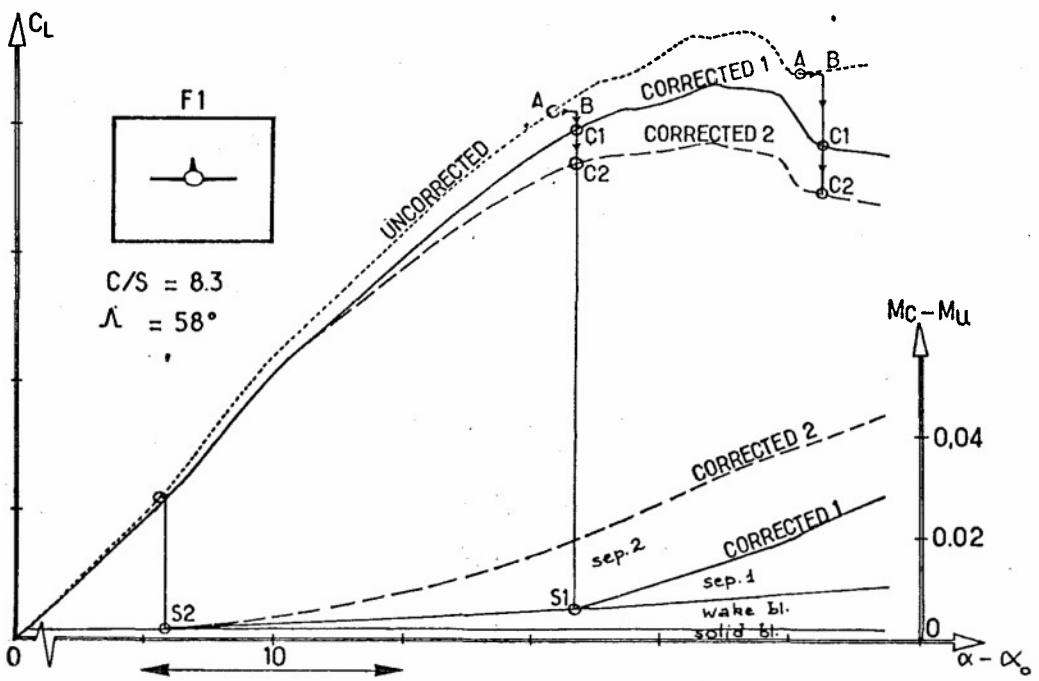

Fig. 8 : Influence de la correction de décollement Courbe CL, M (α)

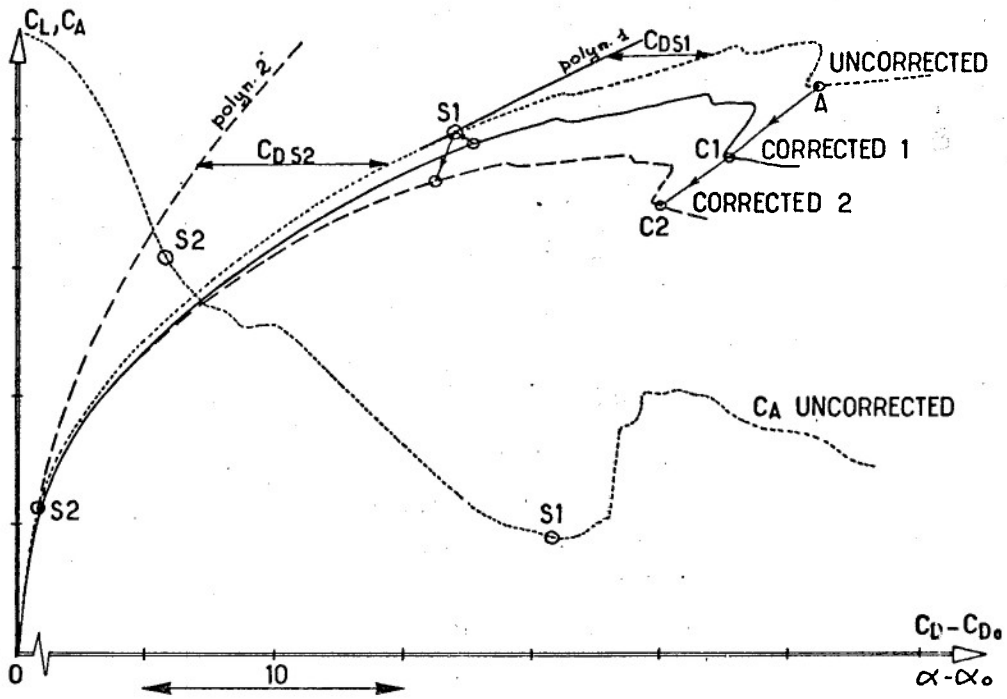

Fig. 9 : Influence de la correction de décollement Polaire - courbe CA (α)

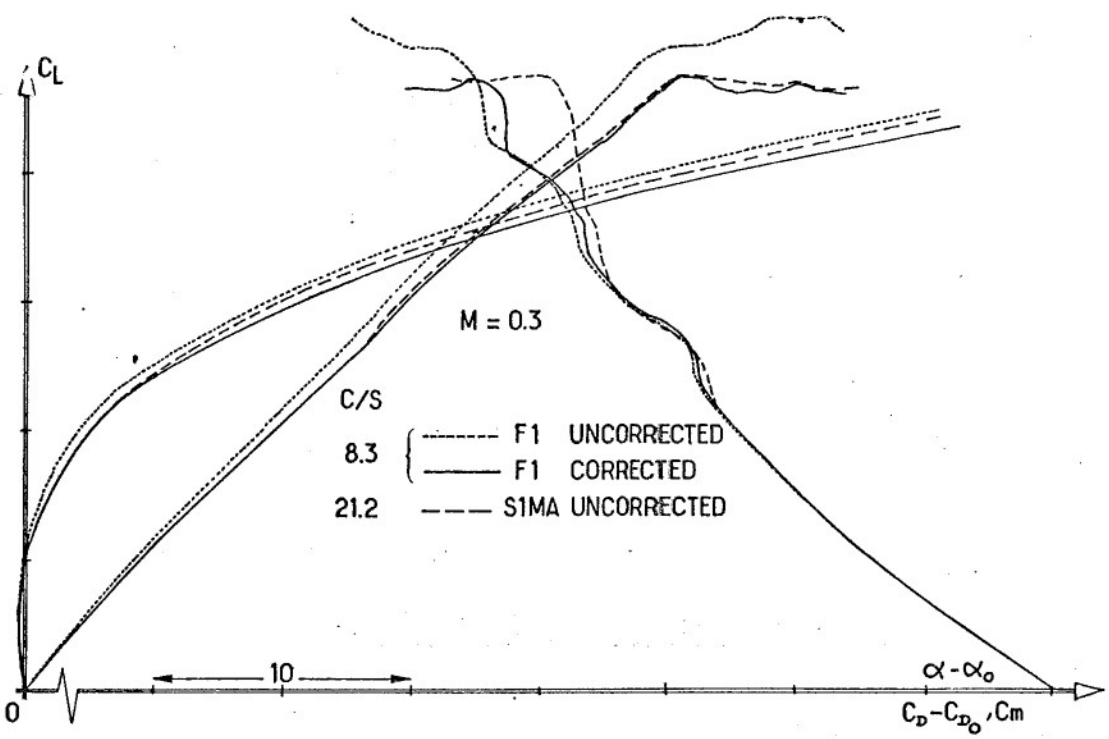

Fig. 10 : Comparaison des souffleries F1 - SIMA Maquette à forte flèche - configuration avec becs

Effect of the model schematisation on the lift correction coefficient

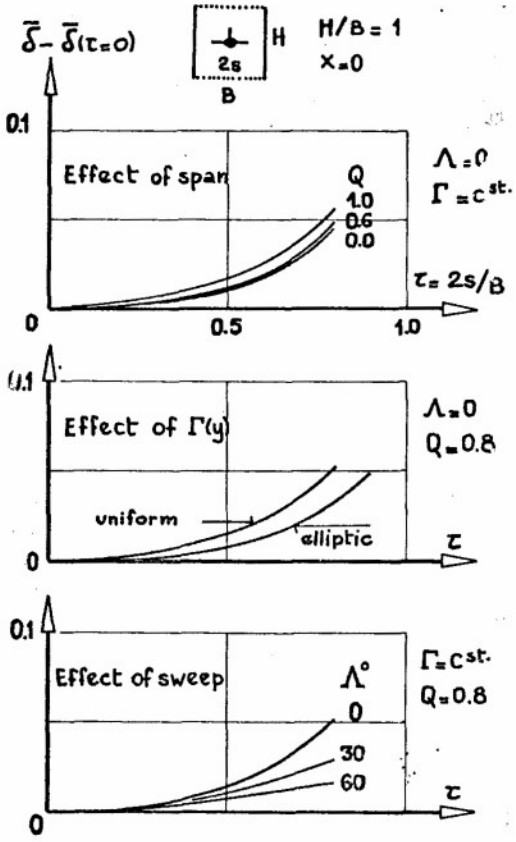

Fig. 11 : Influence de la schématisation de voilure sur la correction d'incidence

Fig. 12 : Influence d'un excentrement vertical de maquette

EFFECT OF VERTICAL MODEL OFFSET

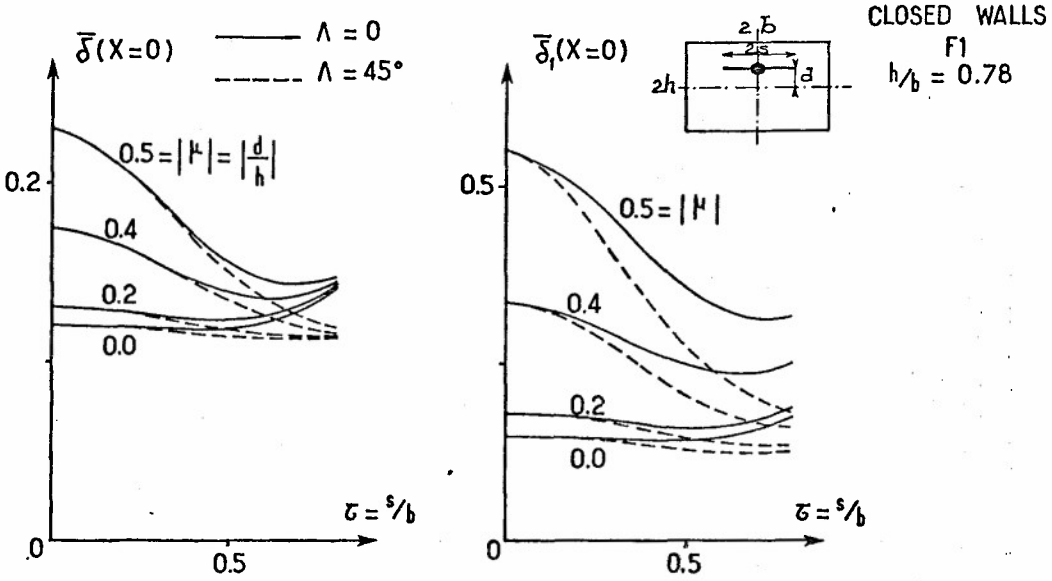

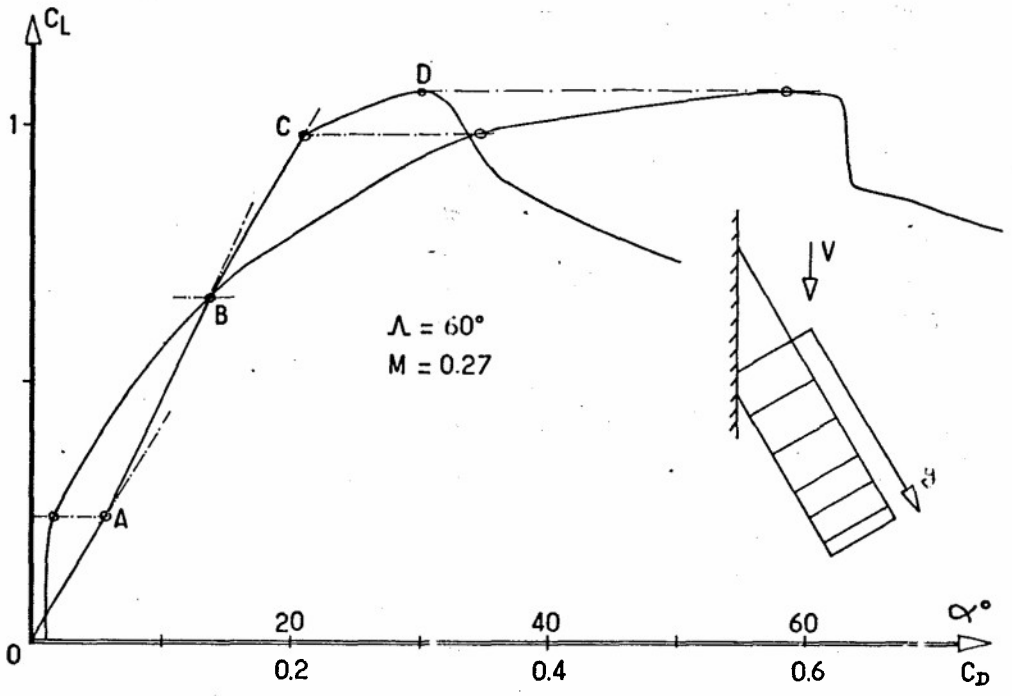

Fig. 13 : Aile à flèche variable $\Lambda = 60°$ Pesées globales - M = 0,27

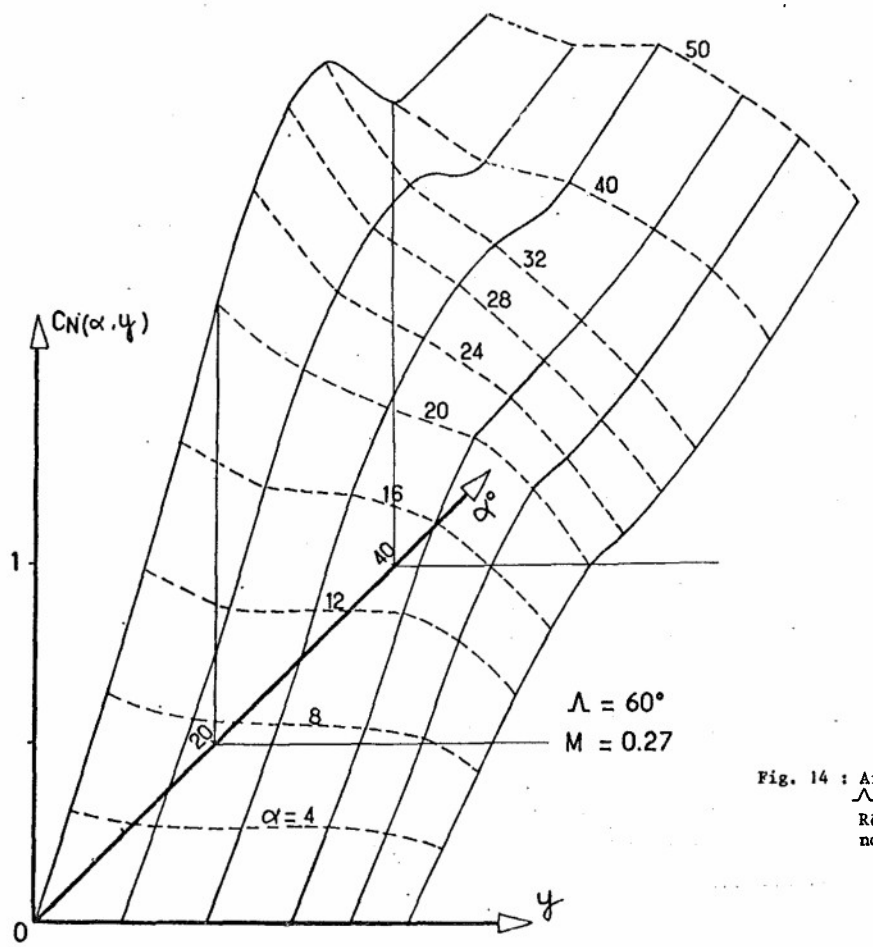

Fig. 14 : Aile à flèche variable $\Lambda = 60°$ - M = 0,27
Répartitions de force normale en envergure

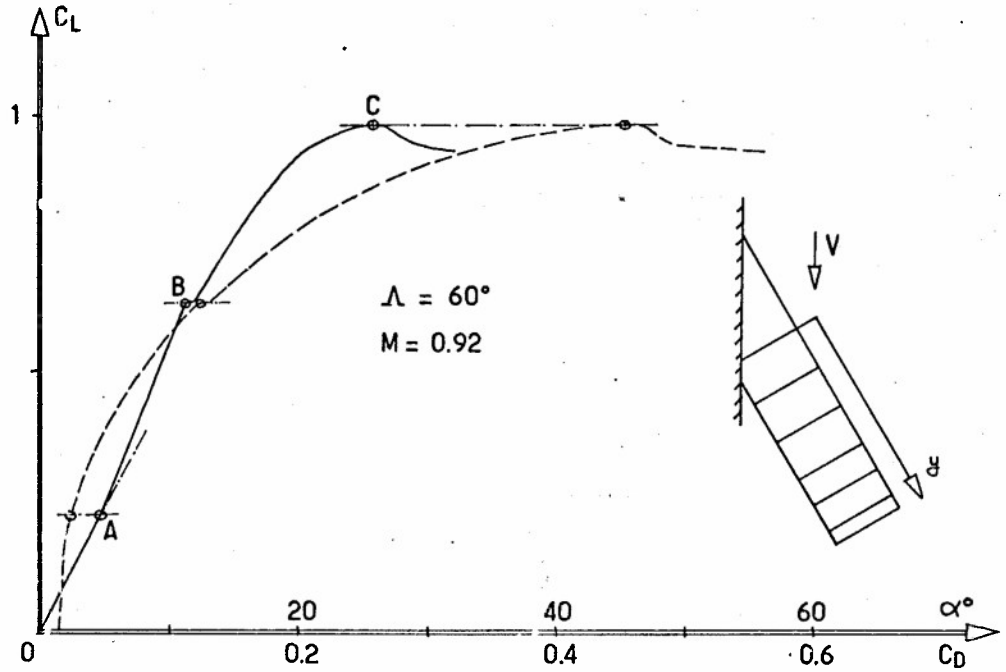

Fig. 15 : Aile à flèche variable Λ= 60° – M = 0,27 Pesées globales – M = 0,92

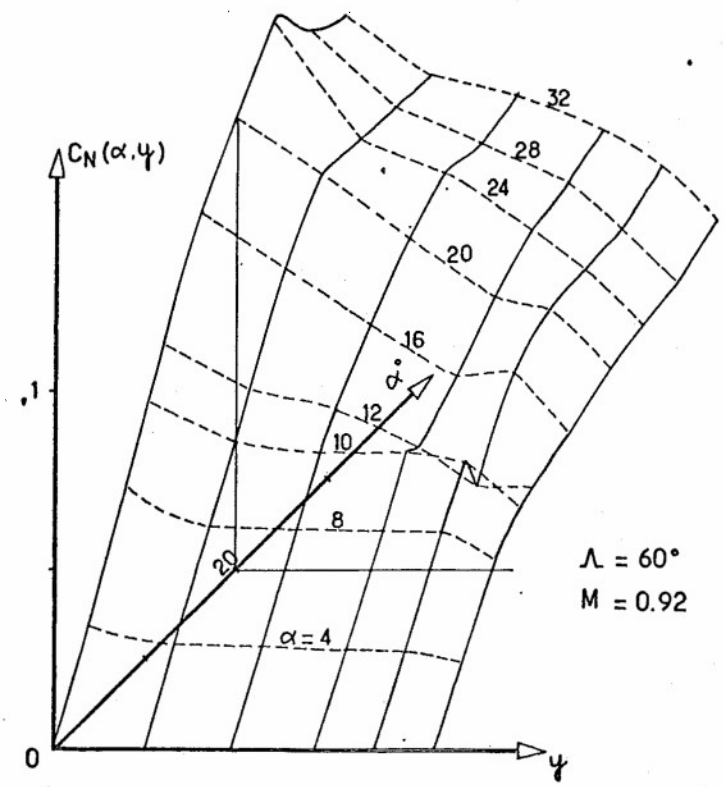

Fig. 16 : Aile à flèche variable Λ= 60° – M = 0,92 Répartitions de force normale en envergure

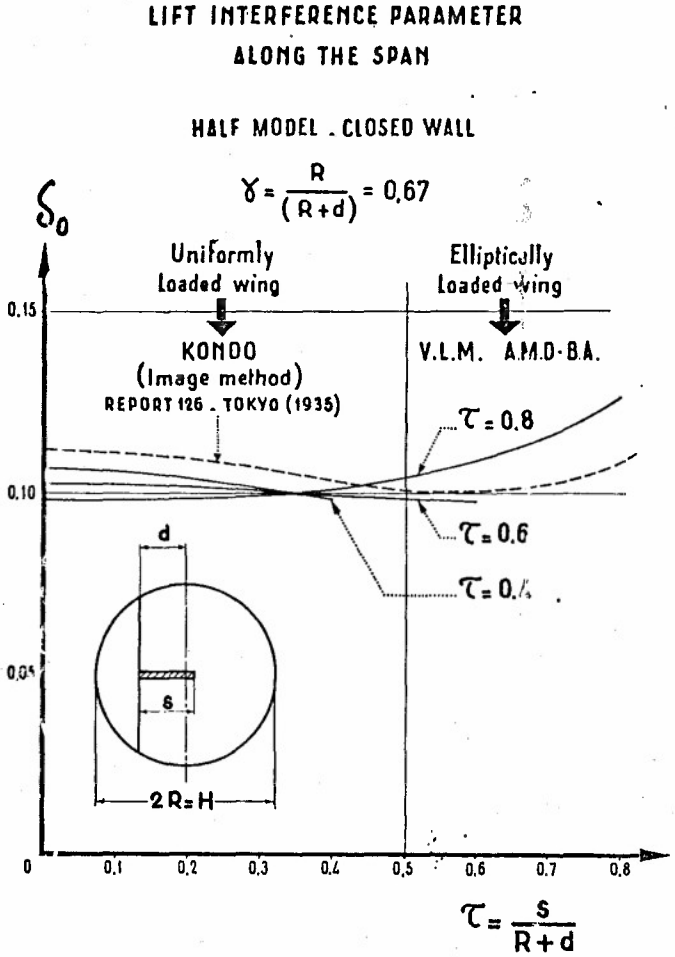

Fig. 17 : Répartition en envergure de correction d'incidence

Fig. 18 : Ecoulement 2D - Corrections à partir des signatures du profil

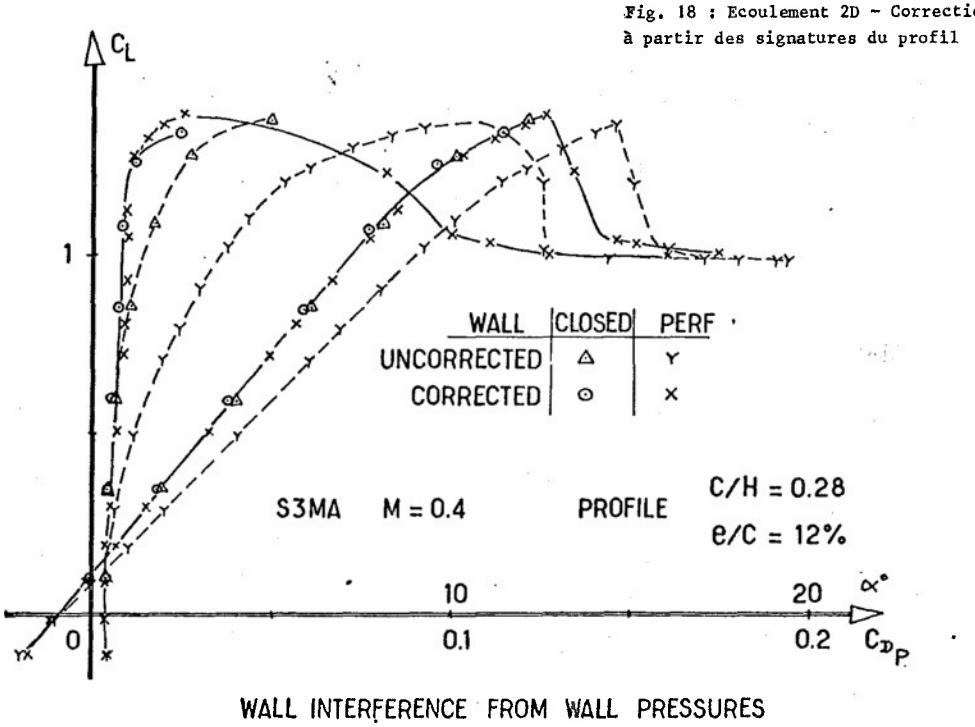

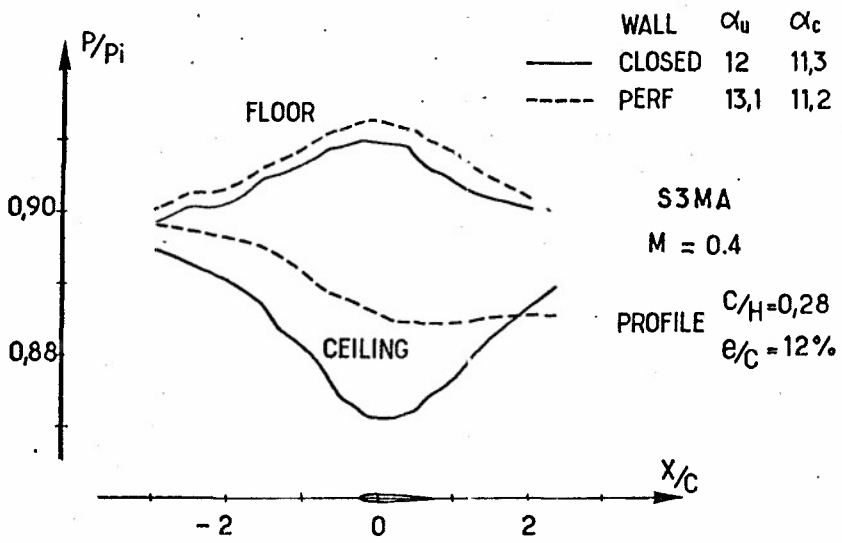

Fig. 19 : Ecoulement 2D - signatures du profil sur plancher et plafond de la veine

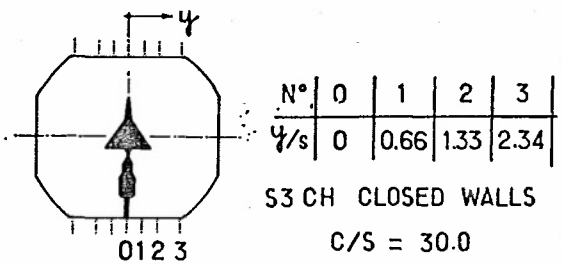

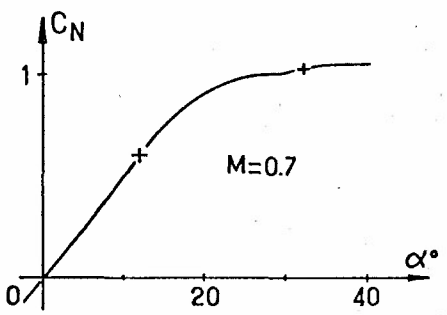

Fig. 20 : Maquette Delta 60° à S3Ch

3D WALL PRESSURES SIGNATURES

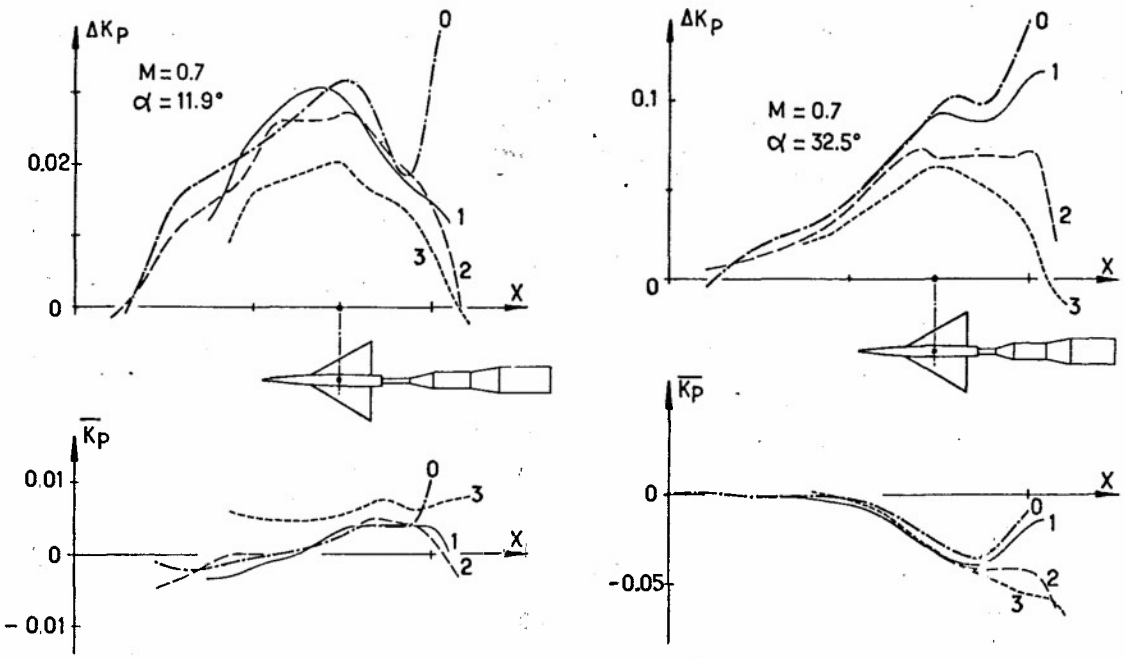

Fig. 21 : Ecoulement 3D - Signatures maquette en termes de blocage et de portance

STING INTERFERENCE ON DRAG

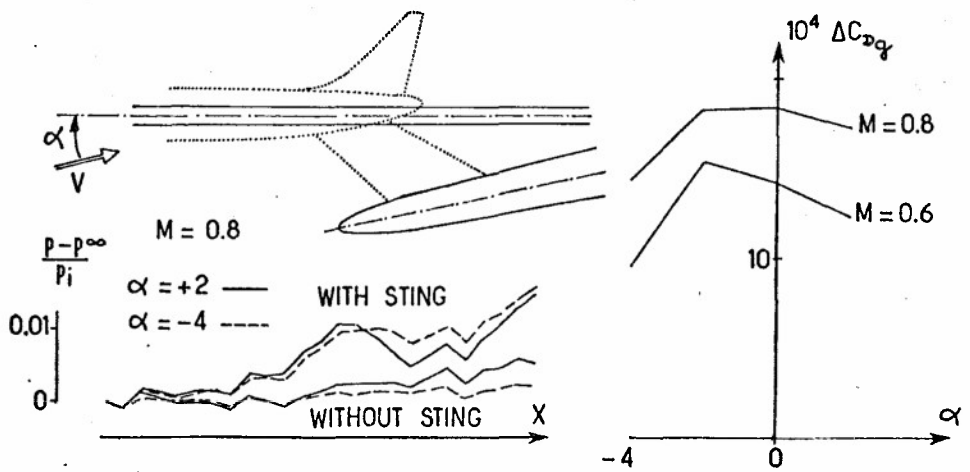

Fig. 22 : Interaction du dard support sur la traînée

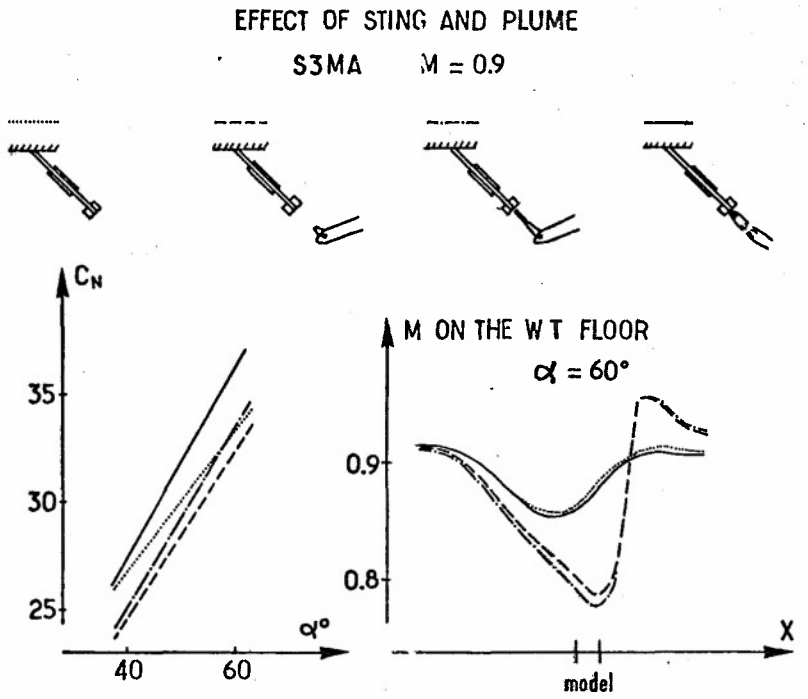

Fig. 23 : Influence des dards et je: sur un missile - S3MA - M = 0,9

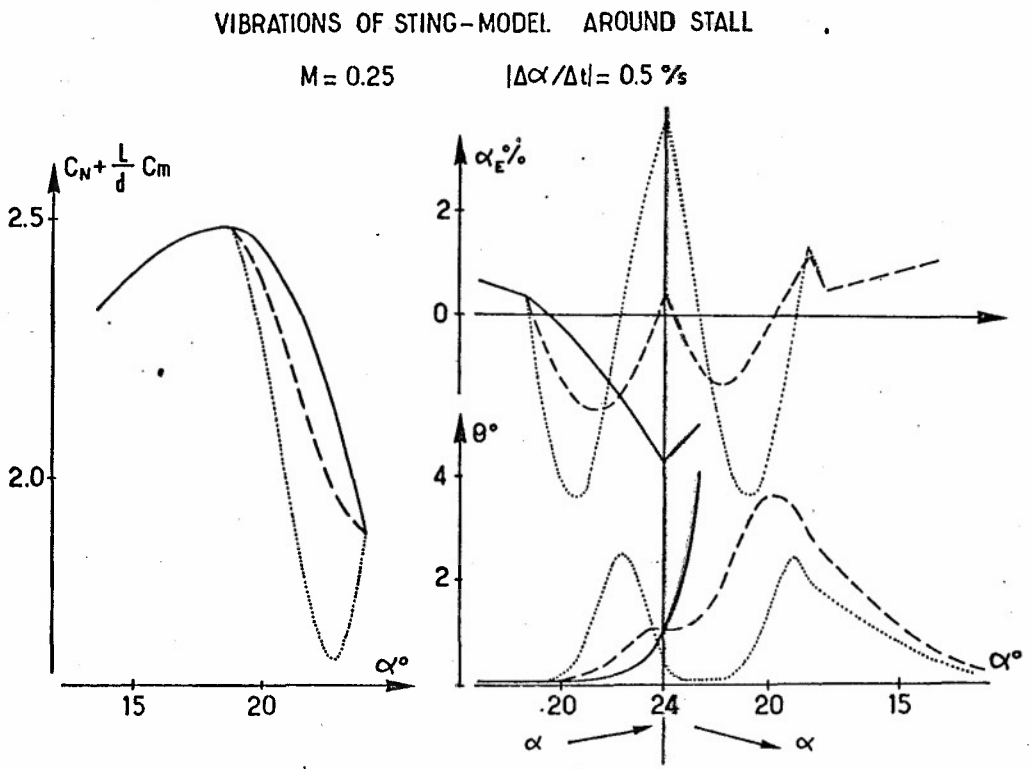

Fig. 24 : Vibrations d'une msquette en dard autour du décrochage

EFFECT OF THE PARAMETER $\Delta\alpha/\Delta t$
ON THE VIBRATION AMPLITUDE

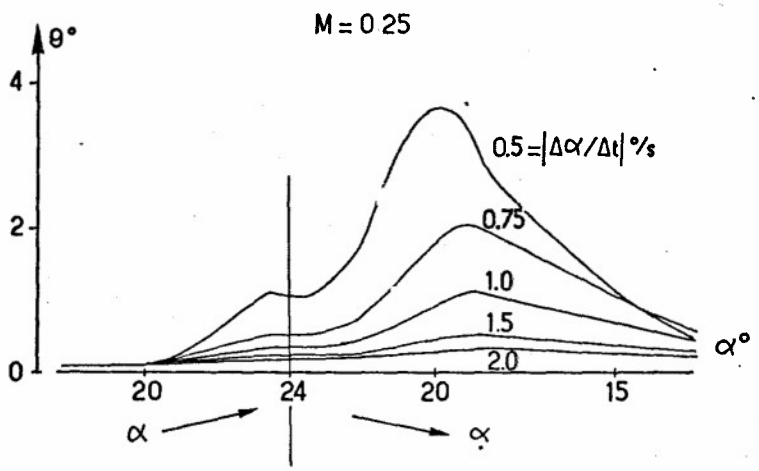

Fig. 25 : Influence de la vitesse de variation d'incidence sur l'amplitude des vibrations

HOW ARE CHECKED WALL CORRECTIONS VALIDITY ?

LEVEL OF MODEL DESCRIPTION

COMPARISONS

W.T., FLIGHT TESTS : R TRANSPOSITION, AEROELASTICITY

W.T., W.T. : SAME REYNOLDS

DIFFERENT MODELS OR W.T. OR WALLS

FLOW QUALITY

SIMILARITY

CORRECTED EQUIVALENT MODEL

STING INTERFERENCE

Fig. 26 : Contrôle de la validité des méthodes de corrections

GERMAN ACTIVITIES ON WIND TUNNEL CORRECTIONS

by

H. Holst
Deutsche Forschungs- und Versuchsanstalt für Luft- und Raumfahrt e.V.
Aerodynamische Versuchsanstalt Göttingen
Bunsenstrasse 10, D-3400 Göttingen, W. Germany

Abstract

To achieve better results from wind tunnel measurements it is necessary to carry out interference free measurements or to improve the methods to correct data to free flight conditions. This paper summarizes the main German activitities in this field.

- o Wind Tunnel interference factors have been calculated for open, closed, slotted and perforated walls using the vortex lattice method with a homogeneous boundary condition.
- o Taking the lift dependent relocation of the trailing vortices into account gives a more realistic pitching moment correction. Some results are presented.
- o For models large in comparison to the test section dimensions, the inhomogeneities of lift and blockage interference parameters throughout the test section have been investigated.
- o A method has been developed using measured wall pressures for the correction of drag in transonic wind tunnels.
- o For closed test sections, the image method and a modified vortex lattice method have been used to evaluate wall pressure signals for correction purposes.
- o A 2-d adaptive wall wind tunnel has been built giving encouraging results. Two different concepts of a 3-d adaptive wall wind tunnel are being pursued.

I. INTRODUCTION

In wind tunnel testing of models, the presence of the boundaries imposes a constraint on the flow not existing in free flight. To correct measured data to free flight conditions different methods have been developed to perform corrections of: Angle of attack (flow direction at the position of the wing), pitching moment (flow direction at the position of the tail), stagnation pressure (blockage effect), the wall induced curvature of the flow (induced camber of the wing), and the inhomogeneities in spanwise direction (effective twist).

To determine these corrections, potential theory can be used to compute interference factors and correct wind tunnel data to free flight conditions such as

- o the image method
- o the vortex lattice method
- o the wall perturbation method
- o and methods using measured wall pressure distributions.

In most cases the lifting system is represented by simple mathematical models such as horseshoe vortices, which are horizontal or follow a given trajectory. However, for high lift configurations this is no longer adequate. The trailing vortices are relocated due to the presence of the wind tunnel boundaries which means that the trajectory of the trailing vortices in the wind tunnel is different from the free flight trajectory. The pitching moment correction is different from that using horizontal trailing vortices. The correction now depends on the circulation of the wing which is not the case for horizontal trailing vortices. For the vortex lattice method computer programs do exist to account the relocation of the trailing vortices in the wind tunnel due to the presence of the tunnel boundaries by means of an iterative procedure.

Increasing the model size and the angle of attack (flow separation, wake blockage) not only leads to an increase of the applied corrections but also to an increase of their inhomogeneities. That means, e.g., that it is probably no longer permitted to apply average corrections for the whole model. One has to be aware of the possibility that the flow field around the model has substantially changed due to the presence of the wind tunnel boundaries. Measured data can then not be corrected to free flight conditions. Excluding these cases (when the flow field is substantially changed) it is most important to know more about boundary-induced effects and their inhomogeneities. This knowledge can be used to estimate the maximum tolerable model size for a given wind tunnel.

Generally there are three methods to avoid large corrections and high levels of their inhomogeneities.

- o reducing model size or very large test sections

- ventilated test sections (longitudinal slots and/or perforated walls to reduce the magnitude of the corrections and their inhomogeneities).
- adaptive wall concept (streamline matched test section) to cancel the corrections at all.

In the following some German work done in the fields mentioned above will be presented.

II. ANGLE OF ATTACK AND PITCHING MOMENT CORRECTIONS IN LOW SPEED WIND TUNNELS WITH ARBITRARY WALL CONFIGURATIONS

a. Open and closed test sections

In the past, corrections were computed using the image technique representing the lifting system by one single horseshoe vortex. Figure 1 shows the system of images. The interference factor δ_o is defined in the following equation:

$$\delta_o = \frac{w \; A_t}{2b \; \Gamma_w}$$

w	boundary induced vertical velocity
b	spanwidth of the model
A_t	cross-sectional area of tunnel
Γ_w	wing circulation.

The angle of attack correction is then given by

$$\Delta\alpha = \delta_o \frac{S_w}{A_t} c_L$$

S_w	wing area
c_L	lift coefficient

δ_o as well as its derivative in x-direction $\delta_1 = d\delta_o/dx$ was calculated at the location of the wing. The interference factor at the tail position (pitching moment correction) could then be found very simply by extrapolation, Figure 2 and Ref. 1.

The vortex lattice method for closed test sections, reported by Joppa[2] in 1967 and for open test sections reported by Doberenz[3] in 1974, has now been introduced for interference calculations in a version reported by Borovik[4] in 1973. This method can compute interference factors for open, closed, slotted and perforated test sections. This program can handle arbitrary cross sections; lift distributions and sweep-back angles of the wing can be prescribed. The representation of the tunnel boundaries by vortex squares or doublet sheets is shown in Figure 3. The lifting system is a set of horseshoe vortices shown in Figure 4. Calculations have been performed to check the validity of the method. The results have been compared (for closed test sections) with results of the Joppa[2] computer program modified by Holst[5].

Figure 5 and Figure 6 show the variation of interference factor in longitudinal and spanwise directions, respectively; parameter is the sweep-back angle Λ. In 1979 Schulz[6] presented computational results of interference factors for closed rectangular test sections using the image method. Figure 7 shows a typical result which gives an impression of the inhomogeneity of the wall interference in the main cross section (model position). Knowing the wall interference throughout the test section (at least along the span of the wing and the span of the tail) one can find average values for the correction factors of wing and tail. Corrections of angle of attack and pitching moment including induced camber and effective twist can then be performed.

b. Slotted wall test sections

As mentioned above the vortex lattice method is capable of calculating interference factors for slotted and/or perforated walls. Calculations were performed to investigate[5] the influence of slot geometry parameter K and porosity parameter R, respectively. Comparisons were made with computational results of an NLR program[7] using sources and sinks to represent the wind tunnel boundaries. Both methods use a homogeneous boundary condition which is shown in Figure 8 for various wall configurations. Figure 9 shows results. The agreement of the two methods is quite good for small values of Q ($Q = (1 + 1/R)^{-1}$). Figure 10 and Figure 11 show the influence of slot geometry parameter K and porosity parameter Q, respectively (see Appendix A for definition of parameters and homogeneous boundary condition).

Measurements were carried out in a wind tunnel with a square cross section of 1,3 m x 1,3 m with longitudinally slotted walls (12% open) at DFVLR-HNW Braunschweig. The experimental results indicated that the effect of the slots was smaller than predicted by theory. This is probably caused by a too small plenum chamber, and, therefore, experiments have begun with no plenum at all (i.e., very large plenum). It is intended to carry

out measurements in the DNW (German Dutch Wind Tunnel) with an 8 m x 6 m rectangular test section equipped with longitudinally slotted walls (0 - 12% open) to check the existing theories.

c. Vortex relocation due to the presence of the tunnel boundaries

For an improvement of pitching moment corrections for high lift configurations it might be necessary to take into account the vortex relocation. In 1973 Joppa[8] presented a vortex lattice method using a single horseshoe vortex as lifting system. He takes into account the vortex relocation due to the presence of the wind tunnel boundaries (closed test section). Equilibrium trajectories for the trailing vortices are found for the wing in tunnel and in free flight; the difference of the induced velocity fields is due to the presence of the wind tunnel walls. The horseshoe vortex model used for the iterative procedure is shown in Figure 12. This method was extended to open test sections by Holst[9] using doublet sheets instead of vortex squares to represent the wind tunnel boundaries and the wing. Figure 13 shows a sketch of the expected wake trajectories for open and closed tunnels. Figure 14 and Figure 15 give some typical results[10]. Figure 16 shows the interference factors with and without vortex relocation for different values of the downwash factor c_L/AR for an open test section (c_L = lift coefficient, AR = aspect ratio of wing).

III. BLOCKAGE CORRECTIONS

In various publications G. Schulz[11, 12, 13] reported about the inhomogeneities of solid blockage corrections throughout the test section. Using the image technique and superimposing point singularities representing the influence of model blockage, he computed τ, defined in the following equation:

$$\frac{\Delta v}{V_\infty} = \tau \cdot K \frac{V_m}{A_t^{3/2}} = \tau \cdot \lambda \left(\frac{S_w}{A_t}\right)^{3/2}$$

K, λ	model shape parameters
V_m	volume of the model
S_w	area of wing
A_t	cross-sectional area of the tunnel
Δv	boundary induced longitudinal velocity
V_∞	free stream velocity
T	$(= \frac{1}{2}\sqrt{\pi}\tau)$ tunnel shape parameter

Figure 17 shows an iso-line diagram of τ in the main cross section (i.e., $x = x_{model}$). Schulz investigated the influence of the following parameters:

span width/tunnel width	b/W
length of fuselage/tunnel width	l_f/W
eccentricity of model (model position)	y, z
tunnel height/tunnel width	H/W
spanwise distributions of volume	V(y)

A variety of computational results is presented in the references mentioned above. Figure 18 and Figure 19 show some results which can be used to determine the maximum tolerable model size for a given wind tunnel or to estimate the achievable accuracy of measurements (so far as blockage corrections are concerned).

IV. CORRECTIONS USING MEASURED WALL PRESSURES

a. Simple blockage corrections in closed subsonic wind tunnels

In 1978 Mercker and Fiedler[19] presented a simple blockage correction method for flows around bodies of arbitrary shape. The correction factor n is obtained experimentally by measuring the wall pressures at appropriate locations. The geometrical blockage ratio S_w/A_t, the thickness of the boundary layer at the model, the thickness of the boundary layer at the tunnel walls and the model shape do not enter into the correction scheme explicitly. They are taken care of by the correction factor n. The method can be applied for total ratios of blockage up to 25%, including boundary layer etc. It has been tested for flows about two-dimensional wedges and cylinders. In principle the method is also applicable to flows around three-dimensional models. For more details see Ref. 19.

b. Drag measurements in transonic wind tunnels

In order to increase the accuracy of drag measurements of slender bodies of revolution at zero angle of attack in transonic wind tunnels a correction method using measured wall pressures was proposed by MBB (Aulehla and Venghaus)[14,15,16]. This method can correct pressure distributions measured in a wind tunnel to free flight conditions. A theoretical wall pressure distribution (free flight, imaginary wall) is computed by a finite element method and compared with the wall pressure distribution which is measured together

with that of the model. The difference of measured and computed wall pressures can be used to find a perturbation potential thus allowing to correct the model pressure distribution. Figure 20 and Figure 21 show the principle of this method. Figure 22 shows one example of a corrected pressure distribution.

. Interference free data are necessary to prove the validity of this correction method and possibly extend it to models at angle of attack.

c. Correction method using measured wall pressures

For large models, high angles of attack and generally in cases with flow separation the computational correction methods based on potential theory are somewhat uncertain. As a contractor of DFVLR-HNW G. Schulz develops a correction method using measured wall pressures.

- o This universal method of correction is supposed to give correction factors for angle of attack, curvature of the flow, pitching moment, and stagnation pressure.
- o The method should provide reliable corrections using only geometric parameters of model and wind tunnel.

The problems that arise are

- o to properly position the static pressure holes at the walls
- o to separate the different corrections
- o to achieve high accuracy of computation as well as of the pressure measurements.

Schulz uses the image method and simple mathematical models to represent the lifting system and the influence of blockage (horseshoe vortices, doublets, sources and sinks) to find influence functions. Figure 23 shows a wall pressure distribution (influence function) in the main cross section for a single horseshoe vortex. The main advantage of the method proposed is that it takes into account the solid blockage and wake blockage automatically. It is not necessary to know more about the model and the flow field in its vicinity than just a few geometric parameters. This method is restricted to closed test sections.

It should be mentioned that the image method is adequate for evaluation of pressures at the tunnel walls because the boundary condition is fulfilled by definition. The singularities used to represent the model and its images are at some distance from the walls. This is not the case for the vortex lattice methods where the boundary condition is just fulfilled at a set of control points and the singularities representing the walls are embedded in the wall.

Schulz[20] presented first results; the validity of his method should be checked by experiments.

d. Modification of the vortex lattice method for wall pressure evaluations

It was mentioned above that the vortex lattice method is not appropriate for wall pressure evaluations. In the usual vortex lattice method the singularities and the control points are lying in the plane of the wall. The boundary condition is fulfilled at the control points. At points in the plane of the wall which are too close to the singularities the velocity field can not be evaluated.

On the other side the image method is not appropriate for slotted and perforated walls, it is restricted to open and closed test sections.

It was, therefore, tried to modify the vortex lattice method. This was done by shifting the plane containing the singularities outwards while keeping the control points at the same locations as before. As far as the angle of attack correction is concernd, this new method was successfully applied to closed test sections.

For the calculation of blockage corrections in closed test sections the vortex squares were substituted by 5 doublets per panel, also using this modified lattice approach.

More details of these methods including first results are given in Appendix B. Calculations for slotted and/or perforated walls will be carried out in the future to check the validity of these new methods.

V. ADAPTIVE WALL CONCEPT

a. 2-dimensional adaptive wall wind tunnel

U. Ganzer[16] reported investigations in a 2-dimensional adaptive wall wind tunnel of TU Berlin. Figure 24 shows schematically the adaptive wall concept. The flow field inside the wind tunnel is supplemented by a fictitious flow field outside the tunnel. Knowing the inner static wall pressure distribution and the shape of the wall a pressure distribution for the fictitious flow field outside the tunnel can be found. The pressure differences

$$\Delta c_p = c_{p_{inside}} - c_{p_{outside}}$$

can be taken to define a new pressure distribution for the fictitious flow outside the tunnel.

$$c_{p_{outside}}(n) + K\,\Delta c_p = c_{p_{outside}}(n+1)$$

with $0 < K < 1$.

This pressure distribution gives a new contour of the wall for an iterative procedure. The advantage of this method is, that measurements as well as computations are very easy to perform due to relatively small curvature of the wall. This method works without knowing anything about the geometry of the model and the flow field in its vicinity.

Results of pressure distribution measurements are shown in Figure 25 and Figure 26 demonstrating the validity of the adaptive wall concept by comparison with nearly interference free results. It should be noted that difficulties arise for flows with high pressure gradients or shock waves.

More recent pressure distribution measurements with a NACA 0012 model of higher accuracy than that used before show even better results than those mentioned above. The iterative procedure of wall adaptation is fully automated. The computer program for the fictitious outer flow field has been optimized, thus reducing the computation time from initially 30 sec for one iteration to now 8 sec on a TR 440.

Theoretical work for 2-dimensional investigations is carried out with a subsonic-panel-program (TU Berlin) and the transonic Bauer-Garabedien-Korn-program. This is necessary to estimate the magnitude of Reynolds number effects (measurements at $Re = 1.0 \,./.\, 1.6 \times 10^6$, comparable measurements mostly at $Re = 6 \times 10^6$) and to investigate the influences of model accuracy and remaining wall interference respectively.

b. 3-dimensional investigations

Two different models will be investigated: the body of revolution ONERA C5 and the wing fuselage combination ZKP-F4. Both models are being constructed now. Measurements will be performed in the 2-dimensional tunnel and in the 3-dimensional octagonal tunnel with 8 flexible walls shown in Figure 27. It is expected that the automatic procedure of wall adaptation for the 2-d test section will be applicable to the 3-d case. Theoretical investigations are carried out for estimation of the accuracy of computation for the 3-d outer flow field and for simulation of the iterative procedure of wall adaptation.

c. Another 3-d concept

At DFVLR Göttingen a feasibility study is being made for a different concept of a 3-d adaptive wall test section. This test section is planned to be a 0.8 m diameter deformable rubber tube. An existing high speed intermittent wind tunnel could then easily be equipped with these adaptive walls. It is planned to optimize the iterative procedure for the acquisition of one data point within 40 seconds.

VI. CONCLUSIONS

The magnitude and inhomogeneity of corrections set a limit to the model size. For real time application during wind tunnel tests appropriate average values should be taken for the correction factors.

A better pitching moment correction could be achieved by taking into account the vortex relocation because the interference factors are lift dependent. Time consuming computations are necessary, so that this correction cannot be applied in real time.

Ventilated test sections reduce the magnitude of interference factors. The inhomogeneities of interference will be investigated in the future. Measurements to check theory have begun.

A promising approach to correct pressure distributions with the aid of simultaneously measured wall pressures has been shown.

A method for corrections of angle of attack, pitching moment and stagnation pressure using measured wall pressures is being developed for closed test sections.

The methods mentioned above find their application in the range of "no substantial change of the flow field around the model" compared to free flight conditions. This sets a limit to or is a criterion for estimating maximum tolerable model size. In some cases the adaptive wall wind tunnel will be the only way to get corrigible or even interference free results.

Existing 2-d adaptive tunnel results are encouraging. A 3-d octagonal adaptive tunnel is being built in Berlin. The Göttingen high speed wind tunnel is being equipped with an adaptive-rubber-tube-test-section.

VII. REFERENCES

1. Kraemer, K., "Windkanalkorrekturen ohne und mit Bodenplatte in einem rechteckigen Freistrahl," Bericht 62A35, DFVLR-AVA Göttingen, 1962

2. Joppa, R.G., "A method of calculating wind tunnel interference factors for tunnels of arbitrary cross sections," NASA CR-845, July 1967

3. Doberenz, M.E., "Wind tunnel interference factors for high lift wings in open jet wind tunnels," Project report 74-18, Von Kármán Institute for Fluid Dynamics, 1640 Rhode St. Genèse, Chaussée de Waterloo 72, Belgium, 1974

4. Berovik, Y., Wasserstrom, E., and Rom, J., "Windtunnel boundary interference corrections, Part I: Theoretical calculations," Laboratory Report 0-124, Department of Aeronautical Engineering, Technion Israel Institute of Technology, Aeronautical Research Center, Haifa, Israel, 1972

5. Holst, H., "Berechnung von Windkanalinterferenzen nach dem Wirbelgitterverfahren," IB 157-80 A 01 DFVLR-HNW Göttingen, 1980

6. Schulz, G., "Beiträge zur Korrektur des Abwindfeldes in geschlossenen rechteckigen Windkanälen. (DNW-AKORR 1)," DFVLR-HNW Porz Wahn, 1979

7. Bleekrode, A.L., "Lift interference at low speed in wind tunnels with partly ventilated walls," Memo WD-75-085, NLR, The Netherlands, 1975

8. Joppa, R.G., "Wind tunnel interference factors for high lift wings in closed wind tunnels," NASA-CR 2191, February 1973

9. Holst, H., "Wind tunnel interference factors for high lift wings in open jet wind tunnels, including wake relocation effects," Project report 76-4. Von Kármán Institut for Fluid Dynamics, 1640 Rhode St. Genèse, Chaussée de Waterloo 72, Belgium, 1976

10. Holst, H., "Einfluß endlichen Strahlquerschnitts bei offenen Meßstrecken beliebigen Querschnitts," IB 157-79 A 08, DFVLR-HNW Göttingen (Vortrag DGLR am 7.2.1979 in Göttingen)

11. Schulz, G., "Die Verdrängungskorrekturen in Unterschallwindkanälen bei sperrigen Modellen und mit Bodensimulation," DLR-FB 74-46, 1974

12. Schulz, G., "Improved Displacement Corrections for Bulky Models and with Ground Simulation in Subsonic Wind Tunnels," AGARD-CP-174, October 1975, London

13. Schulz, G., "Verdrängungskorrekturen sperriger Modelle in geschlossenen rechteckigen Unterschallwindkanälen mit Berücksichtigung der Meßstrecken des Deutsch-Niederländischen Windkanals (DNW), Emmeloord, Holland," DFVLR-HNW, Porz-Wahn, 1979

14. Aulehla, F., "Drag Measurements in Transonic Windtunnels," AGARD-CP 242, October 1977, Paris

15. Venghaus, H.H., and Aulehla, F., "Grundlegende Gedanken zur Windkanalmeßtechnik und ein neues theoretisches Verfahren zur Ermittlung des Einflusses der Windkanalwandinterferenz," Vortrag DGLR am 7.2.1979 in Göttingen

16. Ganzer, U., "Windkanäle mit adaptiven Wänden zur Beseitigung von Wandinterferenzen," ZFW 3, März/April 1979 (Vortrag DGLR am 7.2.1979 in Göttingen)

17. Venghaus, H.H., "Theoretische und experimentelle Untersuchung der Windkanalwandinterferenzen," Forschungsbericht aus der Wehrtechnik, Auftragsnummer T/RF 42/70012/71411

18. Baldwin, B.S., Turner, J.B., and Knechtel, E.D., "Wall Interference in Wind Tunnels with Slotted and Porous Boundaries at Subsonic Speeds," NACA TN 3176, May 1954

19. Mercker, E., and Fiedler, H., "Eine Blockierungskorrektur für aerodynamische Messungen in geschlossenen Unterschallwindkanälen," ZFW 2, 1978, pp. 242-248

20. Schulz, G., "Bestimmung von Strahlgrenzkorrekturen aus Druckdifferenzmessungen an den Wänden des Windkanals. Teil I: Verarbeitung von Wanddrucksignalen für Korrekturzwecke," DFVLR-HNW, Porz-Wahn, 1980

Appendix A

Homogeneous boundary conditions (compare Ref. 4)

a. Longitudinally slotted wall

For an ideally slotted wall the pressure at the slots is assumed constant and equal to the free stream pressure, there is zero normal flow at the strips.

$$\frac{\partial \Phi}{\partial x} = u = 0 \quad \text{at the slot (open boundary)}$$

$$\frac{\partial \Phi}{\partial n} = v_n = 0 \quad \text{at the strips (closed boundary)}$$

Φ velocity potential

u velocity component parallel to free stream

v_n velocity component normal to the wall.

The slot geometry parameter K is defined according to

$$K = -\frac{1}{\pi} \ln \left[\sin \left(\frac{\pi a}{2l}\right)\right].$$

l slot separation
a slot width.

An approximate average boundary condition for a slotted wall was derived by Baldwin, Turner and Knechtel[18]:

$$\frac{\partial \Phi}{\partial x} + K \frac{\partial^2 \Phi}{\partial x \partial n} = 0$$

or using the velocity components

$$u + K \frac{\partial v_n}{\partial x} = 0$$

This is the boundary condition for an ideally slotted wall, disregarding any viscous effects in the slots.

b. Perforated walls

The linearized approximation to a viscous flow through a porous medium is:

$$\frac{\partial \Phi}{\partial n} = v_n = \frac{R}{\rho V_0} \Delta p$$

ρ density
Δp pressure drop across the wall

$$R = \frac{Q}{1-Q}, \qquad Q = \frac{R}{1+R}$$

porosity parameters

Introducing the compressiblity correction factor $\beta = \sqrt{1 - M^2}$ gives the boundary condition for an ideally perforated wall:

$$u + \frac{\beta}{R} v_n = 0.$$

The value for the porosity parameter R must be found experimentally.

c. Homogeneous boundary condition

A homogeneous boundary condition is fulfilled at a set of control points. It can be written in the following way to give a general boundary condition

$$A \frac{\partial \Phi}{\partial x} + K \frac{\partial^2 \Phi}{\partial x \partial n} + \frac{\beta}{R} \frac{\partial \Phi}{\partial n} = 0.$$

or, using the velocity components

$$Au + K \frac{\partial v_n}{\partial x} + \frac{\beta}{R} v_n = 0.$$

This general boundary condition covers all cases of test section boundaries with the proper constants for A (0.0 or 1.0), K and R.

APPENDIX B

Modified vortex or doublet lattice approach

a. Angle of attac correction

For the evaluation of wall pressures the vortex lattice method has been modified. This is shown in the following sketch.

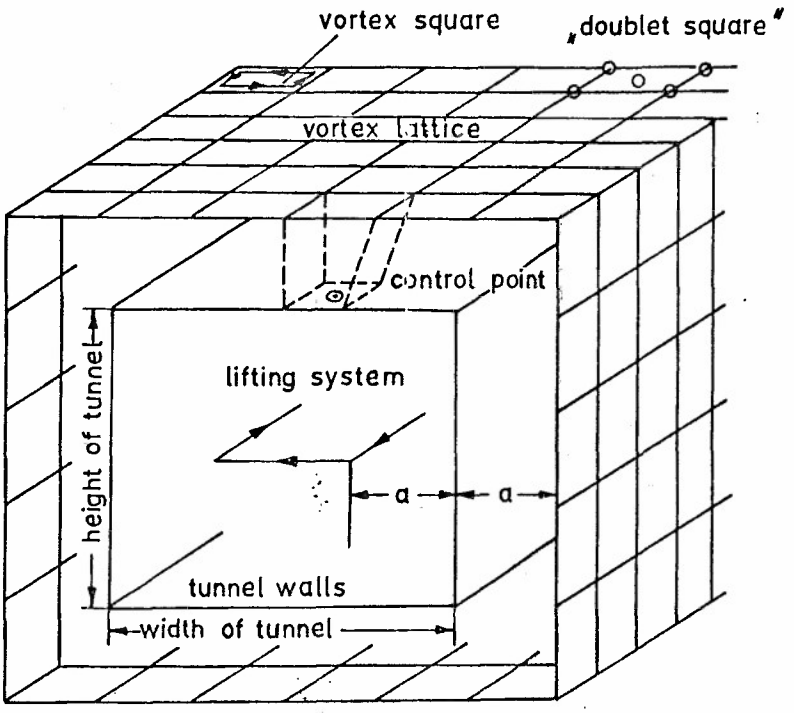

The planes containing the vortex squares are shifted outwards; the distance from the tip of the wing to the wall is the same as the distance from the wall to the vortex lattice. The control points are, of course, kept at the same locations before, i.e., in the plane of the tunnel walls. The homogeneous boundary condition for slotted or perforated walls can easily be applied at the control points.

For closed test sections this method has been proved to give correct results as is shown in the following plot of the wall pressure influence function $\delta x_w / \delta_{zo}$:

$$\delta_{zo} = \frac{wA_t}{2b\Gamma_w} \qquad \text{(at the position of the model)}$$

$$\delta_{xw} = \frac{v_x A_t}{2b\Gamma_w} \qquad \text{(at the walls)}$$

w boundary induced vertical velocity

Γ_w wing circulation

A_t test section cross sectional area

v_x boundary and wing induced velocities in x-direction at the walls

b spanwidth

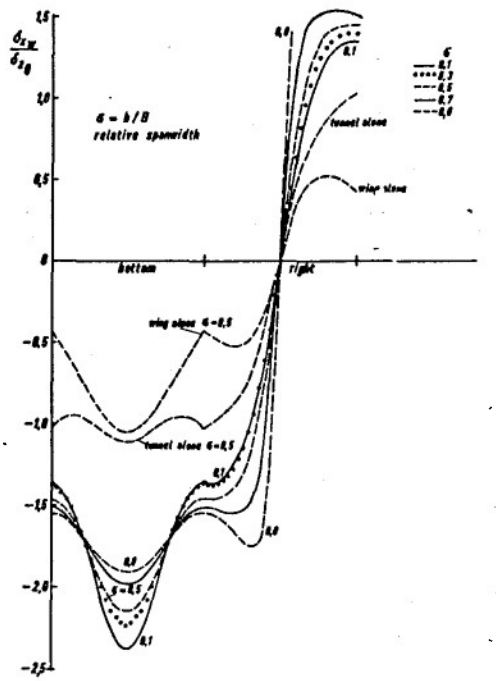

main cross section
($x = x_{model}$)

b. Blockage correction

In the case of calculating blockage interference parameters the lifting system (represented by a single horseshoe vortex or a set of horseshoe vortices) is substituted by a doublet or a set of doublets to represent model blockage. The vortex squares are substituted by "doublet squares" with 5 doublets each. The result is presented in the following figure as an isoline diagram of τ, A single doublet represents the model.

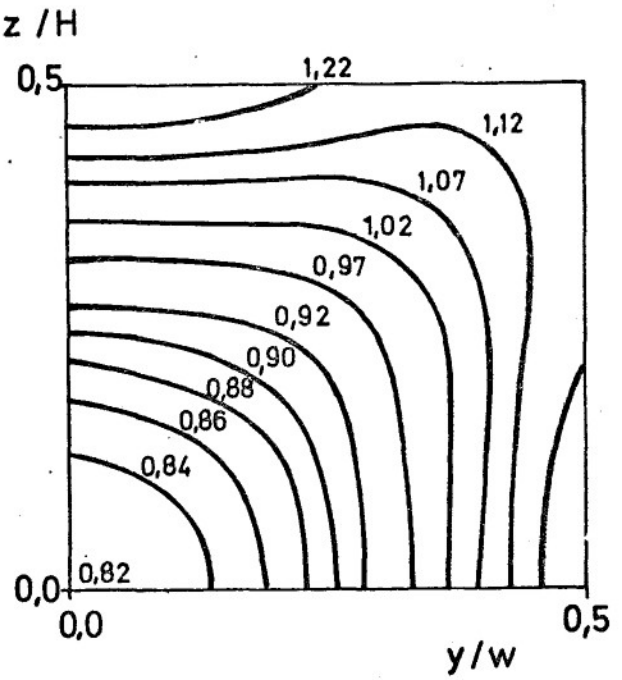

main cross section
($x = x_{model}$)

This new method will be applied to slotted and perforated walls using a homogeneous boundary condition.

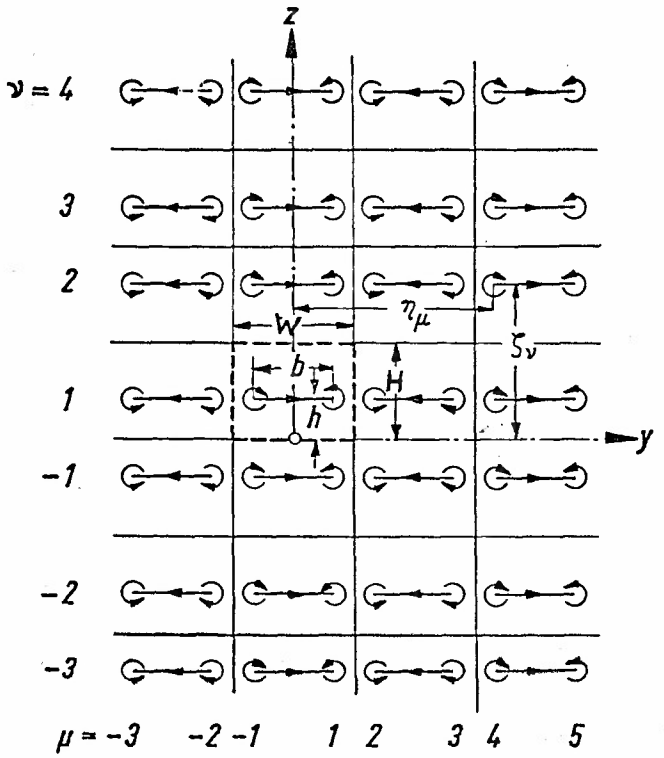

Fig. 1: System of images for an open test section ($x = x_{wing}$, main cross-section).

W width of test section
H height of test section
b spanwidth of model
h height of model
$\eta_\mu = 2W - \frac{b}{2}$
$\zeta_\nu = H + h$

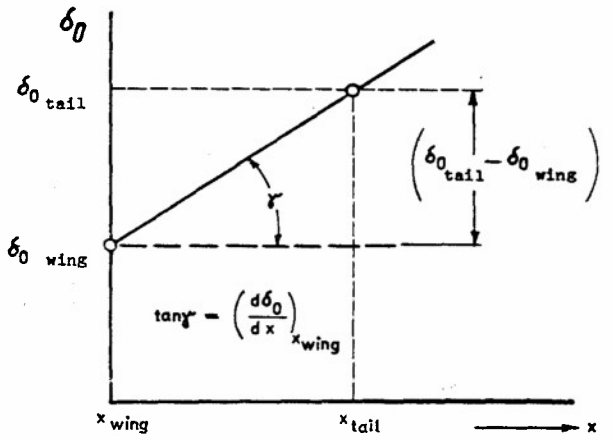

Fig. 2: Simple method to determine the interference factor at the position of the tail by extrapolation.

$$\delta_0 = \frac{w\,HW}{2b\,\Gamma_w} = \frac{w\,A_t}{2b\,\Gamma_w}$$

w boundary induced vertical velocity
b spanwidth of model
W width of wind tunnel
H height of wind tunnel
$A_t = W \cdot H$ cross - sectional area of wind tunnel
Γ_w wing circulation

$$\delta_{0_{tail}} = \delta_{0_{wing}} + \left(\frac{d\,\delta_0}{dx}\right)_{x_{wing}} \cdot x_{tail}$$

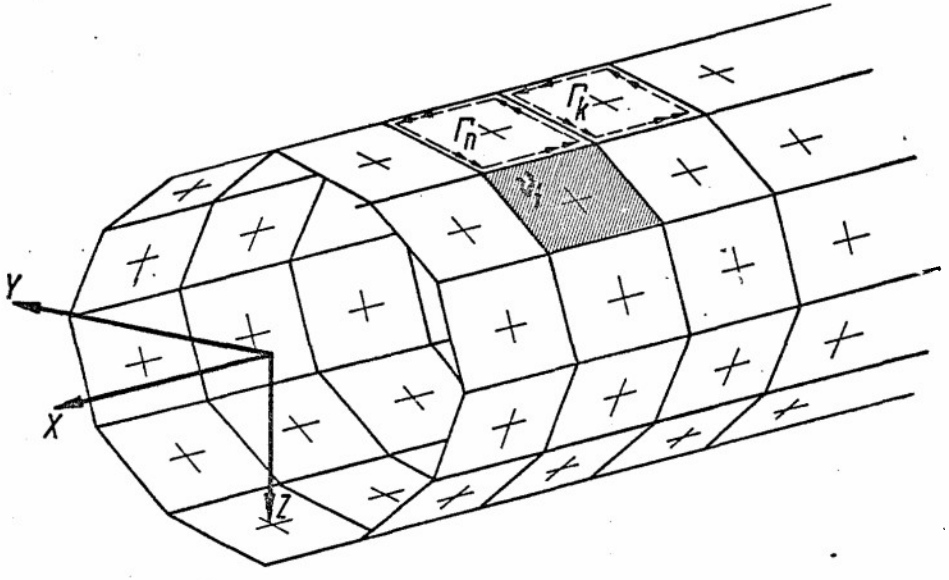

Fig. 3: Representation of wind tunnel boundaries by vortex "squares" or doublet panels. The tunnel may have arbitrary cross section.

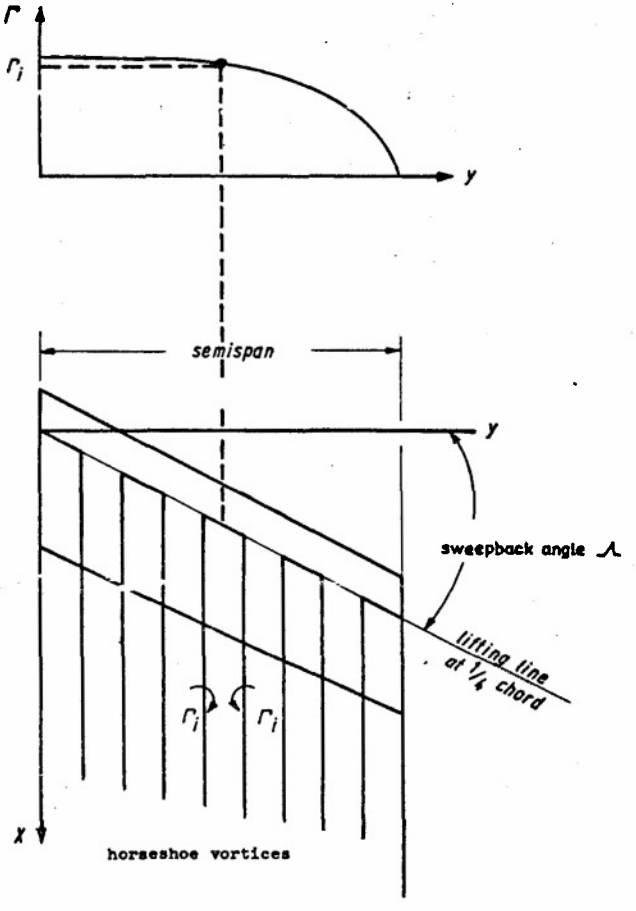

Fig. 4: Mathematical model of the wing

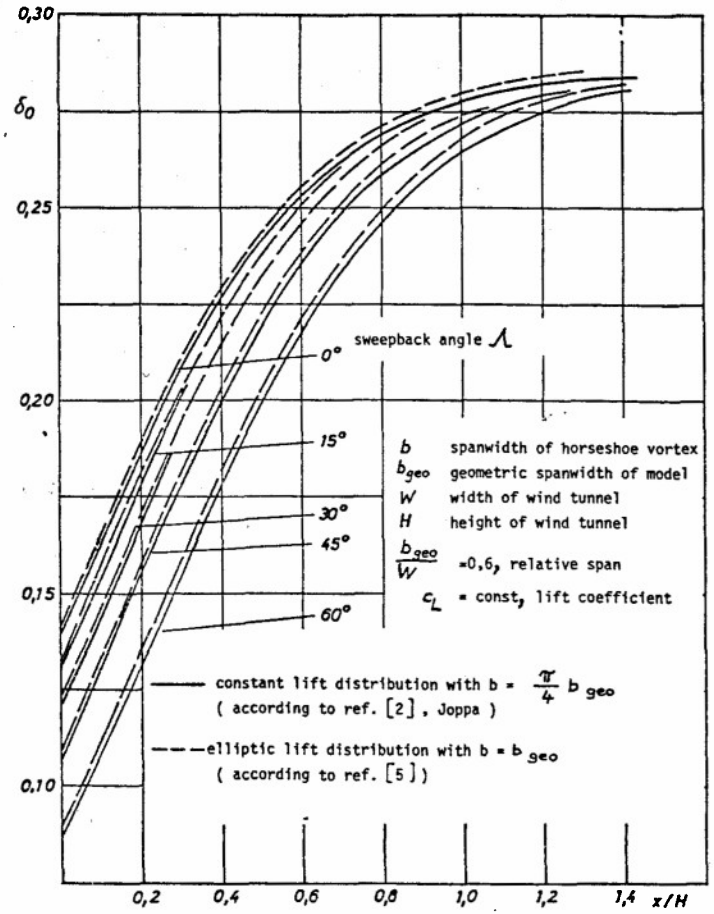

Fig. 5: Interference factors on centerline for a closed square test section, comparison of constant and elliptic lift distribution.

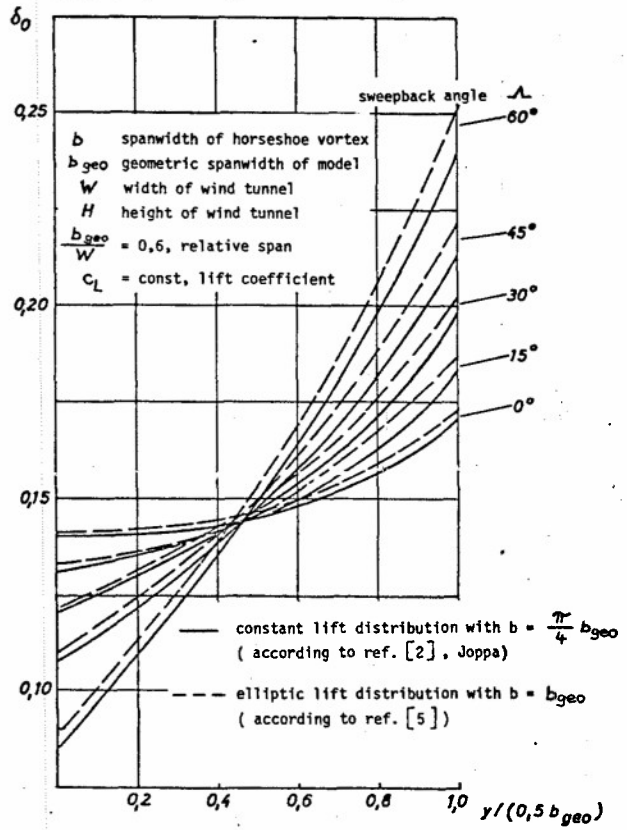

Fig. 6: Interference factors along span for a square closed test section, comparisor of constant and elliptic lift distribution.

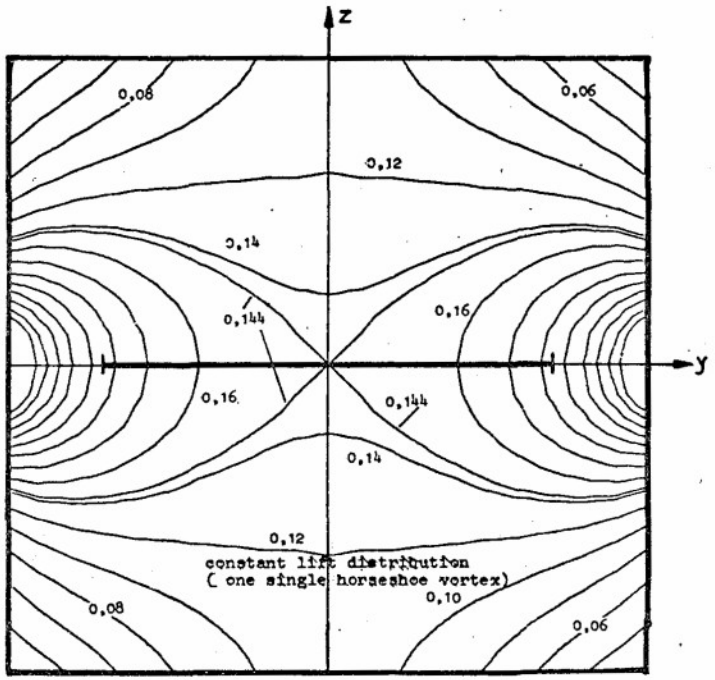

Fig. 7: Downwind corrections in a closed square wind tunnel iso- lines of δ_0 in the main cross section ($x = x_{model}$).

b spanwidth of horseshoe vortex

W width of wind tunnel

H height of wind tunnel

Λ = 0° sweepback angle of wing

$\frac{b}{W}$ = 0,7 relative span of horseshoe vortex

1.	closed walls		v_n		=	0
2.	ideally perforatsd	u +	$\frac{\beta}{R} v_n$		=	0
3.	ideally slotted	u +		$K \frac{\partial v_n}{\partial x}$	=	0
4.	slottsd wall with viscous sffects	u +	$\frac{\beta}{R} v_n$	+ $K \frac{\partial v_n}{\partial x}$	=	0 *)
5.	open boundaries	u			=	0

u induced velocity at the wall (x-direction, parallsl to V_∞ and ths wall)

v_n induced velocity at the wall (normal)

Fig. 8: Homogsneous boundary condition at ths wall for various cases (compars appsndix A).

*) In this cass the porosity parameter R takes into account viscous cross flow in the slots, see also appendix A.

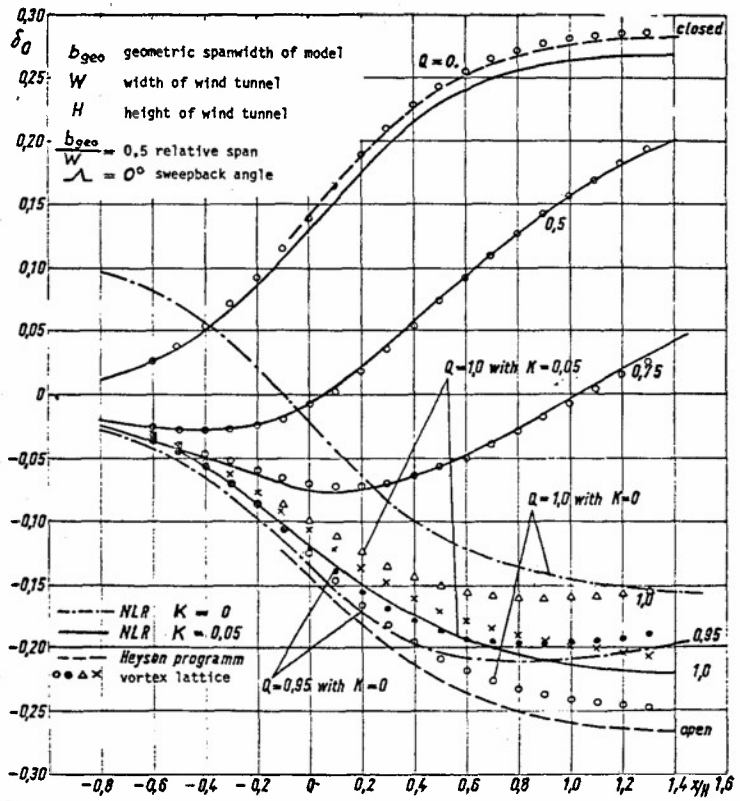

Fig. 9: Comparison of vortex lattice method (ref. 5) with the method using sources and sinks (ref.7) and Heyson program, ventilated walls, square cross section.

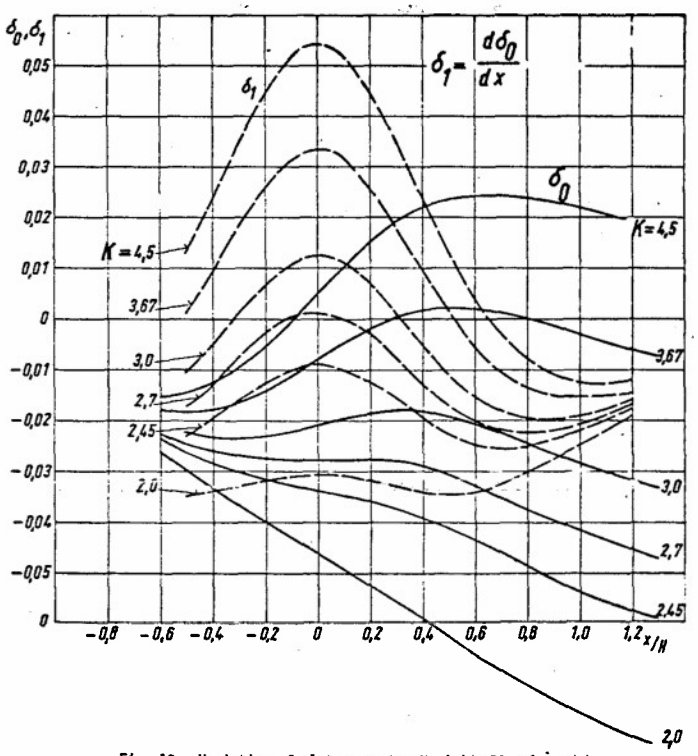

Fig. 10: Variation of slot parameter K (ideally slotted).

b_{geo} geometric spanwidth of model
W width of wind tunnel
H height of wind tunnel
$\frac{H}{W}$ = 0,75 (rectangular cross section)
$\frac{b_{geo}}{W}$ = 0,6 relative span
Λ = 0° sweepback angle
elliptic lift distribution

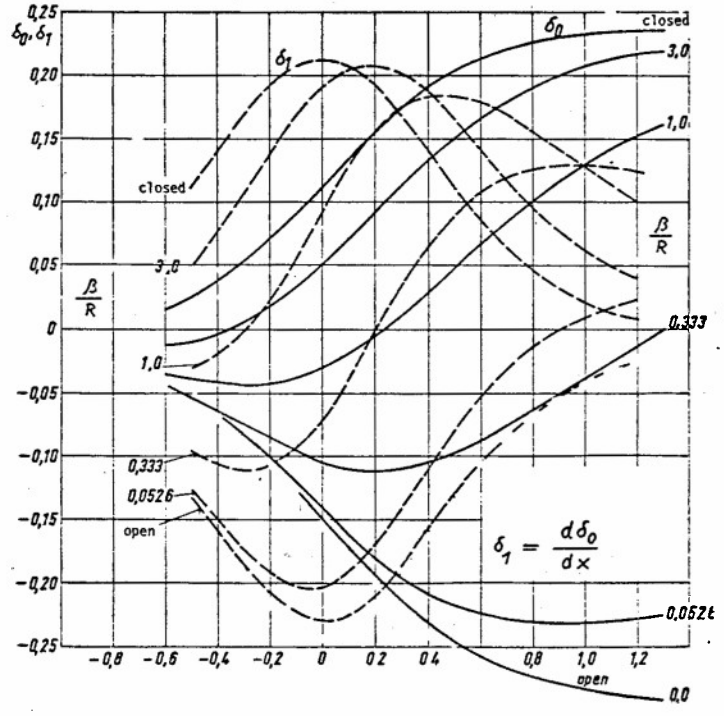

Fig. 11: Variation of porosity parameter $\frac{\beta}{R}$ (ideally perforated).

b_{geo} geometric spanwidth of model
W width of wind tunnel
H height of wind tunnel
$\frac{H}{W} = 0{,}75$ (rectangular cross section)
$\frac{b_{geo}}{W} = 0{,}6$ relative span
$\Lambda = 0^0$ sweepback angle
elliptic lift distribution

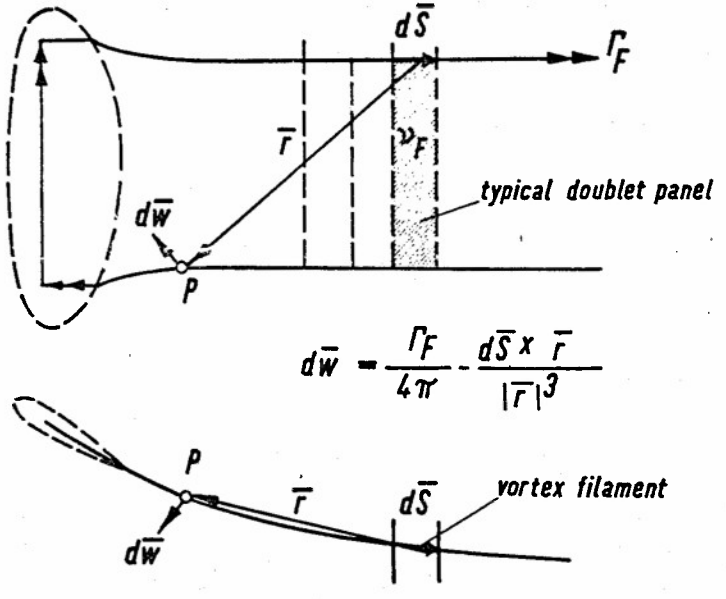

Fig. 12: Representation of lifting system (horseshoe vortex) for iterative procedure

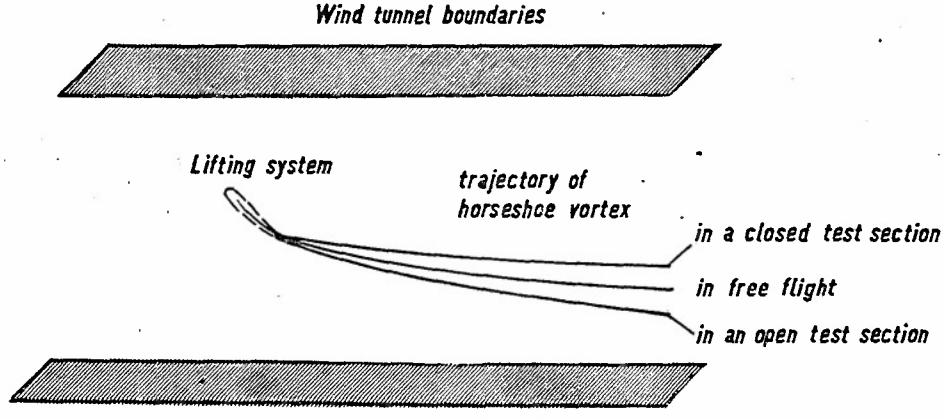

Fig. 13: Relocation of the trailing vortices due to the presence of wind tunnel boundaries

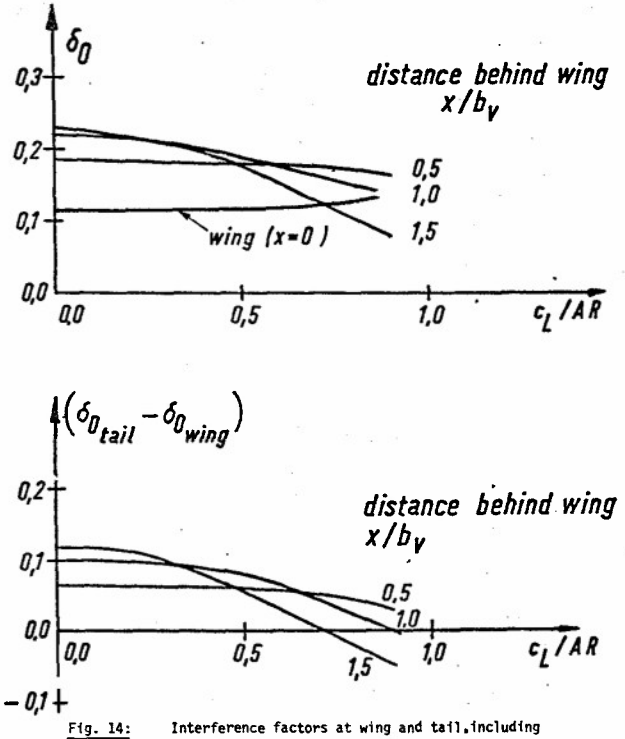

Fig. 14: Interference factors at wing and tail, including relocation effects of the trailing vortices, tail on tunnel centerline, closed test section.

$b_v = b = \frac{\pi}{4} b_{geo} = 0{,}75$ spanwidth of horseshoe vortex
$W = 1{,}5$ width of wind tunnel
$H = 1{,}0$ height of wind tunnel
c_L Lift coefficient
AR aspect ratio
c_L/AR downwash factor

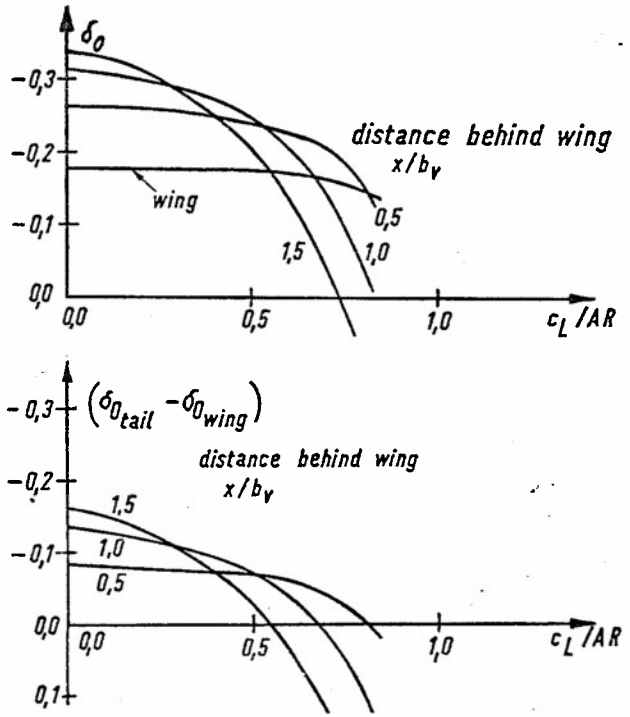

Fig.15: Interference factors at wing and tail, including relocation effects of the trailing vortices, tail on tunnel centerline, open test section

$b_v = b = \frac{\pi}{4} b_{geo} = 0{,}75$ spanwidth of horseshoe vortex

$W = 1{,}5$ width of wind tunnel
$H = 1{,}0$ height of wind tunnel
c_L lift coefficient
AR aspect ratio
c_L/AR downwash factor

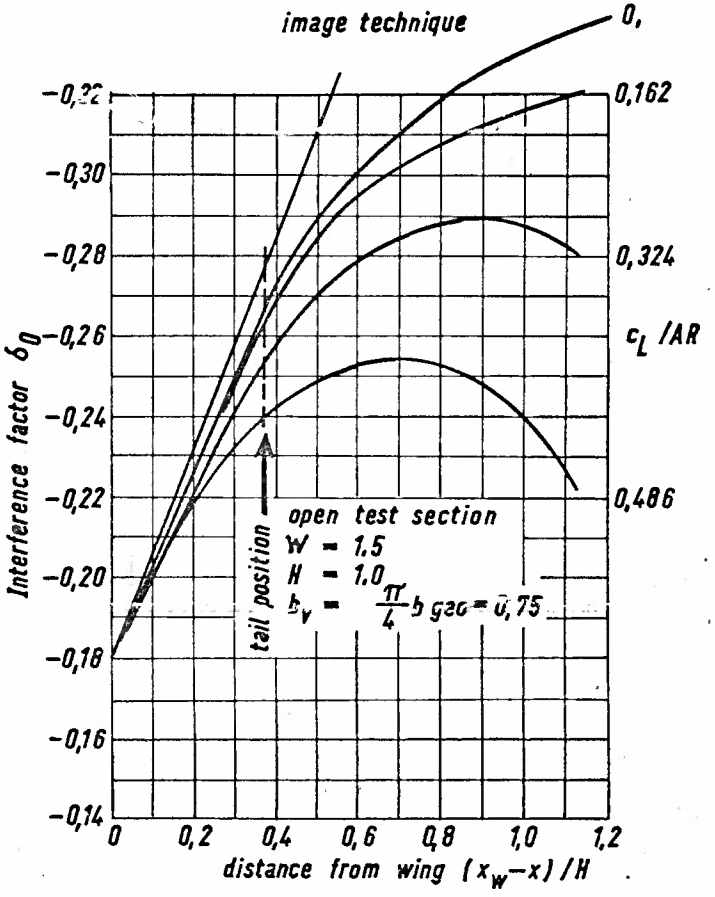

Fig. 16: Influence of downwash factor c_L/AR

W tunnel width
H tunnel height
$\frac{H}{W}$ = 0,7
b spanwidth
$\frac{b}{W}$ = 0,6 relative span

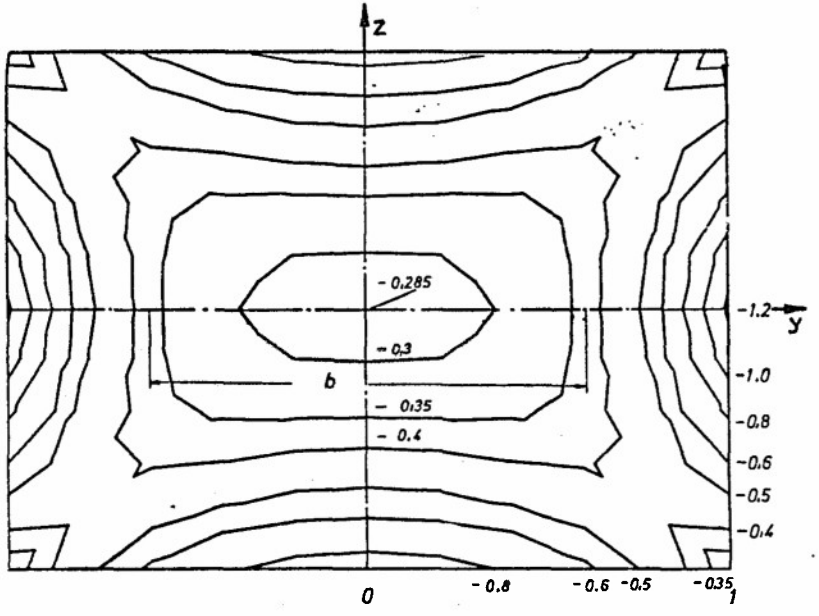

Fig. 17: Open test section, iso-lines of parameter ζ in the main cross-section ($x=x_{model}$), constant volume distribution along the span represents simple airfoil model.

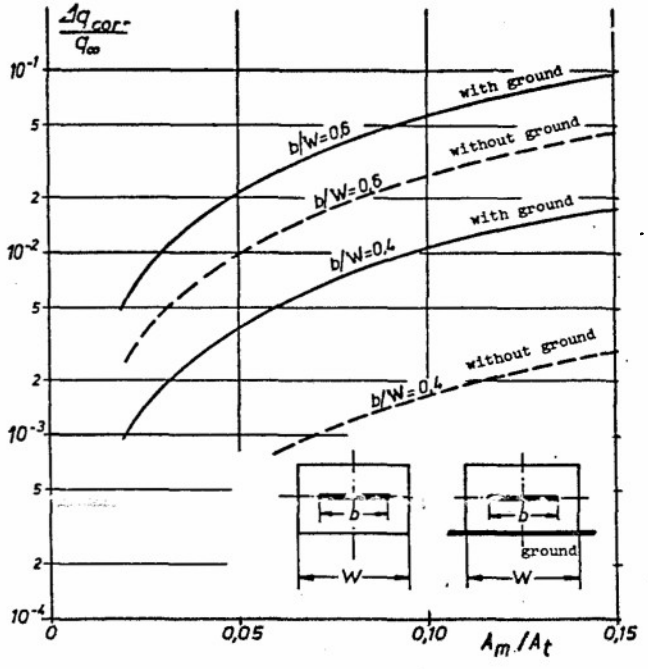

Fig. 18: Inhomogeneity of stagnation pressure for bulky models, open test section, with and without ground simulation.
Constant volume distribution along span represents simple airfoil model.
H tunnel height
W tunnel width
$\frac{H}{W}$ = 0,7
A_t area of tunnel cross- section
A_m model area
λ = 0,6 shape parameter

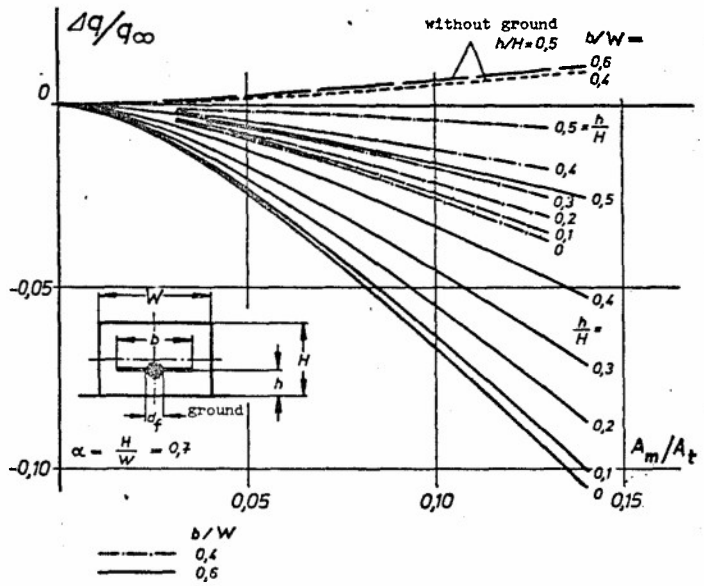

Fig. 19: Inhomogeneity of stagnation pressure for free jet with ground simulation, the model is a body of revolution with a thin airfoil.

$$\frac{A_m}{A_t} = \frac{\frac{\pi}{4}(x^2+y^2)}{A_t}$$

$A_t = H \cdot W$ cross - sectional area of wind tunnel

$A_m = \frac{\pi}{4} d_f^2$ model area

H height of tunnel

W width of tunnel

h height of model

b spanwidth

d_f diameter of fuselage

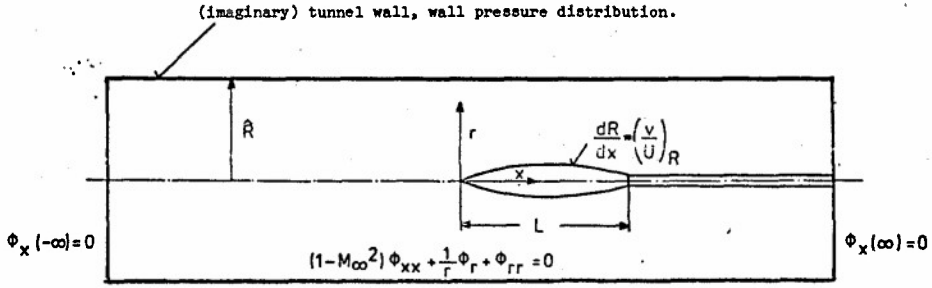

Fig.20: Correction method using measured wall pressures

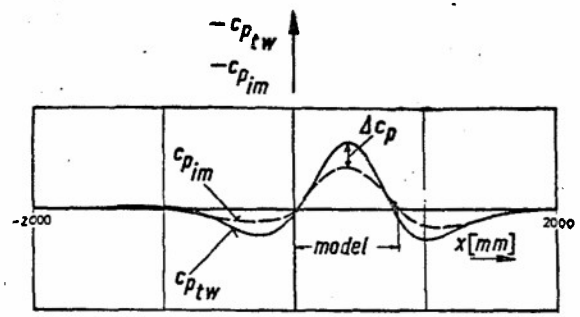

1. The measured wall pressure distribution ie influenced by the preeence of the wind tunnel walls.

2. The difference between meaeured and computed preesure distributione Δc_p along the tunnel wall or a corresponding imaginary wall is a criterion for the magnitude of the mistake

3. and can be used to compute the correction on the tunnel centerline.

4. The correction on the surface of the body corresponds to the correction on the tunnel centerline.

Fig. 21: Correction method ueing measured wall pressures.

c_p pressure coefficient
tw tunnel walls
im imaginary walls

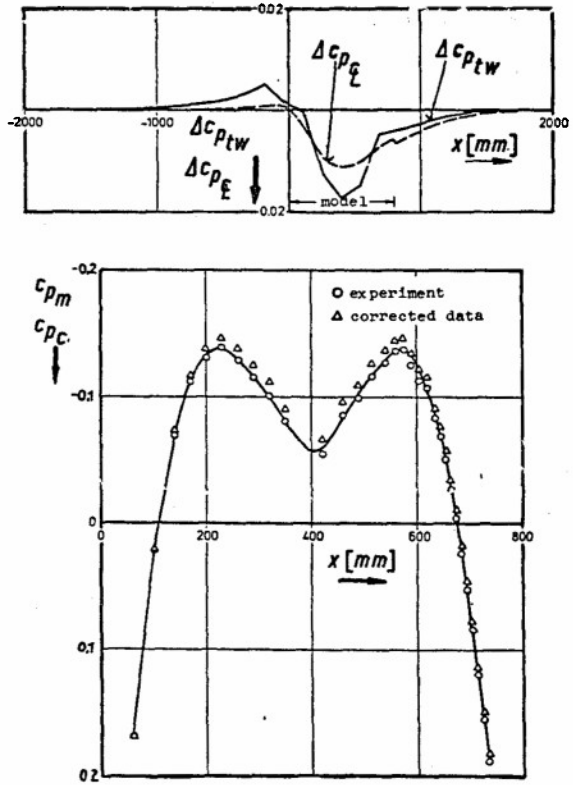

Fig.22: Measured and corrected pressure distribution of the body of revolution MBB M1 at $M_\infty = 0,8$.
c_p pressure cofficient
t_w tunnel walls
m measured
c corrected
$\mathfrak{L}$ centerline

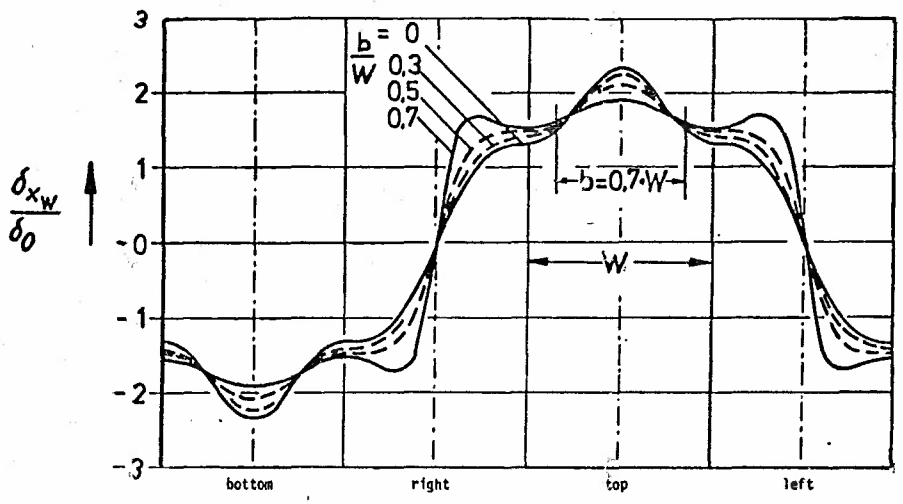

Fig. 23: Wall pressure distribution for a closed square tunnel, main cross section ($x = x_{model}$)

δ_0 interference factor (vertical component of induced velocity due to tunnel walls at the position of the model - not averaged along span)

δ_{x_w} represents induced velocities in x-direction of model and tunnel walls

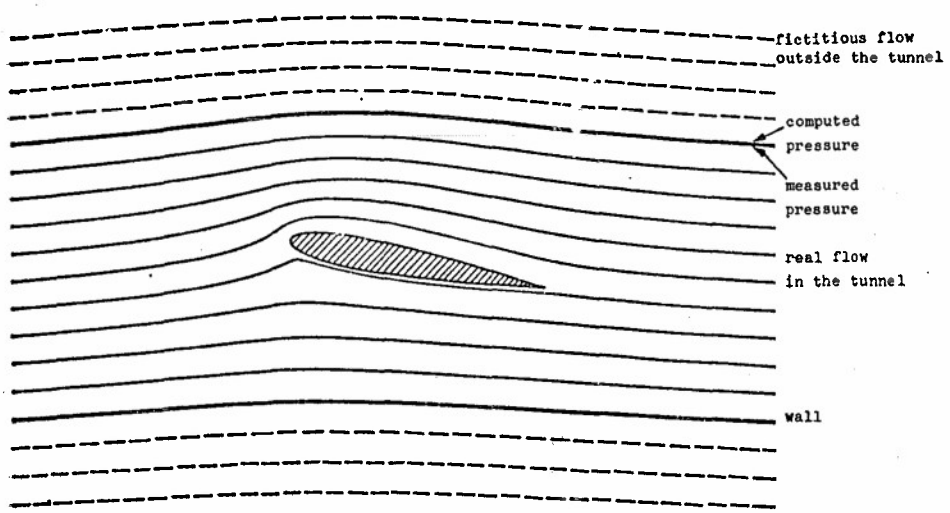

Fig. 24 The principle of adaptive walls.
There is no pressure jump through the wall (fictitious flow field outside the tunnel with computed pressure distribution - real flow field in the tunnel with measured pressure distribution) if the wall contour is a streamline. The shape of the wall is changed by an iterative procedure. If the measured pressure agrees with the computed pressure of the fictitious outer flow field, the inner flow field is interference free.

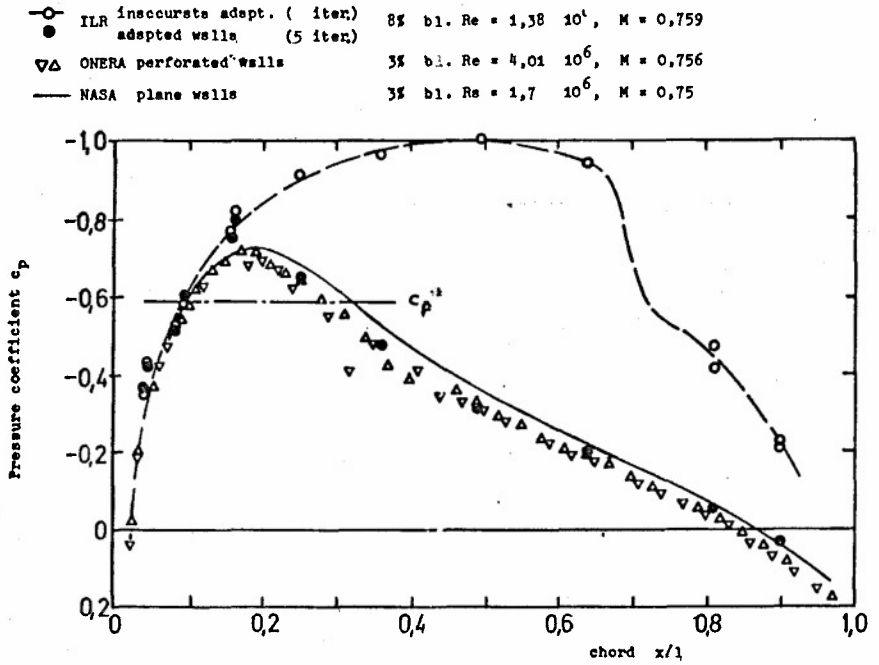

Fig. 25: Pressure distribution for NACA 0012, M = 0,76, α = 0°

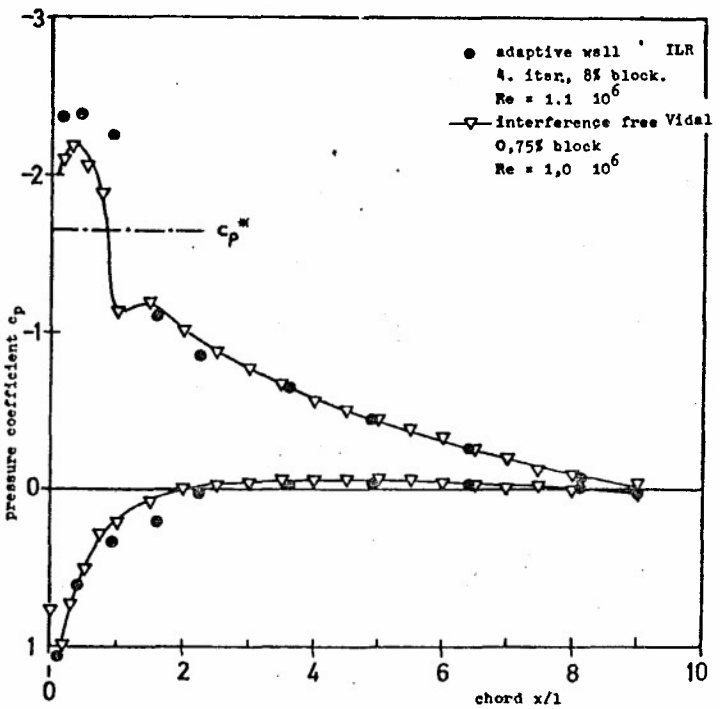

Fig. 26: Pressure distribution for NACA 0012, α = 6°, M = 0,55
Comparison of different measurements.

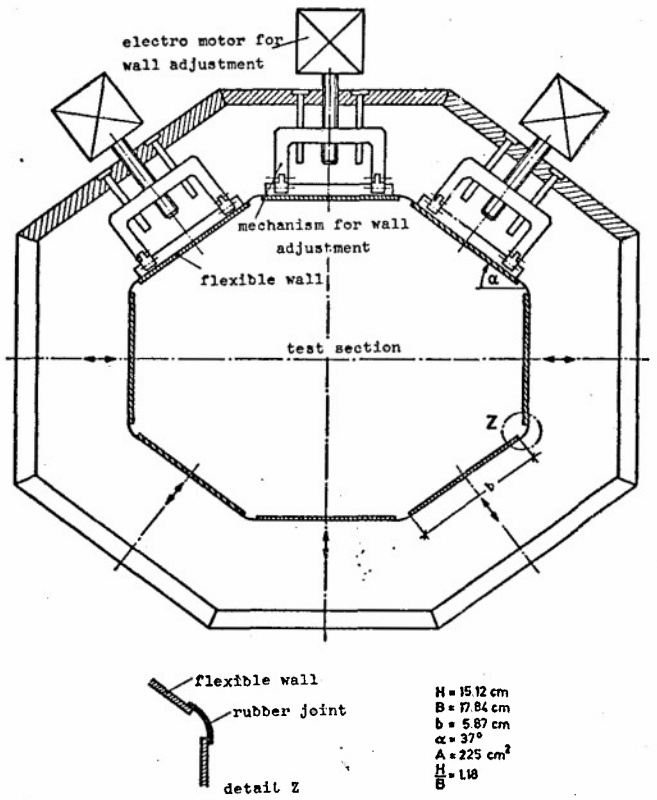

Fig. 27: 3 - D ADAPTIVE WIND TUNNEL
(preliminary design)

A REVIEW OF RESEARCH AT NLR ON WIND-TUNNEL CORRECTIONS FOR HIGH ANGLE OF ATTACK MODELS

by
R.A. Maarsingh
National Aerospace Laboratory NLR
Anthony Fokkerweg 2
1059 CM Amsterdam, The Netherlands

SUMMARY

A survey is given of past, current and planned work at NLR in the field of wind-tunnel wall interference on models at high angles of attack at low-subsonic speeds. Among the new long-term research activities those concerning slotted-wall test sections play a dominant part. It is felt that an approach which makes use of measured distributions of flow quantities near the walls is the most promising one. It may be recommended also as a short-term solution for some special wall correction problems arising from modern low-speed wind-tunnel testing in closed test sections.

LIST OF SYMBOLS

A' = effective aspect ratio of wing
A = influence coefficient matrix
b = tunnel width
$\bar{b}$ = vector of model-induced influences at the collocation points
C = quantity related to static-pressure difference between plenum chamber and upstream infinity (see Fig. 5)
C = cross-sectional area of test section
C_D = drag coefficient of model
C_L = lift coefficient of model
h = tunnel height
K = slot parameter
K_H, K_V = slot parameter, for horizontal and vertical tunnel walls respectively
L = length of ventilated part of test section
L = model lift
n = normal direction (to tunnel wall)
p_c = static pressure in plenum chamber
p_∞ = static pressure of undisturbed flow far upstream
q = dynamic pressure
Δq = dynamic pressure correction
R = radius of rotor model
Q, R = porosity parameter
Q_H, R_H = porosity parameter for horizontal tunnel walls
Q_V, R_V = porosity parameter for vertical tunnel walls
s = model semi-span
S = model reference area or area of tunnel wall
U = velocity in test section
w = wall-induced upwash velocity
x,y,z = co-ordinate system with origin in test-section centre
α = angle of attack of model
Γ = horseshoe vortex strength
δ_0, δ_1 = lift interference factor
$\Delta\alpha$ = angle of attack correction
θ = blockage factor
$\bar{\sigma}$ = vector of source strengths
φ = perturbation velocity potential

1. INTRODUCTION

The NLR research on wind-tunnel wall interference on models at high angles of attack concentrates almost entirely on problems in the low-subsonic speed regime. Especially in this field radical changes in test capabilities and measuring techniques are taking place by the completion of the DNW, the large low-

speed German-Dutch Wind Tunnel, which is entering the operational phase now *).
These charges include firstly a larger variety of models and test conditions in test sections of various dimensions and wall configurations (closed, slotted and open), but secondly they comprise higher requirements on quality, versatility and productivity. An enumeration of the prevailing design principles and of the expected activities is given in figure 1. The msin tunnel design data and test equipment are summarized in figure 2. Further details can be found in previous papers (Ref. 1,2 and 3). Considering both the several ambitious goals and the special features of this facility, it may be concluded that the very combination of these developments, the unusually wide range of test capabilities on the one hand and the high quality of the test data on the other, requires special attention for correction procedures in general and for wall interference in particular.

It is well known that the greater part of the low-speed wall correction methods has been developed many decades ago and is based on elementary model representations and on linear theory. In several respects these methods have not kept pace with modern trends in low-speed wind tunnel testing, like higher angles of attack (large wakes and separated flow), higher lift (vortex wake relocation), and more complete engine simulation (larger jets). Thus, it may be anticipated that real problems may arise when in addition also relatively large model dimensions are applied, attended with requirements on data accuracy (in particular with respect to drag measurement) which are significantly higher than in former days.

In search of means which could help to cope with this new situation and which could be useful to attain that relatively large models can be applied without making concessions to the accuracy of the data, it was decided that all DNW test sections would be provided with longitudinal slots of a continuously variable width (see Fig. 3). Obviously, the adoption of slotted walls can not be considered as a substitute for necessary renewals and improvements of wall correction theory. On the contrary, even new problems arise, since it is not to be expected that an interference-free test section could be created in this way. Therefore, one is still forced to develop a reliable method for the correction of the remaining (reduced and/or more simple) wall effects.

All in all, these developments have given rise to a thorough reorientation in the field of low-speed wall-interference correction procedures for both slotted and closed test sections. In the present paper a review is given of recent, current and planned work (to be) executed at NLR. Some of this research, intended both to improve wall correction methods and to develop new ones, is carried out within the framework of existing DFVLR-NLR co-operation programs.

A survey of the main items of the low-speed wall-interference studies is given in figure 4. This survey is not complete; further items will be mentioned in the text of the present paper. Not mentioned at all, neither in figure 4 nor in the text, is a separate research program set up some years ago for the high-speed regime and intended for closed and slotted-wall test sections. In this frame a new two-dimensional wall correction method is being developed which is based on measured wall pressures and which uses a model representation by point singularities. This approach, started in behalf of the transsonic wind tunnels at NLR and intended to be extended also to three-dimensional test conditions in course of time, concentrates on compressible flow rather than on typical features like high lift, high angles of attack, etc. For this reason this method is out of order now and will not be discussed here further. A description of this method is given in reference 19.

2. PAST AND CURRENT RESEARCH ON SLOTTED-WALL INTERFERENCE

2.1 The design philosophy behind the DNW slotted test sections

Formerly, the application of longitudinal slots in test-section walls of low-speed wind tunnels was not very usual, at least up to several years ago when, particularly in the U.S.A., special V/STOL wind tunnels of large size were built. It was argued then, that typical V/STOL aircraft models in closed test sections can create so large and unpredictable flow distortions that it would be no longer possible to derive reliable wall corrections. Based on the simple reasoning that open and closed test sections create wall effects of different sign, it seemed logical to assume that ventilated walls could largely reduce or even eliminate at least an important part of these wall effects. In fact, the problem was postponed rather than solved, for it was highly uncertain which slot configuration should be chosen and to what extent the wall effects could be reduced actually under the widely varying test conditions which may occur for V/STOL models. However, uncorrected wall effects of unknown but certainly reduced magnitude often were preferred to large wall effects which should be corrected by highly faulty or even clearly failing methods.

The design philosophy adopted for the DNW test sections (except for the 9.5 m x 9.5 test section) is of a different nature, however. In fact the present approach is a middle course between two possibilities: the development of a very complicated analytical correction procedure for closed test sections on the one side and the self-correcting wind tunnel with adaptive walls on the other.

It was realized, that important progress has been and may still be made in the field of computational aerodynamics, so that advanced correction methods might be developed in the near future. As an early example the nonlinear method of Joppa (Ref.5) may be mentioned, in which the wall-induced vortex wake relocation is taken into account by applying a vortex-lattice method in an interative way. Such methods, which are indispensable in several respects, e.g. in assessing the limits of validity of "classical" pitching-moment corrections, do not seem to yield the most practical solution, however, as they are too cumbersome to be used as part of a standard correction procedure in routine wind tunnel testing.

*) The DNW has been built and will be managed and operated by the DNW Foundation, a new organisation established as a subsidiary institute by the German DFVLR and the Dutch NLR.

Since, in addition, for DNW consequent on-line data processing is pursued, such that all data will become available as much as possible in corrected form, it was considered to be more worthwhile to attempt whether slotted walls could be applied in combination with relatively simple correction procedures.

The function of the slotted walls in the DNW, therefore, is limited: they are intended principally for executing some control over the most troublesome wall effects, i.e. the variations of the wall-induced velocities over the model. If such an attempt would turn out to be successful, i.e. if the wall-interference gradients could be reduced sufficiently, the role of the theoretical corrections method also could be limited to derive the remaining corrections for a homogeneous wall-interference field in a reliable way. Besides, some special intentions are present for the slotted floor in the low-speed 9.5 m x 9.5 m test section *) viz.to shift the low-speed test limit which stems from flow breakdown or recirculation phenomena in V/STOL model testing in closed test sections.

2.2 Numerical studies

As it was pointed out above, the adoption of slotted walls in the interchangeable test sections of the DNW was considered neither as a final solution of all wall interference problems nor as a substitute for necessary renewals and improvements of wall correction theory. On the contrary, even two new problems were introduced really:

(i) to find out how effective slotted walls would be in suppressing the inhomogeneity of wall-interference over the model and
(ii) to develop a reliable method for the correction of the remaining wall effects.

In order to explore the first question theoretically, a computer program was developed for calculating lift interference in rectangular test sections with ventilated (slotted of perforated) walls of finite length (Ref. 6). This program is based on a three-dimensional extension of the first-order (linearized, incompressible) version of the method described by Slooff and Piers (Ref.7). It proceeds from a source-panel singularity distribution as a representation of the tunnel walls and it uses a modified form of the "classical" linear homogeneous boundary condition due to Baldwin et al.(Ref. 11). The essential features of this method are summarized in figure 5.

The modification of this analytical boundary condition occurs as a consequence of the finite length of the ventilated part of any actual test section, and consists of the introduction of the quantity C on the right hand side which is proportional to the static-pressure difference between the plenum chamber (adjacent to the ventilated wall) and the undisturbed flow far upstream. In this respect the NLR approach differs from that of reference 8 for instance, where the finite-length aspect is considered separately from the pressure difference between plenum and upstream flow. Even more important, and also different from reference 8, is the fact that in the present approach C is shown to belong to the unknowns of the problem and should be determined therefrom after adopting an additional equation. This equation expresses the plausible physical fact of zero net mass flow through the ventilated wall(s). However, since this modification does not change the basic form (the left hand side) of this boundary condition, some serious objections as to its insufficient theoretical basis and its problematical use in practice remain the same as in its original form.

The principal objection is the rather intuitive introduction of the porosity or viscosity parameter $1/R$ or $Q = (1 + 1/R)^{-1}$, which turns out to have a very large influence on the calculated wall-interference while its magnitude can not be predicted from the actual slotted wall configuration. Nevertheless, this type of boundary condition was used as a basis because (i) it was the only available one at the time and (ii) it was attractive because of its linearity.**) It is also obvious, that for the limited purpose of this investigation, i.e. an assessment of the effectiveness of wall slots in reducing upwash gradients over the model, somewhat lower requirements may be accepted than when it was intended to derive definitive wall corrections. In addition, from the very outset a rather extensive experimental investigation was planned for verifying the computational results.

A parameter study has been carried out using the computer program of reference 6 and a set of input data as summarized in figure 6. This survey represents only the main part of this study; actually also a square test section and both axial and vertical variations of model location have been considered. Further details and the full results have been reported in reference 9 and 10; a summary of the latter report has been included in reference 2.

The principal findings are shown in figure 7 through 10 and may be summarized as follows:
- when not only minimization of streamwise but also of spanwise variations in wall-induced upwash is pursued, all four walls should be ventilated,
- a kind of optimum has been found for a rectangular test section with perforated walls ($K_{H,V} = 0$) at $Q_H = 0.66$ and $Q_V = 0.72$ ($R_H = 1.945$ and $R_V = 2.565$), for in that case $\delta_1 \approx 0$ and $\delta_0(y) \approx$ constant along the lifting line of an unswept wing (see Fig.7); this result was flattering, however, since the absence of streamline curvature occurs only at the lifting line,

*) Strictly speaking, the design considerations pointed out here do not apply at all to the 9.5 m x 9.5 m test section; in this test section only the floor has been provided with slots, whereas in the other test sections slots are present in all four walls.

**) As has been indicated in figure 4, the theoretical work at NLR directed on a more firmly founded analytical boundary condition is still continuing. Presently it has no high priority, however, although it is realized that it is of interest for the design of slotted walls.

- in order to reduce streamline curvature also between wing and tail, and thus to minimize the pitching-moment correction for a complete model with horizontal tail, a slotted test section is to be preferred to a perforated one,
- most favourable with respect to longitudinal variations in lift interference is found to be a (rectangular) test section with almost ideal slots ($Q \approx 1$ or $1/R \approx 0$) of small width and/or large spacing (K large), (see figure 8),
- reductions of both spanwise and streamwise variations may be achieved also for smaller and possibly even more realistic values of Q and K (see Fig.9).

As a tentative conclusion from this exploratory investigation it may be stated therefore, that an actual slotted test section is conceivable which induces only homogeneous, and thus easily correctable, lift interference. It should be noted, that this result was obtained for a relatively large wing model (span ≈ 0.8 tunnel width) as well as for a rotor model (diameter ≈ 0.5 tunnel width) at not too large lift coefficients (see Fig.19). The effect of slot length is small at the lifting line, and remains within bounds elsewhere when this length is not smaller than two times the test section width, at least for not too long models.

2.3 Experiments

Especially in the present case, where the available computational method was imperfect because of a disputable boundary condition applied for a slotted wall, a thorough experimental verification was felt to be indispensable. In the framework of existing DFVLR-NLR co-operation programs an extensive experimental investigation was set up to be executed in a modeltunnel (MUK) of the formerly planned German large low-speed windtunnel (GUK) at DFVLR-Braunschweig.

Sketches of both model and test section are given in figure 11 and 12. The model geometry was chosen as simple as possible; lift, drag and pitching moment are measured by an internal strain gauge balance. Initially it was intended to investigate a large variety of slotted-wall configurations (several slot widths, slot lengths, etc.), but up to now only the configuration shown in figure 12 has been measured. The test section has a square cross section, its open-area ratio is 12 % and the slot length is only 1.3 times the test-section width. As is shown in the sketch in figure 12, the test section was surrounded by a plenum chamber of rather small depth. The plenum walls can also be removed, however.

Up to now a complete set of three-component measurements, i.e. polar runs at seven different tail settings and without tail surfaces, has been carried out three times, viz. in the closed test section, in the slotted test section with and in the slotted test section without plenum chamber *). In preceding calibration tests it was checked that the empty test-section flow did not change significantly with wall configuration, so that differences in results indeed could be ascribed to differences in wall interference. Much attention was paid to differences in pitching moment, which are directly connected with streamline curvature, thus with differences in wall-induced upwash between wing and tail.

An example of the lift measurements without tail is given in figure 13. The most remarkable item is a rather small difference between the uncorrected results for the closed test section and the slotted test section with plenum chamber. This means that the effectiveness of the slots is very small, and that a positive angle-of-attack correction will exist of more than one half of the correction of the closed test section (the corrected lift curve for the closed test section is indicated by flagged circles in figure 13).

Presumably this feature is caused by the small volume of the plenum chamber. When the slotted test section with plenum is considered as a closed test section with inner dimensions equal to those of the plenum chamber, and the measured data are corrected in the usual way for lift interference, a corrected lift curve is found (indicated by flagged squares in figure 13) which coincides almost perfectly with the former. Although the results for the slotted test section without plenum are not yet available, it may be concluded that the small plenum chamber will be the principal cause of the poor slot effectiveness.

For the pitching-moment results a similar correction procedure has been attempted (Fig.14), but in this case the simple interpretation of the slotted test section with plenum as a closed test section with the dimensions of the plenum is not as convincing as in the former case. In fact the uncorrected results are so nearly coinciding that any correction which differs between the closed and the slotted test section will disperse the curves. On the other hand, if from the difference in angle-of-attack correction between the slotted and the closed test section a value of Q is determined (at a known value of K) so that the pitching-moment correction can be calculated, a very good agreement is found between the measured and calculated pitching-moment correction.

As the results of the tests without plenum are not yet available, the issue of this investigation remains undecided. As a tentative conclusion it may be stated, that the slotted test section surrounded by this small plenum chamber may have some characteristics in common with both a slotted test section of small effectiveness (small Q) and a closed test section of enlarged dimensions. The small slot length may be a secondary cause of the small effectiveness of the slots, especially concerning the pitching-moment correction.

3 SOME SOLID-WALL INTERFERENCE STUDIES

3.1 Two-dimensional high angle of attack models (attached flow)

Although it is not exactly of recent date, for the sake of completeness the work of de Vries and Schipholt may be recalled briefly here (Ref. 12). It was argued several years ago, that both improvements

*) The latter measurements have not yet been completed.

of two-dimensional testing methods and developments in the direction of more advanced high-lift devices with high incidences and flap deflections necessitated a check on the validity of the commonly used linearized corrections due to Glauert. This was motivated also by the results of earlier calculations due to De Jager and Van de Vooren (Ref. 13), from which strongly nonlinear effects had been found for an infinitely thin hinged flat plate at zero incidence.

The calculations of De Vries and Schipholt (Ref. 12) were restricted to the inviscid wall-interference effects, thus excluding wake blockage and boundary layer effects, and were carried out by means of an adapted version of a computer program for multi-element aerofoils. This program in turn was based on the NLR panel method. It proceeds from source panels on both the aerofoil contour and the tunnel walls and a prescribed vortex distribution on the mean line of unknown overall strength.

The results substantiated the suppositions in that:

- the correction theory of Glauert breaks down for large flap deflections and may be used for single aerofoils only at not too large angles of attack.
- the results of De Jager and Van de Vooren cannot be used to estimate the pitching-moment correction for a flapped aerofoil with slat.

These results are very similar to those obtained independently by Eriksson (Ref. 14), who states generally that the very displacement of the aerofoil (elements) in vertical direction causes the wall corrections to be nonlinear in C_L.

The final conclusion of reference 12 has been summarized schematically in figure 15. It implies that wall corrections for multielement aerofoils can be estimated from a combination of two types of calculations, i.e. lift interference from a new non-planar vortex lattice method (thus accounting for camber but neglecting thickness effects) and blockage from conventional techniques (thus including thickness and wake effects). This approach has in common with classical approximations that lift interference and blockage are considered to be independent of each other.

Intentions to derive a practical wall-correction procedure along these lines have not been carried out, however, and that for several reasons. The main reason is that such an isolated perfection of the two-dimensional wall corrections received less attention in course of time. In the mean time these plans have been superseded by expectations which may be taken from a more integrated approach: a two-dimensional version of a new method based on measured tunnel-wall pressure distributions to be discussed in section 4.

Wall-interference effects for two-dimensional tests in presence of strong viscous effects, either on the model itself or at the tunnel walls, have not yet received special attention at NLR. However, when flow separation occurs only on the model, it can be considered as a special case of the next item.

3.2 Models with large regions of separated flow

Especially with a view to very high angle of attack conditions (deepstall measurements) of complete models of transport aircraft, as well as for high-lift conditions in general, a need was felt at NLR of a method by which additional blockage effects due to separation bubbles could be estimated.

In a preliminary investigation (Ref. 15) the method due to Maskell (Ref. 16), in a form as recommended by Vayssaire (Ref. 17), was judged to be a tool which could meet a direct need. An important feature of this method is its suitability to be used in a fully computerized on-line data processing system. Last year this method was incorporated into the general low-speed windtunnel data reduction program (APVW) of NLR by way of trial. This new part of the program is being tested now in the usual standard reduction process of representative wind tunnel measurements. A schematic picture of the main features of this procedure is given in figure 16. Its on-line character is due to the fact that the procedure already can be started before the polar run is finished. For, as soon as the ideal polar has been derived from measuring points in a pre-selected low angle of attack range, the correction procedure can be applied immediately to any following measuring point beyond this range.

The experience gained thus far at NLR with this method is not unsatisfactory, although some shortcomings declare themselves clearly. A practical imperfection is found in the case of model configurations with deflected slats, where flow separations occur even in the low-angle-of-attack portion of the polar. In these cases the shape of the ideal polar can be affected to such an extent that very irrealistic values of A', C_{D_m} and/or C_{L_m} are found. But even then the dynamic-pressure correction often turns out to be of a credible magnitude. A more fundamental shortcoming is the fact, that variations over the model of this kind of wall interference can not be accounted for, and thus additional buoyancy corrections are neglected. This means that only the most striking effects are considered and that in particular the drag correction may be not very accurate. Also in this context expectations are set on a method based on measured wall pressure distributions as has been developed at Lockheed-Georgia (Ref. 18).

4 NEW METHODS USING MEASURED FLOW QUANTITIES NEAR THE WALLS

From the previous sections it becomes evident, that in the theory of low-speed wall corrections in slotted and closed test sections, principally two types of problems exist which can hardly be solved satisfactorily by conventional or classical means. Firstly, for slotted test sections a key problem is the lack of an adequate boundary condition for a slotted wall. An analytical approach of this subject would supply a need certainly, particularly in behalf of test-section design, but a solution which would be satisfactory also from a practical point of view can not be expected to be reached at short notice. Secondly, in closed as well as in ventilated test sections problems arise as to the theoretical model representation. These problems are aggravated by several typical features of modern aircraft designs and test requirements (e.g. large models, separated flow, large wakes and jets, etc.).

To some extent both types of problems can be discerned also in transsonic wind tunnel testing, although the origin differs of course, and it is not fortuitous then that the solution is sought in a similar way. At NLR, as well as in many other places (e.g. Ref. 4), it is anticipated that the problems mentioned ask for an approach which uses measured flow quantities in the vicinity of the tunnel walls obtained during the test in addition to measured model forces and/or pressure distributions. The use of measured wall flow quantities (e.g. static pressures) overcomes the need for an analytical boundary condition, as has been pointed out in reference 4, but this experimental information may be used also to detect possible uncorrigible conditions. The same information, possibly in combination with (extra) measured pressures on the model, may be used to overcome problems with respect to the model representation. In this way more certainty will exist about the actual flow phenomena during the test, and appropriate and effective means may be taken at once (e.g. by limited wall control) to such an extent that corrigible conditions arise again.

Returning to figure 4 it is worth mentioning, that the vast part of the work summarized under the heading "Measured boundary conditions" should still be done, and that it can be considered to be of a long-term type. Since the activities in this field have been started only recently, results can not yet be shown.

Firstly, possibilities are being considered presently of developing a new universal method using both measured wall pressures and model forces, which can dispense with a theoretical model representation. It is intended to be applied to both closed and slotted walls and includes both lift interference and blockage. The basic idea is due to mr. J.W. Slooff of NLR and has some aspects in common with the method of Murman described in reference 4. Just like in the "self-correcting" or "adaptive-wall" concept a relatively simple fictitious potential flow exterior to the tunnel is calculated from a measured distribution of the horizontal velocity component along the walls. From this calculation a distribution of the vertical velocity component is obtained which generally differs from the measured one. This difference is a measure of the wall interference. Otherwise than in a self-correcting tunnel, however, it is not the actually measured normal-velocity distribution which is changed by some form of active wall control (by blowing, suction or wall deformation), but the calculated distribution is influenced by modifying the boundary conditions at infinity, i.e. by varying the horizontal velocity component U_∞ and the vertical component V_∞. These components are determined such that both the tangential and normal velocity at the walls are matched in some mean sense (i e. similar to Murman in matching normal and tangential velocities at the airfoil surface, see reference 4). The components U_∞ and V_∞ thus found are the sought corrections on magnitude and direction of the tunnel flow respectively, corresponding with blockage and downwash (lift interference).

Thus, as described so far, this method would require both pressure measurements (to determine the tangential-velocity distribution) and flow direction measurements (to determine the normal-velocity distribution) in the vicinity of the walls. The measurement of the latter does not seem to be attractive in practice. However, this difficulty can be avoided in principle by utilizing relations between the wall velocity distributions and the measured model forces which can be derived from momentum considerations (in two-dimensional flow equivalent to Blasius' theorems). In this way, the matching procedure could be carried out through longitudinal wall velocities and model forces, rather than normal wall velocities*). Presently the feasibility study concentrates on practical and fundamental aspects of this matching procedure, as it is felt that the viability of this method will depend crucially on such points.

An alternative approach is being taken into consideration next, intended especially for complicated models in closed test sections. It proceeds from the method developed at Lockheed-Georgia by Hackett et al. (Ref. 18) for estimating all kinds of blockage corrections, viz. model volume, wake and jet effects and separation bubbles. Typical for the Lockheed-method is that wall pressures are used to define the theoretical model representation. The calculation of the wall interference is similar to classical methods. It is intended at NLR, however, to include lift interference right from the onset and that for high-lift models with or without jet simulation. As a first step a combined numerical and experimental investigation has been started, preliminarily restricted to two-dimensional cases. It may be expected that this method will become operational at relatively short notice and that it will be able to replace several methods for special purposes, like those for multi-element aerofoils, separated flows, etc. (see section 3). Dependent on the results of the present preliminary studies it will possibly be decided to stop the further development of either the first or the second method, so that only a single method might be considered for extension to three-dimensional flow.

5 CONCLUDING REMARKS

For several years it is realized at NLR that some of the commonly used wall correction methods for closed test sections should be re-examined thoroughly before they could be applied satisfactorily to modern low-speed wind tunnel testing. Although for low speeds the development of methods based on purely computational means seems to be conceivable, it may not be expected to result in an optimum solution.
For the new German-Dutch Wind Tunnel (DNW) slotted walls are chosen as a means to minimize the wall interference gradients over the model. In order to derive reliable corrections for the remaining homogeneous wall interference, methods are considered which make use of measured flow quantities near the walls, although also work on analytical boundary conditions is continuing. Besides this long-term research, also attention is payed to short-term solutions for closed test sections. In this context expectations are set on a Lockheed-type of approach as a means for defining the necessary theoretical model representation.

*) It should be noticed that the procedure described here applies to ventilated walls in general. In the special case of a closed wall the situation is more simple because the normal velocity component equals zero at the wall.

6 REFERENCES

1. Seidel, M. and Jaarsma, F.,"The German-Dutch low speed wind tunnel DNW". Lecture given at the Royal Aer. Soc. on February 3rd, 1977. The Aeron. J., April 1978, p. 167-173.

2. Seidel, M. and Maarsingh, R.A.,"Test capabilities of the German-Dutch wind tunnel DNW for rotors, helicopters and V/STOL aircraft". Paper nr. 17 of 5th Europ. Rotorcraft and Powered Lift Aircraft Forum, September 4-7th, 1979, Amsterdam.

3. Fuijkschot, P.H., "The computer infrastructure of the DNW low-speed wind tunnel". Paper prepared for the 8th Int. Congress in Aerospace Simulation Facilities, September 24-26, 1979, Monterey, CA, USA. (NLR MP 79031 U).

4. Murman, E.M., "A correction method for transonic wind tunnel wall interference". AIAA Paper no. 79-1533.

5. Joppa, R.G., "Wind tunnel interference factors for high-lift wings in closed wind tunnels". NASA CR-2191 (1973).

6. Bleekrode, A.L., "Lift interference at low speed in wind tunnels with partly ventilated walls". NLR Memorandum WD-75-085 (1975).

7. Slooff, J.W. and Piers, W.J., "The effect of finite test-section length on wall interference in two-dimensional ventilated wind tunnels". AGARD CP-174, Paper no. 14, London, October 6-8,1975.

8. Ruger, Ch. and Baronti,P., A linear solution of lift interference in square tunnels with slotted test sections of finite length". NASA CR-144980 (N76-27165).

9. Maarsingh, R.A., "Motives and prospects of slotted walls in the DNW". NLR Memorandum AI-77-006 (1976).

10. Maarsingh, R.A.,"Model sizes, testing limits and wall effects for helicopter rotors in the DNW". NLR Memorandum AI-79-008 (1979).

11. Baldwin, B.S.Jr. et al.,"Wall interference in wind tunnels with slotted and porous boundaries at subsonic speeds". NASA TN 3716 (1954).

12. De Vries, O. and Schipholt, G.J.L.,"Two-dimensional tunnel wall interference for multi-element aerofoils in incompressible flow". AGARD-CP-174, Paper no. 20 (1975).

13. De Jager, M. and Van de Vooren, A.J.,"Tunnel wall corrections for a wing-flap system between two parallel walls". NLR TR W.7 (1965).

14. Eriksson, L.E., "Calculation of two-dimensional potential flow wall interference for multi-component airfoils in closed low-speed wind tunnels". FFA (Stockholm) Tech. Note AU-1116 (1975).

15. Maarsingh, R.A., "The blockage correction for models with separated flow, (in dutch)". NLR Memorandum AI-78-015 (1978).

16. Maskell, E.C., "A theory of the blockage effects on bluff bodies and stalled wings in a closed wind tunnel". RAE Report Aero. 2685 (1963).

17. Vayssaire, J.Ch.,"Correction de blocage dans les essais en soufflerie. Effects de décollements". AGARD CP-102, Paper 9 (1972).

18. Hackett, J.E.,"Estimation of tunnel blockage from wall pressure signatures. A review and data correlation". NASA CR-15,224 (1979).

19. Smith, J.,"Preliminary evaluation of a method for determining two-dimensional wall interference. Progress Report". NLR Memorandum AC-77-008 (1977).

PREVAILING DESIGN PRINCIPLES INVOLVED

- HIGH AERODYNAMIC AND AERD-ACOUSTIC QUALITIES
- COMPREHENSIVE AND ADVANCED TEST EQUIPMENT
- LARGE VARIETY OF MODELS AND TEST CONDITIONS
- HIGH TESTING PRODUCTIVITY
- FLEXIBLE AND ECONOMIC OPERATION

MAIN ACTIVITIES FOCUSED ON :

- IMPROVEMENT OF AIRCRAFT LOW-SPEED CHARACTERISTICS (SAFETY, PERFORMANCE AND ECONOMY)
- HIGH-LIFT DEVICES
- V/STOL AERDDYNAMICS
- ENGINE/AIRFRAME INTERFERENCE
- AIRFRAME AND ENGINE NDISE
- ROTOR AERODYNAMICS
- (HIGH-SPEED) HELICOPTERS
- FLUTTER TESTS
- JETTISON TESTS
- OPTIMIZATION DF FULL-SCALE AIRCRAFT COMPONENTS
- REAL ENGINES (INTAKE, JET PLUME EFFECTS)
- NON-AERDNAUTICAL INVESTIGATIONS

Fig. 1 Design principles and expected activities of the DNW facility

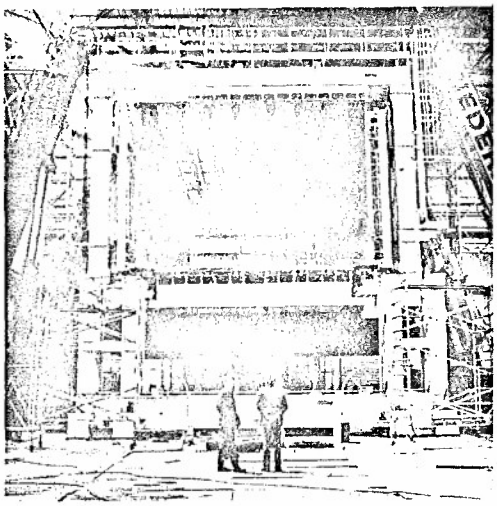

Fig. 3 Upstream view of the convertible 8m x 6m test section with slotted walls

TYPE OF TUNNEL	CLOSED RETURN CIRCUIT (OVERALL LENGTH OF CENTERLINE: 320 m)		
SIZE OF WORKING SECTION	9.5 m x 9.5 m	8 m x 6 m	6 m x 6 m
TYPE OF SECTION	CLOSED *)	CLOSED *) AND OPEN	CLOSED *)
CONTRACTION RATIO	4.8	9.0	12.0
MAX. SPEED (m/s)	62	116 (80)	145
STATIC PRESSURE IN TEST SECTION	ATMOSPHERIC (1 BAR)		
REYNOLDS NUMBER x 10^{-6} *)	3.9	5.2	5.8
MAIN DRIVE	THYR. SYNCHR. MOTOR; NORMAL RATING: 12.7 MW		
AUXILIARY DRIVES	MAINLY FOR COMPR. AIR: ≃7 MW		
FAN	SINGLE STAGE; 8 BLADES; DIRECT DRIVE 225 RPM; CONST. PITCH, WIND SPEED CONTROL BY MOTOR		

*) BASED ON V_{max} AND 0.1 $\sqrt{A}$ (A: TEST SECTION AREA)

*) ALL CLOSED TEST SECTIONS ARE PROVIDED WITH LONGITUDINAL WALL SLOTS OF A CONTINUOUSLY VARIABLE WIDTH RANGING FROM 0 TO 0.12 m AT 1 m PITCH

STANDARD EQUIPMENT

- MODEL STING SUPPORT (VERTICAL MOVEMENT WITH 5 m/s)
- MECHANICAL SIX-COMPONENT BALANCE
- HEAT EXCHANGER (IN THE SETTLING CHAMBER)
- CIRCUIT AIR EXCHANGE (OUTLET & INLET HATCHES, THROTTLE)
- CONTROL, DATA AQUISITION AND REDUCTION SYSTEM (DISTRIBUTED COMPUTER SYSTEM)

SPECIAL EQUIPMENT

• COMPRESSED AIR PLANT WITH AIR STORAGE	6 kg/s CONT., 35 kg/s INTERMITT 50 m^3, 280 bar
• HYDRAULIC DRIVES	
• HYDROGEN PEROXIDE PLANT	FOR HOT GAS SIMULATION
• MOVING BELT GROUND PLANE (INCL BLC)	≃7 m x 6 m, 60 m/s
• Q-STOPPER	RETRO-JET; SAFETY DEVICE FOR FLUTTER TESTS
• SCOOP	REMOVAL OF HOT GAS FROM TEST SECTIONS BY INJECTOR

Fig. 2 Main data and test equipment of the DNW facility

STARTING-POINTS		TYPE OF RESEARCH: OBJECTIVE	TYPE OF RESEARCH: PROCEDURE	APPLICATION	REMARKS (PROSPECTS)
ANALYTICAL BOUNDARY CONDITIONS		EFFECTIVENESS OF SLOTTED WALLS	NUMERICAL STUDIES AND EXPERIMENTAL VERIFICATION	3-D. SLOTTED TEST SECTIONS. ATTACHED FLOW	1) STILL IN PROGRESS (THEORETICAL STUDIES AT LOW PRIORITY) 2) EXPERIMENTS FORM PART OF DFVLR-NLR CO-OPERATION
MEASURED BOUNDARY CONDITIONS	WITHOUT MODEL REPRESENTATION (A)	DEVELOPMENT AND EVALUATION OF A NEW METHOD	1) FEASIBILITY STUDY 2) 2-D. DEVELOPMENT 3) 3-D. EXPENSION POSSIBLY LATER ON	BOTH SLOTTED AND CLOSED TEST SECTIONS (DNW, HST)	FEASIBILITY STUDY STARTED
	WITH MODEL REPRESENTATION (B)	EVALUATION OF A METHOD FOR COMPLICATED MODELS (HIGH LIFT AND/OR LARGE JETS, WAKES, INCL. SEPARATED FLOW)	"LOCKHEED-TYPE" OF APPROACH, (REF. 18) EXTENDED TO LIFT INTERFERENCE	CLOSED TEST SECTIONS, (2-D. AND 3-D.) POSSIBLY EXTENDED TO SLOTTED TEST SECTIONS LATER ON	1) 2-D. FIRST 2) EXTENSION TO SLOTTED T.S. IN PARTICULAR IF METHOD (A) FAILS

Fig. 4 Survey of principal low-speed wall interference studies at NLR

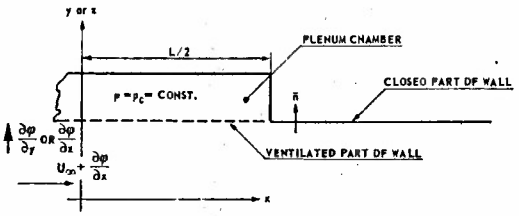

STARTING-POINTS: POTENTIAL FLOW (INCOMPR.) $\Delta\varphi = 0$ (LAPLACE EQUATION)

$\varphi = \varphi_m + \varphi_w$, WHERE φ_m DUE TO MODEL (REPRESENTED BY A SINGLE SWEPT HORSESHOE VORTEX OF KNOWN STRENGTH) φ_w DUE TO WALLS (REPRESENTED BY SOURCE PANELS OF UNKNOWN STRENGTHS σ)

BOUNDARY CONDITIONS: $\frac{\partial\varphi}{\partial n} = 0$ ON CLOSED PARTS OF WALL

$\frac{\partial\varphi}{\partial x} + \frac{1}{R}\frac{\partial\varphi}{\partial n} + K\frac{\partial^2\varphi}{\partial x\,\partial n} = C$ ON VENTILATED PARTS OF WALL

WHERE C IS RELATED TO p_c: $\frac{2C}{U_\infty} = \frac{p_\infty - p_c}{\frac{1}{2}\rho U_\infty^2}$

K IS A FUNCTION OF SLOT GEOMETRY (SLOT WIDTH, SLOT SPACING)

$1/R = (1-\theta)/\theta$ IS AN EMPIRICAL QUANTITY (INTENDED TO ACCOUNT FOR VISCOSITY EFFECTS)

NUMERICAL SOLUTION: BECAUSE φ_m IS KNOWN, THE UNKNOWN SOURCE STRENGTHS σ AS WELL AS THE UNKNOWN QUANTITY C CAN BE SOLVED FROM (1) AND (2)

$$\left.\begin{aligned} &\frac{\partial\varphi_w}{\partial n} = -\frac{\partial\varphi_m}{\partial n} \quad \text{(CLOSED PART)} \\ &\frac{\partial\varphi_w}{\partial x} + \frac{1}{R}\frac{\partial\varphi_w}{\partial n} + K\frac{\partial^2\varphi_w}{\partial x\,\partial n} = C - \frac{\partial\varphi_m}{\partial x} - \frac{1}{R}\frac{\partial\varphi_m}{\partial n} - K\frac{\partial^2\varphi_m}{\partial x\,\partial n} \quad \text{(VENTILATED PART)} \end{aligned}\right\} A\vec{\sigma} = \vec{c} - \vec{b} \qquad (1)$$

$$\iint_{\text{VENTIL. TED PARTS}} \frac{\partial\varphi}{\partial n}\,dS = 0 \quad \text{(ZERO NET MASS FLOW THROUGH VENTILATED WALL)} \qquad (2)$$

Fig. 5 Outline of the NLR calculation method for lift interference in ventilated test sections

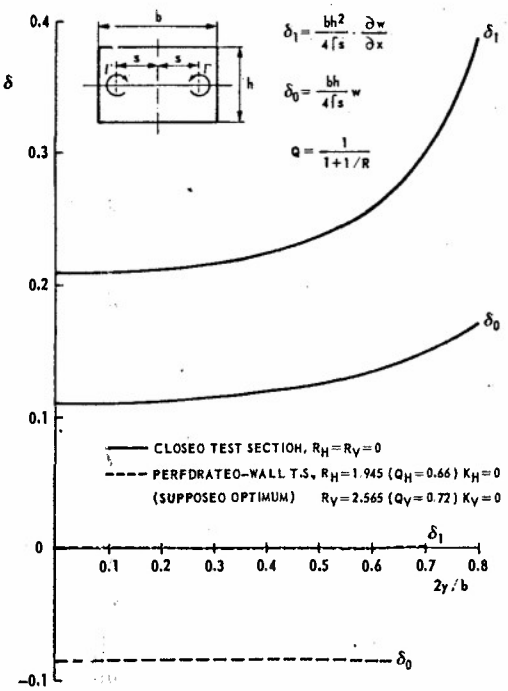

Fig. 7 Example of lift-interference reduction in a perforated test section. h/b = 0.75; 2s/b = 0.7 (representing an unswept wing with span ≈ 0.8b)

TEST-SECTION AND WALL CONFIGURATION	CONSTANT	VARIABLE
HEIGHT/WIDTH: h/b = 0.75	★	
SLOT LENGTH/T.S. WIDTH: L/b = 2 TO 3		★
SLOT PARAMETER K_H (HOR. WALLS), K_V (VERT. WALLS)		★
POROSITY (OR VISCOSITY) PARAMETER Q_H, Q_V (WHERE $Q = \frac{1}{1+1/R}$)		★
MODEL CONFIGURATION AND SIZE		
UNSWEPT WING (AND HELICOPTER ROTOR) REPRESENTED BY A SINGLE HORSESHOE VORTEX OF STRENGTH Γ AND SPAN 2s		
WING MODEL SPAN ≈ 0.8b → 2s/b ≈ 0.7	★	
ROTOR DIAMETER 2R → S/R ≈ 0.87		★

RELEVANT WALL-INTERFERENCE DATA STUDIED

ONLY LIFT INTERFERENCE:

UPWASH $\delta_0 = \frac{w}{V}\frac{bh}{C_L S} = w\frac{bh}{4\Gamma S}$, WHERE $w = \sum_{\text{ALL WALL PANELS}} \iint_{\text{PANEL SURFACE}} \frac{\partial\varphi_w}{\partial z}\,dS$

CURVATURE $\delta_1 = \frac{\partial w}{\partial x}\frac{bh^2}{4\Gamma S}$, WHERE $\frac{\partial w}{\partial x} = \sum_{\text{ALL WALL PANELS}} \iint \frac{\partial^2\varphi_w}{\partial x\,\partial z}\,dS$

Fig. 6 Survey of model and tunnel data used in slotted wall study

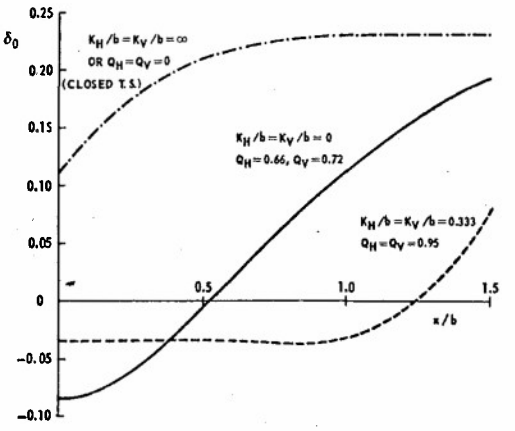

Fig. 8 Distribution of lift interference factor δ_0 along the centre line of a closed, perforated and slotted test section. h/b = 0.75; 2s/b = 0.7 (unswept wing with span ≈ 0.8b)

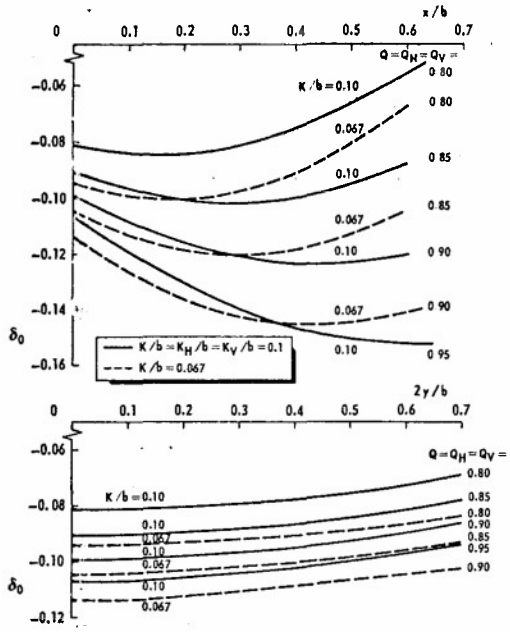

Fig. 9 Distributions of δ_o along test-section centre line and wing span for a rectangular test section. h/b = 0.75; 2s/b = 0.7 (unswept wing with span ≈ 0.8b)

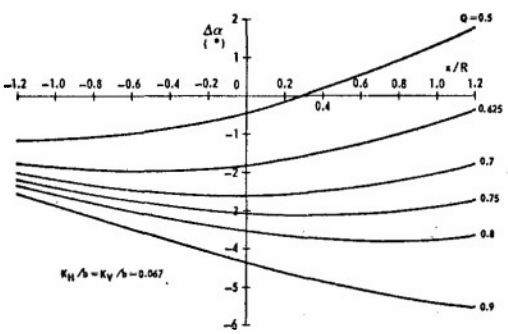

Fig. 10 Distribution of angle of attack correction along the longitudinal axis of a rotor model of 4m diameter in a slotted 8m x 6m test section, h/b = 0.75;

$2R/b = 0.5$; $\alpha = 0^o$; $C_L = \frac{L}{q\pi R^2} \simeq 2.8$

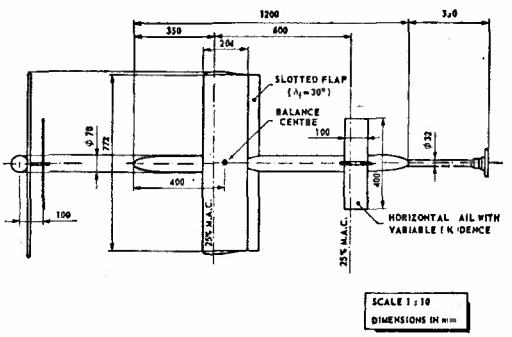

Fig. 11 Geometry of model and sting used in slotted-wall interference study

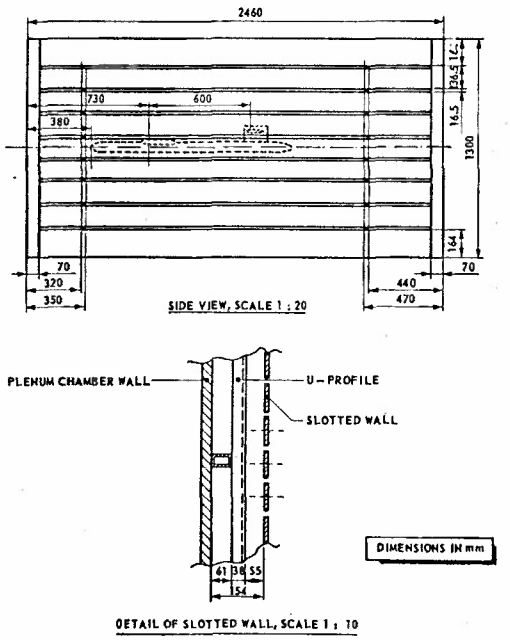

Fig. 12 Test-section wall geometry of model tunnel at DFVLR-Braunschweig

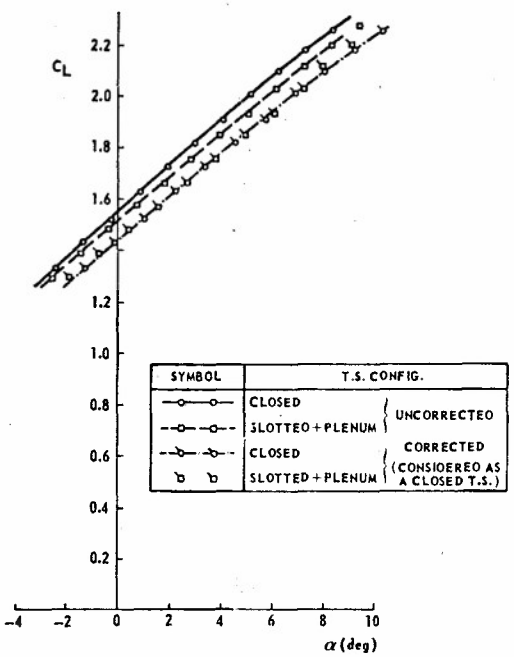

Fig. 13 Influence of the wall configuration and of the correction procedure on C_L (α). Model without horizontal tail, $Re_c \approx 0.68 \times 10^6$

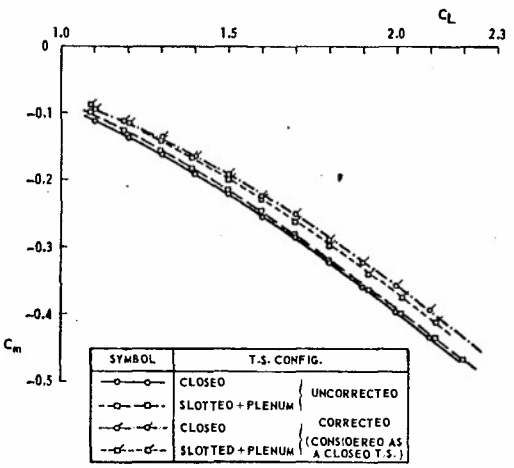

Fig. 14 Influence of wall configuration and correction procedure on C_m (C_L). Model with horizontal tail ($i_t = 0^o$), $Re_c = 0.68 \times 10^6$

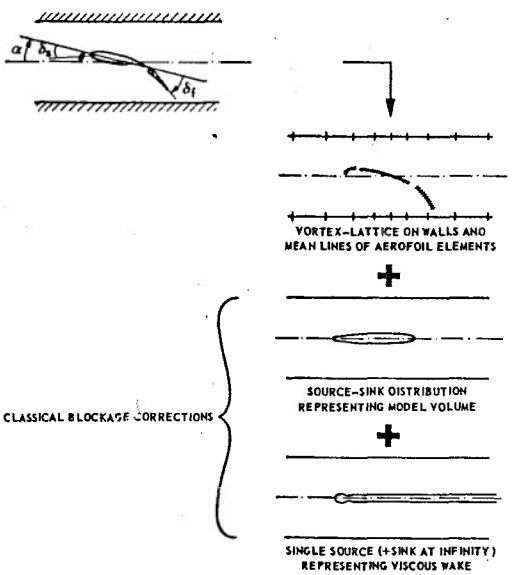

Fig. 15 Scheme of an intended (not realized) correction procedure for two-dimensional multi-element aerofoils in closed test section

$\Delta q/q = \Theta \frac{S}{C} C_{D_s}$, WHERE $\Theta = 2.8 - 0.068\,A'$

S = REFERENCE (WING) AREA

C = CROSS-SECTIONAL AREA OF TEST SECTION

C_{D_s} AND A' TO BE DETERMINED AS OUTLINED BELOW

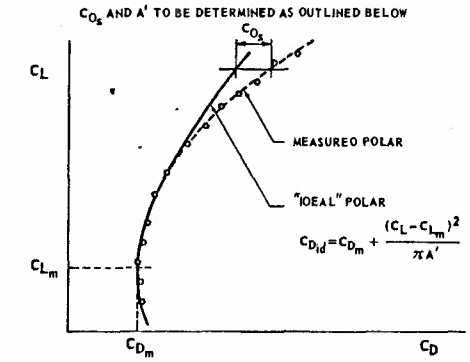

"IDEAL" POLAR : $C_{D_{id}} = C_{D_m} + \frac{(C_L - C_{L_m})^2}{\pi A'} = A_0 - A_1 C_L + A_2 C_L^2$,

WHERE $A_0 = C_{D_m} + \frac{C_{L_m}^2}{\pi A'}$, $A_1 = \frac{2C_{L_m}}{\pi A'}$, $A_2 = \frac{1}{\pi A'}$

ARE CALCULATED FROM A LEAST SQUARES METHOD APPLIED FOR (ABOUT 7) POINTS ON A PRE-SELECTED LOW ANGLE-OF-ATTACK PORTION OF THE MEASURED POLAR CURVE (I.E. A PART WITHOUT FLOW SEPARATION)

THEN C_{D_m}, C_{L_m} AND A' BEING KNOWN, C_{D_s} FOLLOWS FROM

$$C_{D_s} = C_D - C_{D_{id}} = C_D - C_{D_m} - \frac{(C_L - C_{L_m})^2}{\pi A'}$$

Fig. 16 Outline of the Maskell/Vayssaire correction procedure for separation blockage on three-dimensional (wing) models

A REVIEW OF SOME INVESTIGATIONS ON WIND TUNNEL WALL INTERFERENCE CARRIED OUT IN SWEDEN IN RECENT YEARS

by
S.-E. Nyberg
FFA, The Aeronautical Research Institute of Sweden
P.O. Box 11021, S-161 11 BROMMA, Sweden

SUMMARY

A survey is presented of wind tunnel wall interference studies in Sweden relating to testing of models at high angles of attack, published after 1974 or in progress. For subsonic incompressible flow the mutual circulation-induced model - wind tunnel interference has been calculated by panel methods for large multicomponent two-dimensional airfoils, for three-dimensional swept wings, full or half models, and for wing-tail configurations. Wake blockage effects from a swept wing with and without high lift devices have been studied experimentally. The effects of air flow leakage between half model fuselage and reflection wall have been investigated. For transonic flow the flow properties of slotted walls and the influence of wall boundary layer have been studied. Based on these results a numerical method has been developed, and so far axisymmetric calculations have been carried out. The results have been compared with experimental results for large blockage models. The interference-free flow field around a lifting wing-body model has been investigated to establish cross-flow characteristics for ventilated walls. The interference on a half model from a full model support strut has been determined.

SYMBOLS

a	slot width	M	Mach number
A, AR	wing aspect ratio	r	radius vector in cross flow plane (r=1 at tunnel walls, Figs. 28-30), also radial distance model-probe axis, Fig. 16
b	wing span		
B	tunnel width	R	radius of body
c	wing chord	t	wing thickness
c_o	wing root chord	x,y,z	Cartesian coordinates (Fig. 16)
C_D	drag coefficient	X	distance along tunnel axis
$C_{D_{OCLEAN}}$	minimum drag coefficient for clean configuration	X_{cp}	center of pressure in wing-fixed coordinate system
ΔC_D	$\Delta C_D = C_{D_{TOTAL}} - C_{D_{O_{CLEAN}}} - \frac{C_L^2}{\pi A}$	ΔX_{cp}	effect of wind tunnel walls on X_{cp}
C_L	lift coefficient	y_p	coordinate of line in slot centerplane, where plenum pressure is imposed
ΔC_L	effect of wind tunnel wall on C_L	α	angle of attack
C_m	pitching moment coefficient	$\Delta\alpha$	disturbance in α due to wind tunnel walls
ΔC_m	effect of wind tunnel wall on C_m	$\overline{\Delta\alpha}$	mean value of $\Delta\alpha$ over wing area
C_p	pressure coefficient	δ	flap deflection angle
ΔC_p	wall pressure coefficient corrected for solid blockage and lift induced pressures	δ_{LE}	leading edge flap deflection angle
$\Delta C_{p_{max}}$	difference in upstream and downstream pressure coefficient levels	δ_{TE}	trailing edge flap deflection angle
C_R	root moment coefficient	φ	perturbation velocity potential to "exact" problem, also meridional angle model-probe, Figs. 16-23
e	span efficiency factor $e = C_L^2/\pi AC_D$	$\overline{\varphi}$	perturbation velocity potential to approximate (filtered) problem
Δe	effect of wind tunnel walls on e	φ_{25}	wing sweep angle of quarter chord line
h	tunnel height	θ	meridional angle, Fig. 28, also flow deflection angle, positive out from centerline, Figs. 16-23

INTRODUCTION

During the last decade a considerable part of the aerodynamic research and development work in Sweden has been directed to studies of swept wings suitable for trainer and light attack aircraft configurations. The development and optimization of high-lift devices for take-off and landing as well as manoeuvre-devices for high subsonic and transonic speeds have played an important role. The flow patterns encountered in these studies often show strong Reynolds' number effects and it is therefore important that each wind tunnel test is carried out with the largest model possible.

The model size is limited by the wind tunnel wall induced disturbances that can be accepted. If the disturbances can be calculated properly, corrections can be applied for the mean values over the model of the disturbances in angle of attack, velocity and in some cases pitching moment (e.g. for wing-tail configurations). The accuracy of the corrected results will be directly dependent on the accuracy with which the disturbance effects can be calculated. The variation of the disturbances over the model around the mean value causes effects equivalent to the testing of a distorted model (with possible changes in separation pattern, etc.), which can not be corrected for. If, however, these disturbance variations can be calculated with reasonable accuracy, the results can form a basis for the determination of acceptable model size. Relatively large uncorrectable disturbance variations can in many cases be tolerated (for instance in development and optimization of high lift devices, studies of Reynolds' number effects, etc.) compared to what can be accepted when taking stability and control or performance data.

An exploratory study by Hedman [2] with an approximate method of swept wings in a subsonic closed test section showed that the wall interference across the span increased significantly as the sweep angle increased. Hedman suggested more accurate computations with a wing vortex lattice method for representation of the model and the tunnel and that the vertical position of the model parts should be taken into account. Calculations of this kind were made for two-dimensional multi-component airfoils by Eriksson [1], for three-dimensional swept wings by Lind [3] and for wing-tail configurations by Forslund [4]. Some comparisons were made with results calculated by conventional methods. Experimental studies at subsonic speeds were made by Ridder [5] of wake blockage effects from a swept wing with and without high lift devices and by v. Segebaden [6] of the effects of air leakage between half model fuselage and reflection wall.

As far as calculation of wall interference in ventilated transonic wind tunnels is concerned, it was considered that before accurate calculations could be made, deeper knowledge of the boundary condition at the wind tunnel walls had to be established. A theoretical and experimental study by Berndt and Sörensen [10] led to an inviscid theory of wall interference in slotted test sections by Berndt [11]. A method to calculate the influence of the wall boundary layer in slotted wind tunnels has been studied by Löfgren [8,9]. Cross flow characteristics for interference-free ventilated walls for testing of lifting wing-bodies at low supersonic speeds were established theoretically by Hedman and Rizzi [14] and experimentally by Nyberg and Sörensen [14,15]. A numerical method for calculation of wind tunnel interference in slotted test sections based on the theory of Berndt [11] has been developed by Karlsson and Sedin [12,13]. The results hitherto published concern axisymmetric flows, but the method can also be used for the angle of attack case, and some preliminary results have been obtained from the authors [16].

The half-model technique has been developed and used extensively also at transonic speeds. The only report from this work published so far is a theoretical and experimental investigation of the interference effects from a support strut for complete models on the flow around a reflection-plane mounted half model made by Brännström and Lindau [7].

It is the purpose of this paper to present a brief review of those of the above mentioned investigations, which are directly related to testing models at high angle of attack. For the investigations which are more indirectly related to this topic, only a brief abstract without figures, based mainly on the author's summary, is presented.

SUBSONIC FLOW

Two-dimensional flow

Calculation of potential flow wall interference for multi-component airfoils in closed wind tunnels [1]

The numerical method by Eriksson [1], assuming incompressible potential flow around a multi-component airfoil can be summarized in the following points:

- Each airfoil component is approximated by a closed polygon whose corner points are situated on the original contour. The tunnel walls are similarly represented by two straight "polygons" (see Figure 1).
- The straight polygon elements are given a surface vortex distribution that varies linearly over each element and is continuous at all corner points.
- The surface vortex strengths at the corner points are chosen as independent variables.
- A control point is placed at the midpoint of each polygon element. The velocity component normal to the element at this point is taken as a measure of the total flow across the element.

- The boundary condition of zero normal velocity applied at every control point results in a set of simultaneous equations for the vortex variables. The solution to these equations gives the desired surface vortex distribution, from which the pressure distribution, the lift and pitching moment are calculated.

- The method gives the inviscid flow coefficients for both the tunnel case and the free flight case, and from these results the interference corrections are determined.

The author presents results for two test cases. The first is for a symmetric airfoil RAE-102 (t/c = 0.1) with a rather large chord to tunnel height ratio c/h = 0.339. The resulting interference corrections are shown in Figure 2 in comparison with two different analytic methods, a flat plate linear theory method and a finite thickness method by Goldstein. The flat plate theory is correct to order $(c/h)^2$ but takes no account of thickness or camber. Goldstein's method is correct to order $(c/h)^4$ and includes the effect of thickness and camber. None of these methods is, however, in contrast to the method by Eriksson, valid for large angles of attack, when vertical displacement of the airfoil can not be ignored. The results show that Eriksson's calculations agree well with Goldstein's method for small angles of attack, but the discrepancies between the two methods grow rapidly with increasing angle of attack.

The second test case concerns a slightly modified Williams airfoil with flap as depicted in Figure 3. Calculations were made for c/h = 0.184 and 0.339. Some of the results for the large chord are shown in Figure 4. The fact that the C_L and C_m corrections are nonlinear in C_L, which is also the case for the small chord, is interesting, since all analytic methods in practical use give a linear dependence. The nonlinearity is caused by the vertical displacement of the airfoil and flap as the angle of attack and flap deflection are increased. When the flap approaches the lower wind tunnel wall, it experiences a negative lift increment that counteracts the normal tunnel induced lift increase.

Three-dimensional flow

Calculation of wall interference on five swept wings [3]

The panel method by Lind [3] assuming incompressible potential flow around a thin wing is summarized in the following points:

- The real wing in the wind tunnel is replaced by the mean surface of the wing positioned in a constant section thin walled tube modeled from the wind tunnel test section. The combined model is subject to a uniform wind blowing parallel to the test section axis.

- The surfaces are divided into constant pressure panels. The mutual influences from the panels are calculated using vortex singularities. The vorticity on all panels is simultaneously determined from boundary conditions prescribing attached flow.

- The calculations are fully three-dimensional.

- The vortices and control points move with the wing and flap as the flap angle and the angle of attack are varied.

- In the cases presented here, the vortex wake of the wing (and test section) leaves the trailing edge in straight lines parallel to the wind tunnel axis and free stream vector. More detailed models of rolled-up wake are, however, available in the program.

In the present investigation a half-model installation in the FFA low speed wind tunnel LT was studied. The circular test section was therefore doubled by a reflection plane, see Figure 5. Five wings were studied, see Figure 6. The wings were divided into 24 panels, except for the flapped wing W45F, where 48 panels were used. The circular walls of the test section were approximated by a polygon. The mathematical model, which was mostly used, is depicted in Figure 7. Three other models with increased panel numbers were used to check computational model influences.

The calculations were done for the wing alone and for the wing together with the test section. Some of the results obtained with the standard test section model M88 are shown in Figures 8-11. The effect of varying the test section panel number was very small.

As can be seen in Figure 8 the span to width ratio b/B is most important. The wall-induced errors vary approximately as the square of this variable within the range investigated. The large effect on span efficiency factor $\Delta e/e$ should be taken into account when model size for drag measurements is considered.

The variation of the wall induced angle of attack disturbance is presented spanwise along the quarter chord line and chordwise along the root, midspan and tip chords in Figures 9-11. The effect of angle of attack is seen to be small but angle of sweep has considerable effect. The span to tunnel width ratio b/B has as mentioned above a very large effect for large values of b/B. The mean value over the wing area $\overline{\Delta\alpha}/C_L$ of the angle of attack disturbance is shown with full lines in Figures 9, 11a and 11b. Corresponding corrections calculated with conventional handbook methods are shown in the same figures with dotted lines. The agreement is fairly good for the plane wings, but not so good for the flapped wing. This indicates that for the low-lift case the conventional mean value corrections are fairly good, but that for high-lift configurations more sophisticated methods could be necessary for accurate results. Further studies of the high lift case are suggested.

Calculation of wall interference for wing-tail configurations [4]

The computer program by Forslund [4] was developed for calculation and correction of measured pitching moments for wing-tail configurations in low speed wind tunnels. The program, which is valid for incompressible potential flow, is summarized as follows:

- The wing and the stabilizer are replaced by their mean surfaces positioned in a tube with thin walls modeled from the wind tunnel test section.
- The surfaces of the wing, which can have a flap, the stabilizer and the wind tunnel are divided into quadrilateral panels. The influence of each panel on the flow field is simulated by a horse-shoe vortex. Each panel has a control point, and the vorticity on all panels is simultaneously determined from the boundary condition prescribing tangential flow in all control points.
- The vortices and control points on the wing and the stabilizer move with the model as the angle of attack is varied.
- The trailing vortex sheet is made up from a number of horse-shoe vortices. There is at present no wake relaxation in the computer program. To position the wake as correctly as possible, it is recommended to use results from visual observations in the wind tunnel.

The computer program, which is written in FORTRAN IV and can deal with 250 panels distributed on the wing, the stabilizer and the wind tunnel surface, is used to compute the difference in angle of downwash at the position of the stabilizer with and without the wind tunnel walls. It is assumed that a change of downwash at the position of the stabilizer is equivalent to a change in the stabilizer angle in so far as the same moment contribution results. Corrected C_m-α curves are obtained by linear interpolation between C_m-α curves for different stabilizer angles.

An example of where this correction method has been applied is shown in Figure 12. A model of a swept wing-tail combination in a high-lift configuration was tested as a full model at F+W in Emmen and as a half model (the same model) at FFA. The agreement between the F+W results and the corrected FFA results is very good. A corresponding correction using conventional handbook methods gives 96% of the panel method correction at $\alpha = 0^o$ and 67% at $\alpha = 16^o$.

Experimental study of wake blockage effects from a swept wing with and without high lift devices [5]

As a background for his experimental study Ridder [5] presents a review of the current methods of treating the wake blockage problem and discusses possible wake flow patterns for lifting wings. It is concluded that the real wake flow behind three-dimensional wings can in most cases not be characterized with the current oversimplified wake models.

The wind tunnel model used for the measurements was a 35^o swept (25% chord), aspect ratio 1 wing with 10% thick symmetrical section and tested in three configurations: Plane, with leading edge flap only and with leading edge slat and double slotted trailing edge flap. The model was tested as a half model on a reflection plate and the test section wall pressures were measured along a streamwise line on the tunnel ceiling close to the chord plane of the wing at zero angle of attack, see Figure 13.

The measured drag polars for the three wings are shown in Figure 14 and the wake blockage induced pressure distributions along the test section wall for the configurations with high lift devices in Figure 15. The wake blockage induced pressure coefficients ΔC_p were obtained from the measured pressures by subtraction of the pressures measured with the clean configuration set at zero angle of attack and by subtraction of the lift induced pressures calculated from the results obtained by Lind [3].

The pressure distributions in Figure 15 support the concept of an upstream and a downstream velocity level with a rather pronounced acceleration in the vicinity of the model. The effective location of a source to represent the wake flow seems to be quite a distance downstream of the model reference point. Accordingly, the assumption of a mean value of the two velocity levels should not be valid when estimating the effective free stream velocity at the model position. It is shown in the report, however, that the velocity gradient at the test section wall is considerably higher than on the centerline. The conclusion should be that the mean value concept will cause an overestimation of the wake blockage effect.

The difference in upstream and downstream static pressure coefficient levels is called $\Delta C_{p_{max}}$. This pressure coefficient is correlated with the increase in flow separation drag ΔC_D. The ratios $\Delta C_{p_{max}}/\Delta C_D$ are listed in Figure 15. This ratio is found to vary from 0.12 to 0.24. The corresponding value calculated by the classical Maskell/Vayssaire methods for this test configuration is $\Delta C_{p_{max}}/\Delta C_D = 0.585$. It seems likely that these methods could provide the upper limit for wake blockage effects particularly at post stall conditions. However, for wings of the type investigated, the above methods would seem to overestimate the actual wake blockage effect by at least a factor 3 up to and above stall.

Ridder proposes direct measurement of the wake blockage induced pressure difference upstream and downstream of the model as an alternative to the methods of Maskell and Vayssaire. The method has been used by Ridder for several years in wind tunnel tests with thrust reversers where blockage effects are highly pronounced.

Experimental study of the effects of air flow leakage between half model fuselage and reflection wall

When testing half models it is very important to bring friction between the model and its reflection wall to a minimum. At the same time it is also important to keep the leakage of air between model and wall as small as possible so that the flow field remains undistorted.

In connection with a high lift investigation of a 25° swept wing half model v. Segebaden [6] has studied the effects of air flow leakage between the fuselage and the reflection wall.

The effects of four different sealing conditions or gaps between model and wall have been investigated. The different sealing conditions show marked differences that point to the importance of using carefully designed sealings between the half model and the wall if the results are going to be used as absolute values and comparable with results from other tunnels and models. It is also important to design the sealing inside the fuselage so that pressure loads on the sealing do not de-load the true fuselage.

It is, however, so difficult to estimate the effects of leakage that it is probably better to accept a certain amount of friction from an efficient seal.

The results do also show that the effects on lift, drag and pitching moment characteristics do not necessarily appear at the same time due to the fact that large forces may not give any moments at all if they balance around the reference axis.

TRANSONIC FLOW

Wind tunnel wall conditions

Flow properties of slotted walls [10,11]

A theoretical and experimental study of the flow properties of slotted walls for transonic test sections made by Berndt and Sörensén [10] led to a new inviscid theory of wall interference in slotted test sections by Berndt [11]. The classical theory of longitudinally slotted walls, which substitutes an approximate homogeneous wall boundary condition for the true mixed conditions, is extended in several respects. Based on the experimental findings at FFA an inviscid flow model is adopted, in which the flow entering the slot might split up into two different streams, one leaving the slot penetrating into the plenum chamber as a thin jet and one re-entering into the test section, admitting quiescent air from the plenum chamber into the test section and inducing a longitudinal separation bubble at plenum pressure along the slot and adjacent parts of the test section wall. The three-dimensional analysis, based on the assumption that the slots are narrow, retains quadratic cross-flow terms in the pressure equation and allows the slots to be few in number and have non-uniform distribution and geometry. A family of homogeneous boundary conditions is obtained, each of successively higher accuracy. Application to the design of interference-free transonic test sections is discussed.

Unsteady effects also are considered.

Slotted wall boundary layer effects [8,9]

Starting from an idealized physical model of subsonic flow past a slender axisymmetric body in a longitudinally slotted wind tunnel of circular cross section and negligible wall thickness, Löfgren [8,9] has derived a homogeneous wall boundary condition. This is to be used at the wall in connection with the usual mathematical model of non-viscous flow in order to produce approximately the same flow field in the central part of the tunnel as the field obtained from the direct mathematical representation of the idealized physical model. The boundary layer flow is assumed to be laminar, non-viscous and in Reference [8] to have an one-step velocity distribution, while in the method of Reference [9] there is a free choice of the velocity profile.

Interference-free wall boundary condition for tests of lifting wing-body models at low supersonic speed [14,15]

The interference-free flow field at low supersonic speed around a lifting delta-wing-body configuration (see Figure 17) was studied theoretically by Hedman and Rizzi [14] and experimentally by Nyberg and Sörensén [14,15]. The undisturbed pressures and flow angles were obtained at radial locations in relation to the model, where in wind tunnel tests the walls are normally situated. The flow properties were used to establish criteria for cross flow characteristics of interference-free wave-attenuating ventilated wind tunnel walls.

Theoretical calculations were made for the wing-body configuration at small angles of attack with a relaxation method based on the transonic small perturbation (TSP) equation by Hedman and in one axisymmetric sample case for the body alone with a method based on the solution of the full gas dynamics equations (the Euler equations) in a time-dependent finite volume formulation by Rizzi. In the theoretical results obtained using the TSP method the shocks are smeared out, the pressure and flow angle peak values are strongly underestimated, and the agreement with experimental data is generally only qualitative. In the results obtained by the finite volume method for the body alone at zero angle of attack the pressure rise through the shock agrees well with experiments but the shock posi-

tion is not predicted correctly. Details about the theoretical results will not be presented in this review as the calculations only cover zero and small angles of attack. The problems experienced in these calculations indicate, however, that the development of accurate theoretical correction methods for high angle of attack testing with this kind of flow pattern (supersonic flow between the model and the wind tunnel wall with rather strong oblique shocks) will be very difficult.

The experimental test set-up is shown in Figure 16. The model can be translated in the x-direction along the tunnel centerline and it can also be rolled an angle φ around the x-axis. The radial position of the probe used to determine pressure coefficient C_p and flow inclination angle θ is variable. The model (Figure 17) has a 4% thick delta wing.

Examples of the experimentally determined flow field parameters C_p and θ are depicted in Figure 18 together with Schlieren pictures in the same linear scale for a high angle of attack case at $M_\infty = 1.20$. Data points obtained downstream of the reflected bow wave are disturbed by wall interference and are marked with filled symbols. This kind of interference is greatly reduced at $M_\infty = 1.30$ and therefore results for this Mach number were used in Figures 19-22 to demonstrate the effect of angle of attack. It can be seen in Figures 19 and 21 that the influence of angle of attack is small on the strength of the body bow shock but noticeable on its position above and below the model. The α-influence on the wing-induced flow field is very large.

The highest pressures immediately downstream of the body bow shock and of the wing leading edge shock denoted C_{pmax} and the lowest pressure immediately upstream of the wing trailing edge shock denoted C_{pmin} (see Figure 19) are plotted versus angle of attack in Figure 20. The corresponding flow angles are depicted in Figure 22 in the same way. The α-influence is clearly seen. The hatched curves in the wing diagrams representing the mean values of C_p and θ above ($\varphi = 0$) and below ($\varphi = 180^o$) the model demonstrate the lift induced "volume"-effect which for high angles of attack is much larger than the geometrical volume effect at $\alpha = 0$. It is also noted that this pressure disturbance is nearly linear with α and very close to the pressure at the side of the model ($\varphi = 90^o$). The large increase in C_p and θ in the body diagrams at $\alpha = 28^o.3$ below the model ($\varphi = 180^o$) is insignificant and indicates only that the wing leading edge shock has moved upstream and joined the body bow shock, which also can be seen in the Schlieren picture of Figure 18.

The characteristics of a ventilated test section wall are frequently described by the relationship between the pressure drop of the flow when it passes through the wall and the flow angle of this flow at the wall. Each diagram of C_p versus θ in Figure 23 can therefore be interpreted as the required characteristics of an interference-free wall for the location and flow condition investigated. The influence of angle of attack and of distance from the model at $M_\infty = 1.20$ are shown. It can be seen that the disturbance due to lift decays faster than the disturbance due to geometrical volume. Other results, not reproduced here, show that the slope of the curve varies with Mach number. The character of the curves are generally linear or slightly curved with the largest slope in the outflow region. This is in contrast to the cone-cylinder flow field hitherto used as requirement for tunnel wall characteristics, where the largest slope is in the inflow region.

In some areas of the flow field outflow is combined with underpressure and inflow with overpressure. Perforated walls with constant porosity and plenum pressure can not match this requirement. It is suggested by the authors that combined slotted-perforated should be investigated. Another possibility is of course to use perforated adaptive walls with locally variable porosity and/or pressure. The use of solid flexible walls will be difficult as the abrupt local slope changes at the shocks (see Figure 21) have to be at least 5^o for high angle of attack testing.

Wall interference

Calculation of wall interference in slotted test sections - Axisymmetric flows [12,13]

Using the above mentioned inviscid theory by Berndt [11], Karlsson & Sedin [12,13] have developed a method for calculation of transonic wind tunnel interference in slotted test sections. The numerical program can also be used in an inverse mode for design and analysis of optimal slot shapes. The results published so far concern axisymmetric flows, but the program can also be used for the angle of attack case, which will be commented upon in the next section.

The theory by Berndt [11] is built on the calculation of a filtered perturbation velocity potential, neglecting higher order variation caused by the slots and the walls. The theory results in a homogeneous wall boundary condition including the dependence on slot geometry. The small perturbation potential equation is iteratively integrated, repeatedly, with the rapid finite-difference method of Karlsson & Sedin [13], using this wall boundary condition.

Some calculated results from analysis and design of slot shapes in flows with axisymmetric bodies at subsonic free stream Mach numbers published in Reference [13] will be presented here and also some unpublished data comparing calculated and experimental results [16].

Three different bodies, generated by a generalized parabolic arc, were considered in the calculations. Only results for Body I will be presented in this review. This body had the maximum diameter at 50% of the length, a slenderness ratio of $1/(6\sqrt{2})$ and was truncated at 5/6 × length with the cylindrical sting following from that station, see

Figure 24. The body was studied in one small and one large version with blockage area ratios of 0.42 and 2.23% respectively. The tunnel was assumed to be circular in cross section, with the wall defined by r = 1 and provided with 8 uniformly distributed slots. As a start a slot width distribution of a slot called the "FFA" slot as depicted in Figure 25 was studied. This slot shape is close to the slot of the existing transonic wind tunnel HT at the Aeronautical Research Institute of Sweden (FFA).

The small model of Body I with 0.4% blockage had, when calculated in a test section with the non-optimal "FFA"-slot, nearly negligible interference, while the large model with 2.23% blockage had dramatically increased interference as shown in Figure 24. The level of interference had to be diminished by at least an order of magnitude to be acceptable. An optimal slot shape was calculated by running the inverse mode design process. This slot was named M98(I), which means that the optimal design reference Mach number is 0.98 and that the slot is designed for Body I. The shape of the optimal slot M98(I) is found in Figure 25. For this slot, as shown in Figure 26, the agreement between the calculated free air reference pressure distribution and that of the tunnel run is excellent on the body surface and also in good agreement on the wall.

It was observed that for the large model of Figures 24 and 26 a slight discontinuity in the pressure gradients could be recognized at the inflow section, which is a symptom of shortcomings of the assumed inflow boundary condition. The large Body I is currently being experimentally tested at FFA by H. Sörensén to get results for further work on the subject. Some preliminary results comparing calculated and experimental wall pressure distributions [16] are shown in Figure 27. The agreement in shape of the curves is good, but there is a shift in level, which could be a result of the simplified inflow conditions used in the calculations. Another reason for the disagreement could be that no viscous effects have been considered in the slot width distribution. The experiments will continue with surface pressure measurements on the model, and with detailed flow surveys in the slots. Later studies of the effect of slot depth are planned and also tests with optimal slots.

Calculation of wall interference in slotted test sections - Delta wing at angle of attack [16]

The axisymmetric results by Karlsson & Sedin [13] presented in the preceding section look very promising and the theoretical and experimental work will continue to clarify remaining problems. However, a more interesting and natural continuation will be to go on with three-dimensional flow fields, especially when lifting configurations are considered. Berndt's theory [11] and the numerical method of Karlsson & Sedin [13] are capable of handling three-dimensional flow fields. Exploratory calculations with lifting flow fields have already been performed and some of the results have kindly been made available by Karlsson & Sedin [16].

Calculations have been made for a delta-wing as shown in Figure 28. The cross-flow condition at the inner boundary, which is a cylinder with r = 0.5, is for the free-air case obtained by slender-body theory. The test section is circular and has 8 similar slots of constant width and with 9.2% open area. Calculated pressure distributions at the inner boundary and at the tunnel wall for $\alpha = 8.75^{\circ}$ and M = 0.95 are depicted in Figures 29 and 30. The pressures at the inner boundary are higher for the tunnel case than for the free-air case. This could indicate that the open area of the slots is too large. Also from the wall pressures appreciable wall interference can be observed. These first results are certainly very encouraging and it is to be hoped that this important work can be continued as soon as possible and that suitable supporting experiments will be carried out.

Support interference

Interference on a half model from a full model support strut [7]

A theoretical and experimental investigation of the interference in a wind tunnel from the support strut for complete models on the flow around a reflection plane mounted half model has been made by Brännström & Lindau [7].

In the theoretical part a computer program, which could handle up to three components (wing, tunnel and support strut), was used to calculate the interference effects. The components are represented by a mean surface distribution of quadrilateral vortex-ring elements, the strength of which is determined from the boundary condition of zero normal component of velocity at a control point in each element. The trailing vortices are relaxed into the local flow direction by an iterative procedure.

The calculations were carried out for an angle of attack of 5 degrees with four different configurations: without tunnel, tunnel without support strut, tunnel with vertical and tunnel with horizontal support strut. Calculations were made at Mach number zero and by Prandtl-Glauert transformation at Mach numbers 0.6 and 0.8. The results show noticeable interference from the tunnel walls, but very small interference from the support strut. The calculated results for the strut cases are plotted together with the experimental results for comparison in Figures 32, 34 and 35.

The experimental investigation was carried out with a half model of a wing-body combination. The wing had an aspect ratio of 4, a taper ratio of 0.4 and a sweep angle at the quarter-chord line of 35°. Forces and pressure distributions at three wing sections were measured. Four model test cart configurations were tested: without strut, with normal strut in vertical or horizontal position and a strut simulating the strut in the proposed FFA T-2 tunnel. The test arrangement is depicted in Figure 31.

Some results from the force measurements are depicted in Figures 32-35. The strut-effects on C_L, C_m and C_R are small at low angles of attack but are quite large at high angle of attack. For C_D the interference effects are noticeable over the whole range of angle of attack and Mach number. This result in combination with the theoretical result, that there is practically no downwash or vortex relocation interference, indicates that it is primarily a blockage effect of the support strut. This is supported by the fact, that the T-2 strut, which has the largest volume with part of it close to the model, produces the largest interference effects and also that the normal strut interference is independent of whether the strut is vertical or horizontal.

This result is interesting and indicates that very likely there could be interference effects of this kind in many tunnels also in full model tests.

CONCLUDING REMARKS

It has been demonstrated that for subsonic incompressible flow the use of panel methods for the calculation of wind tunnel wall interference will in many cases provide more accurate corrections than the conventional methods. This is certainly the case for instance for wings with high-lift devices and wing-tail configurations, where various model parts are vertically displaced from the horizontal symmetry plane of the wind tunnel. Calculations of this kind can also display the variation of the tunnel-induced disturbances over the model surface, the knowledge of which is of importance for the decision on proper model size with respect to the purpose of the test.

The classical methods by Maskell/Vayssaire seem to provide the upper limit for wake blockage effects, particularly at post stall conditions. For an investigated conventional swept wing with high-lift devices these methods overestimate the wake blockage effect by at least a factor of 3 up to and above stall. As an alternative to these methods, it is proposed to measure the wake blockage induced pressure difference upstream and downstream of the model.

An improved theory for the wall boundary condition at transonic slotted test section walls has been presented.

Criteria for cross-flow characteristics of interference-free wave-attenuating ventilated wind tunnel walls have been established. The results might also have application in the design of adaptive walls for cases where strong shocks extend to the walls.

Based on the new wall boundary condition a numerical method for calculation of transonic wind tunnel interference in slotted test sections has been developed. The program has been used mainly for axisymmetric calculations, but exploratory calculations with lifting flow fields have been performed with encouraging results.

If during a half model test in a wind tunnel the full model support strut remains in its normal position, noticeable strut-interference effects on the half model flow could be encountered.

REFERENCES

[1] Eriksson, L.-E. — Calculation of two-dimensional potential flow wall interference for multi-component airfoils in low speed wind tunnels. FFA Technical Note AU-1116, Part 1, April 1975

[2] Hedman, S. — Schematical computation of wall interference for swept wings as full or half models in the FFA low speed tunnel. FFA Beräkningsbesked AU-1116 (in Swedish), Jan. 1974

[3] Lind, I.A. — Circulation-induced disturbances from low speed wind tunnel walls on five wings calculated by a panel method including realistic vertical panel location. FFA Technical Note AU-1116, Part 2, May 1975 (in contract for FFA by Anasyn AB)

[4] Forslund, R. — A method to calculate wind tunnel interference on measured pitching moments for wing-tail configurations in a low speed wind tunnel. FFA Technical Note AU-1444 (to be published)

[5] Ridder, S.-O. — Experimental study of wake blockage effects from a swept wing with and without high lift devices in a closed low speed wind tunnel. KTH AERO MEMO FI 183, June 1975

[6] von Segebaden, J. — High lift investigation of a 25° swept wing half model with leading edge flap and single slotted trailing edge flap system. Part 2: A study of the effects of air flow leakage between half model fuselage and reflection wall. FFA Technical Note AU-1325, Part 2, Jan. 1974

[7] Brännström, B.
Lindau, R.
Investigation of interference effects in a wind tunnel from a model support strut on a reflection-plane mounted half model.
FFA Technical Note AU-1335, December 1977

[8] Löfgren, P.
Simplifications of the boundary condition at a slotted wind-tunnel wall with a boundary layer.
FFA Technical Note AU-932, March 1975

[9] Löfgren, P.
Derivation of a homogeneous boundary condition for a wind tunnel wall with slots and boundary layer.
FFA Technical Note AU-1229 (to be published)

[10] Berndt, S.B.
Sörensén, H.
Flow properties of slotted walls for transonic test sections.
Paper No. 17 presented at the AGARD FDP-Symposium on Wind-Tunnel Design and Testing Techniques. London, Oct. 6-8, 1975

[11] Berndt, S.B.
Inviscid theory of wall interference in slotted test sections.
AIAA Journal, Vol. 15, Sept. 1977, pp. 1278-1287

[12] Karlsson, K.R.
Sedin, Y.C.-J.
Axisymmetric calculations of transonic wind tunnel interference in slotted test sections.
AIAA Journal, Vol. 17, Aug. 1979, p. 917

[13] Karlsson, K.R.
Sedin, Y.C.-J.
Numerical design and analysis of optimal shapes for transonic test sections - axisymmetric flows.
Paper AIAA P-80-0155 presented at AIAA 18th Aerospace Sci. Mtg., Pasadena, Jan. 14-16, 1980

[14] Nyberg, S.-E.
Hedman, S.G.
Rizzi, A.
Sörensén, H.
Investigation of the boundary condition at a wind tunnel test section wall for a lifting wing-body model at low supersonic speed.
Final Scientific Report prepared by FFA for AFSC and EOARD under Grant No. AFOSR-77-3282, May 1979

[15] Nyberg, S.-E.
Sörensén, H.
Experimental investigation of the interference-free flow field around a lifting wing-body model to establish cross flow characteristics for ventilated wind tunnel walls at low supersonic Mach numbers.
Paper presented at AIAA 11th Aerodynamic Testing Conference, March 18-20, 1980

[16] Karlsson, K.R.
Sedin, Y.C.-J.
Private communication 1980.

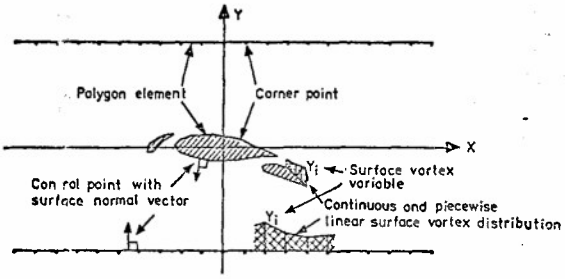

Figure 1. Illustration of the vortex model [1].

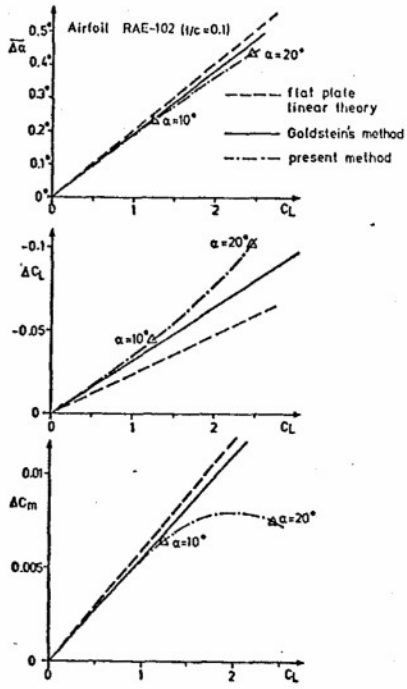

Figure 2. Test case interference corrections. Airfoil RAE-102 t/c = 0.1, c/h = 0.339 [1].

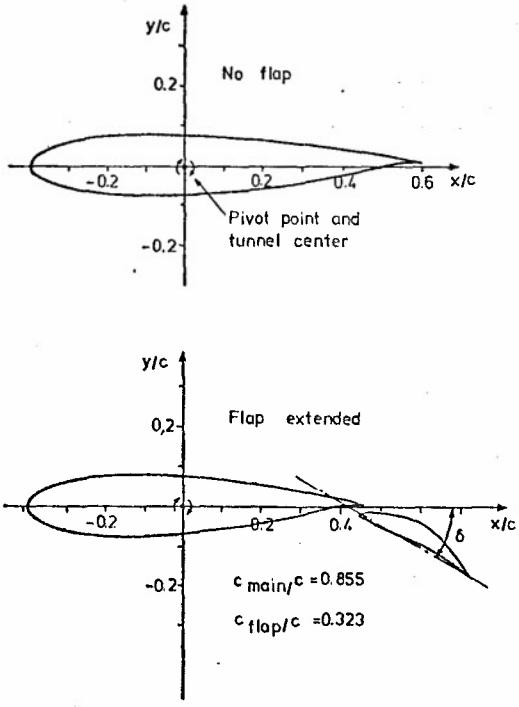

Figure 3. Wing-flap test configuration [1].

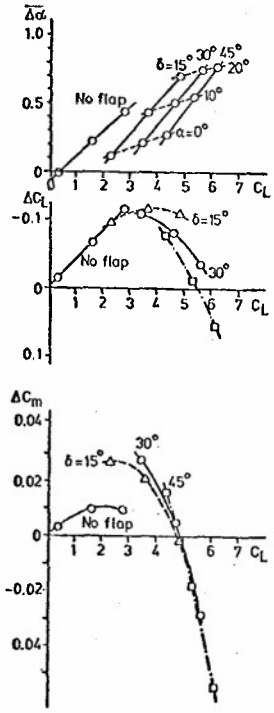

Figure 4. Interference corrections for wing-flap configuration $\overline{\Delta\alpha}$ included, c/h = 0.339.

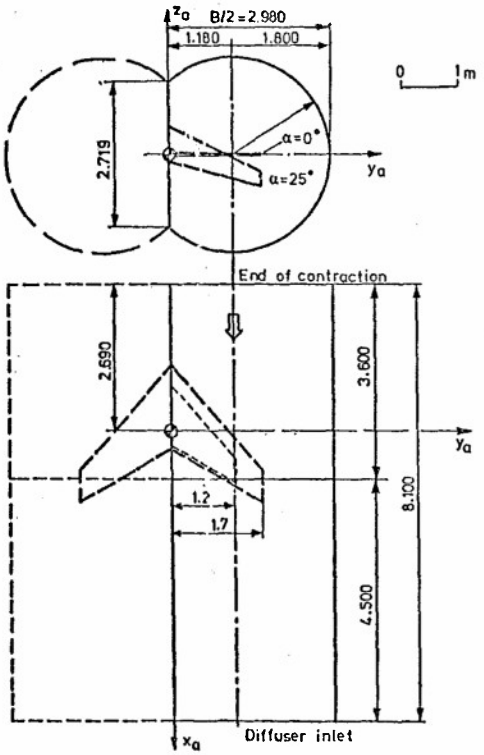

Figure 5. Test section of low speed wind tunnel LT at FFA [3].

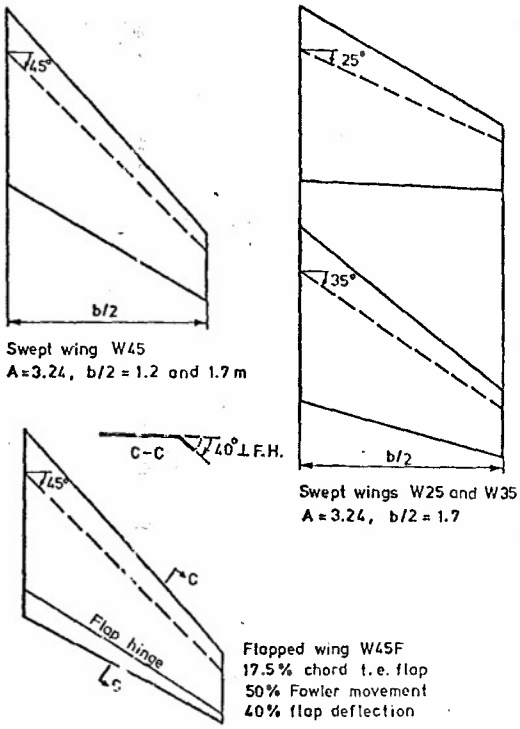

Figure 6. Wing plan forms investigated [3].

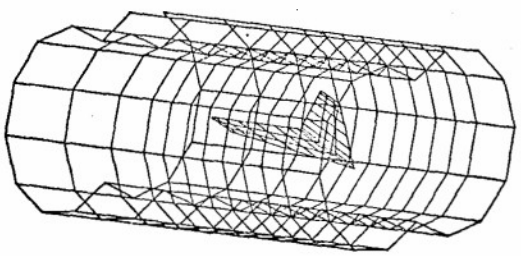

Figure 7. Wing W45 at α = 25° in test section M88 [3].

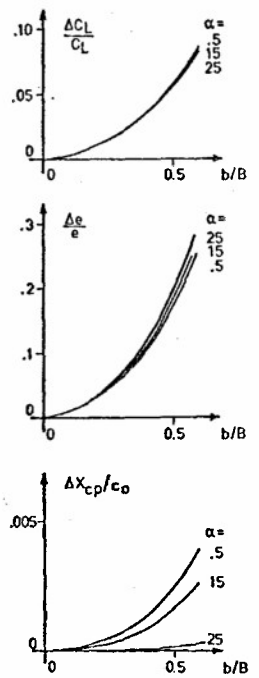

Figure 8. Effect of wind tunnel walls on lift, drag and center of pressure, wing W45 [3].

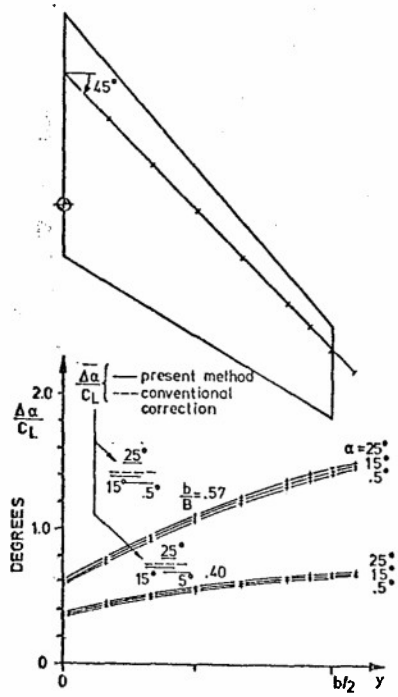

Figure 9. Angle of attack induced by WT walls on quarter chord line of wing W45 [3].

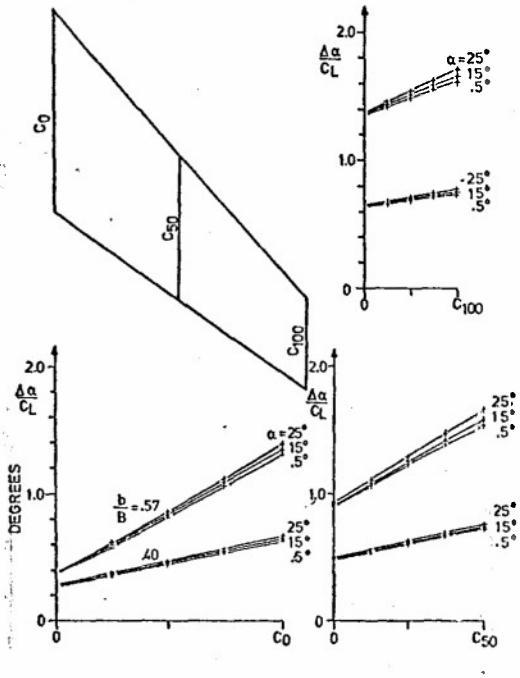

Figure 10. Angle of attack induced by WT walls in three span stations of wing W45 [3].

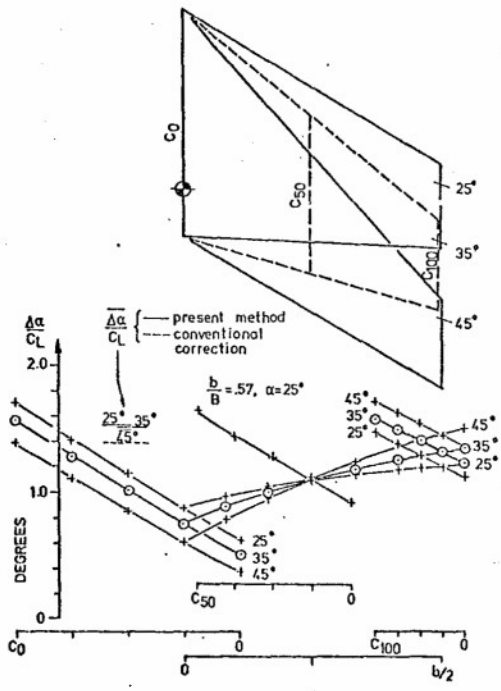

a, Wings W25,W35 and W45

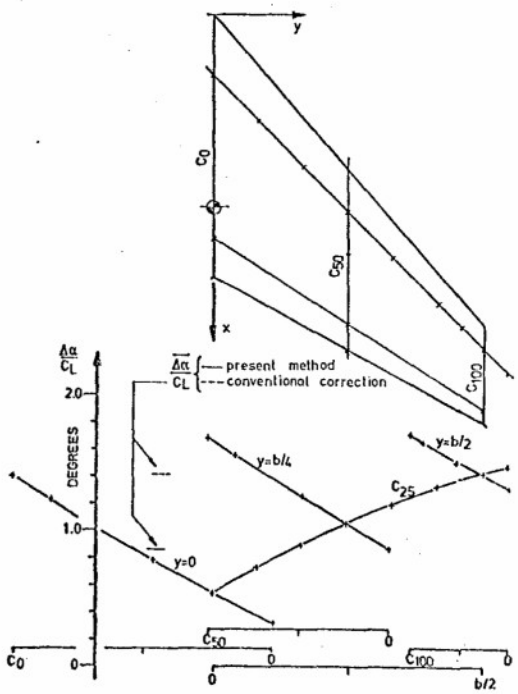

b, Wing W45 F

Figure 11. Angle of attack induced by WT walls on wings, W25, W35, W45 and W45F [3].

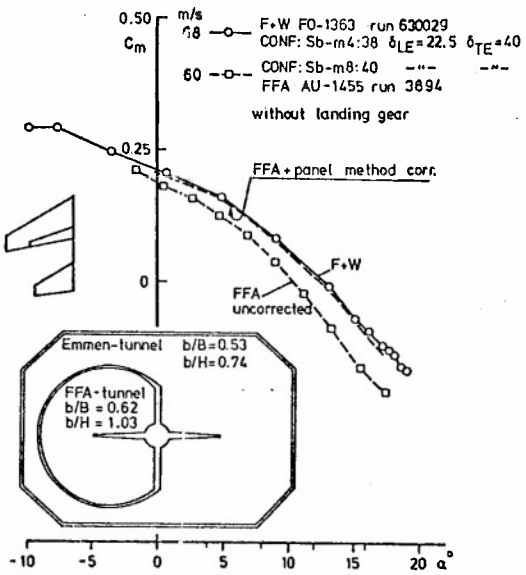

Figure 12. Pitching moment curve, SAAB-wing 7803 with stabilizer [4].

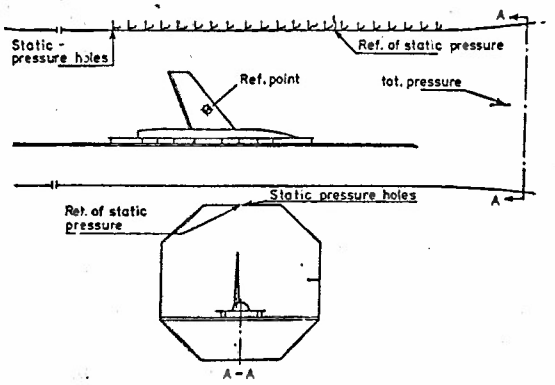

Figure 13. Model installation in test section [5].

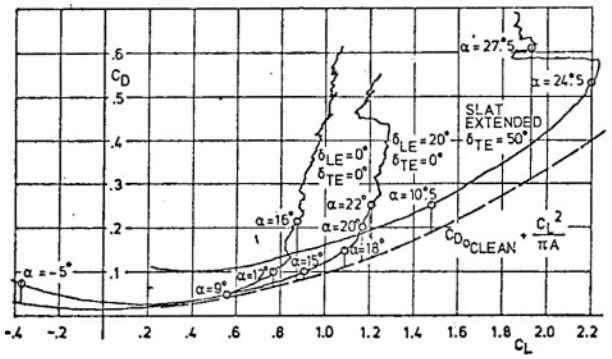

Figure 14. Drag polars for the three wing configurations [5].

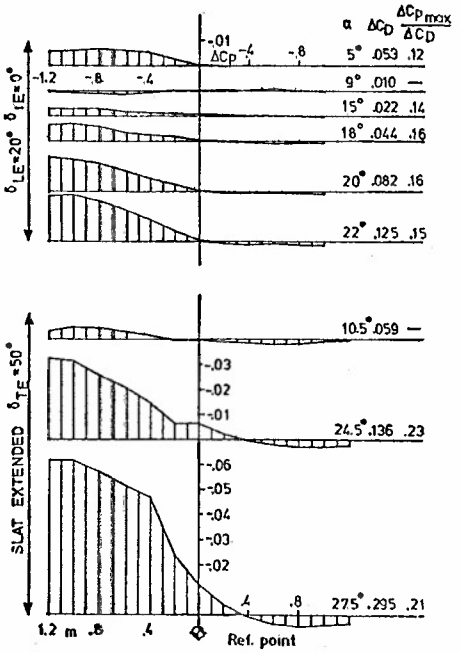

Figure 15. Wake blockage induced pressure distribution along the test section wall (ceiling) [5].

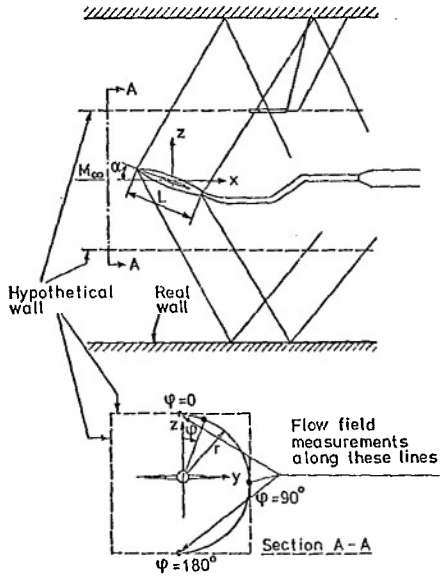

Figure 16. Principle of test arrangement [15].

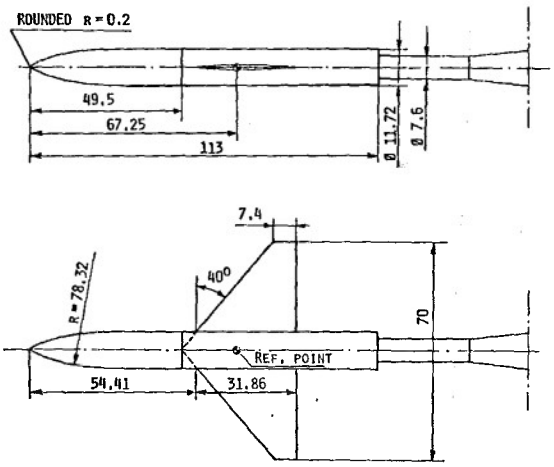

Figure 17. Wing-body model [15].

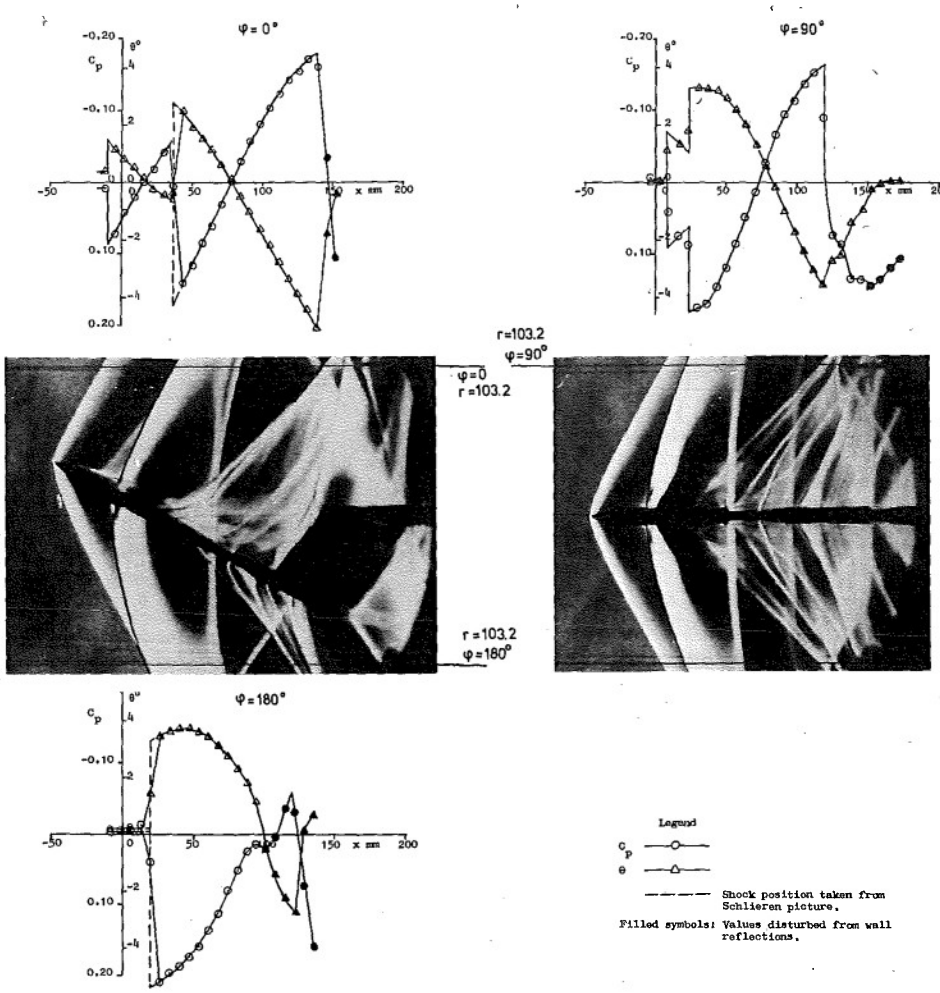

Figure 18. Flow field and Schlieren picture M_∞ = 1.20, $\alpha = 27^\circ.9$, r = 103.2 [15].

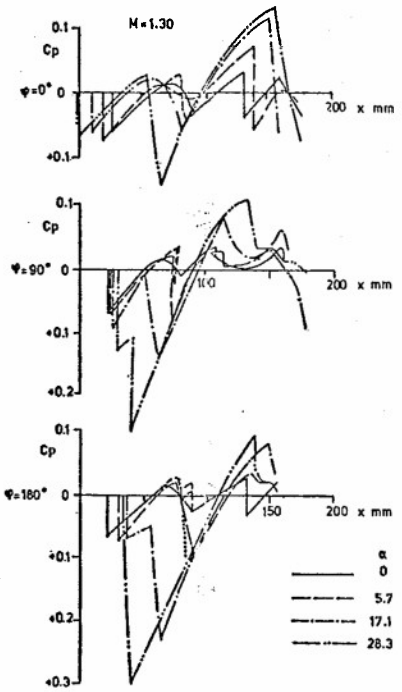

Figure 19. Pressure distributions at r = 105.3 for $\alpha = 0^{\circ} - 28^{\circ}3$ at $M_{\infty} = 1.30$ [14].

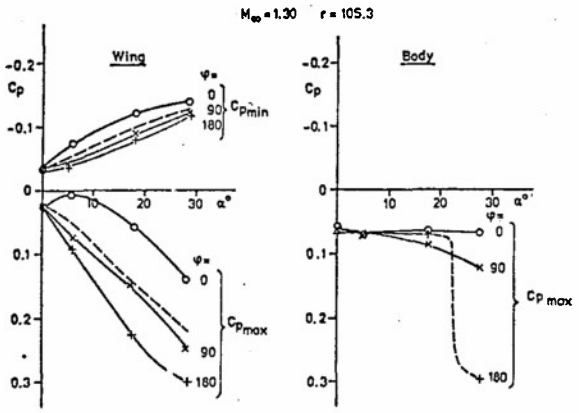

Figure 20. Max. and min. pressure coefficients at r = 105.3 mm and $M_{\infty} = 1,30$ versus angle of attack [14].

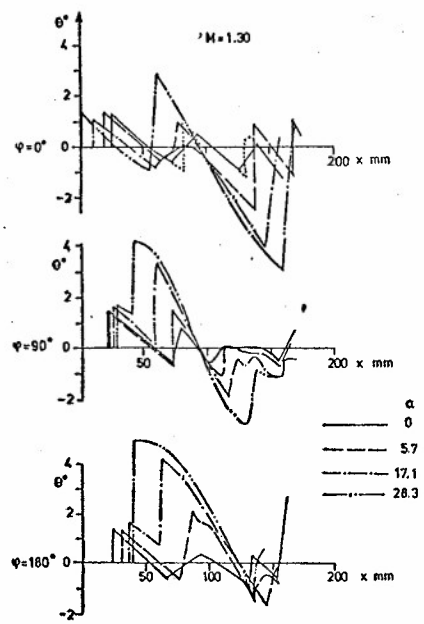

Figure 21. Flow deflection angles at r = 105.3 mm for $\alpha = 0^{\circ} - 28^{\circ}3$ at $M_{\infty} = 1.30$ [14].

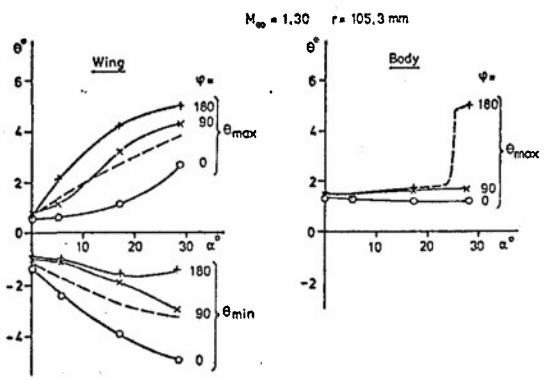

Figure 22. Max. and min. flow deflection angle at r = 105.3 mm and $M_{\infty} = 1.30$ versus angle of attack [14].

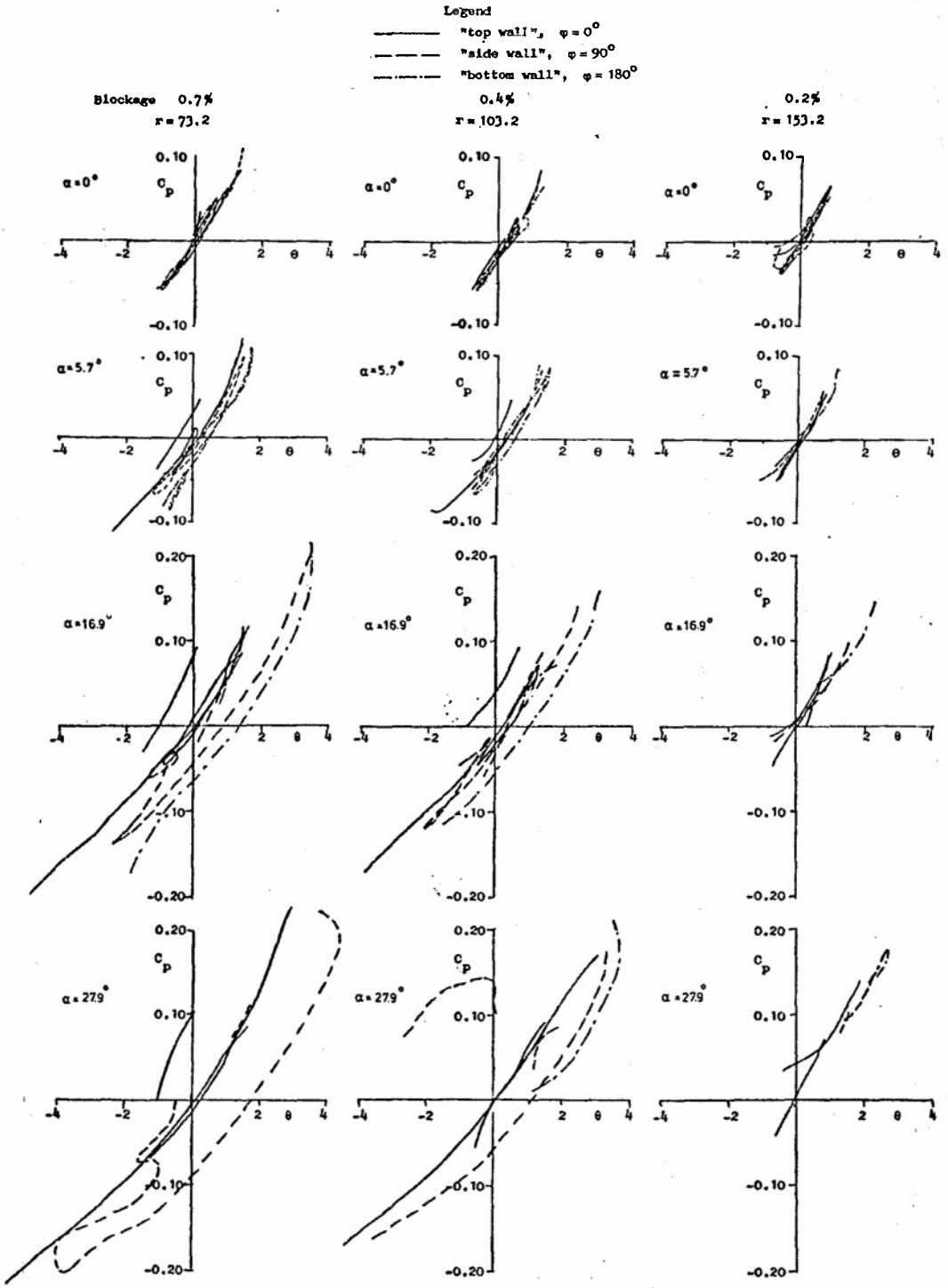

Figure 23. Disturbance distribution $C_p(\theta)$ due to wing-body configuration for model blockage areas 0.2 - 0.7 % and angles of attack $\alpha = 0^o - 28^o$, $M_\infty = 1.20$ [15].

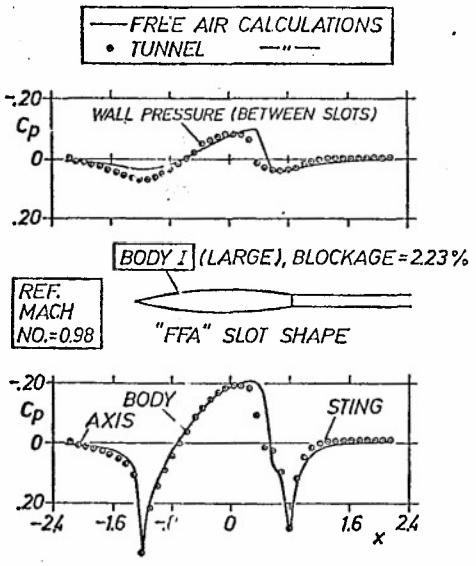

Figure 24. Pressure distributions of body I (large) in tunnel with "FFA" slot at M_∞ = 0.98 [13].

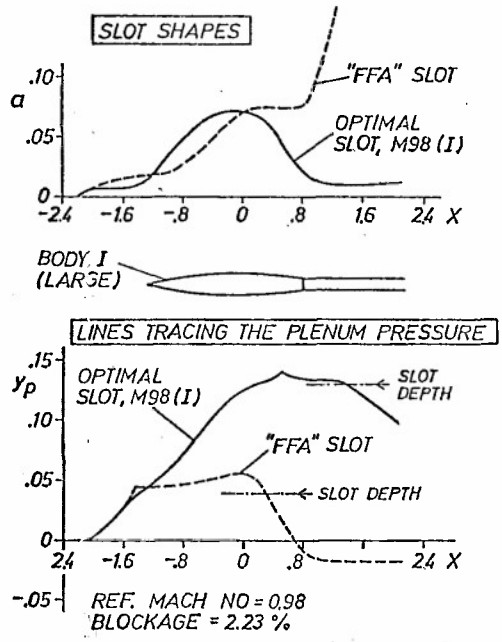

Figure 25. Comparisons between the optimal slot M98 (I) and the "FFA" slot [13].

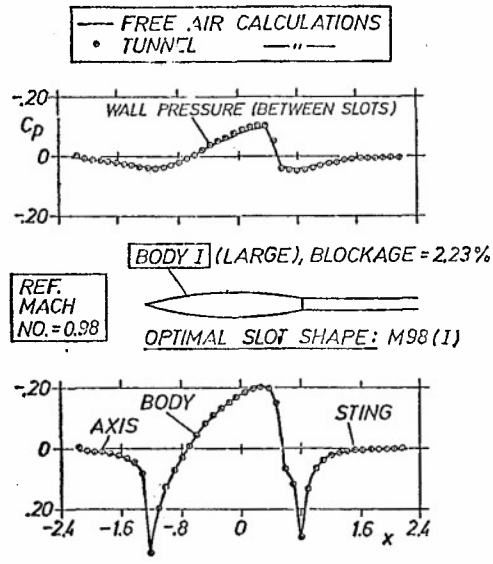

Figure 26. Pressure distributions of body I (large) in tunnel with optimal slot M98 (I) at M_∞ = 0.98 [13].

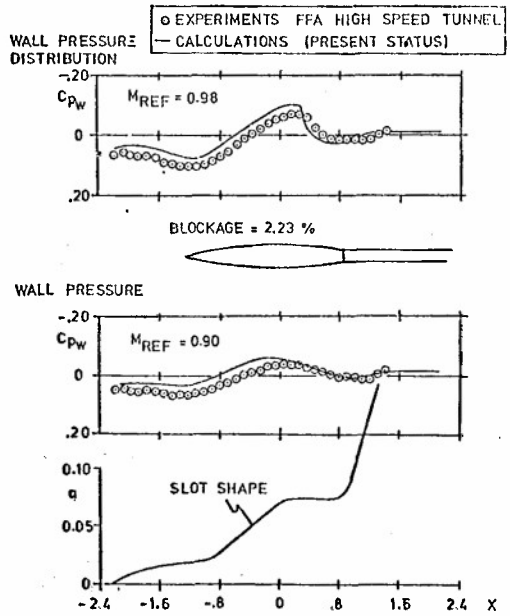

Figure 27. Comparison of calculated and experimental wall pressure distributions [16].

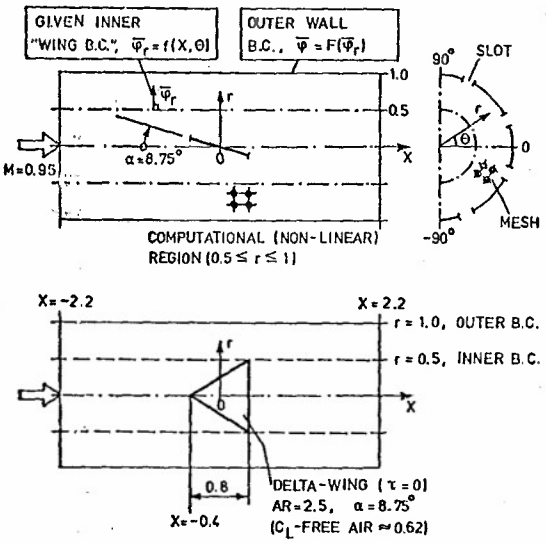

Figure 28. Computational field model for the angle of attack case [16].

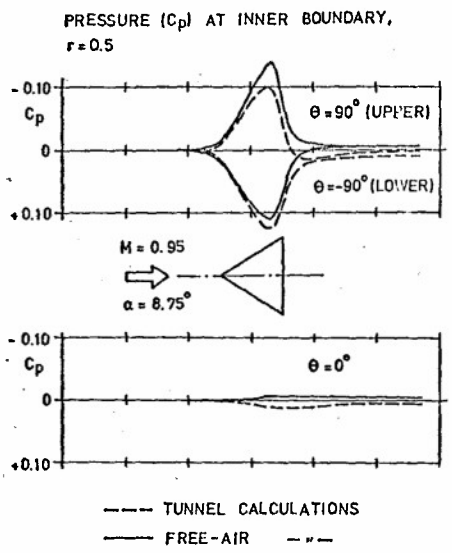

Figure 29. Calculated pressure distributions at inner boundary for an angle of attack case [16].

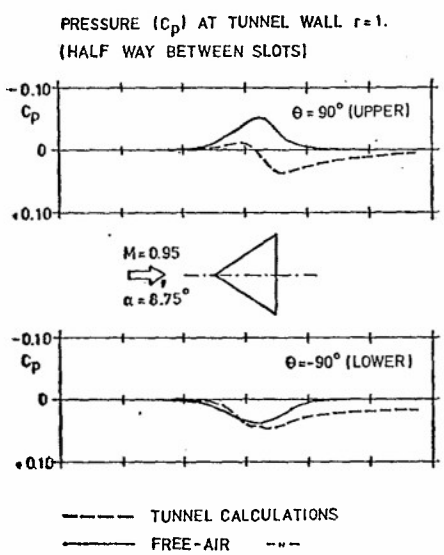

Figure 30. Calculated pressure distributions at tunnel wall for an angle of attack case [16].

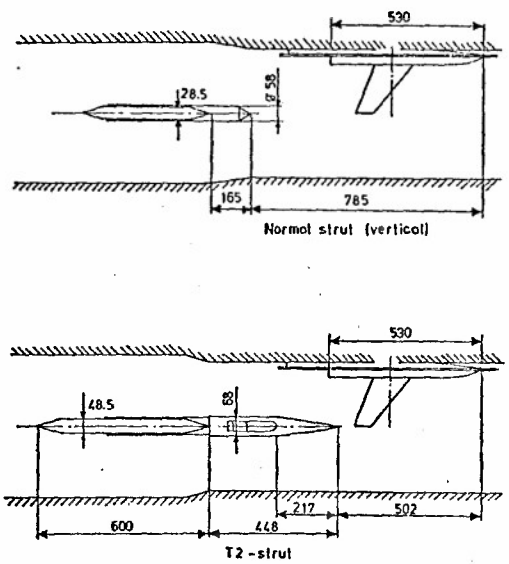

Figure 31. Test arrangement [7].

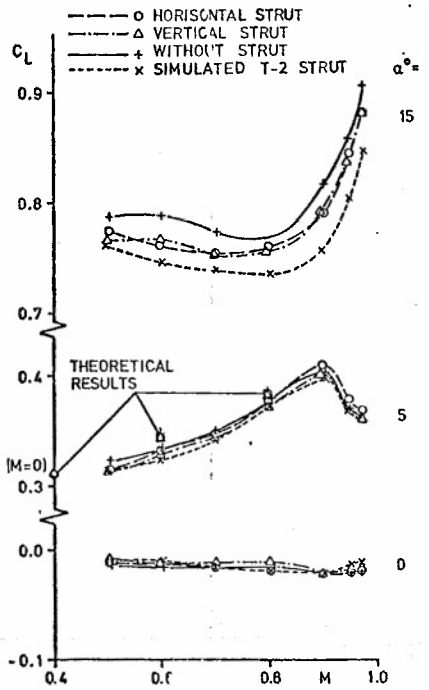

Figure 32. Strut interference effects on C_L [7].

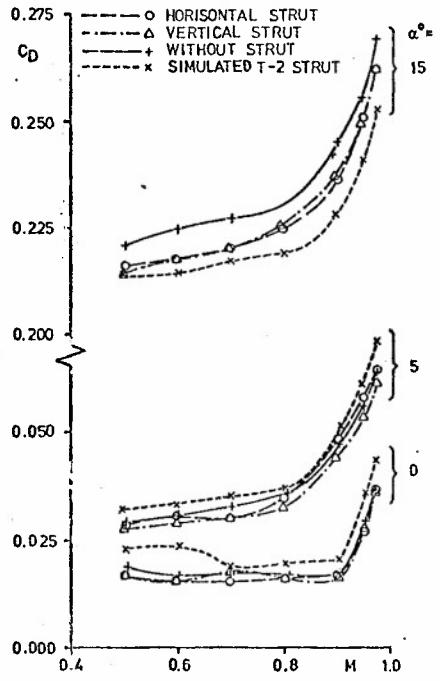

Figure 33. Strut interference effects on C_D [7].

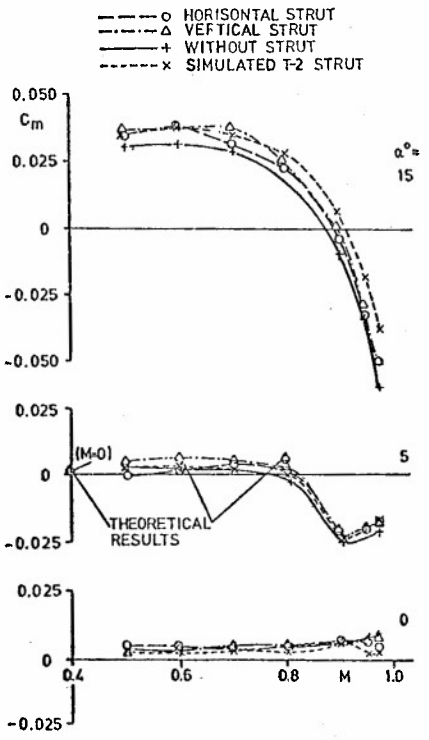

Figure 34. Strut interference effects on C_m [7].

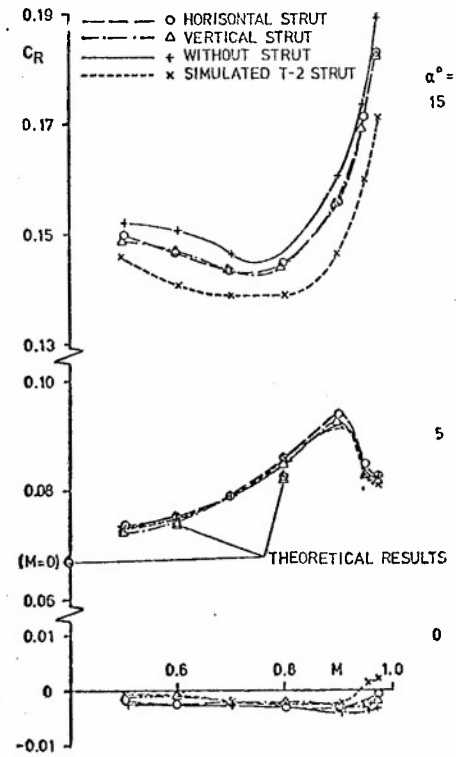

Figure 35. Strut interference effects on C_R [7].

WIND TUNNEL CORRECTIONS FOR HIGH ANGLES OF ATTACK

A BRIEF REVIEW OF RECENT U.K. WORK

by

A. O. Young
(Queen Mary College, London University,
Mile End Road, London, England).

SUMMARY

Only relevant work completed or in progress since the FOP meeting on Wind Tunnel Oesign and Testing Techniques (1975) is covered. It includes the use of adaptive walls (Southampton University), a panel method of model and wake representation for a 2-D model in a wind tunnel with solid walls (British Aerospace), the use of measured pressure distributions on tunnel floor and roof also for a 2-D model and solid walls (RAE), a vortex-lattice representation of the tunnel walls to take account of wake curvature (British Aerospace), interference limitations on tests on V/STOL models with lifting jets (RAE), and work on blockage corrections on models with reverse thrust (British Aerospace).

Some discussion is offered on the limitations on the validity of current methods for determining wind tunnel corrections and it is argued that these limitations are least severe with the use of adaptive walls.

1. INTRODUCTION

Since the AGARO FOP meeting on Wind Tunnel Oesign and Testing Techniques of 1975 the work in the U.K. relevant to the subject of wind tunnel corrections for high angles of attack has been somewhat limited.

This work can be summarised as follows:

a) Work at Southampton University by Dr. Goodyer on the use of adaptive walls.

b) Work at British Aerospace, Kingston-Brough Oivision, by Holt, Storey and Cross on the corrections for a two-dimensional model in a wind tunnel with solid walls. This involves a panel representation of the model and wake coupled with a transformation which dispenses with the need to consider more than one image.

c) Work by Ashill and Weeks, R.A.E., using measured pressure distributions on the tunnel roof and floor to determine the corrections for a two-dimensional model in a tunnel with solid walls up to high subsonic Mach numbers.

d) Work at British Aerospace, Weybridge, by Storey involving a vortex-lattice distribution to represent the tunnel walls but with the limited aim of determining the interference effects arising from differences of wake curvature between the results in 'free air' and tunnel.

e) Work by Trebble, R.A.E., using wind tunnel measurements for models with lifting jets to determine the conditions limiting the validity of wind tunnel testing of V/STOL configurations.

f) Work at British Aerospace, Hatfield, by Farley, McRae and Bryant on blockage corrections on models with reverse thrust.

The salient features of each of the above will be discussed in turn in what follows.

2. WORK OF DR. GOODYER[1,2,3,17] SOUTHAMPTON UNIVERSITY. THE SELF-STREAMLINING WIND TUNNEL.

The essential principle of Goodyer's tunnel is that the pressure distributions and shapes of the top and bottom flexible walls are measured with a model in the tunnel and the pressure distributions are compared with those calculated for an unlimited flow external to the tunnel walls. If the two pressure distributions do not agree then the wall shapes are changed so as to bring the distributions into closer agreement. The measurements are repeated until an acceptable level of agreement between the pressure distributions is attained. Perfect agreement implies that the flow in the tunnel is then the same as for unlimited flow and the tunnel walls are streamlines for unlimited flow. The method includes an allowance for the effective displacement of the tunnel walls due to the boundary layers on them. The process of data acquisition, computation and operation of the jacks determining the wall shapes can be made automatic by means of a suitably programmed on-line computer. The number of iterations required has been reduced to two or three by the application of a process devised by Judd.

Up to the present Goodyer's work has been essentially on two-dimensional models in small tunnels 6 in. between top and bottom walls. An early but striking result that he obtained at low speeds is illustrated in Fig. 1 which shows results he obtained for the flow past a circular cylinder. It will be seen that the self-streamlining tunnel gave satisfactory results even with a cylinder of 29.3% blockage. Some results obtained on an aerofoil with tunnel height (h)/chord (c) = 1.1 at incidences up to and beyond the stall are illustrated in Fig. 2. Here we see encouraging agreement with measurements made on the same model in a much larger Langley tunnel (L.T.P.T.) with h/c = 16, except near and beyond the stall.

In his low speed tunnel some 18 jacks are used on the flexible walls extending three or four chord lengths up and downstream. The method allows for truncation errors due to the finite length of the flexible walls and can also incorporate corrections for any small differences that may remain between the measured and desired wall pressure distributions at a suitable stage in the iterative process.

There appears to be no problem in extending the method to transonic speeds[17], apart from the limitation that it cannot be pursued much beyond the point where a strong shock wave would extend outwards beyond the wall position in unlimited flow.

Goodyer plans to extend his work to three dimensional models, but will continue to keep his sidewalls rigid. The hope is that the major part of the corrections needed for normal wing-bndy arrangements can be dealt with by the shaping of the upper and lower walls and any residual corrections, hopefully small, can be computed with adequate accuracy from the measured pressure distributions. He has constructed a 6 in. square working section for transonic tests and two wing/body models of 4 in. span have been made. These have been tested at Langley in the 7 ft. x 10 ft. transonic tunnel to provide comparative free air results. The tests may range up to stalling incidences. In his work to date he has reached a Mach number of 0.94.

It will be clear that self-streamlining walls offer the possibility of attaining higher Reynolds numbers in a wind tunnel of given size than would otherwise be feasible, and their use in a cryogenic tunnel is particularly attractive.

3. WORK AT BRITISH AEROSPACE, KINGSTON-BROUGH DIVISION[4,5], ON TWO-DIMENSIONAL MODELS IN A WIND TUNNEL WITH SOLID WALLS.

The work is based on the use of a conformal transformation ($\zeta = \xi + i\eta = ie^{\pi z/h}$) which transforms the region between the tunnel floor and roof in the z plane on to the upper half of the ζ plane. Here h is the tunnel height and the real axis in the z plane is along the tunnel centre line. In the ζ plane the wall effect is therefore reduced to that of a single image in the ξ axis of the transformed model. The uniform flow in the z plane transforms to the flow from a source at the origin in the ζ plane.

The model is represented by a system of linearly distributed vortices and uniformly distributed sources over the surface of the model, the latter are symmetrically disposed as described in the method of Maskew & Woodward[6]. The boundary layers are represented by a normal transpiration velocity at the surface related to the rate of change with distance along the surface of the displacement thickness. The wake is similarly represented by linear distributions of vortices and sources over the interface of the two wake layers extending downstream from the trailing edge and lying in the local streamline direction. An allowance for the boundary layers on the walls has yet to be included. An iterative process of solution is adopted to bring into conformity the inviscid and viscous parts of the flow, for the latter Thwaites' method is used for the laminar boundary layers and the lag-entrainment method of Green et al[7] is used for the turbulent boundary layers and wakes.

The method is still under development and the program so far completed has yet to include the wake contribution; it has been applied to a single aerofoil up to stalling incidence for which experimental results at two Reynolds numbers are available for comparison, with the ratio of h/c about 6.9. The calculated curves of C_L and $C_{M\ LE}$ as functions of incidence are about 6% and 8%, respectively, above the experimental data and much closer to the latter than the results for inviscid flow. The inclusion of the wake effects is expected to improve the agreement with the experimental data. The calculations yield values of C_D that are also in reasonable accord with the experimental data.

It is hoped to extend this work to multi-component, high lift arrangements for which an existing wall jet program could be adapted to deal with the use of blowing as well as the interaction of a wake from one component and the boundary layer of the following component.

The inviscid program has, however, also been applied to calculate the lift and pitching moment characteristics of a wing in free air and in a tunnel with a chord/tunnel height = 0.3, for the following configurations:

i) unflapped
ii) 30% trailing edge flap at 30°
iii) 30% trailing edge flap at 45°
iv) 30% trailing edge flap at 60° plus a 10% leading edge flap at 45°.

In each case the corrections ($\Delta\alpha$, ΔC_L, $\Delta C_{M\frac{1}{4}}$) to α, C_L, $C_{M\frac{1}{4}}$* were determined for the calculated tunnel results using the classical standard linearised theory formulae derived from AGARDograph 109[8], and the results for C_L and $C_{M\frac{1}{4}}$ calculated for the wing in free air at the 'corrected' incidence were compared with the corresponding 'corrected' tunnel values (i.e. $C_L + \Delta C_L$, $C_M + \Delta C_M$). Some of the results are set out in Table 1 where suffix 'error' denotes the difference between the calculated free air values of C_L and C_M and the corresponding 'corrected' tunnel values. The ratio of this difference to the corresponding standard theory correction is a measure of the validity of the latter. It will be seen that for the unflapped section at low incidences the standard theory corrections are of acceptable accuracy, but for all other cases they are not adequately accurate. Fig. 3 shows that the uncorrected results can be closer to free air results than after correction by the standard method! Examination of the pressure distributions shows that significant changes in the loading distribution can be induced by the tunnel walls and these do not lend themselves to any simple correlation which could hopefully lead to some generally applicable improvement of the method.

---

* $C_{M\frac{1}{4}}$ denotes the pitching moment coefficient about the quarter-chord point.

4. THE WORK OF ASHILL & WEEKS[9] FOR TWO-DIMENSIONAL MODELS IN THE R.A.E. 8' x 8' TUNNEL.

This work is directed at the corrections needed for aerofoils at subsonic speeds in a tunnel with solid walls. It starts with the argument that within the tunnel the Prandtl-Glauert equation applies in a region S outside a boundary σ enclosing the aerofoil, its wake and areas of supersonic flow (Fig. 4). In S the usual Prandtl-Glauert transformation will lead to Laplace's equation and the complex perturbation velocity can be related by Cauchy's theorem to an integral over the boundaries of S. By considering an aerofoil in free air with the same flow over σ as that of the aerofoil in the tunnel, the difference between them can be ascribed to the integral over the tunnel roof and floor. In this way the tunnel interference can be determined from the measured velocity components over the roof and floor. With solid walls the measured longitudinal component, or the pressure distribution, at the walls provides the basis for determining the tunnel interference. The analysis can be applied to a porous wall tunnel but then the normal velocity distribution is also required. It will be evident that the method will cease to apply if a shock extends from the model to a tunnel wall. Simple extrapolation formulae have been derived to allow for the finite length of working section over which it is possible to make measurements.

The method has been applied to some measurements on aerofoil RAE 5225 with c/h = 0.26 at various Mach numbers and C_L = 0.5 approximately and for various lift coefficients at a Mach number of 0.73. Fig. 5 shows the distribution of wall-induced upwash over the aerofoil chord determined from the measured wall pressures by the above method (vortex distribution method) compared with the distributions given by two versions of the conventional image system method. In the first of these, a distribution of vorticity is placed along the chord line (linearised theory, dashed line) while the second is an approximation to the first, being accurate to second order in $c/\beta_e h$ (linearised theory, full line), where $\beta_e = (1 - M_e^2)^{\frac{1}{2}}$ and M_e is effective free stream Mach number. The agreement between the three methods is reasonably good except towards the trailing-edge where the prediction of the approximate version of the image method deviates from those of the other two methods. The difference in degrees between the induced upwash angles at the leading and trailing edges $\simeq 0.5\ C_L/\beta_e$.

These results clearly provide a warning that the conventional approach of treating tunnel induced upwash as equivalent to an incidence change will be increasingly in error as either C_L or Mach number increases. Furthermore, it may be expected that, in the transonic speed range where there is increased sensitivity to local effective changes of shape, the effect on the pressure distribution of the chordwise variation in upwash is serious.

Some comparisons have been made between the measured pressure distributions at various Mach numbers and corresponding distributions calculated using a program developed by Collyer and Lock[10] (the so-called VGK method - a version of the Garabedian & Korn method[11] coupled with an allowance for viscous effects using the lag-entrainment method of Green et al[7] for calculating the development of the boundary layer). For the latter distributions the calculations were made for the wing section with and without corrections for effective camber changes associated with the upwash distribution given by the approximate version of the image method. Some results are illustrated in Fig. 6 for M = 0.504 and in Fig. 7 for M = 0.749. They are not conclusive in indicating any clear improvement due to allowing for these camber changes, but for these cases the differences are small and not easily distinguished from possible experimental errors (including side-wall effects) and errors in the theories used.

The method for determining tunnel wall interference from measurements of wall pressures can in principle be extended to high lift aerofoils as well as models in three dimensions (by use of Green's theorem provided there is an enveloping region in which the Prandtl-Glauert equation holds). Work on these lines has not yet gone beyond the conceptual stage.

5. WORK AT BRITISH AEROSPACE, WEYBRIDGE. VORTEX-LATTICE REPRESENTATION. WAKE CURVATURE EFFECT.

The method adopted was that due to Joppa[12] in which the model wing is simply represented as a lifting line with a pair of trailing vortices, but these are not assumed rectilinear but are allowed to curve in response to the flow field. The tunnel walls are modelled by a vortex-lattice distribution as illustrated in Fig. 8. The trailing vortex system and associated flow field are first calculated for unrestricted flow ('free air') by an iterative process and then the calculation is repeated for the system in the wind tunnel. The differences between the two sets of calculations for the same wing span and wing circulation are interpreted as the interference effects and the corrections for wind tunnel constraint are derived from them.

The method was applied to two cases: The first was for a 1/15 scale VC10 (span = 9.34 ft) in the Weybridge 13 ft x 9 ft low speed tunnel. From the calculations the interference factors δ and δ' for wing and tail plane incidences, respectively, were determined. These are related to the corresponding incidence and pitching moment corrections by:-

$$\Delta\alpha = \delta \frac{S}{C} C_L \quad \text{and} \quad \Delta C_M = -\delta' \frac{\ell}{h} \frac{S}{C} \frac{\partial C_M}{\partial \eta} C_L$$

Here S = reference area (i.e. wing area), C = tunnel cross-sectional area, ℓ = tail arm, h = tunnel height. η = tail plane incidence, α and η are in radians.

For this model the following results were obtained:-

C_L	δ	δ'
1.1	0.105	0.185
1.9	0.106	0.182

The classical, conventional approach of treating the wake vortices as rectilinear and summing for the images in the tunnel walls gives for all values of C_L :-

$$\delta = 0.104 \quad \text{and} \quad \delta' = 0.178$$

It is clear that for this case the differences between the conventional method and the Joppa method are practically negligible for the values of C_L considered. However, for a similar sized model generating much higher values of C_L the difference in pitching moment correction could become large enough not to be safely ignored.

The second case considered was that of a large rectangular wing model with end plates used for investigations of high lift arrangements. This model had a span of 7.5 ft and a chord of 2.5 ft and was also tested in the 13 ft x 9 ft tunnel.

For this model the Joppa programme resulted in the following values of δ :-

C_L	δ
1.0	0.105
4.0	0.116
5.4	0.126

The conventional method gave $\delta = 0.104$, for all values of C_L ; here there is clearly a major difference in the predicted interference effects for the higher values of C_L considered. This is illustrated in Fig. 9 and 10 showing the resulting curves for C_L as a function of α and C_D as a function of C_L, respectively.

It should be noted that for this model $\Delta\alpha$, the correction to α, is of the order of C_L in degrees and it is questionable whether with such large corrections the chordwise variations of $\Delta\alpha$ resulting in effective changes of model shape can be ignored.

6. WORK BY TREBBLE, RAE, ON LIFTING JETS[13]. LIMITATIONS DUE TO TUNNEL INTERFERENCE.

Trebble investigated the flow field associated with a simple fuselage model with a vertically emerging jet in both the 24 ft tunnel and in the No. 1 11½ ft x 8½ ft tunnel at the RAE (see Fig. 11). The tests in the latter tunnel covered a range of free stream to jet dynamic pressures, q_0/q_j, and various ratios of the height of the nozzle exit above the tunnel floor ($\bar{h}$) to the nozzle diameter (d) and they included pressure measurements on the floor of the tunnel. The model size was such that the 24 ft tunnel results could be taken as free of significant tunnel interference, and they were therefore used as a basis for assessing the interference effects in the smaller tunnel. Earlier tests as well as the flow visualisation experiments in these tests have shown that at low values of q_j/q_0 the jet is diverted downstream in a fairly orderly manner by the main stream. However, as q_j/q_0 is increased the jet comes closer to the tunnel floor and eventually at some critical value of q_j/q_0 it interacts with the tunnel floor boundary layer at some distance downstream of the jet exit. This results in major changes to the flow in the boundary layer and to the surface pressure distribution. At still greater values of q_j/q_0 part of the jet flow spreads laterally and upstream for some distance along the tunnel floor and is associated with the development of a horseshoe vortex which moves upstream and becomes stronger with increase of q_j/q_0.

Clearly this critical value of q_j/q_0 for a given model in a tunnel defines a value above which the flow in the tunnel is sufficiently different from that of flight away from the ground that no correlation by means of simple wind tunnel corrections is possible. Fig. 12 illustrates the nature and degree of the changes that can occur in the downwash in the vicinity of the model fuselage with variations of $\bar{h}/d$ for a given value of q_0/q_j. In this case critical conditions occur for $\bar{h}/d$ about 4.8.

Trebble's measurements show that the onset of critical conditions can be fairly readily identified whether one is looking at dynamic pressure or downwash (Fig.13), and they can be similarly inferred with reasonable consistency from tunnel floor pressure measurements. From an analysis of his own and other workers' results he found that a good empirical relation for the critical value of q_0/q_j as a function of $\bar{h}/d$ is

$$q_0/q_j = 0.25\ (d/\bar{h})^{4/3}$$

for the jet discharging normally to the main stream flow.

Using a semi-empirical formula for the shape of an emerging jet in unrestrained flow, Trebble argued tentatively that for a jet emerging at an angle ϕ_j to the main stream flow the corresponding relation would be

$$(q_0/q_j)^{3/2} = 0.145\ (\cot 50^0 - \cot\phi_j)\ (d/\bar{h})^2 \sin\phi_j ,$$

but there is as yet no experimental result to test this.

Trebble also did some tests with a wing attached to his model and found that the critical conditions were reflected in dramatic changes of lift associated with similar changes of downwash, and these critical conditions were reliably predicted by the above relation for a normal jet in the absence of a wing. He did some preliminary work on an open jet tunnel and found similarly critical effects when the jet impinged on the edge of the mainstream flow.

This work clearly needs pursuing further to examine experimentally what happens with a jet inclined to the main stream and to analyse the interference effects for values of q_0/q_j greater than the critical.

7. B.Ae. HATFIELD.
WORK ON REVERSED THRUST BLOCKAGE CORRECTIONS[14,15].

Measurements made on a HS-125-700 model in a 7ft x 9ft low speed tunnel showed changes in the pressure distributions on the tunnel walls when reverse thrust was simulated. These changes were presumed to be associated with changes in blockage effects which need to he assessed.

The method adopted to do this was briefly as follows. The pressures were measured on the tunnel roof and along the wall and groundboard close to their junction. The pressure distributions with and without the model (but with the nacelles and rig) were determined for various mass flows, and differences were derived due to the various reverse thrust conditions tested. It was assumed that in each case the pressure difference distribution could be associated with an equivalent source-sink distribution along the tunnel axis which was determined from the measured pressure difference distribution (the mean being taken between roof and wall) by means of J.Y.G. Evans' method[16] and influence coefficients. The method then yields a distribution of interference velocity increments due to blockage along the tunnel centre-line. The results showed marked variation of this increment along the centre-line and it was decided to fix on a point half way between the nacelle exit and the mid-chord position for determining a representative value.

Attempts at seeking a collapse of the results for different mass flows (or reverse thrusts) showed a near linear relation could be established between ε (the blockage correction) and C_T (a non-dimensional thrust coefficient) but with some scatter (see Fig.14).

8. CONCLUDING REMARKS

It seems clear that the use of suitable programs, based on some form of panel representation of models and tunnel walls or on measurements of pressure distributions on the walls, can up to a point lead to significantly more accurate estimates of tunnel corrections than the conventional formulae derived from the consideration of simplified image systems. However, such methods must reach their limits of application at the point where the corrections are such that they can no longer be adequately represented as equivalent to the effects of a small change of incidence coupled with a simply represented small change of camber. Beyond such limits the corrections become large enough and vary sufficiently over the body surface to be equivalent to a change of shape which cannot be described as small enough for the effects to be regarded as additive and easily calculated. At that point in trying to determine the wind tunnel corrections we are faced with the need to calculate the flow over a body of prescribed shape. If we could do that accurately we would not have needed the wind tunnel tests in the first place.

The only solution at that stage appears to be the use of adaptive walls. It remains for future research to show how closely we need adjust the walls to the final streamline shapes of unlimited flow. It may well be that judicious use of fairly simple flexible arrangements coupled with measurements of wall pressure distributions to provide residual corrections will prove adequate for most purposes.

Even the use of adaptive walls is limited to cases where strong shocks do not extend to the tunnel walls, but the use of non-linear transonic flow theory for the external flow may ease this limitation.

REFERENCES

1. M.J. Goodyer 1975. "The self streamlining wind tunnel". NASA TM-72699. See also AGARD CP 174.

2. M. Judd, M.J. Goodyer, S.W.O. Wolf 1976. "Application of the computer for on-site definition and control of wind tunnel shape for minimum interference." AGARD CP 210.

3. M.J. Goodyer. "Developments in airfoil testing techniques at the University of Southampton". NASA Conference Publication 2045 Pt. 1. Advanced Technology Airfoil Research Vol. 1, p 415. 1978.

4. P.J. Storey 1977. "Two-dimensional multi-component aerofoils in a wind tunnel". H.S.A. Brough. Note No. YAD3304.

5. O.R. Holt, A.G.T. Cross. "Calculation of viscous, incompressible flow about a single component aerofoil in a closed wind tunnel". B.Ae., Kingston-Brough Division. Note No. YAO 3355. 1978.

6. B. Maskew, F.A. Woodward, 1976. "Symmetrical singularity model for lifting potential flow analysis". J. of Aircraft, Vol. 13, No. 9.

7. J.E. Green, D.J. Weeks, J.W.F. Brooman, 1973. "Prediction of turbulent boundary layers and wakes by a lag-entrainment method." A.R.C. R & M 3791.

8. H.C. Garner, E.W.E. Rogers, W.E.A. Acum, E.C. Maskell, 1966. "Subsonic wind tunnel wall corrections" AGARDograph 109.

9. P.R. Ashill, D.J. Weeks, 1979. "A method of determining tunnel wall constraints effects from measurements of static pressures at the tunnel walls". (To be published).

10. M.R. Collyer, R.C. Lock, 1978. "Improvements to the viscous Garabedian & Korn method (VGK) for calculating transonic flow past an aerofoil". R.A.E. TR 78039.

11. F. Bauer, P.R. Garabedian, D.G. Korn, 1972. "Supercritical wing sections". Lectures notes in Economics & Mathematical Systems. No. 66. Springer - Verlag.

12. R.G. Joppa, 1973. "Wind tunnel interference factors for high lift wings in closed wind tunnels." NASA CR-2191.

13. W.J.G. Trebble. "Investigation of the effects of tunnel walls on the flow near a model containing a lifting jet". Unpublished M.o.D. (PE) material.

14. H.C. Farley, D.M. McRae, 1977. "Reverse thrust blockage corrections". H.S.A. HWT-N-GEN-001705.

15. A.U. Bryant, 1977. "Determination of blockage corrections for a model under reverse thrust conditions." H.S.A. HWT-125-N-001720.

16. J.Y.G. Evans, 1949. "Corrections of velocity for wall constraint in any 10 x 7 rectangular subsonic wind tunnel". A.R.C. R & M No. 2662.

17. M.J. Goodyer, S.W.D. Wolf, 1980. "The development of a self streamlining flexible walled transonic test section". AIAA Paper No. 80-0440, 11th Aerodynamic Testing Conference.

TABLE 1 Coefficient error between corrected tunnel and free stream value as a percentage of the applied correction. (From B.Ae., Brough, Ref. 4 & 5).

SECTION	α	ΔC_M	C_M error	$\frac{\%C_M \text{error}}{\Delta C_M}$	ΔC_L	C_L error	$\frac{\%C_L \text{error}}{\Delta C_L}$
UNFLAPPED SECTION	0	0.0003	0.0000	0.0	0.0015	0.0003	20.00
	5	0.0029	0.0000	0.0	0.0142	0.0031	21.83
	10	0.0054	0.0004	7.41	0.0287	0.0062	21.60
	15	0.0080	0.0014	17.50	0.0467	0.0076	16.27
	20	0.0105	0.0036	34.29	0.0690	0.0307	44.49
	30	0.0153	0.0104	67.97	0.1335	0.0806	60.38
	40	0.0198	0.0198	100.00	0.2309	0.1662	71.98
30° t.e. FLAP SECTION	-10	0.0088	0.0049	55.68	0.0329	0.0249	75.68
	-5	0.0103	0.0049	47.57	0.0440	0.0299	67.95
	0	0.0123	0.0064	52.03	0.0557	0.0394	70.74
	5	0.0148	0.0096	64.86	0.0710	0.0559	78.73
	10	0.0176	0.0149	84.66	0.0922	0.0815	88.39
	15	0.0207	0.0222	107.25	0.1217	0.0179	96.72
45° t.e. FLAP SECTION	-20	0.0139	0.0418	300.72	0.0408	0.0768	188.23
	-15	0.0136	0.0404	297.06	0.0524	0.0805	153.63
	-10	0.0138	0.0410	297.10	0.0603	0.0855	141.79
	-5	0.0146	0.0443	303.42	0.0676	0.0949	140.38
	0	0.0161	0.0509	316.15	0.0772	0.1111	143.91
	5	0.0181	0.0608	335.91	0.0920	0.1359	147.72
	10	0.0204	0.0740	362.74	0.1144	0.1707	149.21
45° l.e. FLAP 60° t.e. FLAP SECTION	-30	0.0293	0.0145	49.49	0.0542	0.0366	67.53
	0	0.0204	0.0080	39.22	0.0923	0.0916	99.24
	5	0.0223	0.0099	44.39	0.1058	0.1161	109.73
	10	0.0248	0.0124	50.00	0.1269	0.1477	116.39
	15	0.0275	0.0154	56.00	0.1572	0.1866	118.70

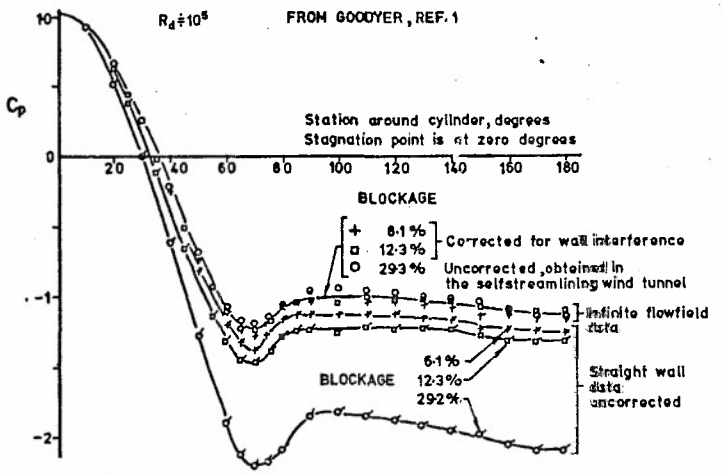

Fig. 1 COMPARISONS OF PRESSURE DISTRIBUTIONS AROUND CYLINDERS MEASURED IN STRAIGHT WALLED AND STREAMLINED TEST SECTIONS

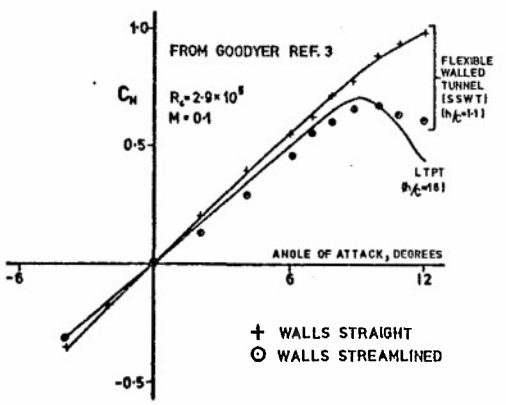

Fig. 2 COMPARISON OF NORMAL FORCE COEFFICIENTS DERIVED FROM PRESSURE MEASUREMENTS ON NACA 0012-64 AEROFOIL IN LANGLEY TUNNEL (h/c=16) AND IN SOUTHAMPTON SELF STREAMLINING TUNNEL (h/c=1·1)

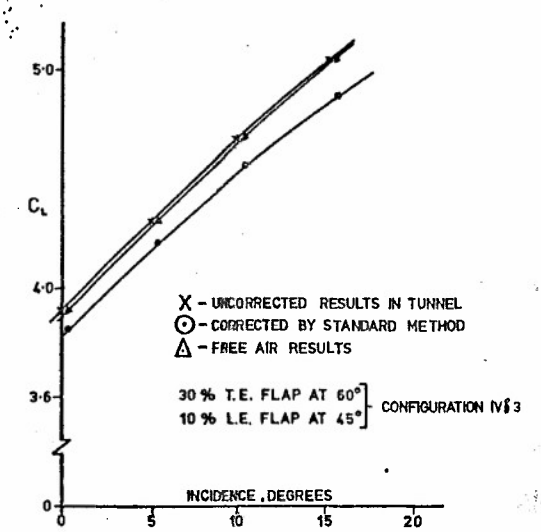

Fig. 3 COMPARISON OF CALCULATED RESULTS FOR SECTION IN TUNNEL 'CORRECTED' AND UNCORRECTED AND IN FREE AIR (BROUGH, REF. 4§5)

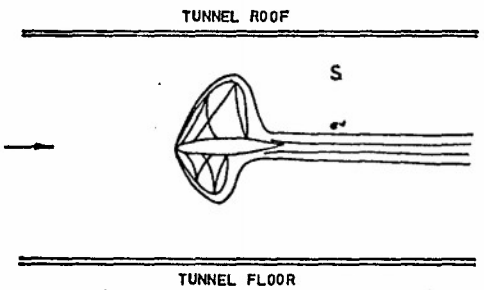

Fig. 4 SKETCH ILLUSTRATING BOUNDARY σ AND REGION S IN WHICH P-G EQU^{N} APPLIES (ASHILL & WEEKS REF. 9)

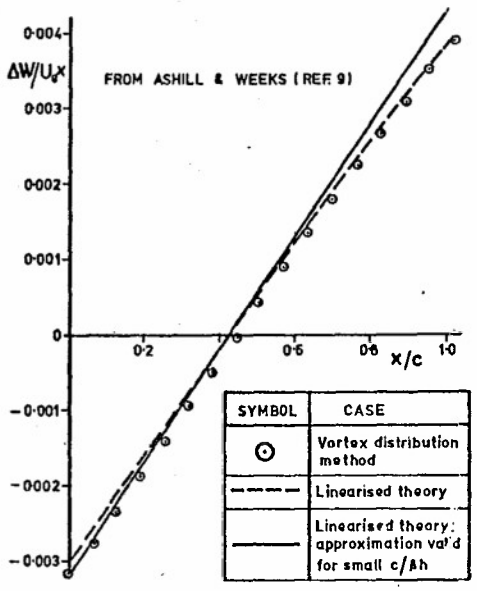

Fig. 5 WALL-INDUCED UPWASH AT AEROFOIL CHORD LINE RAE 5225, M_∞=0·749 C_N=0·560, C_m=-0·238, R_c=20×10^6

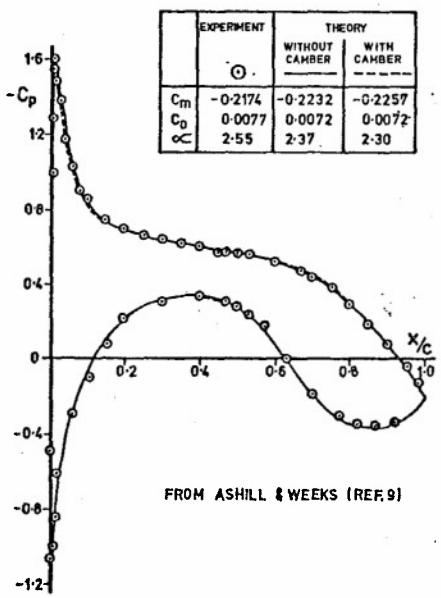

Fig. 6 RAE 5225 PRESSURE DISTRIBUTIONS COMPARISON BETWEEN VGK THEORY AND MEASUREMENT M_∞=0·504, C_L=0·551 R_c=20×10^6

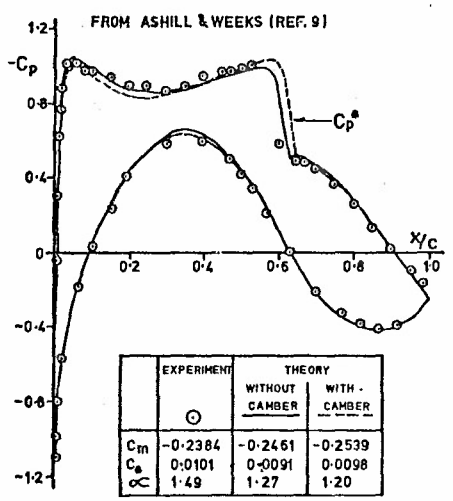

Fig. 7 RAE 5225 PRESSURE DISTRIBUTIONS COMPARISON BETWEEN VGK THEORY AND MEASUREMENT M_∞=0·749 C_L=0·557 R_c=20×10^6

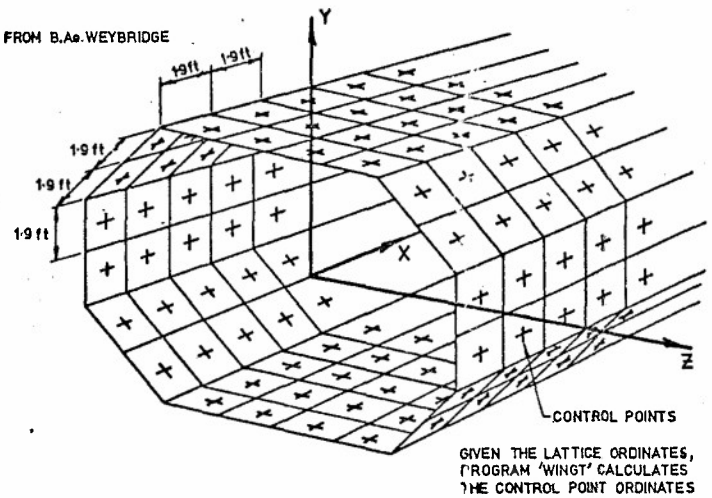

Fig. 8 REPRESENTING 13'×9' LOW SPEED WIND TUNNEL BY VORTEX LATTICE: (Square vortex rings of side 1·9 ft.)

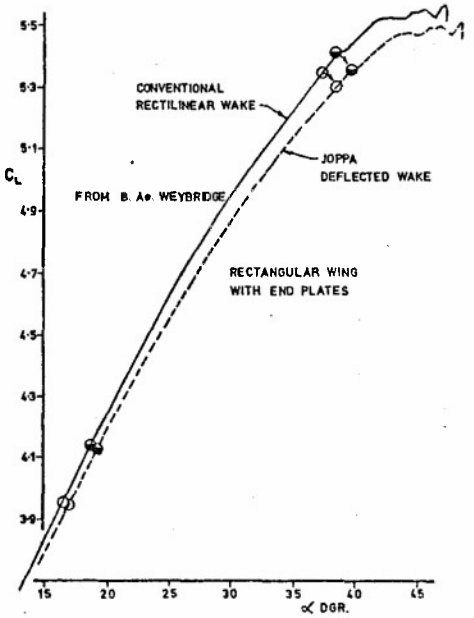

Fig. 9 TYPICAL HIGH LIFT MODEL RESULTS: THE EFFECT OF APPLYING JOPPA'S INTERFERENCE CORRECTION C_L v ∝

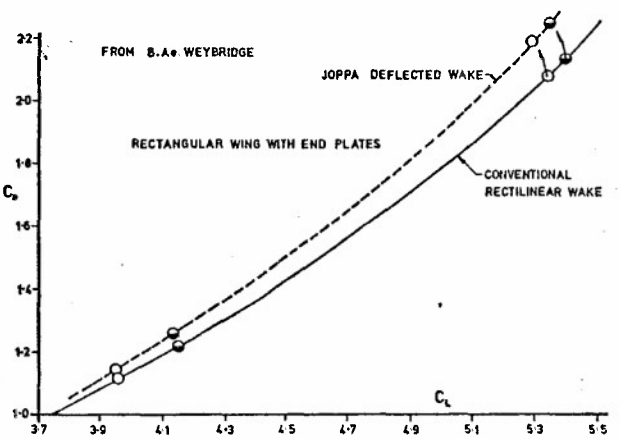

Fig. 10 TYPICAL HIGH LIFT MODEL RESULTS: THE EFFECT OF APPLYING JOPPA'S INTERFERENCE CORRECTION C_D v C_L

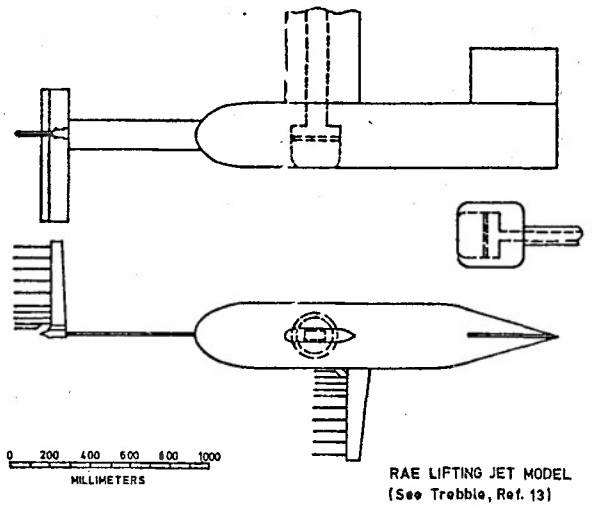

Fig. 11 GA OF MODEL EQUIPPED WITH PITCHMETER RAKES

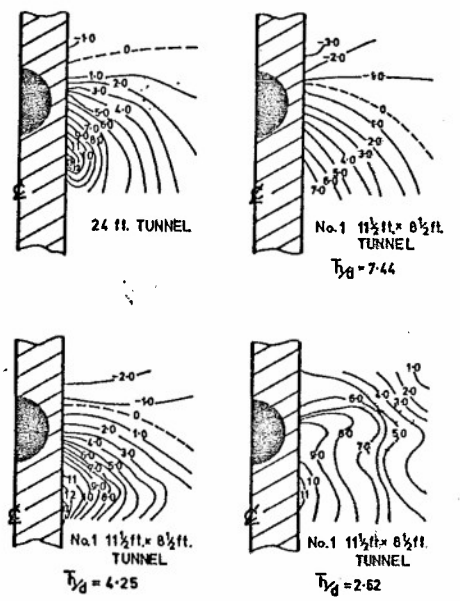

d = 203mm ; $\bar{z}/d$ = −0·80
RAE LIFTING JET MODEL (see Trebble Ref. 13)

Fig. 12 COMPARISON OF THE DOWNWASH ANGLE $\Delta\varepsilon^\circ$
IN THE 24 ft TUNNEL AND
No.1 11½ft × 8½ft TUNNEL AT $\sqrt{q_c/q_j}$ = 0·175

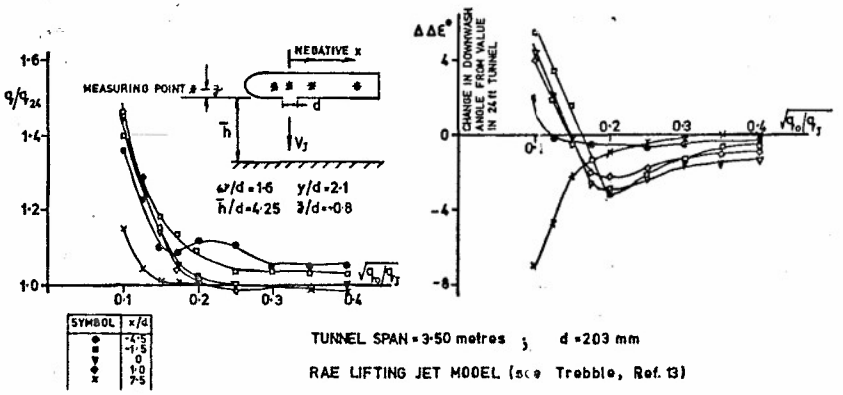

Fig. 13 VARIATIONS IN TUNNEL CONSTRAINT WITH VELOCITY RATIO FOR SEVERAL STREAMWISE LOCATIONS

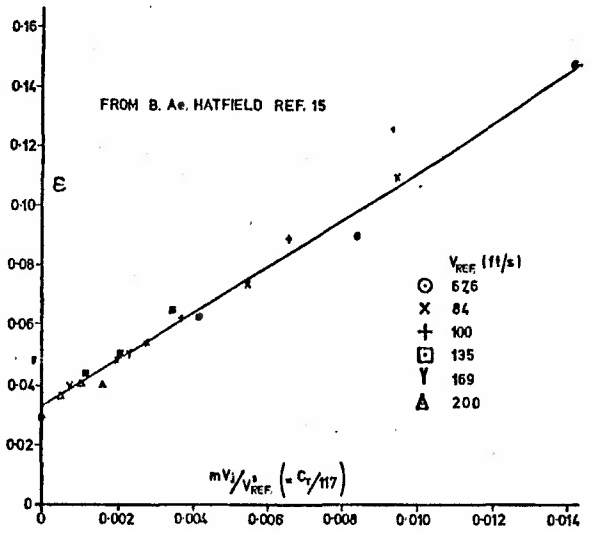

Fig. 14 BLOCKAGE CORRECTION FACTOR ε AS FUNCTION OF REVERSE THRUST COEFFICIENT

REPORT DOCUMENTATION PAGE

1. Recipient's Reference	2. Originator's Reference	3. Further Reference	4. Security Classification of Document
	AGARD-R-692	ISBN 92-835-0283-3	UNCLASSIFIED

5. Originator: Advisory Group for Aerospace Research and Development
North Atlantic Treaty Organization
7 rue Ancelle, 92200 Neuilly sur Seine, France

6. Title: WIND TUNNEL CORRECTIONS FOR HIGH ANGLE OF ATTACK MODELS

7. Presented at: an AGARD Fluid Dynamics Panel Round Table Discussion held in Munich, Germany on 8 May 1980.

8. Author(s)/Editor(s)	9. Date
Various	February 1981
10. Author's/Editor's Address	**11. Pages**
Various	124

12. Distribution Statement: This document is distributed in accordance with AGARD policies and regulations, which are outlined on the Outside Back Covers of all AGARD publications.

13. Keywords/Descriptors

Wind tunnel tests	Adjusting
Angle of attack	Fluid dynamics
Correction	Fluid flow

14. Abstract

This report contains papers on various wind tunnel correction methods used in high angles of attack tests. The papers were solicited from the various NATO countries and presented in a round table discussion following the AGARD Fluid Dynamics Panel Symposium in Neubiberg, Germany in May 1980. Papers given and published here are from Canada, France, Germany, Netherlands, Sweden, United Kingdom and the United States.

Several methods in use or under study are presented for closed, open and ventilated wind tunnels. The Mach number ranges up to the high subsonic and some methods are for incompressible flow. Techniques include vortex lattice, panel, system of images, wall pressure and adaptive walls.

AGARD Report No.692 Advisory Group for Aerospace Research and Development, NATO WIND TUNNEL CORRECTIONS FOR HIGH ANGLE OF ATTACK MODELS Published February 1981 124 pages This report contains papers on various wind tunnel correction methods used in high angles of attack tests. The papers were solicited from the various NATO countries and presented in a round table discussion following the AGARD Fluid Dynamics Panel Symposium in Neubiberg, Germany in May 1980. Papers given and published here are from Canada, France, Germany, Netherlands, Sweden, United Kingdom and the United States. P.T.O	AGARD-R-692 Wind tunnel tests Angle of attack Correction Adjusting Fluid dynamics Fluid flow	AGARD Report No.692 Advisory Group for Aerospace Research and Development, NATO WIND TUNNEL CORRECTIONS FOR HIGH ANGLE OF ATTACK MODELS Published February 1981 124 pages This report contains papers on various wind tunnel correction methods used in high angles of attack tests. The papers were solicited from the various NATO countries and presented in a round table discussion following the AGARD Fluid Dynamics Panel Symposium in Neubiberg, Germany in May 1980. Papers given and published here are from Canada, France, Germany, Netherlands, Sweden, United Kingdom and the United States. P.T.O	AGARD-R-692 Wind tunnel tests Angle of attack Correction Adjusting Fluid dynamics Fluid flow
AGARD Report No.692 Advisory Group for Aerospace Research and Development, NATO WIND TUNNEL CORRECTIONS FOR HIGH ANGLE OF ATTACK MODELS Published February 1981 124 pages This report contains papers on various wind tunnel correction methods used in high angles of attack tests. The papers were solicited from the various NATO countries and presented in a round table discussion following the AGARD Fluid Dynamics Panel Symposium in Neubiberg, Germany in May 1980. Papers given and published here are from Canada, France, Germany, Netherlands, Sweden, United Kingdom and the United States. P.T.O	AGARD-R-692 Wind tunnel tests Angle of attack Correction Adjusting Fluid dynamics Fluid flow	AGARD Report No.692 Advisory Group for Aerospace Research and Development, NATO WIND TUNNEL CORRECTIONS FOR HIGH ANGLE OF ATTACK MODELS Published February 1981 124 pages This report contains papers on various wind tunnel correction methods used in high angles of attack tests. The papers were solicited from the various NATO countries and presented in a round table discussion following the AGARD Fluid Dynamics Panel Symposium in Neubiberg, Germany in May 1980. Papers given and published here are from Canada, France, Germany, Netherlands, Sweden, United Kingdom and the United States. P.T.O	AGARD-R-692 Wind tunnel tests Angle of attack Correction Adjusting Fluid dynamics Fluid flow

Several methods in use or under study are presented for closed, open and ventilated wind tunnels. The Mach number ranges up to the high subsonic and some methods are for incompressible flow. Techniques include vortex lattice, panel, system of images, wall pressure and adaptive walls. ISBN 92-835-0283-3	Several methods in use or under study are presented for closed, open and ventilated wind tunnels. The Mach number ranges up to the high subsonic and some methods are for incompressible flow. Techniques include vortex lattice, panel, system of images, wall pressure and adaptive walls. ISBN 92-835-0283-3
Several methods in use or under study are presented for closed, open and ventilated wind tunnels. The Mach number ranges up to the high subsonic and some methods are for incompressible flow. Techniques include vortex lattice, panel, system of images, wall pressure and adaptive walls. ISBN 92-835-0283-3	Several methods in use or under study are presented for closed, open and ventilated wind tunnels. The Mach number ranges up to the high subsonic and some methods are for incompressible flow. Techniques include vortex lattice, panel, system of images, wall pressure and adaptive walls. ISBN 92-835-0283-3